POLYMER COMPOSITES FOR CIVIL AND STRUCTURAL ENGINEERING

L. Hollaway

Springer-Science+Business Media, B.V.

Polymer Composites for Civil and Structural Engineering

Polymer Composites for Civil and Structural Engineering

by

L. HOLLAWAY
Professor
Composite Structures Research Unit
Department of Civil Engineering
University of Surrey

SPRINGER-SCIENCE+BUSINESS MEDIA, B.V.

First edition 1993

Originally published by Chapman & Hall in 1993
Softcover reprint of the hardcover 1st edition 1993

Typeset in 10/12 pt Times New Roman by Thomson Press (India) Ltd., New Delhi

ISBN 978-94-010-4946-7 ISBN 978-94-011-2136-1 (eBook)
DOI 10.1007/978-94-011-2136-1

A catalogue record for this book is available from the British Library

Library of Congress Cataloging-in-Publication data available

∞ Printed on permanent acid-free text paper, manufactured in accordance with the proposed ANSI/NISO Z 39.48-199X and ANSI Z 39.48-1984

Preface

Synthetic polymers and fibre reinforced polymer composite systems have become increasingly important to the civil and structural engineer over the last decade and now have a wide range of applications in a variety of engineering fields.

A large percentage of all fibre reinforced products are made from unsaturated polyester resins reinforced with glass fibre. However, epoxy and toughened epoxy resins and the high technology thermoplastic polymers, together with the carbon and aramid fibres, are playing an ever more important role in structural engineering, particularly in the aerospace industry, but increasingly in the construction field, and this trend is likely to continue, as chapter 1 convincingly demonstrates. Polymer composites have unique advantages over more conventional materials and these advantages can be enhanced by correct design technology; the engineer has the opportunity to design the composite material and the structural system simultaneously.

An attempt has been made to combine, within one book, information on the various composite systems currently in use in construction, together with fabrication processes, mechanical and physical properties of the matrices, fibres and composites, analytical and experimental testing and design techniques and jointing methods. The section on failure theories is a generic presentation in that structural composites generally consist of various multi-ply laminates which will fail when subjected to a sufficiently large load. It will be realized that the failure of composites is complicated because of the many different ways in which structural systems can collapse. Therefore, this section can serve only as a guide to the prediction of structural integrity.

The aims of this book, therefore, are to provide a simple guide to the principal aspects of the theory and use of composites in construction. It is directed at consulting engineers and designers of polymer composites in the mechanical and civil engineering industries, but will also serve as a reference source for advanced undergraduates and postgraduates studying materials, and material scientists interested in the utilization of composites in engineering.

I would like to express my appreciation to those of my past and present postgraduate students and research assistants at the University of Surrey who have directly and indirectly encouraged and helped me to produce this book. I am particularly indebted to Professor B. Grieveson, Consultant to

the Department of Civil Engineering, with whom I have had many hours of technical discussion and who read the draft of the book and made many valuable suggestions. Finally I would like to thank my wife, Pat, for her help, patience and encouragement.

L.H.

Contents

1 Introduction

It is likely that the mid-20th century into the 21st century will be known as the age of synthetics; these are plastics, man-made fibres, synthetic rubbers, composite materials and synthetic adhesives. Over the past 100 years a massive industry has been created which symbolizes the 20th century just as clearly as iron and then steel characterized the 19th century.

Bakelite was the first completely synthetic polymer produced in 1909; it was named after its inventor, the American chemist Leo Baekeland. Chemically Bakelite is a phenolformaldehyde resin produced when phenol (carbolic acid) and the gas formaldehyde are combined in the presence of a catalyst (see definition in the glossary), if the reaction is allowed to proceed to completion a dark brown tarry substance of little apparent use is produced. However, if the reaction is controlled by terminating it before completion, Baekeland discovered that he had created a material which would flow and could be poured into moulds. If these latter were heated and material pressure applied, a solid heavy plastic material could be formed; this product is used today in certain engineering applications. From this first invention, it is now possible to adapt polymers and to create new ones which can be designed for specific functions. A range of polymers has been developed which do not corrode. These systems can be made to have properties which are flexible or rigid, transparent or opaque and tough or brittle.

The properties of synthetic polymers can be enhanced greatly by adapting techniques utilized in nature. Few natural materials consist of one substance only; most are a mixture of different components which when combined together produce a material which is more able to perform its function than a single substance. Bone, for instance, achieves its combination of lightness and strength (i.e. high specific strength) by combining crystals of apatite (a compound of calcium) with fibres of the protein collagen. These materials are known as composites.

For civil/structural applications, in which both the strength and stiffness of the material are critical, it is necessary to combine the polymer with other materials into composites whose properties transcend those of the constituents. The most commonly employed component is in a particulate or a fibrous form. In the particulate composites, particles of a specific material or materials are embedded in and bonded together by a continuous matrix (the polymer) of low modulus of elasticity. In fibrous composites, fibres with high strength and high stiffness are embedded in and bonded together by the low modulus continuous matrix (the polymer). The fibrous reinforcement

may be orientated in such a way as to provide the greatest strength and stiffness in the direction in which it is needed, and the most efficient structural forms may be selected by the mouldability of the material. To increase the stiffness of the composite still further, the structural units which make up the complete structure may be folded so that the stiffness of the structure is derived from its shape as well as from the material itself. In the construction industry, glass fibre (or carbon or aramid fibre or a combination of these to form a hybrid fibre) and polyester (or epoxy) polymer are used to form a fibrous composite; if glass fibres and polyester resin are formed into a composite, the material is known as glass reinforced polyester (plastics) GRP, or generally as fibre reinforced polymers (FRP). The production of resins, catalysts and accelerators, which are at room temperature, has facilitated the manufacture of GRP by relatively straightforward techniques, using the open mould processes (see section 5.2) without the need to provide presses and steel moulds.

The history of the use of polymers and composites in the construction industry commenced during the Second World War, when rapid progress was made with the manufacture of the first radomes to house electronic radar equipment. Certain aircraft components were also made using GRP. In the late 1940s, GRP continued to be used but it was an expensive material. However, the attraction of the composite with the ease of moulding complex shapes was quickly recognized by designers and in the early 1950s it was available in the form of translucent sheets.

The main growth interest and technology in the glass fibre/polyester composite in the building and construction industry commenced in the 1960s. The production of resins, catalysts and accelerators which cure at room temperature has facilitated the manufacture of GRP by relatively straightforward techniques using the open mould technique (see section 5.2) without the need to provide presses and steel moulds. The main processes, used currently to produce large panel units and small folded plate systems, are the hand lay-up and the spray-up techniques (see sections 5.2.1.1 and 5.2.1.2, respectively).

Two sophisticated GRP structures have played a major role in the development of this material for construction; these are the dome structure erected in 1968 in Benghazi and the roof structure at Dubai Airport built in 1972. The latter structure was designed and fabricated in the United Kingdom and the units were then shipped to Dubai (Figure 1.1).

During the 1970s and early 1980s, other prestigious buildings were erected in the United Kingdom, notably the Morpeth School, Mondial House (the GPO Headquarters in London), Covent Garden Flower Market and the American Express Building, Brighton (Figure 1.2). Apart from the Morpeth school, the buildings were composite systems with either steel or reinforced concrete units as the main structural element and the GRP as the load bearing infill panels.

In the mid-1970s, Lancashire County Council manufactured a classroom

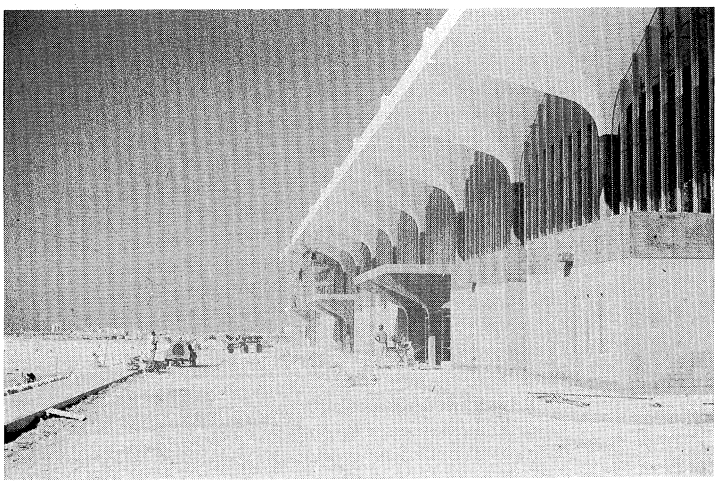

Figure 1.1 Roof structure of Dubai Airport.

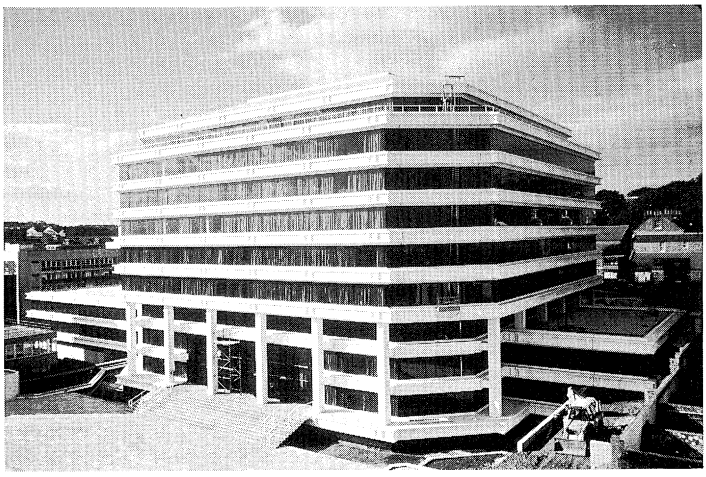

Figure 1.2 American Express building, Brighton.

system using only GRP. This was made possible by folding the flat plate units into a folded plate system so that the overall structural shape provided the stiffness to the building. In this case an icosahedron geometric shape was used.

During the early 1980s, the dome complex at Sharajah International Airport (Figure 1.3) was completed. An example of a continuum space structure is the barrel vault system associated with the Manchester City

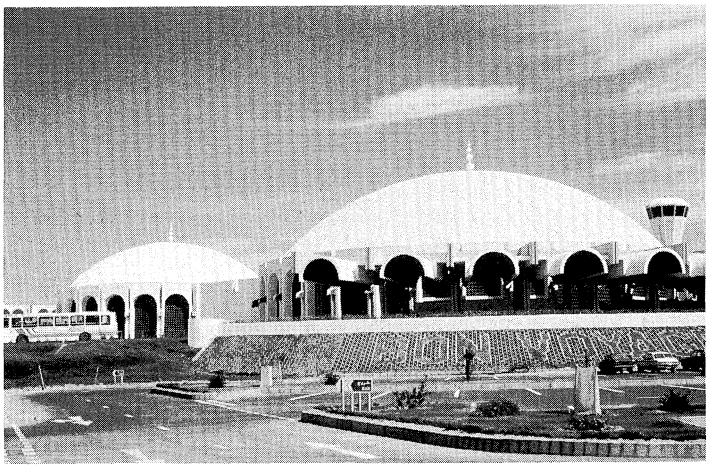

Figure 1.3 Dome complex at Sharajah International Airport.

Football Stand, completed in the mid-1980s. In this structure, glass reinforced polyester gutter sections were fixed to the 1 m deep reinforced concrete beams and onto this gutter section GRP barrel vault modules 5 m by 1.5 m were fixed to span between the reinforced concrete beams.

In the early 1990s, the Neste Corporation (Neste Oy Chemicals Helsinki, Finland) designed and constructed an experimental house (Nestehaus) as a test-bed for polymer-based construction materials and components. Seventy-five percent of the materials used in the 250 m^2 house were manufactured from polymers. Nestehaus has shown that polymers can achieve results that are competitive with traditional materials and are aesthetically, functionally and technically sound.

In addition to conventional building structures, advanced composites have gained significant usage in both Europe and North America where applications have centred around the space industry, buildings in extreme corrosive environments, structures where maintenance inspection access is extremely difficult, and advanced structures for radar transparency.

The analyses and design of composite space structures for communication satellites are likely to be undertaken by some structural engineers using the same techniques as for earth systems; these space systems could be large diameter reflectors in excess of 50 m in diameter and space platforms in excess of 300 m in length will be deployed in space. It is almost certain that these structural systems will be of skeletal form and will be manufactured

Figure 1.4 Perspex model of a deployable skeletal system developed at the University of Surrey. (a) System fully closed; (b) system partially opened; (c) system fully opened.

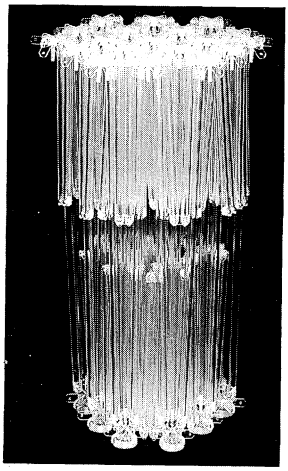

(a)

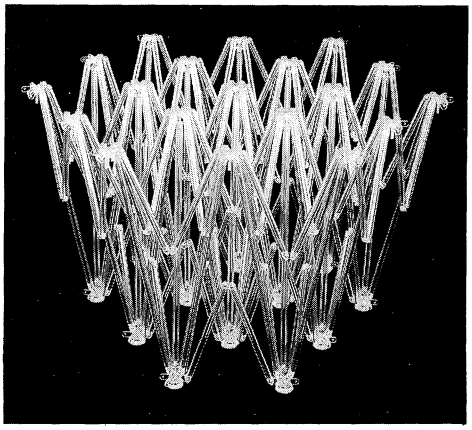

(b)

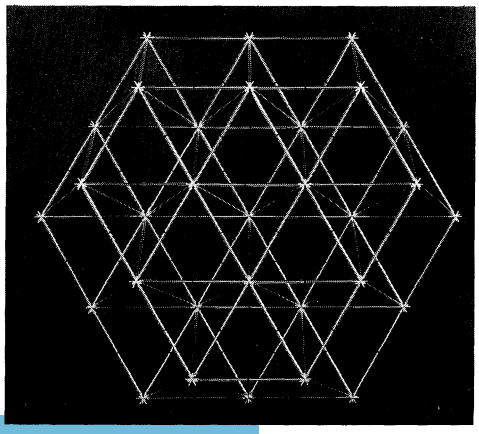

from composite materials because of the latter's unique combination of high specific strength and stiffness, low weight, good thermal stability and high specific damping capacity. Figure 1.4 shows a model of a deployable tetrahedral skeletal system. Intermediate modulus carbon reinforced epoxies (see section 2.8.2) and intermediate modulus carbon reinforced high performance thermoplastic resins (see section 5.4.1) are the principal composite material systems used for space applications.

Glass reinforced polymer beams and columns manufactured by the pultrusion technique (see section 5.2.2.3) have been used for frameworks for buildings in industrial complexes where severe corrosion occurs particularly from acids. An example where this system has been used as the roof support is in a plant manufacturing aluminium in the United States where sodium hydroxide and hydrochloric acid vapours cause major corrosion problems. Tanks for bulk storage of corrosive materials such as sewage plants and chemical storage (where it is mandatory to enclose the material within the container) have been made from glass fibre polymer materials; a typical self-supporting roof made from GRP would be about 25 m in diameter.

The strength and stiffness properties of the pultrusion composite (see section 5.2.2.3) are not yet fully realized in practice and many structural applications that would be possible are never considered. However, this market must soon be exploited because of the need for more energy efficient structures. Single and double layer skeletal roof systems have been described in [1] to illustrate their possible use; further examples of structural systems manufactured by the pultrusion technique are given later in the chapter.

A number of recent studies [2, 3] have examined the possibility of achieving weight savings by the use of composites in various parts of off-shore structures and bridge stays. Areas where composites are well qualified to make significant advances in the short term are:

- walkways, gratings, handrails and cable trays (mainly pultrusion),
- pipework and vessels for all aqueous systems (mainly filament wound),
- panels for separating operating areas and for use in accommodation modules (sandwich and other flat laminates)

In addition, with the improved performance of GRP piping, as cargo and ballast lines for crude products and liquified natural gas carriers, an assessment of the use of GRP piping for sea water systems has been undertaken. It is likely that a large tonnage of composite material will be used in this area within the next 5 years. In addition, composites made from glass fibre and polyester resin are being used in the Gulf of Mexico by Morrison Moulded Fibre Glass Co. to construct small access platforms manufactured entirely from this material. Other uses include structural sections such as gratings and walkways. Composites were selected on the basis of their superior corrosion resistance eliminating maintenance costs.

The construction of prototype footbridges commenced in Europe and

North America in the late 1970s. The first known GRP highway bridge was constructed at Ginzi, Bulgaria, in about 1981 using the hand lay-up technique (see section 5.2.1.1). The main reason for its development was to provide a lightweight military bridge which could be readily transported. Another prototype GRP bridge structure, the Miyun Bridge in Beijing, China, was completed in October 1982. The Shanghai GRP Institute undertook much of the materials research work for this bridge; it has a length of 20.2 m, a width of 7 m and a beam depth of 1.67 m. It is composed of five prefabricated box sections which were glued together on site. The self-weight of the bridge is 300 kN, 80% lighter than an equivalent steel-reinforced concrete bridge. In 1981, the concept of a 'Bridge Enclosure' won a prize in the Civil Engineering Innovative Competition [4]. It was proposed that a floor should be suspended beneath the girders of steel composite bridges to provide inspection and maintenance access. The enclosure would then be sealed onto the underside of the girders to enclose the steelwork and to protect it from further corrosion. At the end of the 1980s an advanced polymer composite construction, fabricated by the pultrusion technique (see section 5.2.2.3), was used in the design of the world's first major bridge enclosure. A cellular glass reinforced polymer composite consisting of interlocking pultruded planks was manufactured and installed as a permanent enclosure to the A19 Tees Viaduct [5].

It is likely that significant advantages can be gained by the construction industry by using complete box girder beam structures manufactured from advanced composites by the pultrusion technique; these advantages will be reflected by cost savings in fabrication and erection. This is particularly true for long span bridges where the stiffness and form of the deck are important with respect to aerodynamic stability. Fibre reinforced polymers offer the potential of eliminating many problems associated with adverse environmental influences which result in the corrosion of metals. Many universities and research institutes throughout the world are investigating the use of advanced composites in bridge construction and repair; Figure 1.5 shows a full-scale structural test which was undertaken in 1992 at the University of Surrey [6] on two 2.3 m wide by 0.76 m deep and 18 m long box beams loaded back to back in pure moment. The beams were manufactured by the pultrusion technique in which a series of hollow stiffened panels of external dimensions 640 mm long and 80 mm deep were joined by 'dog bone' connectors; the panels were bonded, however, along their edge to the corner members.

Many reinforced concrete bridges, particularly in the USA, have suffered from chronic corrosion through deicing salts. To counter the problem over 200 000 tonnes of epoxy-coated steel rebars have been used in bridge decks since 1987, but these have degraded [7]. Glass fibre reinforced polymer (GFRP) rebars which surpass the strength and fatigue properties of steel rebars can be manufactured by the pultrusion process (section 5.2.2.3) and these are now being investigated as a replacement material for steel. Other

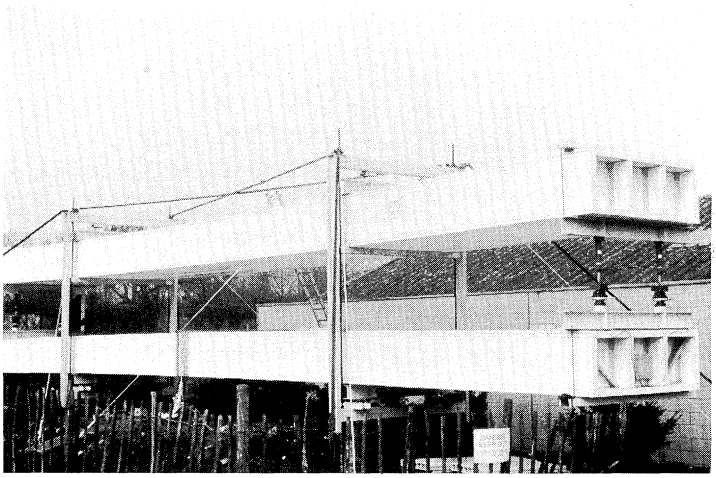

Figure 1.5 Full-scale structural test undertaken at the University of Surrey.

features of these rebars include low weight (although not generally a problem in reinforced concrete) and economy (for example the cost of GFRP rebars is about the same as that of epoxy-coated steel rebars). In addition, as GFRP possesses excellent electrical insulating properties, it would be ideal for use at airports to help solve radar interference with electrical or magnetic fields.

Considerable research has been and is being undertaken into the use of fibre reinforced polymer strands called Polystal (see section 2.8.5) to post tension concrete beams. This technique has been used to construct footbridges in Germany. The first known example using this construction was a small prestressed concrete footbridge erected in Dusseldorf, Germany. In 1986 a continuous two-span highway bridge structure (Die Bruck Ulenbergstrasse) was erected, again in Dusseldorf. The spans of the bridge are 21.3 and 25.6 m, it consists of a 1.57 m deep slab and is 15 m wide. The slab was post-tensioned with 59 Polystal prestressing tendons each made up from 19 glass reinforced polymer rods (nominal diameter 7.5 m). A footbridge was constructed at Marien Flede in Berlin consisting of a two-span continuous double 'T' section beam of spans 27.6 m and 22.9 m; external Polystal tendons were used as prestressing cables.

Aramid fibres (see section 2.8.3) and aramid fibre-reinforced polymers have been used for prestressing, bracing and cable-stay and in particular for the anchoring of oil drilling platforms [8, 9].

The use of carbon fibre (see section 2.8.2) reinforced polymers (CFRP) for applications in bridge construction, in particular for cables in cable-stayed and suspension bridges [10–13] and more recently as prestressing tendons, has been under discussion for some time. An 80 m long prestressed bridge

with a partial reinforcement of CFRP tendons was realized in Ludwigshafen in 1991 [14].

Smart materials and structures are a new class of constructional components that have self-inspection and inherent adaptive capabilities. There are a number of technologies that are strategic in their development but one in particular, namely the fibre optic sensing system, is now being embedded in advanced composite materials in prototype demonstrations [15,16]. This research thrust is an ideal application for this sensing technology since the optical fibres are compatible with the E-glass fibre (see section 2.8.1) but their radial dimensions are an order higher than that of the structural fibre. The sensing system allows the composite component to be monitored during its manufacture, service life and impending failure. Optical fibres can now withstand the 160°C curing temperature associated with the manufacture of smart structural materials.

A large percentage of composites and polymers are used in geotechnical applications; these can be categorized as:

1. (a) soil anchoring techniques;
   (b) ground anchors;
   (c) soil nailing;
   (d) friction anchoring;
   (e) reinforced soil.
2. (a) soil reinforcement techniques;
   (b) reinforced soil rafts;
   (c) embankment slope reinforcement.

The subsequent chapters discuss which types of polymers are used in the most important of the above applications and how these polymers are formed into fibres to provide the reinforcement to the soil.

Foamed polystyrene polymer blocks have been used to form a stable volume of low weight as the sub-base to roads which are built on soft fine-grained subsoils, clays and peat soils where such subsoils often yield unacceptable settlements. The Scandinavian countries and The Netherlands have specifications for expanded polystyrene used for this purpose. In the United Kingdom, such constructions have been used by the Department of Transport for the Western bypass at Great Yarmouth and by the Gateshead Metropolitan Borough Council to provide a second access road to the Metrocentre. In 1992 a new design for the use of expanded polystyrene was adapted and incorporated into an embankment widening for the first stage development of the 60 ha site at Hull for a commercial and leisure complex unit on a former rail sidings land owned by British Rail [17].

Since the early 1950s adhesives have become widely used in civil engineering throughout the world. Many of the uses, however, are non-structural as they do not need to resist the transmission of significant stresses. During recent years there has been a considerable increase in the use of adhesives in

structural applications; one example is the jointing of precast concrete units in the segmental construction of bridges, although in this case the adhesive is in compression. The bonding of external plate reinforcement for the strengthening of concrete structures is another example of adhesive use in the construction industry, in which the joint is designed so that the adhesive provides the shear connection to the composite structural system. Particular grades of two-part epoxy resin adhesive, especially the polyamide type hardeners, can satisfy most of the requirements for external bonding to bridges in the UK's environmental conditions.

Similar requirements are valid for building applications although it is recognized that many epoxy resins exhibit a reduction in mechanical properties above 40°C. Consequently these polymers are limited to situations where fire resistance properties are not important.

It is clear that over the last 20 years considerable advances have been made in the use of composite materials in the construction and building industries, and this trend will continue. The following chapters deal specifically with various aspects of the use, the manufacture, the analyses and the design of composite materials which are or will be of importance to the construction industry. They should enable the engineer and architect to understand the basic principles behind their use and, it is hoped, will encourage the profession to consider the use of this exciting material in the many applications discussed above.

The following sections introduce various aspects of polymer composites in the construction industry, they discuss the mechanical and inservice properties of the material, laminate theory and design methods for composites and some design examples are given. The various bibliographies will enable the reader to broaden his/her knowledge in the subject and to become an expert in the use of composite materials in the construction industry.

References

1. L. Hollaway, Reinforced polymer space structures, in *Studies in Space Structures*, ed. H. Nooshin, Multi-Science Publishing (1991), pp. 265–290.
2. M.M. Salama, Lightweight materials for mooring lines of deep water tension leg platforms, *Marine Technol.*, **21** (1984), 234–241.
3. U. Meier, Future use of advanced composites in bridge construction engineering, in *Proc. 2nd Int. Conf. on Fibre Reinforced Composites*, Institution of Mechanical Engineers (1986), University of Liverpool Paper C46/86.
4. Enclosure put paid to bridge painting, *New Civil Engineer*, 15 October (1981).
5. P.R. Head, GRP walkway membranes for bridge access and protection, in *British Plastics Federation 13th Reinforced Plastics Congress* (1982).
6. L. Hollaway and J. Lee, Bridge Conference, University of Surrey (1993).
7. US bridge tests glass fibre rebars, *New Civil Engineer*, 12 November (1992).
8. C.J. Burgoyne, Structural use of Parafil ropes, *Construct. Building Mater.*, **1** (1987), 3–13.
9. A. Gerritse, Arapree: a non-metallic prestressing tendon, Technical Contribution to the Conference on Durable Reinforcement for Aggressive Environments, Luton (1990).

10. U. Meier, Multiplication of the critical span of suspension bridge through the use of high performance composites, Coloquio de Madrid, *Coloquio International Sobre la Factibilitad de una Comunicacion Fija a través del Estrecho de Gibraltar*, Tomo I (1982) ISBN 84-500-8985-7, pp. 481–484.
11. U. Meier, R. Muller and A. Puck, GFK Biegeträger unter quasistatischer und schwingender Beanspruchung, Tagungsbericht der 18 Offenthehen Jahrestagung der Arbeitsgemeinschaft Verstärkte Kunststoffe e.V., Freudenstadt (1982), 35–112.
12. U. Meier, Proposal for a carbon fibre reinforced composite bridge across the strait of Gibraltar at its narrowest site, *Proc. Inst. Mech. Eng.*, **201** (1987), 73–78.
13. U. Meier, Bruchensanierung mit hochleistungs-Faserverbundwerkstoffen/Réparation des ponts avec des matériaux composites hautes performances, *Mater. Tech.*, **15** (1987) 125–128.
14. Technik Beilage, *Neue Zürcher Zeitung* **216** (1991), P83.
15. N. Furstenau, W. Schmidt, D.D. Janzen and H.C. Goetting, Composite strain sensing with a combined interferometric and polarimetric fibre optic strain gauge, *Proc. 1st European Conf. on Smart Structures and Materials*, Glasgow (1992), session 3, paper 4.
16. R. Davidson and S.S.J. Roberts, Finite element analysis of embedded optical fibre sensors transverse to local reinforcement in CFRP laminates, *Proc. 1st European Conf. on Smart Structure and Materials*, Glasgow (1992), section 4, paper 2.
17. Light answer, *New Civil Engineer*, 5 November (1992).

2 Characterization and mechanism of fibre matrix materials

2.1 Introduction

Composites which are used to form engineering materials and which consist of strong stiff fibres in a polymer resin require scientific understanding from which design procedures may be developed. The mechanical and physical properties of the composite are clearly controlled by their constituent properties and by the micro structural configurations. It is therefore necessary to be able to predict properties when parameter variations take place.

The most important aspect of composite material design is the property of anisotropy; it is necessary to give special attention to the methods of controlling this property and its effect on analytical and design procedures.

Research work undertaken in recent years has resulted in a clearer understanding of the characteristics of fibre/matrix composites. It has been demonstrated that with the correct process control and a soundly based material design approach, it is possible to produce composites that can satisfy stringent structural requirements. However, in the construction industry, because the durability of the composite over a period of say 50 years cannot be scientifically estimated, great care has to be exercised in predicting stress and deformations over this time span.

2.2 Mechanism of reinforcement of fibre reinforced polymers

The reinforcement of a low modulus matrix with high strength high modulus fibres utilizes the plastic flow of the matrix under stress to transfer the load to the fibre; this results in a high strength high modulus composite. The aim of the combination is to produce a two-phase material in which the primary phase that determines stiffness and is in the form of particles of high aspect ratio (i.e. fibres) is well dispersed and bonded by a weak secondary phase (i.e. matrix). The principal constituents which influence the strength and stiffness of the composites are the reinforcing fibres, the matrix and the interface. Each of these individual phases has to perform certain essential functional requirements based on their mechanical properties so that a system containing them may perform satisfactorily as a composite.

2.2.1 *Fibres*

The desirable functional requirements of the fibres in a fibre reinforced composite are:

(a) The fibre should have a high modulus of elasticity for an efficient utilization of reinforcement.
(b) The fibre should have a high ultimate strength.
(c) The variation of strength between individual fibres should be low.
(d) The fibres should be stable and retain their strength during handling and fabrication.
(e) The diameter and surface of the fibres should be uniform.

2.2.2 *Matrix*

The matrix is required to fulfil the following functions:

(a) to bind together the fibres and protect their surfaces from damage during handling, fabrication and during the service life of the composite;
(b) to disperse the fibres and separate them in order to avoid any catastrophic propagation of crack and subsequent failure of the composite;
(c) to transfer stresses to the fibres efficiently by adhesion and/or friction (when composite is under load);
(d) to be chemically compatible with fibres over a long period;
(e) to be thermally compatible with fibres.

2.2.3 *Interface*

The interface between the fibre and the matrix is an anistropic transition region exhibiting a gradation of properties. This is an important region which is required to provide adequate chemically and physically stable bonding between the fibres and the matrix. Its functional requirements vary considerably according to the performance requirement of the composite during its various stages under service conditions.

It will be realized that in the analyses of composite materials, a number of assumptions are made to enable solutions to mathematical models to be obtained, these are:

(a) the matrix and fibre behave as elastic materials;
(b) the bond between the fibre and matrix is perfect and consequently there will be no strain discontinuity across the interface;
(c) the material adjacent to the fibre has the same properties as the material in bulk form;
(d) the fibres are arranged in a regular or repeating array.

The results of the idealized mathematical solution will indicate what is likely to happen in the real composite system.

Clearly the properties of the interface region are of extreme importance when an understanding of the stressed composite material is required. This region is a dominant factor in the fracture toughness property of the material and in the resistance of the composite to aqueous and corrosive environments. Composite materials which have weak interfaces have low strength and stiffness but have high resistance to fracture and those with strong interfaces have high strength and stiffness but are very brittle. This effect is a function of the ease of debonding and pull-out of the fibres from the matrix material during crack propagation.

2.3 Geometrical aspects

The properties of fibre reinforced polymer composites are highly dependent upon the microstructure of the fibre. The most important fibre parameters to be considered when characterizing composite materials are:

1. diameter;
2. length;
3. volume fraction;
4. alignment;
5. packing arrangement.

These parameters will affect the design of the composite and its manufacture.

Composites are manufactured by stacking lamina in a predetermined arrangement to ensure optimum properties and performance. When the elastic properties of the composite are being determined, it is assumed that each lamina is homogeneous and therefore has uniform elastic properties and volume fraction throughout. The fibre arrangement in the various laminae can be continuous or discontinuous; the latter arrangement can be either short length fibres which are unidirectionally aligned or short length randomly orientated fibres. A typical stacking sequence of a laminae, (which is also known as a laminate) is shown in Figure 2.1. Figure 2.1(a) illustrates an orthotropic flat composite (section 3.3) and consists of laminae of unidirectionally aligned fibres which are stacked at 90° to each other. Figure 2.1(b) illustrates a typical lay-up for a pressure pipe in which the two outside laminae have unidirectionally aligned fibres arranged at $\pm 55°$ to the longitudinal axis of the pipe. The inside laminae are made from a randomly orientated fibre arrangement.

When a unidirectional fibre lamina is made, the fibres are aligned parallel to each other. From a theoretical point of view the fibres are assumed to be of uniform circular cross-section, to have a smooth surface and to be arranged in a square or hexagonal lattice. Pickett produced a sophisticated analysis for the elastic moduli of such sections [1]; the arrays are shown in Figure 2.2; the latter configurations are also applicable to organic and

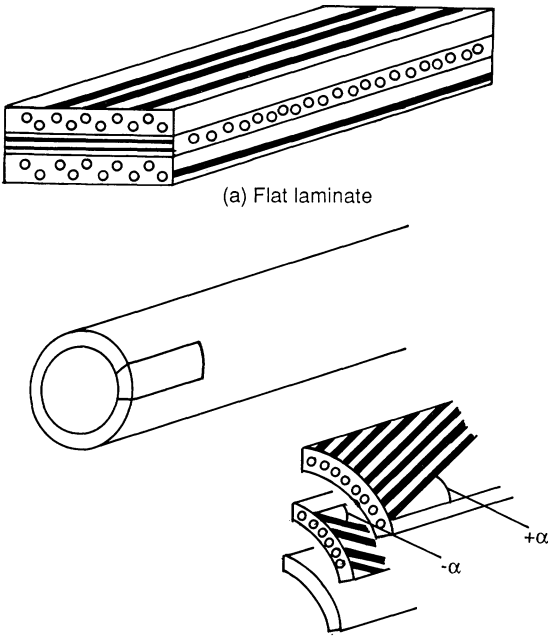

Figure 2.1 Typical stacking sequence. (a) Flat laminate; (b) pressure pipe.

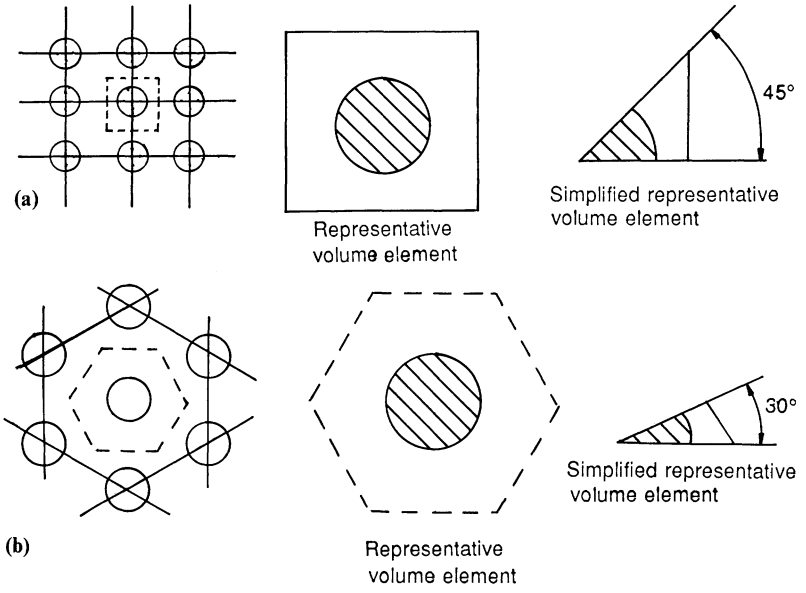

Figure 2.2 (a) A square array and representative volume element. (b) A hexagonal array and representative volume element.

carbon fibres although the carbon fibres, which are approximately circular in cross-section, have very irregular surfaces.

It may be shown that for ideal arrangements (square or hexagonal), the fibre volume fraction V_f is related to the fibre radius as follows:

$$\begin{aligned} V_f &= (\pi/2\sqrt{3})(r/R)^2 \quad \text{(hexagonal)} \\ V_f &= (\pi/4)(r/R)^2 \quad \text{(square)} \end{aligned} \tag{2.1}$$

where $2R$ is the distance between the centres of two adjacent fibres and r is the radius of the fibre. The maximum value of V_f will occur when the fibres are touching, that is when $r = R$ and for this case, the maximum fibre volume fraction for the hexagonal array is 0.907; the corresponding value for a square array is 0.785.

The idealized equations relating the separation of the fibres and the fibre volume fraction are:

$$\begin{aligned} S &= 2[(\pi/2\sqrt{3}\,V_f)^{1/2} - 1]r \quad \text{(hexagonal)} \\ S &= 2[(\pi/4\,V_f)^{1/2} - 1]r \quad \text{(square)} \end{aligned} \tag{2.2}$$

It can be shown by using these equations that if the spacing S is equal to the radius of the fibre, the fibre volume fraction is only 0.3; if the fibres touch other (i.e. $S = 0$), the fibre volume fraction is approximately 0.78 and 0.91 for the square and hexagonal arrays, respectively.

Most design calculations for composite materials are based on the fibre volume fraction, but it is sometimes necessary to use weight fractions, particularly during the manufacturing process and when calculating the density of the composite material.

The relationship between the weight and volume fractions are

$$\begin{aligned} V_1 &= \{W_1/\rho_1\}/\{W_1/\rho_1 + W_2/\rho_2 + W_3/\rho_3 + \cdots\} \\ W_1 &= \{\rho_1 V_1\}/\{\rho_1 V_1 + \rho_2 V_2 + \rho_3 V_3 + \cdots\} \end{aligned} \tag{2.3}$$

where the suffixes 1, 2, 3, etc. refer to the constituents of the material and V, W and ρ are the volume fraction, weight fraction and density of the constituents, respectively.

There are two procedures for obtaining unidirectionally aligned fibres in a laminate, the first is to lay up individual unidirectional laminae at predetermined angles before consolidation, the second method is to weave fibres into a cloth before impregnating it with the polymer. A complete characterization of the woven fibre composite would contain details of the weave spacing, the number of fibres in each roving and the ratio of the number of fibres in the warp and weft directions as well as the variables discussed above. There tend to be areas of higher stress developed at the cross-over points of the woven structure when the composite is under in-plane load; under a compressive load the fibres would tend to buckle

locally at a lower load compared with that of a unidirectionally aligned system of fibres or would tend to straighten out under a tensile load and would therefore have a slightly different characteristic to that of the unidirectionally aligned composite.

If a composite is made from laminae with long in-plane randomly orientated fibres (i.e. hand lay-up or spray-up techniques, see section 5.2), the maximum achievable fibre volume fraction is much lower than that of the aligned laminae (i.e. the pultrusion or filament winding techniques, see section 5.2.2). Typical values of V_f for this type of array are 0.1–0.35 compared with values of 0.6–0.85 for aligned laminae.

The distribution of short in-plane randomly orientated fibre arrays, for example composites manufactured by the injection moulded technique (section 5.2.2.2), has a three-dimensional configuration and consequently the orientation is more difficult to assess. A method is shown in Figure 2.3 in which the unit element represents a thin slice of material which is orientated in a predetermined direction; the position of fibre can be determined by knowing the angles α and β. These angles can be measured by means of optical microscopy. The angle β is given by: $\beta = \tan^{-1}(t/l_\rho)$; α can be measured directly from the optical solution and β can be obtained from the projected length l_ρ. These angles do not completely fix the position of the fibre as the same length of fibre would have been obtained if the projection length had an angle of $(\pi - \beta)$. Barrett and Massalski [2] have discussed the methods for obtaining a graphical representation of the three-dimensional distribution which corresponds to the values of α and β.

Voids in composites must be reduced to a minimum; it has been shown by Judd and Wright [3] that the interlaminar shear strength of composite materials decreases by about 7% for each 1% of voids up to a total void content of 4% and, in addition, other mechanical properties of the material are affected. The presence of voids is more prevalent in composites made by the open mould than by the closed mould techniques (sections 5.2.1 and 5.2.2).

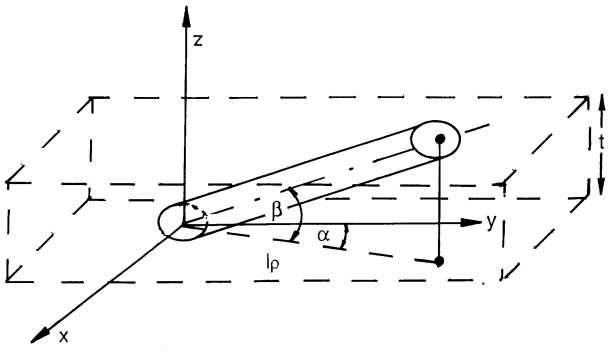

Figure 2.3 Unit element represents a thin slice of material oriented to a predetermined direction.

2.4 Properties of fibres, matrices and composites, elastic properties of continuous unidirectional laminae

2.4.1 Longitudinal stiffness

The stresses at a point in a body are generally represented by stress components acting on the surface of a cube; Figure 2.4 shows the three normal stresses and the three shear stresses. The notation employed in this discussion is such that the first suffix refers to the plane upon which the stress acts and the second suffix is the coordinate direction in which the stress acts; the equivalent strains have the same notation. As laminae are assumed to be sufficiently thin, the through-thickness stresses are zero. Thus $\sigma_{33} = \sigma_{31} = 0$ and plane stress conditions hold.

Figure 2.4 also shows a lamina where the orthotropic layer (see section 3.3) has three mutually perpendicular planes of property symmetry; it is characterized elastically by four independent elastic constants. They are

E_{11}, the modulus of elasticity along the fibre direction;
E_{22}, the modulus of elasticity in the transverse direction;
v_{12}, the strains produced in direction 2 when the specimen is loaded in direction 1;
G_{12}, the longitudinal shear modulus;
v_{21}, the strains produced in direction 1 when the specimen is loaded in direction 2 and is obtained from the equation

$$E_{11}v_{21} = E_{22}v_{12}$$

If the line of action of a tensile or compressive force is applied parallel

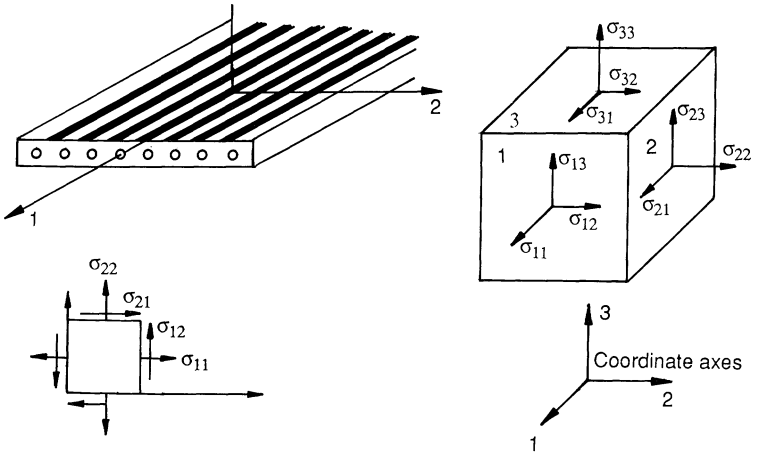

Figure 2.4 Unidirectional fibre composite (orthotropic material).

to the fibres of a unidirectional lamina, the strain in the matrix will be equal to the strain in the fibre, provided the bond between the two components is perfect. As both fibre and matrix behave elastically, then

$$\sigma_f = E_f\varepsilon_f \quad \text{and} \quad \sigma_m = E_m\varepsilon_m, \quad \text{where } \varepsilon_f = \varepsilon_m \tag{2.4}$$

As $E_f > E_m$, the stress in the fibre must be greater than the stress in the matrix and will therefore bear the major part of the applied load.

The compressive load

$$P_c = P_m + P_f \tag{2.5}$$

or

$$\sigma_c A_c = \sigma_m A_m + \sigma_f V_f \tag{2.6}$$

$$\sigma_c = \sigma_m V_m + \sigma_f V_f \tag{2.7}$$

where A is the area of the phase, V is the volume fraction of the phase with $V_c = 1$. As the bond is perfect

$$\varepsilon_c = \varepsilon_m = \varepsilon_f \tag{2.8}$$

From eq. (2.7)

$$E_c\varepsilon_c = E_m\varepsilon_c V_m + E_f\varepsilon_c V_f \tag{2.9}$$

$$E_c = E_m V_m + E_f V_f \tag{2.10}$$

$$E_c = E_{11} = E_m(1 - V_f) + E_f V_f \tag{2.11}$$

This equation is often referred to as the law of mixtures equation.

2.4.2 Transverse stiffness

The same approach can be used to obtain the transverse modulus of a unidirectional lamina E_{22}. The applied load transverse to the fibres acts equally on the fibre and matrix and therefore

$$\sigma_f = \sigma_m \tag{2.12}$$

$$\varepsilon_f = \sigma_{22}/E_f \quad \text{and} \quad \varepsilon_m = \sigma_{22}/E_m \tag{2.13}$$

$$\varepsilon_{22} = V_f\varepsilon_f + V_m\varepsilon_m \tag{2.14}$$

Substituting eq. (2.13) into eq. (2.14),

$$\varepsilon_{22} = V_t\sigma_{22}/E_f + V_m\sigma_{22}/E_m \tag{2.15}$$

Substituting $\sigma_{22} = E_{22}\varepsilon_{22}$ into eq. (2.15) and rearranging gives

$$E_{22} = E_f E_m/\{E_f(1 - V_f) + E_m V_f\} \tag{2.16}$$

Equation (2.16) produces E_{22} with reasonable agreement when compared

with experimental results. Equation (2.17) has been proposed and takes account of Poisson contraction effects.

$$E_{22} = E'_m E_f / \{E_f(1 - V_f) + V_f E'_m\} \tag{2.17}$$

where $E'_m/(1 - v_m^2)$.

2.4.2.1 Poisson's ratio v_{12}. Figure 2.5 shows an element ABCD under a mean normal stress σ_{11}, Poisson's ratio is given as

$$v_{12} = -\varepsilon_{22}/\varepsilon_{11}$$

ε_{22} is the lateral strain in direction 2 and is a function of two components, the fibre component, $-v_f\varepsilon_{11}$, and the matrix component, $-v_m\varepsilon_{11}$. The lateral displacements in the two directions due to the strains are dependent on the geometry of the fibre and on the cross-sectional form of the element. The assumptions that are made in the following discussion are that the fibre extends over the whole thickness of the element, is of rectangular cross-section and the strain effects in the lamina, in direction 3, are negligible. The lateral displacement of the fibre $= -v_f\varepsilon_{11}(V_f b)$ and the lateral displacement of the matrix $= -v_m\varepsilon_{11}(V_m b)$.

Total lateral displacement in direction 2 equals $[-v_f\varepsilon_{11}(V_f) - v_m\varepsilon_{11}(V_m)]b$, where b is the breadth of the element. The lateral strain in direction $2 = \varepsilon_{22} = -(v_f V_f + v_m V_m)\varepsilon_{11}$. Therefore

$$v_{12} = \frac{\varepsilon_{22}}{\varepsilon_{11}} = -[v_f V_f + v_m V_m] \tag{2.18}$$

Equation (2.18) is approximate but predicts the value of v_{12} with a reasonable degree of accuracy.

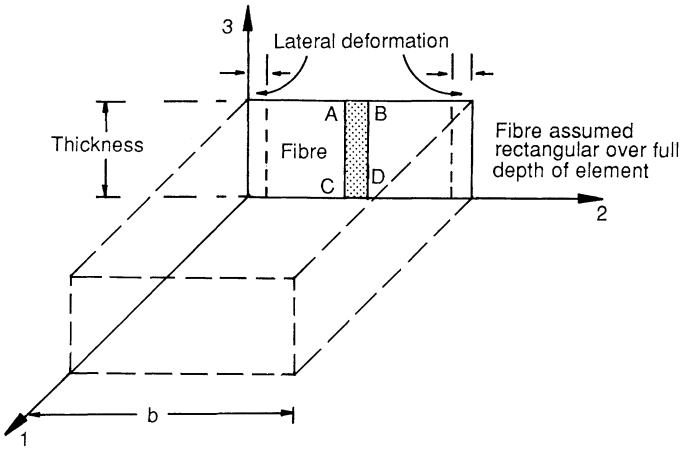

Figure 2.5 Lateral strain in an element under mean normal stress σ_{11}.

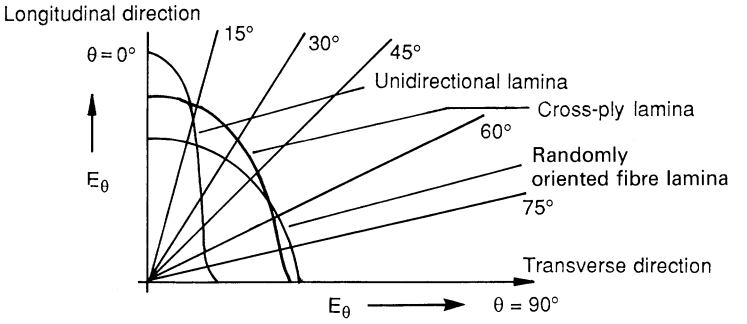

Figure 2.6 The relationship between E_θ and θ between 0 and 90°.

2.4.2.2 The modulus of rigidity G_{12}. The derivation of G_{12} is analogous to that for E_{22}, consequently the full derivation of G_{12} is not given here but it can be shown that

$$G_{12} = (G_f G_m)/(G_m V_f + G_f V_m) \tag{2.19}$$

2.4.2.3 Elastic properties of in-plane random long fibre laminae. Laminae that are manufactured from long randomly orientated fibres in a polymer matrix are macroscopically isotropic in the plane of the lamina; fibre end effects can be neglected when predicting the moduli. The general equation (the proof is given in [4]) relating the modulus of elasticity in directions 1 and 2, the modulus of rigidity G_{12} and the angle θ which defines the direction of the required stiffness is

$$\frac{1}{E_\theta} = (1/E_{11})(\cos^4\theta) + (1/E_{22})(\sin^4\theta) + [(1/G_{12}) - (2\nu_{12}/E_{11})]\cos^2\theta \sin^2\theta \tag{2.20}$$

where E_θ is the modulus of elasticity of the composite at θ to direction 1.

Figure 2.6 shows the relationship between E_θ values when angle θ varies between 0° and 90°. It can be seen that laminae can be made with predetermined fibre orientation distribution so that elastic and other mechanical properties can be designed to meet specific needs.

2.5 Stress and strain distribution around fibre ends of discontinuous fibres

When a composite containing uniaxially aligned discontinuous fibres is stressed in tension parallel to the fibre direction, it is assumed that the fibres terminate at the surface of the laminate or that they are sufficiently long that the effects associated with fibre ends can be neglected. However, as the aspect ratio (l/d) of the fibre becomes progressively smaller, there is a portion at the end of each finite length of fibre where the stress

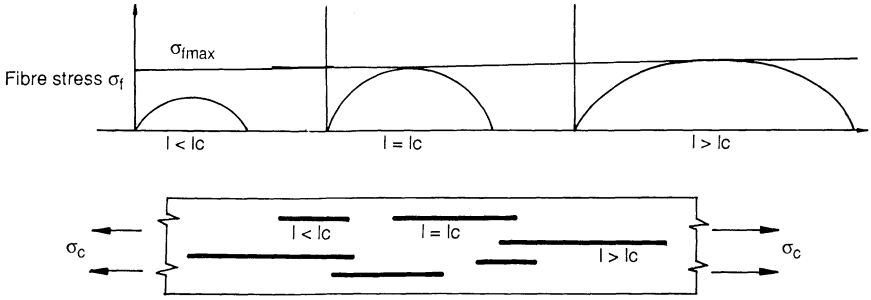

Figure 2.7 Schematic representation of discontinuous fibre/matrix composite.

and strain fields in it and in the adjacent matrix are modified. The efficiency of the fibre to reinforce and stiffen the composite decreases as the fibre length decreases. Consequently, the length of discontinuous fibres plays an important role in the fracture of the composite.

The critical transfer length over which the fibre stress is decreased from σ_{max} to zero (Figure 2.7) is referred to as $\frac{1}{2}l_c$ and a quantity α may be defined as the ratio of the area under the stress distribution curve over the length $\frac{1}{2}l_c$ to the area of the rectangle represented by the product

$$\sigma_{fmax} \times \tfrac{1}{2}l_c$$

The fibre end of length $\frac{1}{2}l_c$ may be considered as supporting a reduced stress α, (σ_{fmax}) or may be reduced to an effective length of $\frac{1}{2}\alpha l_c$ subjected to a stress σ_{fmax}.

Figure 2.8(a) shows a diagrammatic representation of the deformation

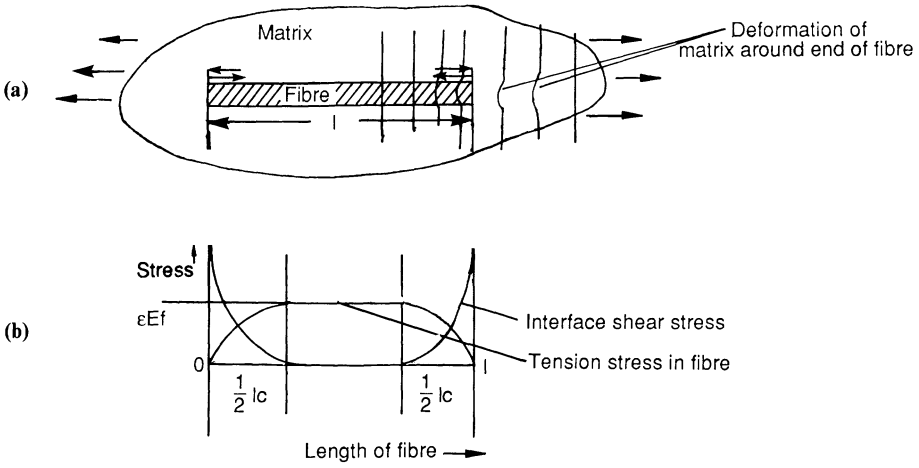

Figure 2.8 (a) A schematic representation of displacement around the tip of a discontinuous fibre. (b) Tensile stress in the fibre and the interface shear stress between the fibre and the matrix.

around a discontinuous isolated fibre embedded in a matrix and subjected to a tensile load parallel to the fibre. The stress applied to the matrix will be transferred to the fibre across the interface; at the fibre ends, the strain in the fibre will be less than in the matrix.

Cox [5] showed that for an applied stress in the resin, the fibre tensile stress parallel to the fibre and the shear stress at the interface between the fibre and matrix are given by

$$\sigma_f = E_f \varepsilon_m \left\{ \frac{1 - \cosh \beta(\frac{1}{2}l - x)}{\cosh \frac{1}{2}\beta l} \right\} \tag{2.21a}$$

$$\tau = E_f \varepsilon_m \left\{ \frac{G_m}{2E_f \ln(R/r)} \right\}^{1/2} \left\{ \frac{\sinh \beta(\frac{1}{2}l - x)}{\cosn \frac{1}{2}\beta l} \right\} \tag{2.21b}$$

$$\beta = \left\{ \frac{2G_m}{E_f r^2 \ln(R/r)} \right\}^{1/2}$$

$2R$ is the interfibre spacing.

A diagrammatic representation of the variation of stress along the fibre is shown in Figure 2.8(b). It can be seen that the tensile stress is zero at the fibre ends and is a maximum at the fibre centre or when the fibre length is equal to the critical length; in this case the stress is a maximum at half critical length. The shear stress is a maximum at the fibre ends and falls to zero at half critical length.

It will be clear that the load transfer between fibre and matrix is dependent on their interface bond. High shear stresses are developed at the ends of the fibres and therefore failure of the composite could be as a result of:

1. shear debonding at the interface;
2. cohesive failure of the matrix;
3. shear yielding of the matrix;
4. cohesive failure of the fibre;
5. the ultimate strength of the fibre being reached.

2.6 Elastic properties of short fibre composite materials

If a unidirectionally aligned fibre array was under the action of a tensile or compressive force, as discussed in section 2.4.1, the law of mixture eq. (2.11) would be modified by the inclusion of a length coefficient factor η. The law of mixture equation becomes

$$E_c = E_{11} = \eta E_f V_f + E_m(1 - V_f) \tag{2.22}$$

Cox derived a value for η as

$$\eta = 1 - (\tanh \tfrac{1}{2}\beta l)/\tfrac{1}{2}\beta l \tag{2.23}$$

where β has been defined in eq. (2.21b).

Halpin [6] expressed the composite longitudinal modulus of elasticity as

$$E_{11} = E_m \frac{1 + \xi\eta V_f}{1 - \eta V_f} \tag{2.24}$$

where

$$\eta = [(E_f/E_m) - 1]/[(E_f/E_m) + \xi] \tag{2.25}$$

$\xi = l/r$; l and r are the length and radius of the fibre, respectively. Equation (2.24) is specific to the Halpin–Tsai general equations [7] which are

$$E_{11} = E_f V_f + E_m(1 - V_f)$$
$$\nu_{12} = \nu_f V_f + \nu_m(1 - V_f) \tag{2.26}$$

and $M/M_m = (1 + \xi\eta V_f)/(1 - \eta V_f)$, $\eta = [(M_f/M_m) - 1]/[(M_f/M_m) + \xi]$, M is the composite property $E_{22}G_{12}$ or ν_{23}, M_f is the fibre property E_f, G_f or ν_f and M_m is the matrix property E_m, G_m or ν_m.

Krenchel [8] has used eq. (2.11) by introducing an orientation efficiency factor η_o to take account of randomly orientated fibres. The modified formula is

$$E_{11} = \eta_o E_f V_f + E_m(1 - V_f) \tag{2.27}$$

where η_o is 1 for a unidirectionally aligned fibre array, 0.5 for a bidirectionally aligned fibre array and 0.375 for a randomly orientated fibre array.

2.7 Polymeric materials

Organic polymers consist primarily of two elements: carbon and hydrogen. The existence of the vast number of carbon compounds that are found in nature or which can be synthesized can be accounted for by the fact that carbon possesses four valencies and has the ability to satisfy any of these valencies by combining with other carbon groups or other groups of atoms having an unsatisfied valency. Polymers are organic materials with very high molecular weight constructed from simpler repeating chemical units under suitable conditions of temperature and catalytic action. When a large number of these small molecular units, which are called monomers, are combined by the chemical polymerization process, long chain molecules are formed and the resulting product is a high polymer; natural materials such as bitumen, rubber and cellulose have this type of structure. There are two main types of polymerization. In the first a material is produced which is known as a thermoplastic polymer; this consists of a series of long-chain polymerized molecules, which are separated and can slide over one another. In the second type, because the chains are cross-linked, a solid material is produced which cannot be softened and which will not flow.

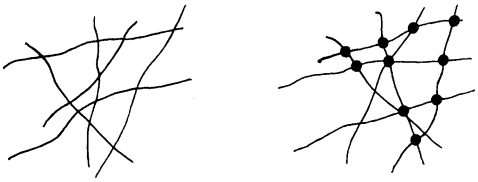

Figure 2.9 Schematic representation of the two mean polymer types. (a) Thermoplastic polymer; (b) thermoset polymer.

Such solids are called thermosetting polymers. These two groups classify polymer materials. Figure 2.9 shows a schematic representation of these polymers.

There are two distinct types of polymerization processes; condensation polymerization which creates by-products during linking of the molecules, usually water, nitrogen or hydrogen gas, and addition polymerization which creates no by-products.

2.7.1 Thermoplastic polymers

In a thermoplastic polymer, the long chain molecules are held together by relatively weak Van der Waals forces but the chemical valency bond along the chain is extremely strong, therefore they derive their strength and stiffness from the inherent properties of the monomer units and the very high molecular weight. These polymers will be either amorphous which implies a random structure with a high concentration of molecular entanglement or they will be crystalline with a high degree of molecular order or alignment. In the amorphous polymer, the random structure will become disentangled during heating and will change the material from a rigid solid to a viscous liquid, whereas heating the crystalline polymer will change it to an amorphous viscous liquid. However, it is difficult to make a polymer which has a pure crystalline structure because of the complex physical nature of the molecular chains, consequently, the so-called 'crystalline' polymers should more correctly be described as semi-crystalline polymers.

2.7.2 Thermosetting polymers

Thermosetting polymers are usually made from liquid or semi-solid precursors which harden irreversibly; this chemical reaction is known as polycondensation, polymerization or curing and on completion, the liquid resin is converted to a hard solid by chemical cross-linking which produces a tightly bound three-dimensional network of polymer chains. The molecular units forming

the network and the length and density of the cross-links of the structure will influence the mechanical properties of the material; the network and length of the units are a function of the chemicals used and the cross-linking is a function of the degree of cure.

The curing procedure is important to enable the optimum properties of the polymer to be achieved. Most thermosets will polymerize at room temperature but it is usual to expose the material to a relatively high temperature for final cure to minimize any further cure and change in properties during its service life.

Shrinkage stresses during the polymerization process, which is an exothermic reaction, and thermal stresses due to differences between the thermal coefficient of expansion of the matrix and fibre may have an effect on the microstresses within a composite material; these stresses are in addition to those developed from the external load. The stresses produced from the shrinkage of the polymer can be sufficient to produce microcracks even in the absence of any external load.

2.7.3 Foamed polymers

Rigid polymer foam is the name generally used to describe the two-phase system of a gas dispersed in a solid polymer. In most cases the polymer represents only a minor portion of the volume of the system but contributes largely to its properties and utility. Foamed polymers are produced by adding a blowing agent to chemical formulations and this causes the material to expand and to increase its original volume many times by the formation of small cells. The properties of foams and the optimum use of these properties is a complicated subject which reflects not only the polymer properties but also the method of manufacture. A complete characterization of the foam structure would require the knowledge of the size and spatial location of the cells with respect to each other but this is difficult to achieve and the subject has not been fully investigated.

Like solid polymers, rigid polymer foams can be thermoplastic or thermosetting materials and they share the advantages and limitations of the solid phase; in addition, the density, cell geometry and gas phase composition can be varied to modify the products. Sections 7.3–7.6 give the various types of foam polymer and their properties.

2.7.4 Elastomers

Another member of the polymer family is the elastomer, the most common of which is rubber. The material consists of long chain molecules which are coiled and twisted in a random manner and the molecular flexibility is such that the material is able to undergo very large deformations. If the material has not been cured by a process known as vulcanization, the elastomer would not recover completely from the large deformations received

under load; this is because the molecules would have moved irreversibly relative to each other. After a curing process, the molecules are cross-linked and, like a thermosetting polymer, they do not slide relative to each other when under load. As the vulcanization process does not change the form of the coiled molecules, but merely prevents them from sliding, the elastomeric material will completely recover the original shape after the removal of a force.

2.7.5 The major thermoplastic resins

There are many thermoplastic polymers available to the engineer, each can be placed into specific groups which have their own specific area of use in the construction industry. The areas of subdivision are:

(a) geotextiles: polypropylene, polyethylene (low, high, ultra-high) density, modacrylics, polyamide (nylons), aramids, polyesters; the first two polymers can be in sheet form and all these polymers can be formed into fibres (geosynthetics [9] is a generic term that encompasses flexible synthetic materials used in geotechnical engineering such as geogrids and geotextiles);
(b) medium technology structural components in conjunction with fibre reinforcement: fibre filled nylons;
(c) high technology structural components in conjunction with fibre reinforcements: fibre reinforced polyethersulphones and polyetheretherketone;
(d) non-load bearing units: PVC, acrylics;
(e) semi-load bearing units: PVC, acrylics.

Sections 5.3 and 5.4 discuss the manufacturing methods for unreinforced and reinforced thermoplastic polymer systems which could be used to manufacture specific components in items (b) and (c). Section 2.8.4 discusses the method of manufacture of the synthetic (thermoplastic) fibres.

2.7.6 The major thermosetting resins

The major thermosetting resin used in the construction industry is the polyester resin, three principal types of which are used as a laminating resin: the orthophthalic type is a general purpose resin, the isophthalic one has superior weathering and chemical resistance properties and the hot acid type is used for flame-retardant purposes. Fillers and pigments may be used in resins, the former principally to improve mechanical properties and the latter for appearance and protective action. Fillers such as aluminium trihydrate may be used to improve flame-retardant characteristics (see sections 6.4.2.5 and 6.9.4), but it is important that the correct amount should be incorporated; if too high a proportion is employed, adverse effects on weathering properties may result. This is only applicable for composites exposed to the weather; for internal applications, where water or chemicals are not in contact with the polymer, it is not affected. Ultraviolet stabilizers (see section 6.4.2.3)

can be incorporated into the resin at the time of fabrication and a gel coat surface coating can be applied to the composite for increased weather protection.

The epoxy resin is another of the thermosetting resins which is utilized in the construction industry, although, in comparison to the polyester resin, it has a limited but very specialized use. The toughness of the epoxies is superior to that of the polyester resins and therefore they will operate at higher temperatures. They have good adhesion to many substrates, low shrinkage during polymerization and are especially resistant to alkali attack. This allows mouldings of high quality, with good dimensional tolerance, to be manufactured.

The most important epoxide resins are oligomers, produced from the reaction of bisphenol A and epichlorohydrin, and they range from medium viscosity liquids through to high melting solids. The different resins are formed by varying the proportions of the two reactions. The mechanical properties of these polymers are given in section 2.9.

2.8 Fibres

Very often it is necessary to increase the stiffness and strength of polymer materials and this is done by the addition of a filler to the resin formulations. The physical form of a filler may range from powders with random shape, flakes or platelets and spheroidal objects to fibres. However, for the maximum contribution to mechanical properties, fibres are normally used.

Inorganic and organic fibres can be used; the glass fibre is the only inorganic fibre that is discussed here; all the other fibres reviewed are organic.

No real material has a strength approaching a small fraction of its theoretical ultimate strength. One reason for this relative weakness is the presence of minute cracks and blemishes on the surface of the solid; stresses are concentrated around the tips of each of the cracks to a level far above the average stress for the object as a whole. At these points, the stresses exceed the strength of the material and the cracks begin to grow, and eventually the whole solid fails by brittle fracture.

As fibres are drawn progressively finer and finer during their manufacturing process, their relative strength begins to increase until at their finest they begin to approach their theoretical value. The reason is that freshly drawn fibres have very smooth surfaces, free from the type of blemish which causes brittle fracture. Consequently the fibres are very much stronger than the predrawn condition. If, however, these fine fibres are handled, their ultimate strength immediately falls and the final value will depend on the degree of handling. It is vitally necessary, therefore, that fibres are not roughly handled prior to placing in the resin if the final composite is to have enhanced properties.

A wide range of amorphous and crystalline materials can be used as the fibre in reinforced polymer composites; these include glass and carbon. The process of making a fibre is one involving axial alignment of molecules of the material; the high tensile strength is associated with improved intermolecular attraction resulting from this alignment.

A relatively new and potentially important class of fibre is based on the high strength and stiffness that is possible in fully aligned polymers. Probably the most important commercial organic fibre currently has been developed by the Du Pont Company with the trade name Kevlar (see section 2.8.3). Other organic fibres are made from polymers whose chemical composition and geometry are basically crystalline and whose intermolecular forces are strong. As the extensibility of the material has already been utilized in the process of manufacture, fibres have a low elongation.

The following sections discuss the manufacturing techniques and the make-up of specific fibres which are used to enhance polymers.

2.8.1 Glass fibres

Glass is the common name given to a number of mutually soluble oxides which can be cooled below their true melting point without crystallization taking place. They are clear, amorphous solids and fail with typical conchoidal fracture surfaces.

The main chemical composition of the most important grades of glass used in commercial production is shown in Table 2.1 [10] and the main oxide is silica in the form of silica sand; the other oxides such as calcium, sodium and aluminium are incorporated to reduce the melting temperature and impede crystallization.

The most important grades of glass are:

1. E-glass, low-alkali content, is the most common glass fibre on the market and is the major one used in the construction industry. However, it was not until the advent of polyester resin in 1942 that this glass was used successfully and it is now widely used with polyester and epoxy resins.
2. S-glass, a stronger and stiffer fibre than E-glass, was originally developed for military applications.

Table 2.1 The chemical composition of E-glass and S-glass (after Phillips [10])

	Oxides used				
	CaO	Al_2O_3	MgO	B_2O_3	SiO_2
For E-glass	17.5	14.0	4.5	10.0	54.0
For S-glass	—	25.0	10.0	—	65.0

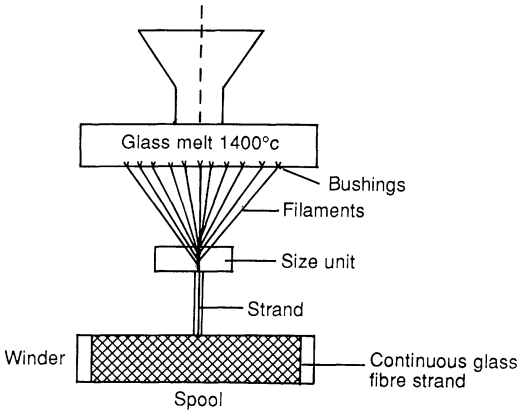

Figure 2.10 Schematic representation of the manufacture of glass fibre.

3. R-glass, a civil version of the S-glass fibre, is used for high technology applications.
4. C-glass, a fibre use for chemical resistance, mainly against acid attack.
5. Cemfil, a fibre used for resisting alkali attack in Portland cement.

Glass fibres are manufactured by continuous and rapid drawing from the melt into very fine filaments; these range from 3 to 24 μm in commercial production. Figure 2.10 illustrates schematically the manufacturing procedure. At the base of the electrically heated furnace, the molten glass passes into electrically heated platinum alloy nozzles called spinnerets and as the molten glass gathers at the spinneret, the filaments are draw by hand into a thread which is wound onto a rotating drum. On emerging from the spinnerets, 200 of the individual filaments are drawn together into a strand; the filaments are treated with a size which binds the filaments before they are wound onto the drum. Further strands may be brought together to form an untwisted bundle of fibres called rovings.

The size has four main functions:

1. to facilitate the manufacturing technique;
2. to reduce the abrasive effect of the filaments against one another;
3. to reduce damage to the fibres during mechanical handling;
4. to provide a chemical link between the glass fibre and the polymer.

The strands and the rovings can be woven into a variety of cloths, which have been virtually standardized, and rovings may be chopped into strands or into strand mats which form random arrays of fibres; the latter system is held together by a size. The strands can be made into thin random veils (also known as surface tissue mats) which are used to produce resin-rich surfaces for composite structural units.

There are five forms in which glass fibre strands may be used to reinforce thermosetting polymers, namely:

1. chopped fibres;
2. chopped strand;
3. chopped strand mats;
4. woven fabrics;
5. surface tissue.

(a) *Chopped fibres* may be divided into three groups, these are milled fibres, short fibres and long fibres. The first group are finely ground fibres of lengths varying between 30 and 3000 μm with aspect ratios of about 30; these fibres are utilized in the injection moulding process. Short chopped fibres have lengths up to about 6 mm and aspect ratio of about 800 and the long chopped fibres have lengths of about 50 mm. The fibre lengths for the DMC and the SMC processes (see section 5.2.2.1) would be about 3 mm and 12 mm long, respectively, and the lengths for the spray-up technique would be about 50 mm long.

(b) *Chopped strand mats* are manufactured from chopped strands which are bonded together in a random two-dimensional manner with a resinous binder which must be compatible with the laminating resin; binders are chosen according to the application. The strands are normally 50 mm in length. This type of reinforcement is considerably cheaper than woven fabric when measured on a weight basis and would be used as a reinforcing material in a laminate either by itself or in conjunction with a woven fabric except when high strength and stiffness are required, in which case it would probably be replaced by glass cloth.

(c) *Woven rovings* are used in mouldings and laminates to produce high directional strength characteristics. Unidirectional roving cloths have great strength in the direction of the fibre. Bidirectional roving cloth laminates have directional strength and stiffness in the direction of the reinforcement. It is difficult to produce a woven roving laminate with a good surface finish and the interlaminar cohesion between layers is not good.

(d) *Woven fabrics* are produced in cloth form similar to that used in the textile industry. The thinner cloths produce laminates of high tensile strength but lower interlaminar cohesion and on a weight basis are more expensive to use than the heavier fabrics.

(e) *Surface tissues* are thin glass fibre mats bonded with a readily wetted medium. They are used when a resin rich surface is required or when the coarse fibre pattern of the load bearing laminate is to be concealed. The mechanical properties of glass fibres are given in section 2.10, Table 2.4.

2.8.2 Carbon fibres

Carbon fibres are manufactured by controlled pyrolysis and cyclization of certain organic fibre precursors, the most common of which is the precursor polyacrylonitrile (PAN) and precursor mesophase pitch (MPP);

the first is a synthetic fibre and the second is produced from the destructive distillation of coal.

The processing steps involved in the fabrication of carbon fibre are shown in Figure 2.11(a). The process consists of a sequence of procedures: stabilization, carbonization, graphitization and surface treatment. In the first step of the PAN fibre fabrication (i.e. stabilization), a polyacrylonitrile (PAN) copolymer filament tow is stretched and passed through a low temperature oxidation furnace to achieve dimensional stability. This is sometimes called the infusible step. In the subsequent step of carbonization, polymer backbones are converted at higher temperature (800°C under an inert atmosphere) into ribbons of continuous carbon hexagonal rings. During the heating period, most elements other than carbon are removed and carbon crystallites are preferably orientated along the fibre length. In the successive heat treatment at higher temperatures above 2000°C (graphitization), the size of the carbon crystallites increases and the orientation of the fibre crystallites improves. Finally, the fibre passes through the surface treatment chamber to promote fibre adhesion. The processing steps for the pitch-based fibre are similar, except for the initial step in which fibre is melt spun from processed isotropic or anisotropic pitches as shown on the lower left corner of Figure 2.11(a). The crystallite size, crystal

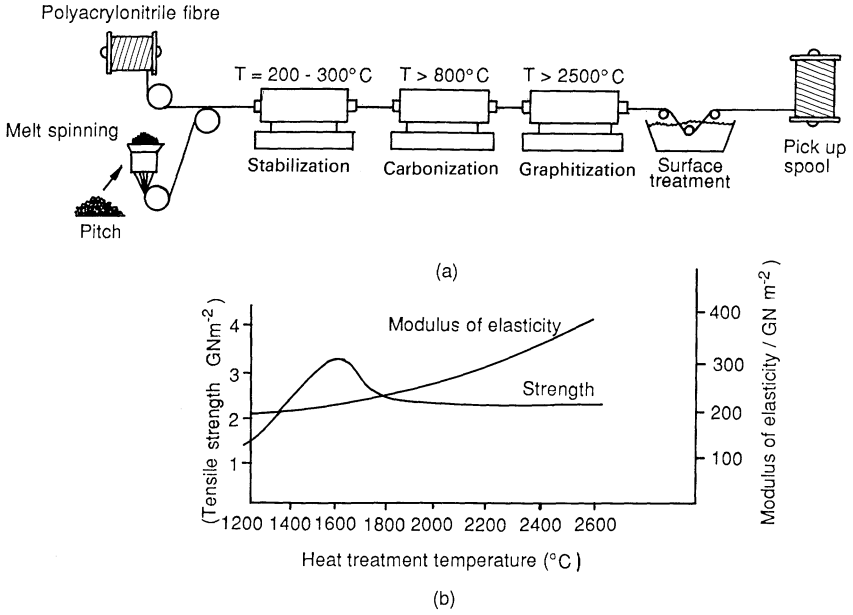

Figure 2.11 (a) Manufacturing process of carbon fibre. Precursors of carbon fibre are either polyacrylonitrile fibre or melt spinning of pitch. (b) Heat treatment temperature versus tensile strength and modulus of elasticity.

orientation, fibre porosity and impurity are major factors affecting the final physical properties of the filament.

The mechanical properties of the fibres and the effect of temperature on them is discussed in section 2.10 and the properties are given in Table 2.4.

Carbon fibre filaments are typically between 5 and 8 μm in diameter and are combined into tows containing 5000 and 12 000 filaments. These tows can be twisted into yarns and woven into fabrics similar to that for glass fibre described in section 2.8.1. Hybrid fabrics containing glass and carbon fibres are also commercially available.

As the heat treatment to the carbon fibre increases, the modulus of elasticity rises exponentially throughout the temperature range as shown in Figure 2.11(b); the reason for this is that the crystallinity of the fibre increases and consequently the amorphousness decreases. On the other hand, tensile strength increases in value to a maximum at about 1600°C and then falls to a constant value as the temperature rises to the greatest value used. Three distinct types of carbon fibre have been identified from the heat treatment temperatures, these are:

1. Type 1 is the stiffest carbon fibre and requires the greatest heat treatment temperature.
2. Type 2 is the strongest carbon fibre and has been carbonized at the temperature that gives the greatest tensile strength.
3. Type 3 is the cheapest carbon fibre; the stiffness is lower than the previous types but the strength is good. This type has the lowest heat treatment temperature.

Although currently carbon fibres tend to be used mainly for aerospace and space applications, they are being considered for use in the construction industry. A high modulus (HM20) carbon fibre manufactured from a newly developed liquid crystal petroleum pitch by Petoca in Japan has modulus of elasticity and strength values of 200 GPa and 2000 MPa, respectively; its cost is comparable to that for glass fibre. These may be used in conjunction with either a polymer or a cement matrix.

2.8.3 Aramid fibres

Aramid fibres are organic, man-made fibres which have a high degree of crystallinity; they have found applications in the field of composites. The molecular chains are aligned and made rigid by means of aromatic rings linked by hydrogen bridges. This combination explains their very high strength and their chemical structure is indicated in Figure 2.12. Two grades of stiffness are generally available; one has a modulus of elasticity in the range of 60 GPa and the other has a modulus of elasticity of 130 GPa. The higher modulus fibre is the one that is used in polymer composites.

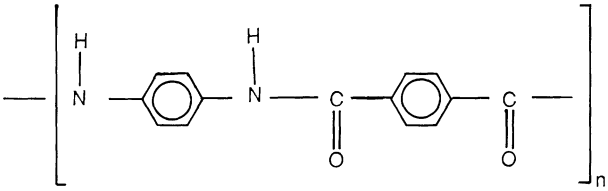

Figure 2.12 Schematic diagram showing a combination of rigid benzene rings para-linked with hydrogen bonds in the transverse direction.

The fibre is typically produced by an extrusion and spinning process. A solution of the polymer in a suitable solvent at a temperature of between −50°C and −80°C is extruded into a hot cylinder which is at 200°C; this causes the solvent to evaporate and the resulting fibre is wound onto a bobbin. The fibre then undergoes a stretching and drawing process to increase its strength and stiffness properties.

There are various types of Aramid fibres on the market including Kevlar® aramid which is produced in several versions by Du Pont in the USA and Northern Ireland, Twaron which is made by Enka in The Netherlands and Technora which is manufactured by Teijin in Japan. The mechanical properties of Aramid fibres are given in section 2.10, Table 2.4.

2.8.4 Synthetic fibres

Synthetic fibres are manufactured from certain thermoplastic polymers; the most important ones are the polyolefins (polypropylene and polyethylene), polyamide (nylon) and polyester. The polyolefins are used in the production of cement/mortar composites but this family, together with the other two types, are also used in geosynthetics; the application of these materials is briefly discussed in sections 2.7.5 and 2.7.6.

It is possible to chemically, mechanically and physically engineer synthetic fibres to achieve the particular requirements for geotechnical engineering applications. Natural fibres such as cotton and jute and the majority of the regenerated fibres such as cellulose and rayon are seldom used to make geotextiles because they are biodegradable. However, these latter fibres may be used in temporary situations where biodegradation is desirable.

The manufacture of synthetic fibres, which is shown schematically in Figure 2.13a, involves many stages from the transfer of the raw polymer from a solid to a liquid form through to the extension and the drawing process. There are two methods available to change the solid polymer into a liquid form; the polymer may be dissolved in solution or it may be heated until it becomes molten. Polymers such as acrylic, modacrylic, aramid and vinyl polymers utilize the former process whereas the polyester polymers are changed to the liquid form by the utilization of the second

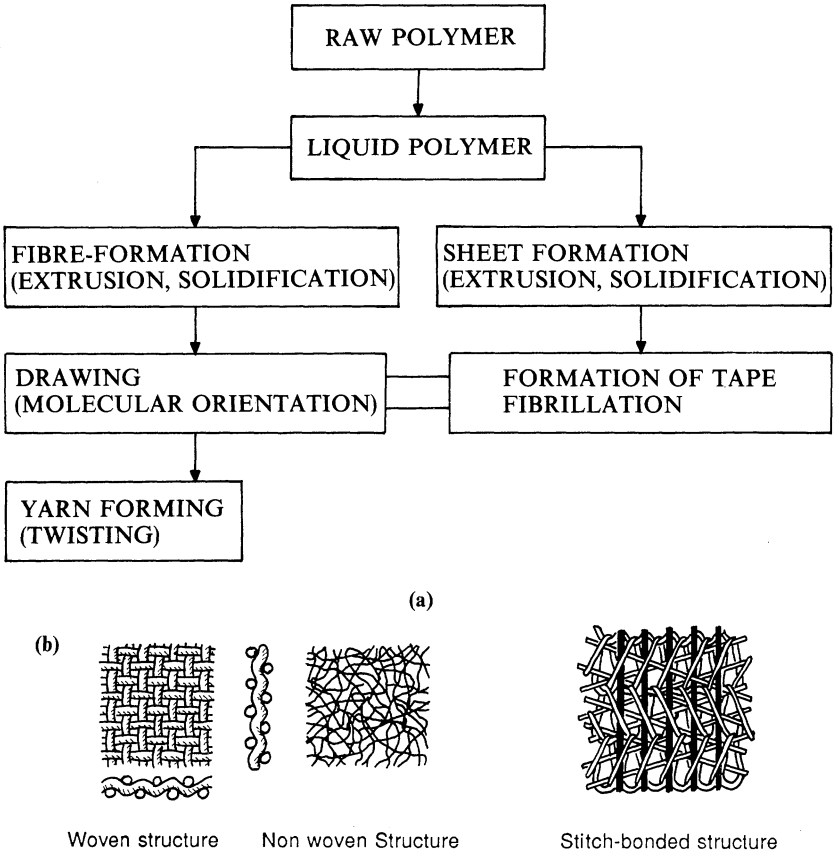

Figure 2.13 (a) Manufacture of synthetic fibres. (b) Typical geotextile constructions.

method. A multi-hole spinneret is used to convert the polymer into filaments and these are then stretched in the direction of their longitudinal axes, to increase the orientation of the molecular chain within the filament structure. This latter process improves the stress–strain characteristics of the fibre (see Table 2.5). From the above manufacturing techniques seven different types of synthetic fibres or yarns may be produced. These are: monofilament fibres; heterofilament fibres; multifilament yarns; staple fibres; staple yarns; split-film tapes; fibrillated yarns.

Much of the engineering interest in the use of synthetic fibres lies in the field of reinforced soils with the possibilities presented by geotextiles. These systems possess a number of intrinsic characteristics that make them ideal for soil reinforcement applications. They are composed of highly stable and durable thermoplastic polymers (the polyolefins and the high modulus polyester fibres) which are engineered during manufacture to

provide the required mechanical properties (i.e. tensile strength and extension) and form; the latter provides specific geometric shapes which optimize the 'bond' characteristics between the geotextile and the adjacent soil.

Geotextiles can be divided into two categories:

(a) conventional geotextiles which include woven, non-woven, knitted and stitched-bonded geotextiles; these are shown in Figure 2.13(b);
(b) special geotextiles which are of non-textile origin and include geostrips, geogrids, geobars and geocomposite materials; these are illustrated in Figures 5.10(b) and 5.10(c) and their uses are given in Figure 6.3.

The non-woven geotextiles consist of a random arrangement of fibres bonded together by heat (melt bonded) or by physical entanglement (needle punch). The fibres can be in the form of either staple (short lengths) or continuous filaments.

The woven geotextiles consist of orthogonally arranged fibres in various configurations. The monofilament wovens are manufactured from fibres with circular or elliptical cross-section and the multifilament (and fibrillated tape) wovens are made by gathering fibres into parallel arrays arranged orthogonally. The knitted geotextiles consist of fibres that are interlooped and stitch-bonded geotextiles are manufactured by stitching together fibrous yarns.

The manufacturing processes for the special geotextile such as the geogrids and geostrips are discussed in section 5.3.5. The geocomposites are manufactured by placing high strength fibres within a polymer sheet, the former component providing the tensile property and the latter component the geometrical shape and protective medium for the fibre. A range of values for some representative properties of geotextiles is given in Table 2.6.

2.8.5 Prestressing fibres

There are two polymer-based fibres and one inorganic fibre material that are suitable for use as prestressing tendons for concrete; these materials are possible replacements for the high tensile strength steels. These are glass, aramid and carbon fibres. The first two fibre types have been utilized as prestressing tendons whereas the latter fibre is available but no actual applications are known.

The three commercial systems all utilize parallel filaments but they differ in construction techniques. 'Polystal' is a pultrusion of glass fibre in a resin material (see section 5.2.2.3); 'Parafil' is a rope that derives its strength from aramid yarns; 'Arapree' is a pultrusion of aramid fibres.

1. *Polystal* is produced by Bayer AG in association with Strabag AG in Germany and has been available since 1978. The tendon consists of bundles of bars or rods, each containing E-glass filament fibres in an unsaturated polyester resin. Each bar is typically 7.5 mm in diameter and has

a fibre volume fraction of 68%; 19 of these bars are incorporated into a tendon which has a working load capacity of 600 kN. After prestressing, the tendon is grouted into the duct, using a resin-based mortar. The modulus of elasticity of the Polystal bars is 51 GPa and has a linear stress–strain characteristic to failure at 1520 MPa; the strain at failure is 3.3%. It is necessary to be aware that glass does suffer from stress ageing where cracks develop at surface flaws and propagate through the thickness. Long-term tests are being undertaken on Polystal to investigate this problem.

2. *Parafil* is a rope that contains a core of unidirectionally aligned fibre encapsulated in a polymer sheath. Polyester, Kevlar 29 and Kevlar 49 fibres are frequently used in rope form and are known as Type A, Type F and Type G, respectively; the most suitable rope for use as prestressing tendons is Type G. All three types possess the basic properties of high strength high modulus and low residual creep; Table 2.2 gives a comparison of the properties of Parafil cables and a prestressing strand. These basic properties, along with corrosive resistance and ease of handling, suggest that the cables could be used in a hostile environment, especially in the construction of ground anchors, where the potential for corrosion can be a major problem with steel tendons. The replacement of the steel tendon with Parafil cables might be a desirable option.

The ropes have been used as prestressing tendons in prestressed concrete. Tests have allowed engineers to predict that a Parafil rope will sustain a load of 50% of the short-term ultimate strength for 100 years [12], and applying a material factor of 1.5 to this load level gives a permanent sustainable working stress of about 650 MPa.

3. *Arapree* is a prestressing tendon consisting of aramid filaments embedded in epoxy resin and is manufactured by the pultrusion technique (section 5.2.2.3), using the aramid fibre Twaron (section 2.8.3). The tendon was developed by AKZO in association with Hollandsche Beton Group (HBG).

Table 2.2 Comparison of properties of Parafil cables and prestressing strand

Material	Parafil cable type A	Parafil cable type F	Parafil cable type G	Prestressing steel low relaxation
Ultimate tensile strength (GPa)	0.62	1.93	1.93	1.49
Modulus of elasticity (GPa)	12	77.5	126.5	200
Relaxation losses (% of initial load)	14 after 144 h	22 after 1000 h	8 after 1000 h	1.1 after 1000 h
Creep strain (%)	0.50 after 1000 h	0.23 after 1000 h	0.12 after 1000 h	0.056 on diameter of 1.56 mm

Typical strip-like tendons are available in 20 mm wide, 1.5 mm thick sections; these tendons have tensile strengths of 34 kN.

An effective and economic long-term use of these aramid/epoxy tendons for reinforcement and prestressing may be expected where:

- concrete is exposed to aggressive atmospheric attack;
- chlorides are present (sea water/de-icing salts);
- use of calcium chloride in the concrete matrix can increase productivity;
- thin and light elements are required;
- large deformation capacity is required (impact, explosions, earthquakes) high fatigue requirements are to be met;
- electromagnetic currents are to be prevented.

For practical use as a prestressing tendon in concrete structures, the following long-term aspects must be considered:

- creep/relaxation behaviour (see section 2.9.1);
- behaviour in different environments (e.g. alkaline and carbonated);
- stress rupture/stress corrosion behaviour;
- residual strength under sustained loading;
- fatigue data and fatigue on bond.

2.9 Mechanical properties of polymers

Unreinforced polymers exhibit relatively poor mechanical behaviour when under load. The properties of the cured resins can be determined from

Table 2.3 Comparison of some of the most important mechanical properties of unreinforced polymers with traditional structural materials

Material properties	Specific weight	Ultimate tensile strength (MPa)	Modulus of elasticity in tension (GPa)	Coefficient of linear expansion (10^{-6}/°C)
Thermosetting				
Polyester	1.28	45–90	2.5–4.0	100–110
Epoxy	1.30	90–110	3.0–7.0	45–65
Phenolic (with filler)	1.5–1.75	45–59	5.5–8.3	30–45
Thermoplastic				
PVC	1.37	58.0	2.4–2.8	50
ABS	1.05	17–62	0.69–2.82	60–130
Nylon	1.13–1.15	48–83	1.03–2.76	80–150
Mild steel	7.8	370–700	210	12–13
Aluminium	2.8	450	70	23
Timber (Douglas Fir)	0.5	74	10	4

specimens prepared by casting the uncured polymer into moulds. Table 2.3 compares the most important mechanical properties of some unreinforced thermoplastic and thermosetting polymers with traditional structural materials, the properties of the polymers, however, are subjected to wide variations depending upon the chemical system used and the cure conditions. It is seen that the magnitudes of most properties of polymers are of similar value to those of timber apart from the modulus of elasticity which is about one-third that of timber. The thermosetting polymer is usually isotropic and unlike the thermoplastic polymer, it does not melt on heating but it does lose its stiffness property at the heat distortion temperature; this defines an effective upper limit for its use in structural components. Polyester resins are generally inferior to epoxy resins regarding strength and elastic properties; the latter resins have a much lower shrinkage on curing and a lower coefficient of thermal expansion than the former; the strength of the interface bond between resin and fibre is greater in the case of epoxy resin. However, there are disadvantages in using epoxy resins compared with polyester. The former has higher viscosity before curing and is more expensive.

The thermosetting polymers are generally regarded as brittle materials, however, this statement does require qualification. The characteristic of the polymer is generally investigated by a tensile test which is performed on a uniaxial specimen. The failure stress will be of the order of 60 MPa at a strain of 2.0% and failure will appear to be a brittle one with no sign of yielding. If, however, a compressive uniaxial test is performed, the failure stress will be of the order of 120 MPa and there will be considerable yielding of the material. The tensile failure of the specimen is associated with flaws in the material which give the appearance of a brittle failure

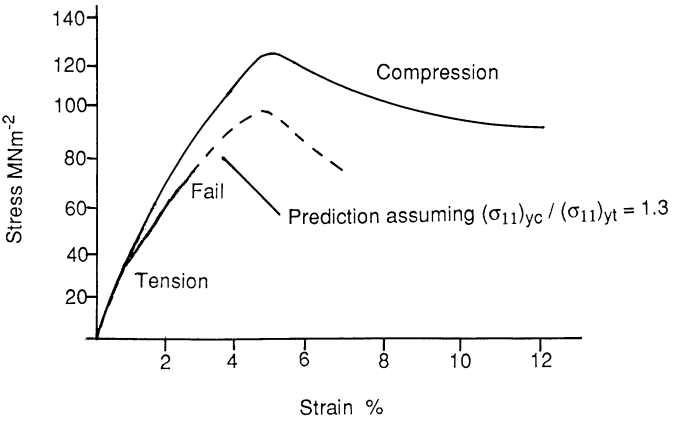

Figure 2.14 Typical stress–strain relationship for general purpose polyester resin.

whereas the compressive failure allows plastic deformation to occur in the polymer. The failure theory of polymers is discussed in section 3.7.

Figure 2.14 shows a typical stress–strain curve for a general purpose polyester resin tested in tension and compression; the broken line is predicted by assuming $(\sigma_{11})_{yc}/(\sigma_{11})_{yt}$ is equal to 1.3. The graph shows a non-linear relationship and this is a function of the viscoelastic nature of the material. If a constant load is allowed to remain on a polymer specimen for a length of time the material will creep; this characteristic is discussed in the following section.

2.9.1 Creep deformation and rupture

In classical elasticity, the form of the relationship between stresses and deformation is independent of the magnitude and the rate of the deformation. The true relationship between stress and deformation is, however, dependent on the properties of the material and other parameters such as temperature, humidity, etc.

Polymers are the largest class of materials whose mechanical properties have characteristics of both elastic solids and viscous fluids and hence they are classified as viscoelastic materials. The most important characteristics of this class of material are its history, the nature of the applied load, the dependence of the mechanical measurements on the rate at which these measurements are made and the temperature and moisture environment. The creep characteristic of a polymer composite is also dependent on the direction of alignment, the type and the volume fraction of the fibres. It should be mentioned here that there is a second mechanism that contributes to the creep properties of polymeric composites and that is the time dependent nature of the micro-damage in composite materials subject to stress.

Under short-term low applied stress levels, the properties of polymers and polymer composites are assumed to behave elasticity; however, polymers in construction will generally be subjected to long-term and moderately high load levels. This section, therefore, concentrates on the long-term deformational characteristic of polymer composites.

The relationship between stress and strain may be represented by the equation

$$\sigma = E\varepsilon \tag{2.28}$$

where E is the stiffness of the material. (It must be said that this relationship is highly idealized even for pure materials.) Equation (2.28) can be modelled as a linear spring.

The creep of a viscoelastic material, of which the polymer is one example (a definition of this term is given in the glossary) is a function of the viscous fluid characteristic of the material and the relationship between

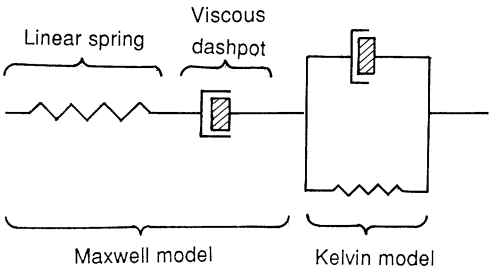

Figure 2.15 Standard linear solid model.

the stress and rate of strain. This relationship can be represented by the equation

$$\sigma = \eta \frac{d\varepsilon}{dt} = \eta \dot{\varepsilon} \tag{2.29}$$

where η is the viscosity of the fluid. Equation (2.29) can be modelled as a linear dashpot.

Early models were developed to represent the creep characteristics of viscoelastic materials and the simplest of these mechanical analogues is the standard linear solid model shown in Figure 2.15. This model consists of the Maxwell model joined in series with the Kelvin model; these two models are a series and a parallel combination of a linear spring and viscous dashpot, respectively.

Polymers will behave in a linear viscoelastic manner when the applied stress levels are low; this implies that the strain in the material is directly proportional to the stress at any instant of loading, and this condition is represented by the equation

$$\varepsilon = f(t)\sigma \tag{2.30}$$

where $f(t)$ is the creep compliance of the material. This condition also implies that the principle of superposition can be invoked for changes in applied stresses which, in the design of structural materials, may be subjected to a complex case history.

Consider that, in a creep experiment, a polymer material is subjected to a stress at time zero (t_0), the strain after time (t_1) will be given by

$$\varepsilon(t_1) = f(t_1)\sigma_0 \tag{2.31}$$

If at time t_1 a stress σ_1 is added to the system, then for a linear viscoelastic material, the strain at time t_2 will be

$$\varepsilon(t_2) = f(t_2)\sigma_0 + f(t_2 - t_1)\sigma_1 \tag{2.32}$$

and the final strain is a linear superposition of the two separate strains

acting independently; this is an example of the Boltzmann's principle of superposition [13].

The equation can be generalized to

$$\varepsilon(t) = \sum_{t_i=-\infty}^{t_i=t} f(t-t_1)\sigma_1 \tag{2.33}$$

and for a continuous loading cycle, the equation may be written as

$$\varepsilon(t) = \int_{-\infty}^{t} f(t-\tau)\frac{d\sigma}{d\tau}d\tau \tag{2.34}$$

An analogous expression can be written for stress, with strain as the independent variable in stress relaxation problems. The analogous equations are

$$\sigma_{(t_1)} = \sum_{t_i=-\infty}^{t_i=t} G(t-t_i)\varepsilon_1$$

$$\sigma_{(t)} = \int_{-\infty}^{t} G(t-\tau)\frac{d\varepsilon}{d\tau}d\tau \tag{2.35}$$

If the level of applied stress is high, the viscoelastic behaviour of the polymer can become highly non-linear. In this case, the creep compliance is a function of both the stress and the time and consequently eq. (2.30) then becomes

$$\varepsilon = f(t_1\sigma) \tag{2.36}$$

Superposition rules can be used to solve for non-linearity under certain limiting conditions. The simplest method is to separate the time and stress functions of the creep compliance and the superposition integral is then modified to form a linear integral which is given by

$$\varepsilon = f(t)g(\sigma)$$

$$\varepsilon = \int_{-\infty}^{t} f(t-\tau)\frac{dg(\sigma)}{d\tau}d\tau \tag{2.37}$$

In addition to the stress level, the creep behaviour for composites is further compounded by the influence of temperature which also has a detrimental effect on polymer strength. Indeed, such is the complexity of modelling creep that the most favoured approach is to develop a law based on data from experimental work. Obtained empirically, one of the most widely applied laws for creep is Findley's power law given in its most general form by

$$\varepsilon = \varepsilon_0 + m(t/t_0)^n \tag{2.38}$$

where ε is the time dependent creep strain, ε_0 and m are functions of

stress, t is the time duration, t_0 is a constant and n is independent of stress.

By representing the parameters and m by hyperbolic functions [14], the creep expression becomes

$$\varepsilon = \varepsilon'_0 \sinh(\sigma/\sigma_0) + \varepsilon_t(t/t_0)^n \sinh(\sigma/\sigma_t) \tag{2.39}$$

which may be further refined to

$$\varepsilon = \varepsilon'_0(\sigma + \sigma_0) + \varepsilon_t(t/t_0)^n(\sigma/\sigma_t) \tag{2.40}$$

where ε'_0, ε_t, σ_0 and σ_t are material constants that can be written as

$$\varepsilon = \sigma(1/E_0 + t^n/E_t) \tag{2.41}$$

$E_0 = \sigma_0/\varepsilon_0$ is the initial elastic modulus independent of time and $E_t = \sigma_t/\varepsilon_t = \sigma/m$ is the modulus that characterizes the time dependent behaviour. From this a viscoelastic modulus can be obtained given by

$$E_v = E_0E_t/(E_t + E_0^n) \tag{2.42}$$

If during an experimental set-up there is a constant applied load, $\varepsilon_0 = \varepsilon'_0$, and the initial stress is equal to the applied stress, the value of the viscoelastic modulus can be determined directly.

2.9.2 Time dependent behaviour: long-term tests

The two methods used for the evaluation of time dependent behaviour of polymers are stress relaxation and creep.

Stress relaxation is the decay in stress with time when the material is under a constant strain condition. To measure this parameter when the material is under a tensile stress relaxation experiment, the load that is required to maintain the constant strain is divided by the original cross-sectional area of the specimen to obtain the stress value. The secant modulus of the material within its limit of proportionality is then obtained by dividing the stress by the fixed strain. A curve of the secant modulus is obtained as a function of time. To obtain a time dependent yield strain, the yield stress is obtained as a function of time on the basis of the original cross-sectional area.

In the creep method, the strain is measured as a function of time for a constant value of stress applied to the material and the creep data may be presented in a variety of ways. A recommended way is to produce a set of creep curves in which the strains are measured at constant stress levels and plotted as a function of time (isostress creep curves), usually by $\log t$, due to the long-term tests. An alternative method of presenting the data is to provide isochronous stress–strain curves. BS 4618 [15] (there is no ISO equivalence) recommends a procedure for cross-plotting from the creep curves at constant times and this yields a family of stress–strain curves, each relevant to a particular time of loading. In this standard,

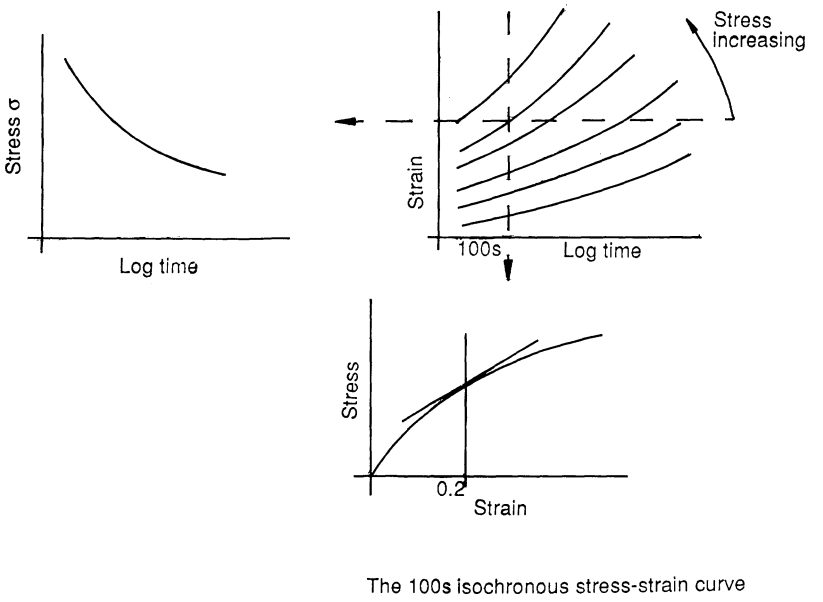

Figure 2.16 Creep curves: isochronous stress–strain curve (derived from BS 4618 [2]).

constant load tests are carried out under controlled conditions for the following durations: 60 s, 100 s, 1 h, 2 h, 100 h, 1000 h, 1 year, 10 years and 80 years. A family of creep curves for any material may be obtained by varying the stress as shown in Figure 2.16. From these curves, isochronous stress–strain curves may be drawn, each corresponding to a specific loading duration. Thus, a 100 s isochronous stress–strain curve implies that the total strain at the end of 100 s has been plotted against the corresponding stress level, and it will be seen that the slope of this curve is not constant. Consequently, it is necessary to specify at which point in the curve the slope has been determined, and this slope is then defined as the creep modulus.

Isometric stress–time curves (isostrain creep curves) are obtained by cross-plotting from the creep curves at constant strains, as shown in Figure 2.16. Creep information in this form may be required in design calculations where strain is the limiting criteria. From these curves, it is possible to read directly the constant stress value which produces a given strain at the end of a specified time. A simpler form of these curves, the stress–rupture (creep–rupture) curve, is more commonly used to predict the expected lifetime of load-carrying elements. The stress–rupture curves represent the time-to-rupture (failure) of the material when loaded at different stress levels. It is seen from Figure 2.17, which shows the stress–rupture characteristics of glass fibre reinforced polymers (GFRP) (a similar form of graph exists for a pure polymer), that the rupture stress value decreases with time under a constant stress condition. The long-term strength properties

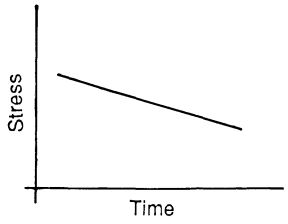

Figure 2.17 Stress rupture characteristics for GFRP.

of GRP under load may be specified by using the relevant graphs associated with stress/rupture/time relationships.

Creep coefficients can be determined by linearizing the isostress–creep curves into strain versus log time axes. When plotted in this manner, most polymeric materials approximate to a linear relationship. The equation for the total strain of the material becomes

$$\varepsilon_{(t)} = \beta \log t + \varepsilon_0 \quad t > 0 \tag{2.43}$$

where $\varepsilon_{(t)}$ is the total extension in the material after time period t, ε_0 is the strain value at unit time and β is the creep coefficient (creep rate parameter) $= d\varepsilon_{(t)}/dt$.

The graph of this equation is shown in Figure 2.18. The creep coefficient is dependent on the level of stress applied to the material and is a measure of its rate of creep. It provides a convenient means of comparing the rate of creep of different polymeric materials. Figure 2.19 shows that β increases for increase in applied stress and is typical for all polymers. It

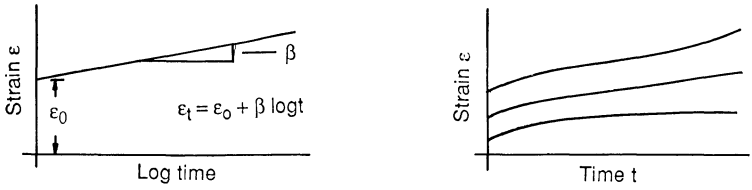

Figure 2.18 Isostress creep curve.

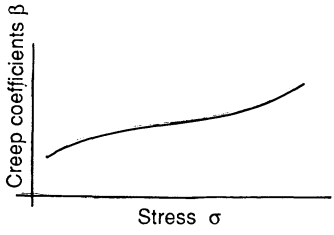

Figure 2.19 Typical relationship between creep coefficient and stress.

should be emphasized that the manufacturing techniques of polymers can significantly alter the rate of creep of a particular polymer. In addition, this expression has the disadvantage that at time zero, the strain would be minus infinity, but it can be used at all practical time values (say from 1 s).

A stress/strain ratio may be defined at any point in the above three graphs, and in the linear case where $\sigma/\varepsilon = 1/f(t)$ (eq. (2.30)), the ratio is known as the creep modulus; this quantity will also depend on the stress level to which the material is subjected. Consequently, an alternative relationship to those mentioned above is provided by the creep modulus/time curves which may be obtained from the relationship σ/ε from any one of the above families of curves. The creep modulus/time curves may be presented at either constant stress or constant strain loadings.

To obtain the creep characteristics of polymer and polymer composite materials, long-term tests are generally required. It is possible, however, for data to be taken over a few days or weeks and an extrapolation to be made beyond the test duration via a mathematical equation. If this procedure is adopted, it does imply that the continuous creep process will obey the same law as existed at the commencement of the test. Generally the creep data are modelled by a power law function and when plotted on a logarithmic axes (i.e. log creep strain/log time), they will present a linear graph. This method should yield a confident extrapolated value up to twice the test duration. If a value of creep strain is required in excess of this, a more accurate method should be employed. A sophisticated mathematical model which could represent the complex viscoelastic damage growth does not currently exist and therefore other empirical methods have to be employed.

One successful method is based on the time–temperature superposition principle (TTSP). This technique utilizes the accelerating effect of increased temperature on the creep behaviour of polymers. A single creep equation can model a family of creep curves at different test temperatures. Identical test specimens are placed under the same stress level, but are exposed to different temperatures and the creep compliance data are plotted on a

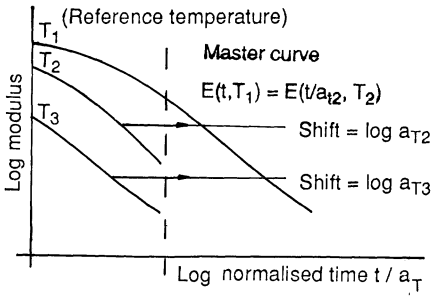

Figure 2.20 Typical schematic graph for extrapolation procedure for TTSP.

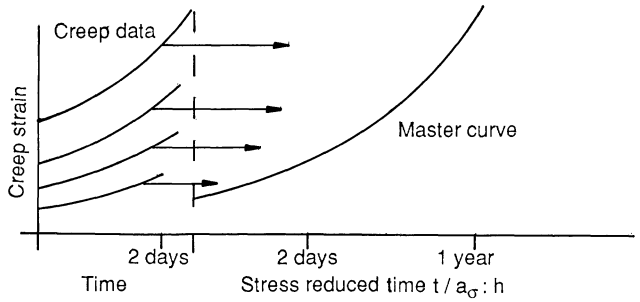

Figure 2.21 Typical schematic graph for extrapolation of creep data using TSSP.

logarithmic scale against a logarithmic time scale. Assuming time–temperature correspondence, a master curve can be constructed by shifting the higher temperature curves parallel to the time axes and the amount of shift to achieve the superposition of the data gives the reduced time factor for each test temperature. Figure 2.20 illustrates this technique. Likewise, the applied stress time superposition principle (TSSP) can be used for polymers and polymer composite materials and Figure 2.21 shows a typical creep stress–time relationship. The time–temperature and stress–time superposition principles have been discussed more fully in [16] and [17], respectively.

2.9.3 Experimental techniques to determine creep properties

The techniques used for characterizing the time dependent behaviour of polymers are those involving tensile, compressive, flexure and shear; the first method only will be discussed.

In this test, a uniaxial tensile load is applied to a suitably shaped test specimen and the creep deformation is measured as a function of time. The tests are generally performed at various stress levels to provide some indication of the non-linearity of the material. A typical total creep curve for polymers under a given uniaxial stress and constant temperature T can be divided into five parts; a graph for a highly idealized material is

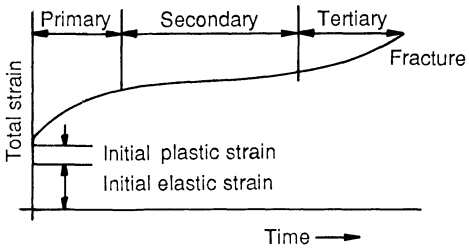

Figure 2.22 Highly idealized creep–time graph.

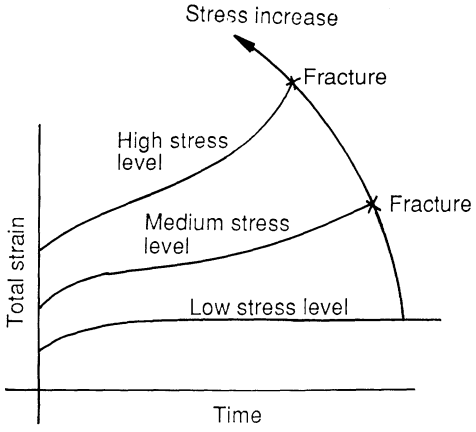

Figure 2.23 Typical family of creep curves.

shown in Figure 2.22. It should be realized that some materials do not exhibit a secondary type creep and others do not have a tertiary region; also, it is common to find that in some polymers the tertiary creep is evident only at high stresses. A typical family of creep curves is given in Figure 2.23.

2.10 Mechanical properties of fibres

The non-linear stress–strain material behaviour of the polymer does not rule out its utilization as the matrix or secondary phase in a composite

Table 2.4 Typical mechanical properties for glass, aramid and carbon fibres

Material	Fibre	Elastic modulus (GPa)	Tensile strength (MPa)	Ultimate strain (%)	Density (g/cm^2)	Max temp (°C)
Glass	E	72.4	2400	3.5	2.55	250
	A	72.4	3030	3.5	2.50	250
	S-2	88.0	4600	5.7	2.47	250
Aramid	49	125	2760	2.4	1.44	180
	29	83	2750	4.0	1.44	180
Teijin	Technora	70	3000	4.4	1.39	–
Carbon	XAS HS	235	3800	1.64	1.79	600
Grafil	HS	235	3450	1.64	1.79	600
	IM-S	290	3100	1.64	1.76	600
	HM-S6K	370	2750	1.64	1.86	600
Toray	T-300	230	3530	1.5	1.77	600
	M-46-J	450	4100	2.4	1.82	600

material. Section 2.2 discusses the mechanism of reinforcing the matrix material.

The mostly frequently used reinforcement for polymers in construction is the E-glass fibres; to a much lesser extent carbon fibre and Kevlar are used as unidirectional reinforcement placed in the high stress region of the composite. It is possible to use a hybrid of glass and carbon fibre to increase the stiffness of the primary phase. Glass fibre combines good mechanical behaviour with relatively low cost and the carbon or Kevlar fibre provides a stiff laminate. Table 2.4 gives the mechanical properties of these three fibres. It can be seen that the ultimate strength and stiffness of these fibres, which would be utilized as the dispersed phase (i.e. the primary phase), are high compared with those of the matrix.

Synthetic and natural fibres such as polyamides (nylons), polyester, high

Table 2.5 Typical mechanical properties of synthetic fibers used in construction

Fibre type	Specific weight	Ultimate tensile strength (MPa)	Elongation at break (%)	Maximum working temp °C
Natural				
Cotton	1.5	500–880	7–14	—
Jute	1.5	460	4	—
Sisal	1.45	850	2.5	—
Synthetic				
Acrylics	1.14–1.18	300–400	20–40	180
Chlorofibres				
Polyvinyl Chloride	1.38–1.40	340	20	80
Polyvinylidene Chloride	1.70	300–400	20–40	80
Fluorofibres	2.30	105–175	40–100	220
Modacrylics	1.31–1.37	300–400	20–40	170
Nylons				
Nylon 6	1.13	450–750	20–40	70
Nylon 6,6	1.14	450–1000	12–30	130
Aramids	1.38–1.45	500–2900	2–12	450
Polyolefins				
Polypropylene	0.90	400–700	10–20	100
Polyethylene				
Low density	0.92	80–120	25–50	55
High density	0.95	350–500	20–30	65
Ultra-high density	0.96	2400–2700	3–4	90
Polyesters	1.38	500–1400	8–30	170
Polyurethane Elastomers	1.00–1.32	70–110	400–800	150

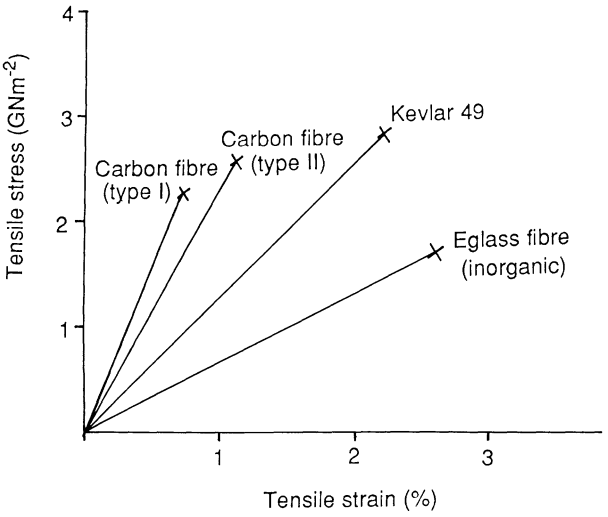

Figure 2.24

density polyethylene, sisal and jute can be combined with resins to form fibre/matrix composites. Some of these laminates have been used for special purposes in civil engineering applications; these fibres and the fibre/matrix composites have been mentioned in section 2.7.5. Table 2.5 gives typical mechanical properties of synthetic (organic) fibres and Figure 2.24 shows the comparative strength/extension characteristics of some thermoplastic fibres. Table 2.6 gives typical representative properties of some geotextiles.

2.11 Mechanical properties of structural composites

There are two major requirements when designing structural composite components for the construction industry.

1. The deformation under load must be within the prescribed functional and aesthetic considerations.
2. Fracture and rupture should not take place within their scheduled lifetime.

To satisfy these requirements it is necessary to have information on two particular mechanical properties, namely stiffness and strength. Therefore discussion of the mechanical characteristics will largely revolve around these properties.

It is shown in sections 5.2.1 and 5.2.2 that composites are manufactured as a combination of a number of laminae where each lamina is assumed to be homogeneous although microscopic studies have revealed considerable evidence of microheterogeneity.

Table 2.6 Representative properties of geotextiles (table from Exxon Chemical—Geotextiles Designing for Soil Reinforcement, Table 1)

Geotextile construction	Tensile strength (kN/m)	Extension at max. load (%)	Apparent opening size (mm)	Water flow ($l/m^2/s$)[a]	Unit weight (g/m^2)
Conventional geotextiles					
Non-wovens					
Melt-bonded	3–25	20–60	0.02–0.35	25–150	70–350
Needle-punched	7–90	50–80	0.03–0.20	30–200	150–2000
Wovens					
Monofilament	20–80	9–35	0.07–2.5	25–2000	150–300
Multifilament[b]	40–800	9–30	0.20–0.9	20–80	250–1350
Flat tape	8–70	10–25	0.07–0.15	5–20	90–250
Knitteds					
Welt	2–5	300–600	0.2–1.2	60–2000	
Warp	20–120	12–15	0.4–5.0	100–2000	
Stitch-bonded	30–1000	8–30	0.07–0.5	30–80	250–1200
Special geotextiles					
Geogrides					
Cross-laid strips	25–200	3–20	50–300	NA	300–1200
Purchased sheets	10–200	11–30	40–150	NA	200–1100
Geocomposites					
Strips	20–150[c]	3–20	NA	NA	NA
Bars	20–500[c]	3–20	NA	NA	NA
Link structures	100–4000	3–20	NA	NA	600–4500

[a] Normal to the plane of the geotextile with 10 cm constant head
[b] Fibrillated tapes are included in this category
[c] Measured in kN (not kN/m).

However, for engineering design a laminate made from a number of laminae fabricated from randomly orientated fibres in a polymer matrix is considered to be quasi-isotropic in the plane of the lamina on a macro scale. Non-isotropic composites associated with construction using orthotropic laminae (unidirectionally aligned fibres in a polymer matrix) in a symmetric lay-up (see section 2.4.1) have three mutually perpendicular planes of material symmetry and the properties at any point are different in three mutually perpendicular planes of symmetry (see Figure 2.4). A typical lamina stacking sequence is to produce either unidirectionally aligned or bi-directionally aligned composites.

In an orthotropic composite, the tensile strength and stiffness are, of course, greater in the directions in which the fibres are aligned than in any other direction. Futhermore, in the unidirectional strand composite,

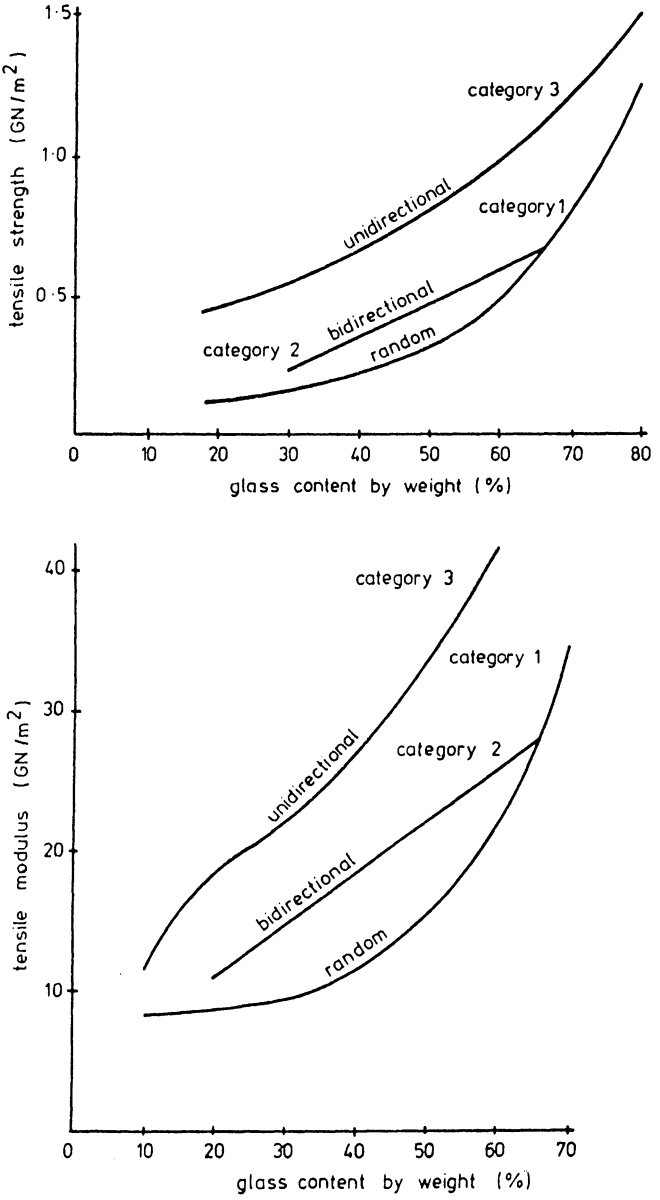

Figure 2.25 Typical tensile strengths and tensile moduli versus glass content.

the planes perpendicular to the alignment in which the strength and stiffness do not vary with direction, are transversely isotropic.

From the above it may be seen that the strength and stiffness of composites depend upon a number of parameters, these are:

1. the stiffness and strength of the component parts;
2. the fibre orientation;
3. the fibre/polymer composite volume fraction;
4. the method of manufacture of the composite.

Three aspects of a fibre/polymer composite can be broadly considered. Firstly, the condition in which the fibres are randomly orientated in the matrix; in this case, the maximum proportion of the glass in the composite is about 50% by weight (category 1). Secondly, where the fibres are orthogonally arranged and where the maximum proportion of glass is about 65% by weight; in this category are the woven rovings and cloth laminates (category 2). Finally, the condition in which the fibres are laid in one direction; because they are then packed more closely, the percentage of glass used in the composite can be as high as 85% by weight (category 3). However, the practical value is generally nearer 70%. Figure 2.25 shows typical tensile strengths and tensile moduli against glass content; the relationships are for the three categories discussed above.

Table 2.7 gives the tensile characteristics of the different types of glass fibre/polyester composites and illustrates the parameters on which the strength and stiffness depend.

Table 2.7 Typical mechanical properties for glass reinforced polymer composites

Material	Glass content (% by weight)	Specific weight	Tensile modulus (GPa)	Tensile strength (MPa)
Unidirectional rovings (filament winding or pultrusion	50–80	1.6–2.00	20–50	400–1250
Hand lay-up with chopped strand mat	25–50	1.4–1.6	6–11	60–180
Matched dye moulding with preform	25–50	1.4–1.6	6–12	60–200
Hand lay-up with woven rovings	45–62	1.5–1.8	12–24	200–350
DMC polyester (filled)	15–20	1.7–2.0	6–8	40–60
SMC	20–25	1.75–1.95	9–13	60–100

2.12 Stress–strain relationships for fibre/polymer materials

It is particularly difficult to compare the polymer and polymer composite material characteristics given in one publication with those presented in another because property values vary according to the manner in which they are determined and unless there is a unified testing standard for composite material, this problem will persist (see chapter 4 for test procedures for composites). Routine type tests undertaken in one laboratory, while satisfying quality control considerations and perhaps as an indication of service performance if interpreted carefully, will rarely give the designer the values on which to base his calculations. The largest gap between most published data and performance behaviour lies in the time scale; for instance, what is the extent of the degradation of the material at the end of its life and what is the relationship between the rate of loading of the laboratory specimen and that of the prototype structure. Accelerated tests will often provide useful guides and frequently are the only solution to such demands. However, it will be realized that to undertake accelerated tests, some variables have to be intensified, for example, the temperature raised, the nature of the environment changed or the frequency of stressing increased. These changes may themselves induce effects which would never occur at the normal ambient temperature.

It is clearly necessary to unify test procedures for composite materials and with this in mind, a working group was inagurated in 1980 by the Composite Research Advisory Group (CRAG). Its terms of reference included a requirement to survey and rationalize the enforced test procedures for fibrous composite materials (see chapter 4). Test methods were agreed for the generation of materials design data, primarily on unidirectional composite materials for use in design aids such as laminated plate theory but also on multidirectional fibre composites. The third and final report was written in 1988 [18]. Although this report was written mainly for composites used in the aerospace industries, it is, nevertheless, an extremely useful document for composite testing generally.

The uniaxial tensile stress–strain curves for composites are commonly obtained at constant rates of elongation often following the test procedures prescribed in national standards such as BS 2782 [19] (equivalent ISO are also given) or the corresponding standard of the American Society for Testing and Materials [20]. At relatively low strains, the stress–strain curves exhibit a linear relationship; these curves are established in a short period of time, usually of the order of a few minutes. At higher levels of strain, the slopes of these curves are generally less than their initial values and the change occurs at a point that is often referred to as the knee in the stress–strain curve. The knee is associated with crazing or cracking of the matrix material and once this point has been passed, the composite is permanently damaged and, although it is still capable of

undergoing considerable strain deformation, it will not return to its original dimensions when the load causing strain is removed. This characteristic is more noticeable with higher fibre contents and the position of the knee on the stress–strain curve is dependent on the stiffness of the matrix; for very flexible matrices, cracking may be eliminated altogether.

Because the polymer component of the composite is a viscoelastic material, its deformational behaviour is highly dependent on the way in which it is subjected to stress and strain. Although glass, on the other hand, is linearly elastic, the composite will exhibit viscoelastic properties and, under different conditions of testing, the stress–strain behaviour will appear different; it is imperative, therefore, that a standard test procedure is adhered to.

The mechanical behaviour of composite materials might be more realistically established by applying constant loads over longer periods of time; these investigations may be defined as creep tests (see section 2.13). These tests produce curves of elongation against time at different stress levels and although they are not able to produce data that may be converted directly to stress–strain curves, constant time sections through families of such creep curves have been used to produce isochronous stress–strain curves (see section 2.9.2).

2.13 The deformation characteristics of composites

There are at least three different ways in which uniaxial tension can be applied to a composite specimen being tested in a laboratory and the three most important are discussed here.

The constant rate of elongation test closely approximates the constant rate of strain test as prescribed by BS 2782 [19]: these tests lead to secant and tangent moduli values which vary significantly with different strain rates. It is, therefore, necessary to define the rate of strain if results are to be intelligible.

The constant rate of loading test is relatively uncommon because of the difficulty of applying constant rates of loading (i.e. constant rate of stressing) using standard testing equipment, but if used, it is necessary to define the rates of stress used. The constant load tests (creep tests) amount to a series of different constant stress levels applied over varying time intervals and correspond directly to those met in many structural applications of polymers. These tests can cover long as well as short periods of loading and therefore the results are to be preferred to the above two cases when structural design of viscoelastic materials is being undertaken. Greater time and effort are required to obtain the values compared with the test procedures laid down in BS 2782 [19], however, for design purposes the creep tests are the preferred ones to obtain the deformational behaviour of polymers. This is exemplified by the Recom-

mendations of the British Standards Institution for Presentation of Plastics Design Data [15]. It will be realized that creep tests do not immediately provide isochronous stress–strain curves but these may be obtained by taking constant time sections through creep curves (see section 2.9.2).

The importance of the isochronous stress–strain curves lies in the fact that the slopes obtained from the three methods of test loading are different and they decrease in the order constant stress rate, constant strain rate and constant stress.

The constant rate of elongation test makes polymers appear stiffer than they are under the constant load tests and, therefore, the information it provides on the stiffness of polymers is over-optimistic. It may also be observed that the constant load or creep tests relate directly to civil engineering structural problems under long-term loading, but the stiffness of components under short-term loading will be underestimated by this test procedure and will err on the side of safety.

Although many testing laboratories undertake the more ad hoc testing procedures, the unreliability of the creep results and the long-term modulus of elasticity given by these, clearly indicate that the isochronous stress–strain characteristics of GRP should be obtained. It does, however, require considerably more time and effort to produce these curves compared with those obtained under the test procedures in BS 2782; a further requirement is that the tests should be performed at known temperatures and relative humidities. There is a certain justification for adopting BS 2782 or ASTM Part 36, when the superimposed loads applied to civil engineering GRP structures are of short duration (e.g. wind and snow); the results of the test will underestimate the stress–strain relationship which will be a function only of the ageing effect of the material.

2.14 Fatigue in composite materials

The anisotropic characteristics of composite materials cause a complex failure mechanism under static and fatigue loading and this is accompanied by extensive damage to the composite. Unidirectional continuous fibre composites, on the other hand, have excellent fatigue resistance and are essentially linear to failure. If, however, the composite contains off-axes plies, various damage mechanisms can occur under load, causing it to be redistributed, and the stress–strain response will become non-linear. The four basic failure mechanisms are:

1. matrix cracking;
2. delamination;
3. fibre breakage;
4. interface debonding.

The type and degree of these damage mechanisms vary depending on

(a) material property;
(b) stacking sequence;
(c) type of fatigue.

2.14.1 Matrix cracking

Matrix cracking in the off-axis plies is usually the first damage mechanism and as the load increases, the density of the cracks increases. If a [0°/90°/$\pm$45°] laminate is subjected to a tensile load, the cracks would occur in the 90° plies followed by the $\pm$45° plies. The first cracks to appear can be estimated analytically with a fair degree of accuracy, but it is difficult to produce analytically the $\pm$45° plies; this might be due to the influence of the original cracks in the 90° plies. The density of the cracks increases as the load increases until they appear to stabilize at a unique value for a given laminate. Reifsnider and co-workers [21, 22] have called this state the 'characteristic damage state'. It is possible to obtain 0° plies splitting perpendicularly to the fibre direction, this being a form of matrix cracking caused by the Poisson's ratio mismatch between adjacent plies. The 0° plies are also susceptible to cracking in the fibre direction as a result of the transverse stress in the 0° ply of a multidirectional laminate. Under static loading, axial cracking in the 0° direction plies might not occur because the transverse stress is usually small, but under fatigue loading, cracking in cross-laminates can occur.

2.14.2 Delamination

Delamination occurs between layers of a composite laminate and is attributed to the existence of interlaminar stresses which exist in the neighbourhood of a free edge under an in-plane loading. These out-of-plane stresses arise because the transverse and shear stresses in each ply must decay to zero at the free edge; this gives rise to interlaminar stresses which can be either tensile or compressive, depending on the stacking sequence. The magnitude and distribution of these stresses vary depending on the laminate, the stacking sequence, the properties of the component materials and the type of loading. Delamination will generally start on the free edge of the composite and propagate inwards.

In addition to interlaminar tensile stresses, there are other mechanisms such as transverse cracking and interlaminar shearing which could be significant during the process of delamination. For example, a symmetric 0°/90°/$\pm$45° laminate under a static tensile stress would not show any delamination, but under a fatigue tensile load it would show considerable delamination between the +45° and −45° plies.

2.14.3 Fibre breakage and interface debonding

The properties of component materials in fibre reinforced polymers are highly dependent on the fibre and interface strengths. In a unidirectional composite, under a tensile force made from carbon fibre with a polymer matrix, it is likely that defects in the fibre will cause it to fail before the matrix. This crack will extend into the matrix as the load is increased and its path will be dependent on the properties of the interface bond between fibre and matrix. If the bond is strong, cracks will extend into the matrix, whereas if the interface bond is weak, the crack will lead to interfacial debond and fibre pull-out.

Although the above discussion refers to composites under both static and fatigue loading, the sensitivity of the matrix, interface and fibre to fatigue loading must be considered in the design.

Damage to the composite caused under cyclic loading will inevitably produce significant changes in the mechanical response of the specimen. These changes fall into three main groups:

1. the strength and modulus of elasticity of the material will decrease with increase in damage;
2. the hysteresis losses will increase with increase in cycles of load (see Figure 2.26);

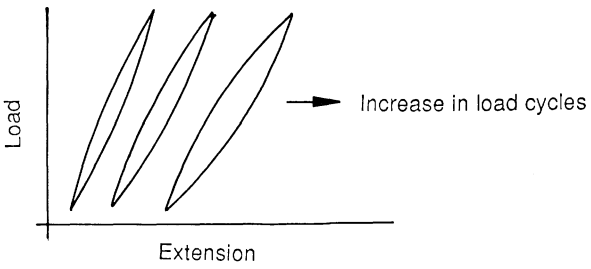

Figure 2.26 Schematic representation of hysteresis loop change for short glass fibre reinforced nylon.

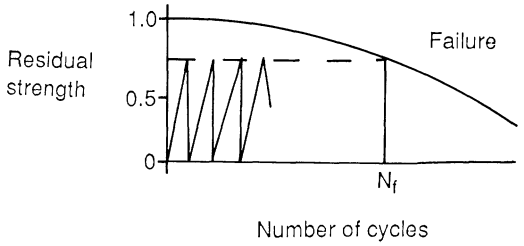

Figure 2.27 Typical GFRP and KFRP composite: wear-out model of fatigue.

3. the residual strength of the composite decreases with increase in fatigue cycling (see Figure 2.27).

The effect of damage on the composite will depend upon the type of laminate and the nature of the loading. For instance, a multidirectional composite under a fatigue load shows a gradual reduction in strength and stiffness values, whereas a unidirectional composite (0 fibre direction only) will show little damage until immediately before failure.

2.14.4 Fatigue behaviour

The fatigue behaviour of polymer/fibre composites is generally presented as a stress–number of cycles (S–N) relationship. This quantity is primarily dependent on the properties of the component materials. Unidirectional materials show good fatigue resistance which reflects the importance of fibre orientation. Figure 2.28 shows a comparison of the fatigue performance of three composites (viz. glass fibre reinforced polymers, Kevlar fibre reinforced polymers and carbon fibre reinforced polymers). Curtis [23] has given the strain life curves for four different carbon types with their stiffness varying over a 40% range; the fibres were placed in the same matrix. It was shown that there is no significant difference in the fatigue performance between these types. Curtis has also shown that by using the same fibre, but placing it in different epoxy resins (for example toughened and standard epoxies), higher static strengths can be achieved, but at the expense of steeper 'fall-off' of their S–N curves after a certain number of cycles (see Figure 2.29).

The fatigue failure due to damage accumulation in a GFRP cross-ply laminate would cause a rapid stiffness reduction initially which would be associated with an increased density of transverse ply cracks; some fibre breakage may occur in the 0 direction. This stage is followed by an approximately linear region of stiffness reduction and an increase in matrix crack density in the transverse direction but at a much reduced rate; some

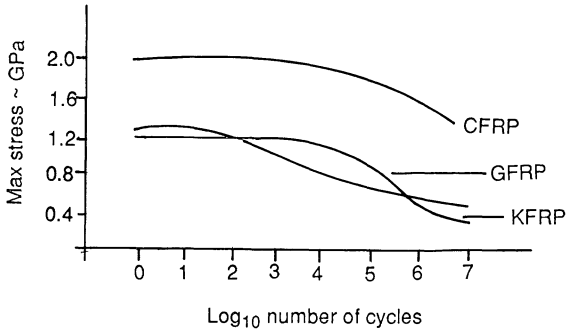

Figure 2.28 Typical S–N curves for unidirectional composites.

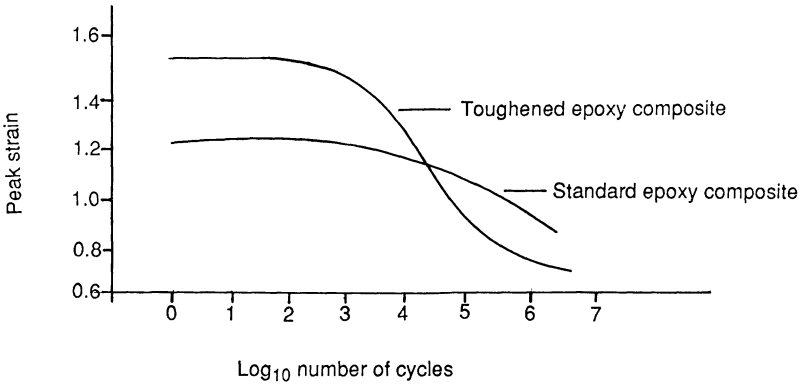

Figure 2.29 Peak strain versus number of cycles for the same fibre type in two different matrices (after Curtis [22]).

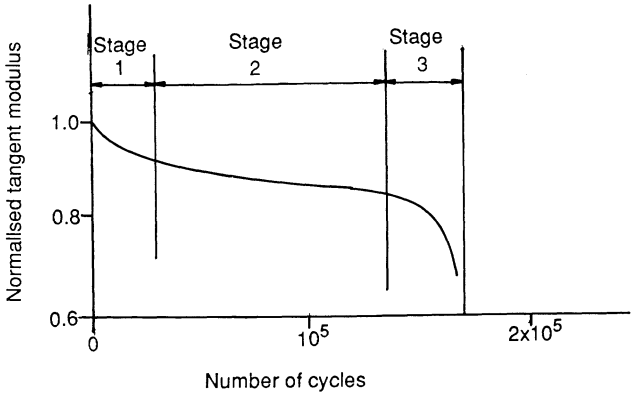

Figure 2.30 Damage development and modulus reduction in a 0°/90° glass fibre/epoxy resin matrix laminate.

delamination at the 0°/90° interface will take place as well as fibre breakage in the 0° direction. The third stage is associated with a rapid stiffness reduction with macro-cracks forming in the highly stressed region of the matrix prior to failure of the laminate. Figure 2.30 shows a typical damage development and modulus reduction for a symmetrical 0°/90° laminate.

The fatigue performance of randomly orientated composites has been documented by Owen and co-workers [24, 25]. The onset of fatigue damage in a chopped strand glass fibre mat/polyester resin matrix was identified by Owen using optical microscopy to identify and quantify the damage as a function of cycling; Figure 2.31 shows the relationship between stress amplitude and the log of the number of cycles in a randomly orientated

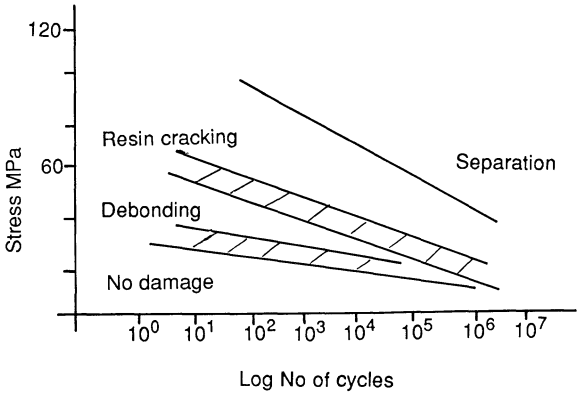

Figure 2.31 The onset of debonding and resin cracking in fatigue under zero mean stress in a randomly oriented glass fibre/polyester resin matrix.

glass fibre/polyester matrix laminate and identifies the fibre/matrix debonding, resin cracking and separation.

From the brief discussion on the fatigue behaviour of composites given above, it will be realized that the reduction in stiffness of the material due to the failure mechanisms can be large, whereas in homogeneous materials, where little cracking takes place until near to final failure, the reduction in stiffness is small. Consequently, it is advisable to use a stiffness rather than strength based failure criterion for design with composites.

References

1. A. Pickett, Elastic moduli of fiber reinforced plastic composites, in *Fundamental Aspects of Fibre Reinforced Plastic Composites*, eds. R.T. Schwartz and H.S. Schwartz, Interscience, New York (1968) Ch. 2.
2. C.S. Barrett and T.B. Massalski, *Structure of Metals*, Mc Graw-Hill, New York (1966).
3. M.C. Judd and W.W. Wright, Voids and their effects on the mechanical properties of composites—an appraisal, *SAMPE J.*, Jan/Feb (1974), 10–14.
4. J.E. Ashton, J.C. Halpin and P.H. Petit, *Primer on Compositie Materials: Analysis*, Technomic, Westport, CT (1969); J.C. Halpin, Revised 2nd edition, *Primer on Composite Materials Analysis*, Technomic, Basel, Switzerland (1992).
5. H.L. Cox, The elasticity and strength of paper and other fibrous materials, *Br. J. Appl. Phys.*, **3** (1952), 72–79.
6. J.C. Halpin, Stiffness and expansion estimates for orientated short fibres composites, *J. Composite Mater.*, **3** (1969), 732–734.
7. J.C. Halpin and S.W. Tsai, Environmental factors in composite materials design, Air Force Materials Laboratory Technical Report AFML-TR-67-423 (1967).
8. H. Krenchel, *Fibre Reinforcement*, Akademisk Forlag, Copenhagen (1964).
9. C. Lawson, Geosynthetics in *Polymers Polymer Composites in Construction*, ed. L. Hollaway, Thomas Telford (1990).
10. D. Hull, *An Introduction to Composite Materials*, Cambridge University Press, Cambridge (1981, reprint 1990).
11. L.N. Phillips, Introduction in *Design with Advanced Composite Materials*, ed. L.N. Phillips, The Design Council (1989).

12. J.J. Chambers, Long term properties of parafil, in *Proc. Symp. on Engineering Applications of Parafil Ropes* (1988), pp. 21–28.
13. G. Gross, *Mathematical Structure of the Theories of Viscoelasticity*, Paris Hermann et Cie, (1953).
14. W.N. Findley and W.J. Worley, Some static fatigue and creep tests of a glass fabric laminated with a polyester resin AF, *Technical Report No. 6389*, Engineering Experimental Section, University of Illinois, April (1951).
15. British Standards Institution, *Recommendations for the presentation of plastics design data Part 1: Mechanical Properties*, British Standard 4618 (7 sections, no ISO equivalence) British Standards Institution, London (1970).
16. J.J. Aklonis and W.J. MacKnight, *Introduction to Polymer Viscoelasticity*, 2nd edn, Wiley, New York (1983), pp. 36–56.
17. L.C. Cessna, Jnr., Stress-time superposition for creep data for polypropylene and coupled glass reinforced polypropylene, *Polymer Engineering Science*, **13**, May (1971), pp. 211–219.
18. P.T. Curtis, ed., CRAG Test Methods for the Measurements of the Properties of Fibre Reinforced Plastics. *MOD Technical Report 88012*, Farnborough, February (1988).
19. British Standards Institution, *Determination of tensile properties*, British Standard 2782: Method 10003 1977 (≡ EN61: ≠ ISO/R527, ISO 3268),* British Standards Institution, London (1983).
20. *ASTM Standards on Plastics* (annual book on ASTM standards), ASTM, Philadelphia, USA.
21. K.L. Reifsnider and A. Talug, Analysis of Fatigue Damage in Composite Laminates *Int. J. Fatigue* **2** (1) (1980), 3.
22. K.L. Reifsnider and A. Highsmith, Advances in Fracture Research, Vol. 1, I.C.F.5, Cannes (1981).
23. P.T. Curtis, The fatigue behaviour of fibrous composite materials, *J. Strain Anal.* **24** (4) (1989), pp. 235–244.
24. M.J. Owen, ASTM STP 772 (1982) p. 64.
25. M.J. Owen and R.J. Howe, The accumulation of damage in a glass-reinforced plastic under tension and fatigue loading, *J. Phys. D.: Applied Physics* **5** (1972), 1637–1649.

* The symbol ≡ indicates an identical standard, i.e. a BSI publication identical in every detail with a corresponding international standard ISO. The symbol = indicates a (technically) equivalent standard, i.e. a BSI publication in all technical respects the same as a corresponding international standard ISO although the wording and presentation may differ quite extensively. The symbol ≠ indicates a related but not equivalent standard, i.e. a BSI publication, the content of which to any extent at all short of complete identity or technical equivalence, covers subject matter similar to that covered by a corresponding international standard ISO.

3 Laminate theory: macroanalyses of composite laminates

3.1 Introduction

It has been shown in chapter 2 that composite materials are manufactured as laminates, consequently in analysing the lamina, the primary aim is to obtain predictions of the average behaviour of the composite from the properties of the components. From the point of view of the mechanical properties of the composite lamina, the area of interest to the designer will be its stiffness and strength; these are influenced by the following:

(a) the mechanical properties of the fibre and matrix;
(b) the fibre volume fraction of the composite;
(c) the fibre cross-section;
(d) the fibre orientation within the matrix;
(e) the method of manufacture of the composite.

The fibres are generally assumed to be linear elastic to failure and although the resin is practically linear in the low stress region, it does exhibit non-linear properties at higher stress levels. However, the ultimate strain of the brittle fibre is invariably less than that of the 'ductile' matrix and consequently, to justify the assumption of linear elasticity of the matrix, the latter's stress would be relatively low at failure of the composite. In addition, the effect of creep in the polymer matrix on the stress distribution within, and on the stiffness characteristics of the composite can be minimized by ensuring that the fibres are positioned in the most effective way, which for axial forces would be along the line of action of the applied force. By increasing the proportion of the glass fibre in the composite, a greater percentage of the load will be taken by the fibres and therefore a smaller percentage will be carried by the matrix. Conversely if the fibre content is low, the matrix material will carry a greater percentage of the total load but in this case the load would be sufficiently low to ensure low creep.

The following assumptions are made in the development of the relationships between stresses and the corresponding strains of composite material properties:

(a) the tension and compression characteristics are the same;
(b) the composite material has linear elastic properties.

In the following sections rigorous mathematical detail is not presented.

3.2 Isotropic lamina

The mechanical properties of the composites are controlled by their constituent properties and by the microstructural configurations (see chapter 2). It is therefore necessary to be able to predict properties under varying conditions. The notation of the stress components used in this chapter is given in section 2.4, and Figure 2.4.

3.2.1 Elastic properties of a randomly orientated fibre lamina

For homogeneous isotropic laminae (i.e. randomly orientated fibres in a polymer matrix), the stress–strain relationship for a lamina and laminates is

$$\begin{aligned}\sigma_{11} &= E/(1-v^2)(\varepsilon_{11} + v\varepsilon_{22})\\ \sigma_{22} &= E/(1-v^2)(\varepsilon_{22} + v\varepsilon_{11})\\ \sigma_{12} &= [E/2(1-v)]\varepsilon_{12}\end{aligned} \tag{3.1a}$$

In matrix form

$$\begin{bmatrix}\sigma_{11}\\ \sigma_{22}\\ \sigma_{12}\end{bmatrix} = \begin{bmatrix}Q_{11} & Q_{12} & 0\\ Q_{21} & Q_{22} & 0\\ 0 & 0 & Q_{33}\end{bmatrix}\begin{bmatrix}\varepsilon_{11}\\ \varepsilon_{22}\\ \varepsilon_{12}\end{bmatrix} \tag{3.1b}$$

where

$$\begin{aligned}Q_{11} &= E(1-v^2) = Q_{22}\\ Q_{12} &= Ev(1-v^2) = Q_{21}\\ Q_{33} &= E/2(1+v) = G\end{aligned}$$

or

$$[\sigma] = [Q][\varepsilon]$$

The $[Q]$ matrix is known as the material matrix.

There are two independent constants in these equations: these are E and v and this indicates isotropic material properties.

The corresponding set of equations to those in eq. (3.1b) relate the strains to stresses as

$$\begin{bmatrix}\varepsilon_{11}\\ \varepsilon_{22}\\ \varepsilon_{12}\end{bmatrix} = \begin{bmatrix}S_{11} & S_{12} & 0\\ S_{21} & S_{22} & 0\\ 0 & 0 & S_{33}\end{bmatrix}\begin{bmatrix}\sigma_{11}\\ \sigma_{22}\\ \sigma_{12}\end{bmatrix} \tag{3.2}$$

where

$$S_{11} = 1/E = S_{22}$$

$$S_{33} = 1/G$$

$$S_{12} = -\nu/E = S_{21}$$

or

$$[E] = [S][\sigma]$$

The $[S]$ matrix is known as the compliance matrix.

3.3 Orthotropic lamina

The orthotropic lamina can be assumed to be isotopic in plane 1 (i.e. the plane normal to the axes direction 1) as the properties are independent of direction in that plane. The stress–strain relationship for an orthotropic lamina is

$$\begin{bmatrix} \sigma_{11} \\ \sigma_{22} \\ \sigma_{12} \end{bmatrix} = \begin{bmatrix} Q_{11} & Q_{12} & 0 \\ Q_{21} & Q_{22} & 0 \\ 0 & 0 & Q_{33} \end{bmatrix} \begin{bmatrix} \varepsilon_{11} \\ \varepsilon_{22} \\ \varepsilon_{12} \end{bmatrix} \tag{3.3}$$

where

$$Q_{11} = E_{11}/(1 - \nu_{12}\nu_{21})$$

$$Q_{22} = E_{22}/(1 - \nu_{21}\nu_{12}),$$

$$Q_{33} = G_{12}$$

$$Q_{12} = E_{22}\nu_{12}/(1 - \nu_{12}\nu_{21})$$

$$Q_{21} = E_{11}\nu_{21}/(1 - \nu_{21}\nu_{12})$$

As the Q matrix is symmetric, we have $E_{11}\nu_{21} = E_{22}\nu_{12}$. The Poisson's ratio ν_{12} refers to the strains produced in direction 2 when the lamina is loaded in direction 1. Similarly ν_{21} refers to the strains produced in direction 1 when the lamina is loaded in direction 2.

There are four independent constants in these equations; these are E_{11}, E_{22}, ν_{12} and ν_{21}. This indicates orthotropic material properties.

From the above equation, it can be seen that the shear stress σ_{12} is independent of the elastic properties $E_{11}, E_{22}, \nu_{12}, \nu_{21}$ and therefore no coupling between tensile and shear strains takes place.

The corresponding set of equations to those in eq. (3.3) which relate strains to stresses are

$$\begin{bmatrix} \varepsilon_{11} \\ \varepsilon_{22} \\ \varepsilon_{12} \end{bmatrix} = \begin{bmatrix} S_{11} & S_{12} & 0 \\ S_{21} & S_{22} & 0 \\ 0 & 0 & S_{33} \end{bmatrix} \begin{bmatrix} \sigma_{11} \\ \sigma_{22} \\ \sigma_{12} \end{bmatrix} \tag{3.4}$$

where

$$S_{11} = 1/E_{11}$$
$$S_{22} = 1/E_{22}$$
$$S_{33} = 1/G_{12}$$
$$S_{12} = -\nu_{21}/E_{22}$$
$$S_{21} = -\nu_{12}/E_{11}$$

3.3.1 *Orthotropic lamina: arbitrary orientation*

The relationships defined in eq. (3.3) are related to the principal directions of the material. Consequently, because of material symmetry, the effects of the normal stress are independent of those of the shearing stresses and hence the total effects can be obtained by superposition.

If the lamina principal axes (1, 2) do not coincide with the reference axes (x, y) but are at some arbitrary orientation θ to them (Figure 3.1), then the above constitutive relationship for each individual lamina must be transformed to the reference axes.

This may be achieved by applying the following transformation:

$$\begin{bmatrix} \sigma_{11} \\ \sigma_{22} \\ \sigma_{12} \end{bmatrix} = [T] \begin{bmatrix} \sigma_{xx} \\ \sigma_{yy} \\ \sigma_{xy} \end{bmatrix} \tag{3.5a}$$

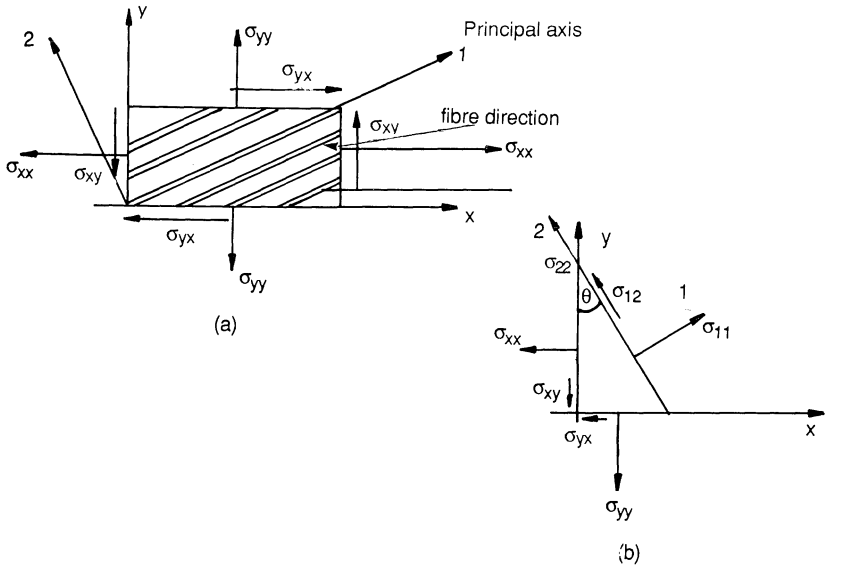

Figure 3.1 Orientation of orthotropic lamina about the reference axes. (a) Lamina principal axis (1,2) at θ orientation with reference axis (x,y); (b) element under stress on axes (x,y) and (1,2).

or

$$\begin{bmatrix} \sigma_{xx} \\ \sigma_{yy} \\ \sigma_{xy} \end{bmatrix} = [T]^{-1} \begin{bmatrix} \sigma_{11} \\ \sigma_{22} \\ \sigma_{12} \end{bmatrix} \tag{3.5b}$$

The transformation matrix is given by

$$[T] = \begin{bmatrix} m^2 & n^2 & 2mn \\ n^2 & m^2 & -2mn \\ -mn & mn & m^2 - n^2 \end{bmatrix} \tag{3.6a}$$

and

$$[T]^{-1} = \begin{bmatrix} m^2 & n^2 & -2mn \\ n^2 & m^2 & 2mn \\ mn & -mn & (m^2 - n^2) \end{bmatrix} \tag{3.6b}$$

where $m = \cos\theta$ and $n = \sin\theta$.

The following relationship in matrix form is allied to strains in the principal axes (1, 2) and the reference axes (x, y):

$$\begin{bmatrix} \varepsilon_{11} \\ \varepsilon_{22} \\ \varepsilon_{12}/2 \end{bmatrix} = [T] \begin{bmatrix} \varepsilon_{xx} \\ \varepsilon_{yy} \\ \varepsilon_{xy}/2 \end{bmatrix} \tag{3.7a}$$

where $[T]$ is the transform matrix in eq. (3.6a)

$$\begin{bmatrix} \varepsilon_{xx} \\ \varepsilon_{yy} \\ \varepsilon_{xy}/2 \end{bmatrix} = [T]^{-1} \begin{bmatrix} \varepsilon_{11} \\ \varepsilon_{22} \\ \varepsilon_{12}/2 \end{bmatrix} \tag{3.7b}$$

It will be seen that, comparing eqs (3.5) and (3.7), the stress and strain transformation equations are identical.

Ashton *et al.* [1] show that, from the elasticity theory, the stress–strain relationship in the x, y coordinate system at an angle θ to the principal material direction becomes

$$\begin{bmatrix} \sigma_{xx} \\ \sigma_{yy} \\ \sigma_{xy} \end{bmatrix} = \begin{bmatrix} \bar{Q}_{11} & \bar{Q}_{12} & \bar{Q}_{13} \\ \bar{Q}_{21} & \bar{Q}_{22} & \bar{Q}_{23} \\ \bar{Q}_{31} & \bar{Q}_{32} & \bar{Q}_{33} \end{bmatrix} \begin{bmatrix} \varepsilon_{xx} \\ \varepsilon_{yy} \\ \varepsilon_{xy} \end{bmatrix} \tag{3.8}$$

where the $\bar{Q}_{ij}$ component is known as the transformed reduced stiffness matrix and the components of this matrix have the following values:

$$\bar{Q}_{11} = Q_{11}m^4 + Q_{22}n^4 + 2(Q_{12} + 2Q_{33})n^2m^2$$

$$\bar{Q}_{12} = \bar{Q}_{21} = (Q_{11} + Q_{22} - 4Q_{33})n^2m^2 + Q_{12}(n^4 + m^4)$$

$$\bar{Q}_{13} = \bar{Q}_{31} = (Q_{11} - Q_{12} - 2Q_{33})nm^3 + (Q_{12} - Q_{22} + 2Q_{33})n^3m$$

$$\bar{Q}_{22} = Q_{11}n^4 + Q_{22}m^4 + 2(Q_{12} + 2Q_{33})n^2m^2$$

$$\bar{Q}_{23} = \bar{Q}_{32} = (Q_{11} - Q_{12} - 2Q_{33})n^3m + (Q_{12} - Q_{22} + 2Q_{33})nm^3$$

$$\bar{Q}_{33} = (Q_{11} + Q_{22} - 2Q_{12} - 2Q_{33})n^2m^2 + Q_{33}(n^4 + m^4)$$

where n and m have been defined in eq. (3.6) and $Q_{11}, Q_{22}, Q_{12}, Q_{21}$ and Q_{33} have been defined in eq. (3.3).

Ashton *et al.* [1] also show that an equivalent expression for strain components in the reference axes x, y in terms of the stress components in that axis can be obtained by utilizing the compliance matrix $[S]$ to describe the relationship between these components as

$$\begin{bmatrix} \varepsilon_{xx} \\ \varepsilon_{yy} \\ \varepsilon_{xy} \end{bmatrix} = [S] \begin{bmatrix} \sigma_{xx} \\ \sigma_{yy} \\ \sigma_{xy} \end{bmatrix} \tag{3.9}$$

The matrix $[S]$ is a 3×3 matrix where the components are

$$\bar{S}_{11} = S_{11}m^4 + S_{22}n^4 + (2S_{12} + S_{33})n^2m^2 \tag{3.10a}$$

$$\bar{S}_{12} = \bar{S}_{21} = S_{12}(n^4 + m^4) + (S_{11} + S_{22} - S_{33})n^2m^2 \tag{3.10b}$$

$$\bar{S}_{13} = \bar{S}_{31} = (2S_{11} - 2S_{12} - S_{33})nm^3 - (2S_{22} - S_{12} - S_{33})n^3m \tag{3.10c}$$

$$\bar{S}_{23} = \bar{S}_{32} = (2S_{11} - 2S_{12} - S_{33})n^3m - (2S_{22} - 2S_{12} - S_{33})nm^3 \tag{3.10d}$$

$$\bar{S}_{22} = S_{11}n^4 + S_{22}m^4 + (2S_{12} + S_{33})n^2m^2 \tag{3.10e}$$

$$\bar{S}_{33} = 2(2S_{11} + 2S_{12} - 4S_{22} - S_{33})n^2m^2 + S_{33}(n^4 + m^4) \tag{3.10f}$$

where m and n have been defined in eq. (3.6) and $S_{11}, S_{22}, S_{12}, S_{21}$ and S_{33} have been defined in eq. (3.4).

3.3.1.1 Engineering constants relationships. Using the approach outlined above, expressions may be obtained for the elastic properties E_{xx}, E_{yy}, G_{xy} and v_{xy}, corresponding to the $x - y$ axes, which have an orientation θ to the principal axes of the material, in terms of the elastic constants in the principal axes. By inserting the elastic constants into eq. (3.10a), we obtain

$$\frac{1}{E_{xx}} = \frac{1}{E_\theta} = \frac{1}{E_{11}}m^4 + \left[\frac{1}{G_{12}} - \frac{2v_{12}}{E_{11}}\right]n^2m^2 + \frac{1}{E_{22}}n^4 \tag{3.11}$$

Similarly for eq. (3.10e), we obtain

$$\frac{1}{E_{yy}} = \frac{1}{E_{11}}n^4 + \left[\frac{1}{G_{12}} - \frac{2v_{12}}{E_{11}}\right]n^2m^2 + \frac{1}{E_{22}}m^4 \tag{3.11a}$$

Similarly for eq. (3.10f)

$$\frac{1}{G_{xy}} = 2\left(\frac{2}{E_{11}} + \frac{2}{E_{22}} + \frac{4v_{12}}{E_{11}} - \frac{1}{G_{12}}\right)n^2m^2 + \frac{1}{G_{12}}(n^4 + m^4) \tag{3.11b}$$

Similarly for eq. (3.10b),

$$v_{xy} = E_{xx}\left(-\frac{v_{12}}{E_{11}}(n^4 + m^4) + \left(\frac{1}{E_{11}} + \frac{1}{E_{22}} - \frac{1}{G_{12}}\right)n^2m^2 \right) \qquad (3.11c)$$

Thus if E_{11}, E_{22}, G_{12} and v_{12} are known, the elastic properties at any angle to the principal axes can be calculated.

3.4 Properties of laminates

The above sections have discussed the properties of individual lamina but in practice the composite is a laminate manufactured from a number of laminae where the properties of the former are dependent on those of the latter. Because the fibre reinforced polymer is susceptible to residual stresses, the lay-up has to be correctly designed. To reach mechanical and thermal compatibility between the individual lamina (plies) and to prevent distortion after curing, several considerations have to be taken into account; some of these are:

1. The stacking sequence of the plies should be symmetrical and a minimum of three different fibre angles should be used. This leads to non-warping of the structural system and a minimum of load on the matrix. Figure 3.2 illustrates a symmetrical and a non-symmetrical lay-up.
2. The angle of the fibre between two adjacent plies should be as small as possible to prevent severe interlaminar stresses developing.
3. If possible, plies with equal fibre directions should not be stacked adjacent to each other.

An outline of the approach to predict the properties of laminates based upon classical laminate theory is given below.

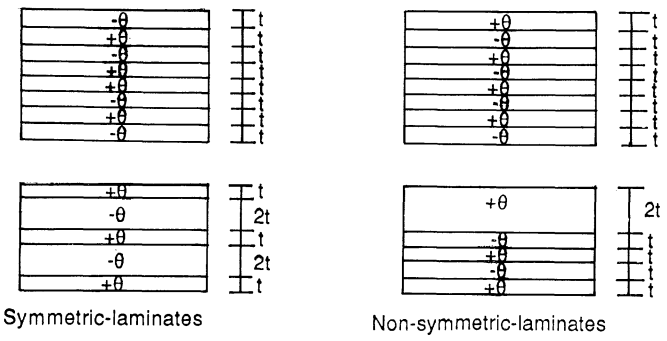

Figure 3.2 Typical stacking sequence for symmetrical and non-symmetrical angle-ply laminate.

The following four points should be mentioned.

1. there is a complete bond between all laminae, i.e. the strains at any section in each lamina are the same;
2. the bond line between the lamina is infinitely thin;
3. the laminate has the properties of a thin sheet:
4. the laminae have the same stress–strain relationship but are, of course, orientated at different directions to each other.

The stress–strain relationship for the mth layer of the laminate in the x, y coordinate system at an angle θ to the principal material directions is

$$\begin{bmatrix} \sigma_{xx} \\ \sigma_{yy} \\ \sigma_{xy} \end{bmatrix}_m = \begin{bmatrix} \bar{Q}_{11} & \bar{Q}_{12} & \bar{Q}_{13} \\ \bar{Q}_{21} & \bar{Q}_{22} & \bar{Q}_{23} \\ \bar{Q}_{31} & \bar{Q}_{32} & \bar{Q}_{33} \end{bmatrix}_m \begin{bmatrix} \varepsilon_{xx} \\ \varepsilon_{yy} \\ \varepsilon_{xy} \end{bmatrix}_m \tag{3.12}$$

the values of the various $\bar{Q}_{ij}$ have to be computed for each layer to enable the stress distribution to be evaluated for a given strain and then the resultant forces and moments per unit length acting on the laminate can be determined by integrating each lamina stress through the thickness of the composite.

Two examples to illustrate the above are considered; the first is a symmetric balanced cross-ply laminate fabricated from laminae as shown in Figure 3.3(a)

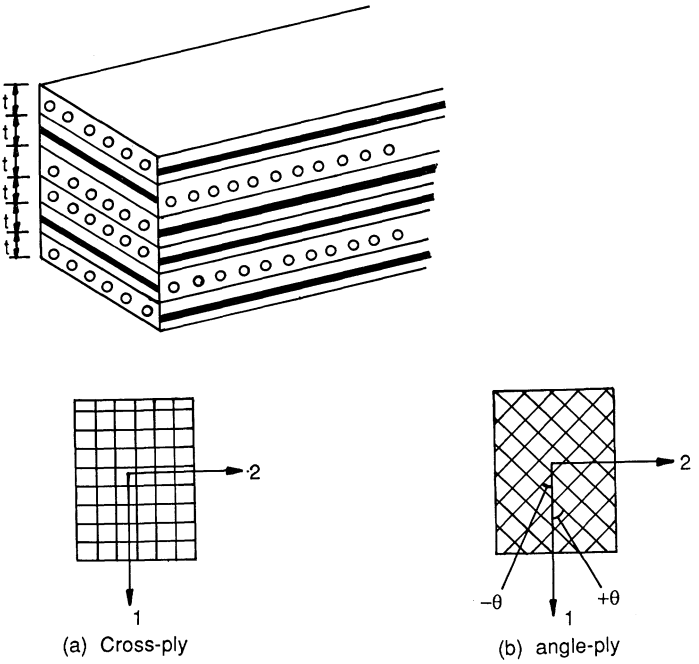

Figure 3.3 Symmetric balanced laminate.

and the second is a balanced symmetric angle-ply laminate shown in Figure 3.3(b).

The ratio of the thickness of each type of lamina for the balanced cross-ply is at_1/bt_2, consequently, the ratio of the volume fraction is V_a/V_b. The laminate has orthotropic elastic properties and consequently the stress–strain relationship for this laminate when tested in the principal material directions is

$$\begin{bmatrix} (\sigma_{11})_c \\ (\sigma_{22})_c \\ (\sigma_{12})_c \end{bmatrix} = \begin{bmatrix} (Q_{11})_c & (Q_{12})_c & (Q_{13})_c \\ (Q_{21})_c & (Q_{22})_c & (Q_{23})_c \\ (Q_{31})_c & (Q_{32})_c & (Q_{33})_c \end{bmatrix} \begin{bmatrix} (\varepsilon_{11})_c \\ (\varepsilon_{22})_c \\ (\varepsilon_{12})_c \end{bmatrix} \tag{3.13}$$

where $(Q_{13})_c = (Q_{23})_c = (Q_{31})_c = (Q_{32})_c = 0$ and the subscript c refers to the cross-ply lamina.

The value of the reduced stiffness matrix $(Q_{ij})_c$ in eq. (3.13) is obtained from the stiffness of the individual laminae.

$$(Q_{ij})_c = \sum_{m=1}^{m=M} [\bar{Q}_{ij}]_m V_m \tag{3.14}$$

Therefore

$$\begin{aligned} (Q_{11})_c &= V_a Q_{11} + V_b Q_{22} \\ (Q_{12})_c &= V_a Q_{12} + V_b Q_{21} = Q_{12} \\ (Q_{22})_c &= V_a Q_{11} + V_b Q_{22} \\ (Q_{33})_c &= V_a Q_{33} + V_b Q_{33} = Q_{33} \end{aligned} \tag{3.14a}$$

where Q_{11}, Q_{22}, Q_{33} and Q_{12} are given in eq. (3.3).

The balanced symmetric angle-ply laminates shown in Figure 3.3(b) have orthotropic elastic properties, consequently the reduced stiffness modulus $(Q_{ij})_a$, where the angles of the plies are at $\pm\theta$ to the principal axes of the material (direction 1) are

$$\begin{aligned} (Q_{11})_a &= \bar{Q}_{11}, \qquad (Q_{12})_a = \bar{Q}_{12} \\ (Q_{22})_a &= \bar{Q}_{22}, \qquad (Q_{33})_a = \bar{Q}_{33} \end{aligned}$$

The subscript a refers to the angle-ply lamina; these values are given in eq. (3.8). The terms $(Q_{13})_a$ and $(Q_{23})_a$ are zero for the special case of balanced and symmetric angle-ply laminates, as the contribution from each layer to the $(Q_{13})_a$ and $(Q_{23})_a$ cancel each other out.

3.4.1 Stress within individual laminae

The fracture mechanism of a lamina which causes failure of the composite may be due to

(a) fibre fracture;

(b) transverse tensile cracking parallel to fibre;
(c) shear fracture parallel to fibres.

The strain–stress equation for a laminate is the inverse of the stress–strain equation and is written as

$$\begin{bmatrix} (\varepsilon_{11})_c \\ (\varepsilon_{22})_c \\ (\varepsilon_{12})_c \end{bmatrix} = \begin{bmatrix} (S_{11})_c & (S_{12})_c & (S_{13})_c \\ (S_{21})_c & (S_{22})_c & (S_{23})_c \\ (S_{31})_c & (S_{32})_c & (S_{33})_c \end{bmatrix} \begin{bmatrix} (\sigma_{11})_c \\ (\sigma_{22})_c \\ (\sigma_{12})_c \end{bmatrix} \tag{3.15}$$

where the subscript c refers to the cross-ply laminates.

Considering a cross-ply or an angle-ply laminate of constant thickness shown in Figure 3.3 in which the line of action of the load is along the principal axes of the composite which in turn lie along the line of symmetry, the strain values in the principal directions 1 and 2 are

$$\begin{aligned} (\varepsilon_{11})_c &= (S_{11})_c(\sigma_{11})_c + (S_{12})_c(\sigma_{22})_c \\ (\varepsilon_{22})_c &= (S_{21})_c(\sigma_{11})_c + (S_{22})_c(\sigma_{22})_c \\ (\varepsilon_{12})_c &= 0 \end{aligned} \tag{3.15a}$$

For the situation regarding the symmetric cross-ply laminate, shown in Figure 3.3(a), where θ is equal to 0° and 90° (i.e. the principal axes of the laminae coincide with the fibre directions) and the various laminae are fabricated alternately in these two directions, the strains in lamina 1 in direction 1 are

$$(\varepsilon_{11})_1 = (\varepsilon_{11})_c, \qquad (\varepsilon_{22})_1 = (\varepsilon_{22})_c, \qquad (\varepsilon_{12})_1 = (\varepsilon_{12})_c \tag{3.16}$$

and the strains in lamina 2 in direction 2 (i.e. in the fibre direction for lamina 2) are

$$(\varepsilon_{22})_2 = (\varepsilon_{22})_c, \qquad (\varepsilon_{11})_2 = (\varepsilon_{11})_c, \qquad (\varepsilon_{12})_2 = (\varepsilon_{12})_c \tag{3.17}$$

The stresses in the individual lamina are obtained from eq. (3.3), consequently, stresses in direction 1 and 2 for lamina 1 can be obtained:

$$\begin{aligned} (\sigma_{11})_1 &= Q_{11}(\varepsilon_{11})_c + Q_{12}(\varepsilon_{22})_c \\ (\sigma_{22})_1 &= Q_{12}(\varepsilon_{11})_c + Q_{22}(\varepsilon_{22})_c \\ (\sigma_{12})_1 &= Q_{33}(\varepsilon_{12})_c \end{aligned} \tag{3.18}$$

Substituting eq. (3.15a) into eq. (3.18) gives

$$\begin{aligned} (\sigma_{11})_1 &= Q_{11}[(S_{11})_c(\sigma_{11})_c + (S_{12})_c(\sigma_{22})_c] + Q_{12}[(S_{12})_c(\sigma_{11})_c + (S_{22})_c(\sigma_{22})_c] \\ (\sigma_{22})_1 &= Q_{12}[(S_{11})_c(\sigma_{11})_c + (S_{12})_c(\sigma_{22})_c] + Q_{22}[(S_{12})_c(\sigma_{11})_c + (S_{22})_c(\sigma_{22})_c] \\ (\sigma_{12})_1 &= 0 \end{aligned} \tag{3.18a}$$

If the line of action of the load is parallel to direction 1 then $(\sigma_{22})_c = 0$ and eq. (3.18a) becomes

$$\begin{aligned}(\sigma_{11})_1 &= (\sigma_{11})_c[Q_{11}(S_{11})_c + Q_{12}(S_{12})_c] \\ (\sigma_{22})_1 &= (\sigma_{11})_c[Q_{12}(S_{11})_c + Q_{22}(S_{12})_c]\end{aligned} \tag{3.18b}$$

The values of $(S_{11})_c$, $(S_{22})_c$, $(S_{12})_c$ and $(S_{33})_c$ may be obtained by inversion of eq. (3.13):

$$\begin{aligned}(S_{11})_c &= \frac{(Q_{22})_c}{(Q_{11})_c(Q_{22})_c - (Q_{12}^2)_c} \\ (S_{22})_c &= \frac{(Q_{11})_c}{(Q_{11})_c(Q_{22})_c - (Q_{12}^2)_c} \\ (S_{12})_c &= \frac{-(Q_{12})_c}{(Q_{11})_c(Q_{22})_c - (Q_{12}^2)_c}\end{aligned} \tag{3.19}$$

By combining eqs (3.3), (3.14a), (3.18) and (3.19) and assuming $V_A = V_B = 1/2$, then

$$\begin{aligned}\frac{(\sigma_{11})_1}{(\sigma_{11})_c} &= \frac{1/2E_{11}(E_{11} + E_{22}) - v_{12}^2E_{22}^2}{1/4(E_{11} + E_{22})^2 - v_{12}^2E_{22}^2} = A \\ \frac{(\sigma_{22})_1}{(\sigma_{11})_c} &= \frac{1/2v_{12}E_{22}(E_{11} - E_{22})}{1/4(E_{11} + E_{22})^2 - v_{12}^2E_{22}^2} = B\end{aligned} \tag{3.20}$$

Similarly

$$\begin{aligned}\frac{(\sigma_{11})_2}{(\sigma_{11})_c} &= \frac{1/2v_{12}E_{22}(E_{22} - E_{11})}{1/4(E_{11} + E_{22})^2 - v_{12}^2E_{22}^2} = C \\ \frac{(\sigma_{22})_2}{(\sigma_{11})_c} &= \frac{1/2E_{22}(E_{11} + E_{22}) - v_{12}^2E_{22}^2}{1/4(E_{11} + E_{22})^2 - v_{12}^2E_{22}^2} = D\end{aligned} \tag{3.21}$$

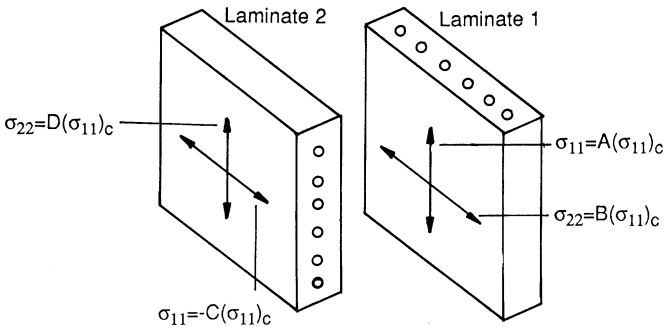

Figure 3.4 Symmetric angle-ply: laminate stresses.

Note that in eq. (3.21), the suffixes for the stresses refer to the coordinate axes for lamina 2 shown in Figure 3.4 where direction 1 is the direction of the major axes for that lamina.

Similar equations, but more complicated than those developed above, may be obtained for the angle-ply laminates.

3.5 Yield strength of polymers

The yield strength of polymers is highly dependent upon the biaxial stress conditions of the material. Figure 3.5 shows the locus of yield strengths of polymers in a biaxial stress field [2].

A failure theory related to the applied tensile or compressive stresses that cause failure in uniaxial tests irrespective of whether it was a normal or shear failure is the von Mises criterion; this criterion was originally applied to homogeneous isotropic material. For the case where $\sigma_{zz} = 0$, von Mises biaxial state of stress may be stated as

$$\sigma_{xx}^2 + \sigma_{yy}^2 - \sigma_{xx}\sigma_{yy} = \sigma^{*2} \tag{3.22}$$

This equation does not define precisely the polymer condition at failure which must take account of the differences in σ_{yc} and σ_{yt} and the influence of the mean normal stress. The stresses σ_{11} and σ_{12} are the principal stresses and the stresses σ_{yc} and σ_{yt} are the yield strength in compression and tension, respectively, of the material. Equation (3.22), therefore, is refined to

$$\sigma_{11}^2 + \sigma_{22}^2 + (\sigma_{11} + \sigma_{22})(\sigma_{yc} - \sigma_{yt}) - \sigma_{11}\sigma_{22} = \sigma_{yc}\sigma_{yt} \tag{3.23}$$

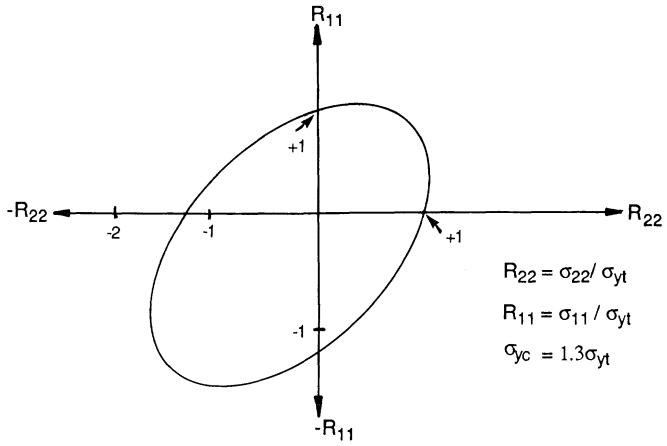

Figure 3.5 A typical locus of yield strength of a polymer in a biaxial stress field (based on [2]).

If eq. (3.23) is normalized by introduction ratios

$$R_{11} = \sigma_{11}/\sigma_{yt} \quad \text{and} \quad R_{22} = \sigma_{22}/\sigma_{yt}$$

eq. (3.24) is formed:

$$R_{11}^2 + R_{22}^2 - R_{11}R_{22} + (R_{11} + R_{22})\left(\frac{\sigma_{yc}}{\sigma_{yt}} - 1\right) = \frac{\sigma_{yc}}{\sigma_{yt}} \tag{3.24}$$

Figure 3.5 shows a number of different polymers where the results have been normalized.

3.6 Strength theories of undirectional laminae

3.6.1 Longitudinal tensile strength

In section 2.4 the micro-analysis of unidirectional laminae was discussed and the relationship between the stress of the composite σ_c and the stress in the fibre and matrix was given as

$$\sigma_c = \sigma_{11} = \sigma_f V_f + \sigma_m V_m \tag{3.25}$$

where the suffixes f and m refer to fibre and matrix, respectively.

This relationship is an over-simplification and although in some cases it is a good approximation, it takes no account of the statistical scatter in fibre strengths and the influence of the micro-structural defects. Equation (3.25) may be modified to include these effects, thus the equation becomes

$$\sigma_{11} = \beta\sigma_\beta V_f + \sigma_m V_m$$

where σ_β is the fibre bundle strength and β is the matrix efficiency factor (this value lies between 1 and 2).

The response of the composite as the load increases to failure will depend on the relative strains to failure of the matrix and the fibre. There are two possible conditions, either ε_f^* is greater than ε_m^* or ε_m^* is greater than ε_f^* where the * refers to the failure strain in uniaxial tension. The first and second conditions are represented in graphical form in Figure 3.6 and it will be seen that there are two distinct failure modes for each condition. For low V_f when ε_f^* is greater than ε_m^* the lamina strength is primarily dependent on σ_m^*. When the matrix fails, all the load is transferred to the fibre and if the magnitude of the fibre volume fraction is low, the fibres will fail and complete rupture of the composite will take place. If, however, the magnitude of the V_f is high, the fibre will take the excess load and the composite will not fail until

$$\sigma_{11}^* = \sigma_f^* V_f$$

If the strain in the matrix is greater than the strain in the fibre, a similar argument applies. With a low fibre volume fraction, the extra load applied

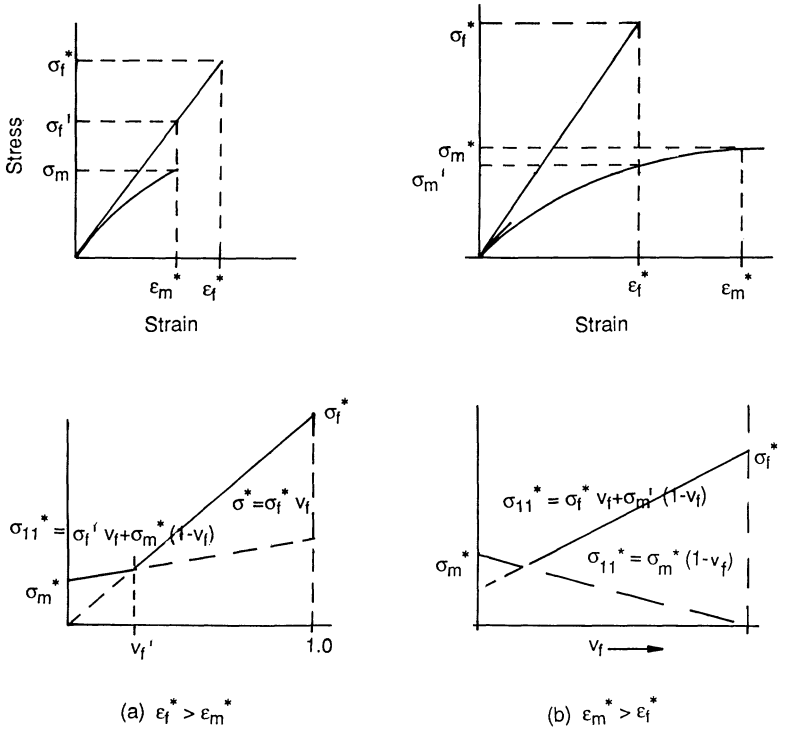

Figure 3.6 Stress–strain curves for fibre and resin and fracture strength–fibre volume fraction of laminate. (a) $\varepsilon_f^* > \varepsilon_m^*$; (b) $\varepsilon_m^* > \varepsilon_f^*$.

to the matrix when the fibres fail will not be sufficient to fail the matrix. When V_f is large, the load transferred to the matrix is also large and it fractures; at this point the equation is

$$\sigma_{11}^* = \sigma_f^* V_f + \sigma_m(1 - V_f) \tag{3.26}$$

where σ_m fails immediately σ_f fails.

3.6.2 Transverse tensile strength

Unidirectional laminae have very low transverse tensile strength and this does present a problem in some designs of composite structures. Ideally fibres would be orientated to lie parallel to the external loads but transverse stresses cannot always be avoided and they may lead to fracture failures of the composite. The transverse strength depends on the properties of the fibre and matrix components, the interface bond and the internal strain distribution due to the presence of voids within the composite. The constraints placed on the matrix by the fibres cause strain and stress concentrations in the

matrix adjacent to the fibre and thus result in composite failure at a much lower strain than the strain at which the unrestrained matrix material would fail. Therefore, unlike the increase in longitudinal strength and stiffness and the transverse modulus, the transverse strength is reduced in the presence of the fibres, this implies the fibres have a negative reinforcing effect.

The transverse tensile strength of a composite can be predicted assuming that it is controlled by the matrix ultimate strength. It is also assumed that the composite strength is lower than the matrix strength by a factor s defined below. The composite transverse strength can be expressed as

$$\sigma_{tu} = \frac{\sigma_m^*}{s} \quad \text{or} \quad \varepsilon_{tu} = \frac{\varepsilon_m^*}{s'}$$

where s is the strength reduction factor, s' is the strain magnification factor, σ_m^* is the ultimate failure stress of the matrix and ε_m^* is the ultimate failure strain of the matrix. If Poisson's ratio effects are negligible, then

$$\begin{aligned} s &= \{1 - V_f[1 - E_m/E_f]\}/\{1 - (4V_f/\pi)^{1/2}[1 - E_m/E_f]\} \\ s^1 &= 1/\{1 - (4V_f/\pi)^{1/2}[1 - E_m/E_f]\} \end{aligned} \tag{3.27}$$

where the notation has its usual meaning.

Nielsen [3] has proposed an empirical formula for the prediction of the transverse tensile strength of fibrous composites. The composite strain at failure may be approximated as

$$\varepsilon_c^* = \varepsilon_m^*(1 - V_f^{1/3}) \tag{3.28}$$

where ε_c^* is the ultimate failure strain of the composite in the transverse direction and ε_m^* is the ultimate failure strain in the matrix.

3.6.3 Longitudinal compressive strength

The longitudinal compressive strength is dependent on a number of parameters which include the fibre volume fraction, the fibre and matrix mechanical properties, void content and the interface bond strength.

The longitudinal failure of a unidirectional composite under a compressive load is generally associated with the local and overall buckling of fibres and it is assumed that each fibre acts independently of its neighbour. However, the fibres are restricted by the matrix surrounding them. From the Rosen model [4], the buckling compressive strength for low fibre volume fractions is represented by an out-of-phase mode (the extensional mode) and it is assumed that adjacent fibres will buckle with equal wavelengths at the ultimate load.

$$(\sigma_{11}^*)_c = 2V_f[V_f E_m E_f/3(1 - V_f)]^{1/2} \tag{3.29}$$

and is represented in Figure 3.7(a).

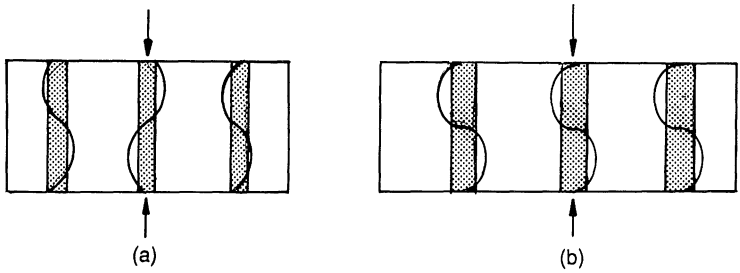

Figure 3.7 Schematic representation of (a) out-of-phase and (b) in-phase mode of buckling in unidirectional laminate.

For high fibre volume fractions, the buckling compressive strength is represented by an in-plane mode (the shear mode) given by

$$(\sigma_{11}^*)_c = G_m/(1 - V_f) \tag{3.30}$$

and is represented in Figure 3.7(b).

For both buckling modes, the fibres are regarded as plates with thickness h and separated by a matrix of width $2c$. Each fibre is subjected to a compressive load P and is of length L. The fibres are also regarded as being much stiffer than the matrix (that is $G_f \gg G_m$) so the fibre shearing deformations are neglected.

In the practical range of V_f the shear mode tends to dominate and the compressive strength is then highly dependent on the shear modulus of the matrix. Hull [2] has given a comparison of experimental and predicted values of longitudinal compressive strength of unidirectional laminae; these values are reproduced in Table 3.1. The agreement is poor; it can be seen that the predicted values are much greater than the experimental values. This would indicate that either the modelling is wrong or that the assumptions are over-simplified. By comparing the results of Table 3.1, it may be concluded that a different model is required for different fibre/resin systems.

Fibre buckling can also be caused by shrinkage stresses developed during

Table 3.1 Comparison of experimental and predicted values of longitudinal compressive strength of unidirectional laminae $V_f \sim 0.50$ (after Hull [2])

Material	$(\sigma_{11}^*)_c$ experimental (MPa)	$(\sigma_{11}^*)_c$ predicted eq. (3.29) (MPa)	$(\sigma_{11}^*)_c$ predicted eq. (3.30) (MPa)
Glass/polyester	600–1000	8700	2200
Carbon/epoxy (type 1)	700–900	22800	2900
Kevlar 49/epoxy	240–290	13200	2900

curving of the composite. The shrinkage stresses result from the matrix having a higher thermal coefficient of expansion than the fibre.

The factors which will have a de-stabilizing effect on the buckling strengths of undirectionally aligned composites are:

(a) fibre and resin rich areas within the composite;
(b) voids within the resin;
(c) fibres that are poorly aligned;
(d) fibre debonding due to poor compaction of the matrix around the fibre; it may also occur due to the different Poisson's ratio of fibre and resin;
(e) matrix ultimate strain.

An observation that has been made is that transverse splitting or debonding might be the initiating component, this has led to the formulation of a simple theoretical expression for the maximum composite strength as

$$\sigma_{c_{max}} = \{(E_f V_f + E_m V_m)(1 - V_f^{1/3})\varepsilon_{mu}\}/\{\nu_f V_f + \nu_m V_m\} \tag{3.31}$$

where ε_{mu} is the ultimate strain of the matrix.

3.6.4 Shear strength

It has been suggested by Ewins and Ham [5] that shear stresses developed in a unidirectional laminate when under compressive loading may cause a shear mode failure as shown in Figure 3.8. The shear stress would then be

$$(\sigma_{12}^*)_s = \sigma_{11} \sin\theta \cos\theta \tag{3.32}$$

the maximum value of the shear stress will occur when $\theta = 45°$ and $(\sigma_{12}^*)_{s_{max}} = 1/2(\sigma_{11})_c$. If the above strength is less than that for the buckling , then the failure mechanism will be shear.

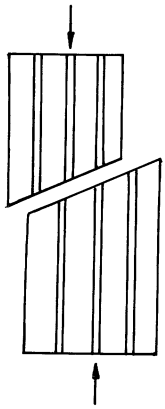

Figure 3.8 Diagrammatic view of shear fracture under a longitudinal compressive load.

3.7 Strength and failure criteria of orthotropic laminates not loaded in the principal directions

The results of the orthotropic material analysis are based on the uniaxial strength properties in the three principal axes. These tests will determine the modulus of elasticity, Poisson's ratio and the strength characteristics in the direction of the principal axes and, as stated earlier, will eliminate any coupling effects of shearing and normal strains that would occur if the laminate were tested in any other direction.

The orthotropic material properties must be determined in the direction of the principal axes from separate tests. This means that independent ultimate uniaxial strengths must be determined in the 1, 2 and 3 directions and a separate test to determine the shear strengths in these directions must be undertaken. These tests are shown schematically in Figure 3.9.

The stress conditions in orthotropic materials are considered in connection with the normal and shearing components relative to their principal axis.

The simple failure criteria which follow have been derived on the assumption that the macromechanical values are based on the average stresses and strains in a single orthotropic layer loaded in plane (i.e. $\sigma_{33} = \sigma_{13} = \sigma_{23} = 0$).

The Grant–Sanders criterion is a simplified version of a criterion based on a three-dimensional laminate and is included to illustrate the relative complexity of failure criteria which are based on distinct observed failure modes.

3.7.1 Maximum stress theory of fracture

The maximum stress theory of failure assumes that failure occurs when the stress in the principal material axis reaches a critical value. There are three possible modes of failure and the conditions for these are:

$$\sigma_{11} = \sigma_{11}^* \qquad \sigma_{22} = \sigma_{22}^*, \qquad \sigma_{12} = \sigma_{12}^*$$

where σ_{11}^* and σ_{22}^* are the ultimate tensile or compressive stress in direction

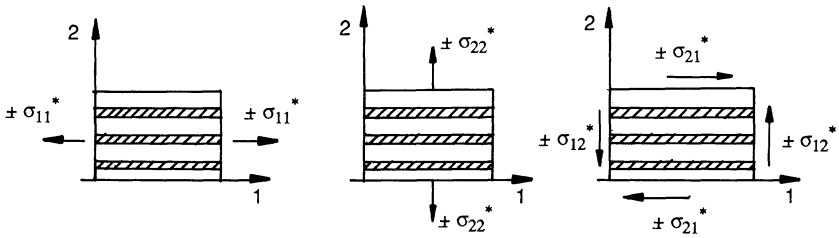

Figure 3.9 Critical stress value in the principal material axes.

1 or 2 respectively, and σ_{12}^* is the ultimate shear stress acting in plane 1 in direction 2.

If the load were applied to the laminate at an angle θ to the principal axis direction (i.e. the off-axis ultimate tensile strength, see Figure 3.1(a)), then by transformation:

$$\begin{aligned}\sigma_{11} &= \sigma_{xx}\cos^2\theta = \sigma_\theta \cos^2\theta \\ \sigma_{22} &= \sigma_{xx}\sin^2\theta = \sigma_\theta \sin^2\theta \\ \sigma_{12} &= -\sigma_{xx}\sin\theta\cos\theta = -\sigma_\theta \sin\theta\cos\theta\end{aligned} \tag{3.33}$$

If $\theta = 0°$, $\sigma_\theta = \sigma_{11}$ and failure would occur in the longitudinal direction. If $\theta = 90°$, $\sigma_\theta = \sigma_{22}$ and failure would occur in the transverse direction. The off-axis ultimate tensile strength σ_θ is the smallest value of the following

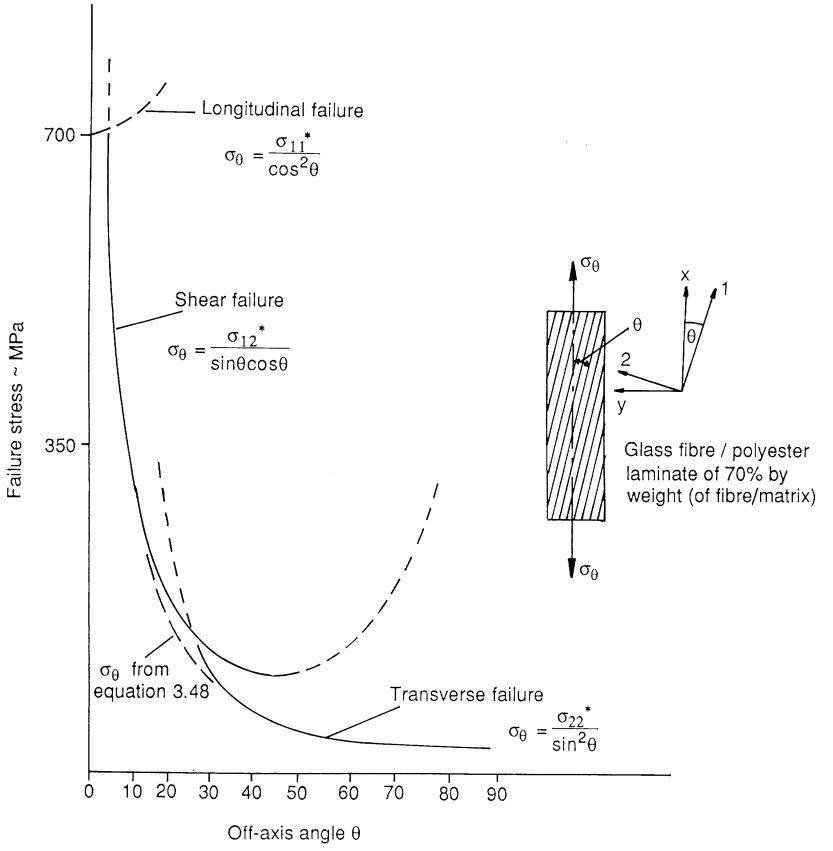

Figure 3.10 Typical failure stress of unidirectional glass fibre–polyester polymer laminae predicted by maximum stress theory for off-axis tests.

stresses:

$$\sigma_\theta = \sigma_{11}^*/\cos^2\theta$$
$$\sigma_\theta = \sigma_{22}^*/\sin^2\theta \qquad (3.34)$$
$$\sigma_\theta = \sigma_{12}^*/\sin\theta\cos\theta$$

Figure 3.10 shows a typical failure envelope, based on eq. (3.34), for a unidirectional glass fibre-polyester polymer lamina as θ varies between 0° and 90° (cf. Figure 2.6).

3.7.2 Maximum strain theory of fracture

The maximum strain theory of fracture assumes that failure occurs when the strains in the principal material axes reach a critical value. There are three possible modes of failure, these are:

$$\varepsilon_{11} = \varepsilon_{11}^*, \qquad \varepsilon_{22} = \varepsilon_{22}^*, \qquad \varepsilon_{12} = \varepsilon_{12}^* \qquad (3.35)$$

where ε_{11}^* and ε_{22}^* are the maximum tensile or compressive strains in direction 1 or 2, respectively, and ε_{12}^* is the maximum shear strain on plane 1 in direction 2.

3.7.3 Interaction theory (Tsai–Hill failure criterion)

There have been many theories and hypotheses developed to enable predictions of 'failure surfaces' under combined loading conditions where interaction between different failure modes is important, but none is wholly satisfactory and more investigative work is required in this area.

The Tsai–Hill criterion is one of the best known and is based on the von Mises failure criterion for homogeneous isotropic bodies, modified by Hill [6] to suit anisotropic materials and finally applied to composite materials by Tsai [7].

In the development of the deviational strain energy for isotropic material, it is assumed that the normal stresses causing failure are the principal stresses. If the failure stresses had not been the principal stresses, the lamina's plane of failure would have been subjected to shear stresses in addition to the normal stresses. This would have given rise to additional shear strains. The additional deviational strain energy is

$$\tfrac{1}{2}\sigma_{xy}\varepsilon_{xy} + \tfrac{1}{2}\sigma_{yz}\varepsilon_{yz} + \tfrac{1}{2}\sigma_{zx}\varepsilon_{zx} \qquad (3.36)$$

and shear strain energy is

$$\{(1+\nu)/E\}[\sigma_{xy}^2 + \sigma_{yz}^2 + \sigma_{zx}^2] \qquad (3.37)$$

The total deviational strain energy, therefore, is the sum of the components

from the normal strain and the shear strain energies:

$$U_D = \{(1+\nu)/6E\}[(\sigma_{xx}-\sigma_{yy})^2+(\sigma_{yy}-\sigma_{zz})^2+(\sigma_{zz}-\sigma_{xx})^2] + \{(1+\nu)/E\}[\sigma_{xy}^2+\sigma_{yz}^2+\sigma_{zx}^2] \tag{3.38}$$

Equating eq. (3.38) to the failure in a uniaxial test in terms of the deviational strain energy, gives

$$\{(1+\nu)/6E\}[2\sigma^{*2}] = \{(1+\nu)/6E\}[(\sigma_{xx}-\sigma_{yy})^2+(\sigma_{yy}-\sigma_{zz})^2+(\sigma_{zz}-\sigma_{xx})^2] + [(1+\nu)/E][\sigma_{xy}^2+\sigma_{yz}^2+\sigma_{zx}^2]$$

or

$$1 = \frac{1}{2\sigma^{*2}}[(\sigma_{xx}-\sigma_{yy})^2+(\sigma_{yy}-\sigma_{zz})^2+(\sigma_{zz}-\sigma_{xx})^2] + \{3/\sigma^{*2}\}[\sigma_{xy}^2+\sigma_{yz}^2+\sigma_{zx}^2] \tag{3.39}$$

If eq. (3.39) is the assumed failure criterion for orthotropic materials, then the final equation must be expressed in terms of the stresses in the principal directions together with the three normal strengths σ_{11}, σ_{22} and σ_{33} and the three corresponding shear strengths $\sigma_{12}, \sigma_{23}, \sigma_{31}$; the yield criterion is given as

$$H(\sigma_{11}-\sigma_{22})^2+G(\sigma_{22}-\sigma_{33})^2+F(\sigma_{33}-\sigma_{11})^2 + 2N\sigma_{12}^2+2M\sigma_{23}^2+2L\sigma_{31}^2 = 1 \tag{3.40}$$

which is analogous to eq. (3.39). The parameters F, G, H, L, M and N are the Hill's yield strength and are regarded as the failure strengths of the lamina.

If σ_{12} acts on the lamina only, then at failure

$$2N = 1/\sigma_{12}^{*2} \tag{3.41}$$

The values of M and L are given in terms of the shearing strengths relative to the axes 2–3 and 3–1, respectively; under plane stress $\sigma_{23} = \sigma_{31} = 0$. Also if σ_{11} acts on the lamina only, then

$$F + H = 1/\sigma_{11}^{*2} \tag{3.42}$$

and if σ_{22} acts on the lamina only, then

$$G + H = 1/\sigma_{22}^{*2} \tag{3.43}$$

Similarly

$$F + G = 1/\sigma_{33}^{*2} \tag{3.44}$$

On combining equations (3.42), (3.43), and (3.44)

$$2H = \frac{1}{\sigma_{11}^{*2}} + \frac{1}{\sigma_{22}^{*2}} - \frac{1}{\sigma_{33}^{*2}}$$

$$2G = \frac{1}{\sigma_{22}^{*2}} + \frac{1}{\sigma_{33}^{*2}} - \frac{1}{\sigma_{11}^{*2}}$$

$$2F = \frac{1}{\sigma_{33}^{*2}} + \frac{1}{\sigma_{11}^{*2}} - \frac{1}{\sigma_{22}^{*2}} \tag{3.45}$$

For a undirectional lamina (i.e. orthotropic materials) under plane stress when the fibres are in direction 1, then $\sigma_{33} = \sigma_{13} = \sigma_{23} = 0$ and, in addition, from geometrical symmetry, $\sigma_{22}^* = \sigma_{33}^*$. Thus the failure criterion in terms of the lamina strengths $\sigma_{11}^*, \sigma_{22}^*$ and σ_{33}^* becomes

$$\frac{\sigma_{11}^2}{\sigma_{11}^{*2}} - \frac{\sigma_{11}\sigma_{22}}{\sigma_{11}^{*2}} + \frac{\sigma_{22}^2}{\sigma_{22}^{*2}} + \frac{\sigma_{12}^2}{\sigma_{12}^{*2}} = 1 \tag{3.46a}$$

The equation, known as the Tsai–Hill condition, describes a failure envelope. Consequently, failure of the lamina will not occur provided that σ_{11}, σ_{22} and σ_{12} all lie inside the failure envelope.

For most composite materials $\sigma_{11}^* \gg \sigma_{22}^*$ so that the second term in eq. (3.46a) tends to zero and the simplified equation is

$$\frac{\sigma_{11}^2}{\sigma_{11}^{*2}} + \frac{\sigma_{22}^2}{\sigma_{22}^{*2}} + \frac{\sigma_{12}^2}{\sigma_{12}^{*2}} = 1 \tag{3.46b}$$

For a bi-directional lamina (i.e. orthotropic material) Puppo and Evensen [8] have given the Puppo–Evensen criterion (which was originally suggested for the prediction of laminate failure). This can be written as:

$$\frac{\sigma_{11}^2}{\sigma_{11}^{*2}} - \mu\left(\frac{\sigma_{11}^*}{\sigma_{22}^*}\right)\left(\frac{\sigma_{11}}{\sigma_{11}^*} \cdot \frac{\sigma_{22}}{\sigma_{22}^*}\right) + \mu\frac{\sigma_{22}^2}{\sigma_{22}^{*2}} + \frac{\sigma_{12}^2}{\sigma_{12}^{*2}} = 1 \tag{3.47}$$

Using the Tsai–Hill eq. (3.46a) in conjunction with eq. (3.34), a prediction can be made of the failure strength in direction θ to the principal axes (see Figure 3.1) of a unidirectional lamina by the use of the design equation:

$$\sigma_{xx} = \sigma_\theta = \left[\frac{\cos^4\theta}{\sigma_{11}^{*2}} + \frac{\sin^4\theta}{\sigma_{22}^{*2}} + \frac{\sin^2\theta\cos^2\theta}{\sigma_{12}^{*2}} - \frac{\sin^2\theta\cos^2\theta}{\sigma_{11}^{*2}}\right]^{-1/2} \tag{3.48}$$

It has been shown that there is a reasonable agreement between this theory and experimental results for E-glass/epoxy composites [9]. Hull [2] has found close agreement between carbon fibre/epoxy resin laminate. It may therefore be concluded that this failure criterion is suitable for off-axes tests on unidirectional laminae at various orientations of load applications and that it represents a more realistic criterion for the failure of composite materials than the previous two theories.

The significance of the material anisotropy in polymer composites is illustrated in Figures 2.6 and 3.11; the graphs of E_θ (Figure 3.11a) and σ_θ (Figure 3.11b) have been plotted as a function of orientation angle θ for typical

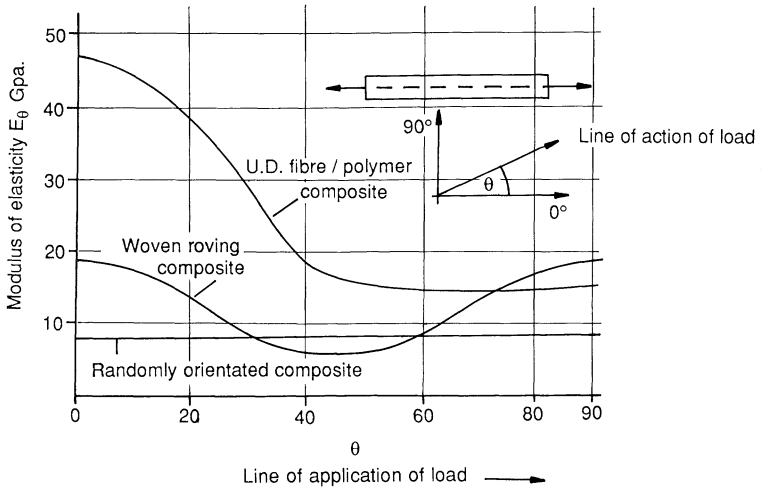

(a)

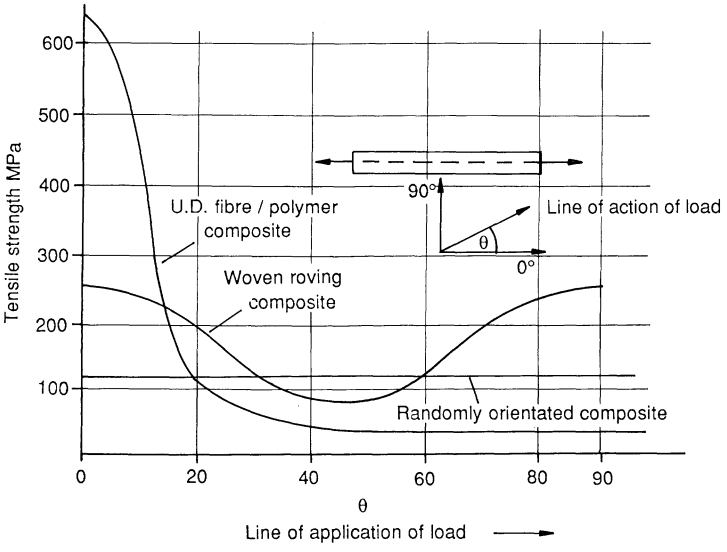

(b)

Figure 3.11 Typical variations of modulus of elasticity and strength values of laminae of glass fibre–polyester resin.

GFRP composites of unidirectional aligned glass/polyester, woven rovings glass/polyester and randomly orientated glass/polyester with typical fibre matrix ratios of 70%, 50% and 30% respectively. One specific feature of the graphs is the large reduction in properties of the woven roving composite at 45° to the warp direction. These graphs have been computed from eqs (3.11) and (3.48).

3.7.4 Grant–Sanders method

This method employs a number of separate criteria, some of which are simple while others are more complicated and involve the interaction between stress and strain components, to assess the possibility of failure in each of the distinct modes identified by a study of individual layers in multilayered laminates.

For individual lamina the criteria are

$$\sigma_{11} = (\sigma^*_{11})_c = (\sigma^*_{11})_t$$

where the suffixes c and t refer to compression and tension loading states,

$$(\varepsilon_{11})_m = \varepsilon^*_m, \qquad (\varepsilon_{22})_m = \varepsilon^*_m$$
$$\sigma_{12} = (\sigma^*_{12})_f = (\sigma^*_{12})_m \tag{3.49}$$

For combined tension and shear

$$\left(\frac{\varepsilon_{12}}{(\varepsilon^*_{12})_m}\right)^2 + \left(\frac{\varepsilon_{11}}{\varepsilon^*_m}\right)^2 = 1 \tag{3.50}$$

or

$$\left(\frac{\varepsilon_{12}}{(\varepsilon^*_{12})_m}\right)^2 + \left(\frac{\varepsilon_{22}}{\varepsilon^*_m}\right)^2 = 1 \tag{3.51}$$

For combined compression and shear

$$\frac{\sigma_{12}}{K(\sigma^*_{12})_m} - \frac{\sigma_{11}}{\sigma^*_{11}} = 1$$

where K is a factor determined by experiment and is usually ~ 1.5.

3.8 Characteristics of laminated composites

In the previous sections attention has been directed towards single lamina composites. However, in practice composite materials consist of a number of individual lamina which are effectively 'bonded' together by the polymer used in the manufacture of the lamina. If the separate lamina had been manufactured by utilizing randomly orientated fibres in the matrix, the

resulting laminae (composite) will also possess similar in-plane properties and the whole will be considered to be quasi-isotropic. If, however, the separate lamina possess orthotropic properties by virtue of the orientation of the fibres in the matrix material, then the resulting composite will have properties depending upon the final arrangement of each individual lamina within the composite.

If the thickness of the laminated composite is produced from several laminae, whose properties vary in given directions, the composite may not be uniform about the centre-line of the cross-section and under in-plane forces, a complex stress situation will result in which flexural stresses will be developed. Shear stress would be developed through the cross-section of the composite and the limiting values of these stresses would depend upon the shear strength of the polymer.

3.8.1 Laminated composite beam behaviour

The theory of composite plates may be developed by first considering a composite beam which is a special case of a plate spanning in one direction only. The theory is discussed by considering different lamina stacking arrangements within the cross-section of the beam.

Consider a composite beam made from stacking randomly orientated fibre lamina to give a symmetric section (isotropic material) the general equation for the resultant axial force N per unit width is

$$N_{xx} = Et\left(\frac{du_0}{dx}\right)$$

and for the bending moment per unit width M_{xx} is

$$M_{xx} = (Et^3/12)\frac{d^2w}{dx^2}$$

These are the standard equations for axial and flexural effects in a rectangular beam of unit width.

The general equations for multilayered symmetric cross-sectional laminated beams are of similar form to the above but are more complex. A portion of a beam consisting of three laminates is shown in Figure 3.12(a). The stiffness expression for the in-plane forces gives a 'rule of mixture' result in which each separate component of the equation represents the stiffness of the respective composite section. In addition, the stiffness expression for the flexural forces is obtained from the separate second moments of area for the individual sections. In the above two cases, the deflections produced by the in-plane and flexural forces are uncoupled.

For a multilayered symmetric cross-section beam, in-plane and flexural expressions are produced similar to those for the symmetric sectioned beam;

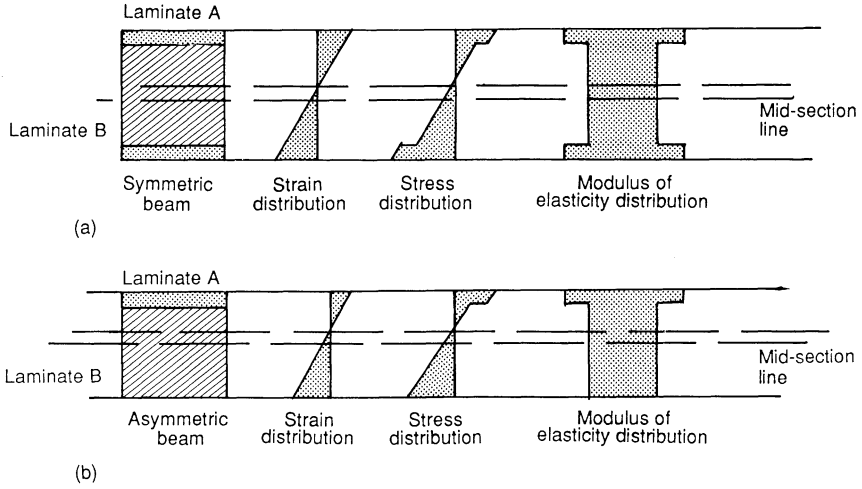

Figure 3.12 Cross-sections of laminated beams. (a) Variation of stress, strain and modulus of elasticity of a symmetric beam; (b) variation of stress, strain and modulus of elasticity of an asymmetric beam.

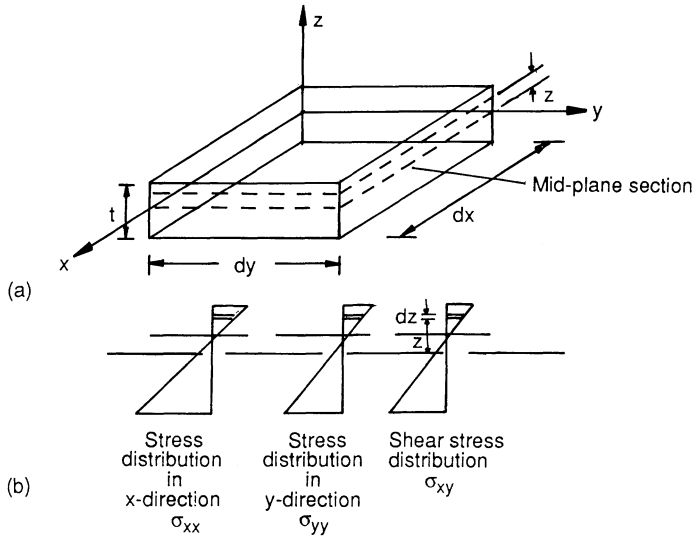

Figure 3.13 Plate element under load. (a) Rectangular plate element of thickness *t*; (b) stress distribution in an isotropic plate.

Figure 3.12(b) illustrates a two-layer beam with each layer having different material properties. In this case the deformations from the two loading components are coupled because the separate applications of in-plane and flexural forces produce both axial and flexural deformations.

The general equation for composite beams with symmetrical and asymmetrical cross-section may be expressed in the form

$$N = A\frac{du_0}{dx} + B\frac{d^2w}{dx^2} \qquad M = B\frac{du_0}{dx} + D\frac{d^2w}{dx^2} \tag{3.52a}$$

or

$$\begin{bmatrix} N \\ M \end{bmatrix} = \begin{bmatrix} A & B \\ B & D \end{bmatrix} \begin{bmatrix} du_0/dx \\ d^2w/dx^2 \end{bmatrix} \tag{3.52b}$$

For symmetrical cross-sections, the coefficient B becomes zero but it will be non-zero for asymmetrical composite cross-sectioned beams.

3.8.2 Laminated composite plate behaviour

The general case of the two-dimensional plate theory may be developed from the one-dimensional beam theory with a linear element of length dx, by considering a rectangular element with sides dx and dy as shown in Figure 3.13. The important section in these plates is the mid-plane as this will determine the symmetric or asymmetric nature of the plate.

In laminated plates, the flexural deformations can take place in both the x and y directions and also in-plane shear distortions can develop. In laminate plate theory, the following assumptions are made:

1. plane sections before deformation remain plane after deformation;
2. normals to the mid-plane surface remain normal after deformation;
3. no stresses are developed in the transverse direction.

Considering Figure 3.13a which shows an element in the xy plane, it is assumed that the displacement varies linearly through the plate thickness and the origin 0 remains fixed during bending of the laminate. For general deformations, this is not the case, consequently vectors u_0, v_0 and w_0 representing the displacement of the origin must be added to the displacement equations.

The displacements δ_u, δ_v in the x and y directions can be expressed as

$$\delta_u = \delta_{u_0} - z\frac{\delta_w}{\delta_x} \quad \text{and} \quad \delta_v = \delta_{v_0} - z\frac{\delta_w}{\delta_y}$$

The normal and shear strains can be expressed as

$$\begin{aligned} \varepsilon_{xx} &= \partial u/\partial x = \partial u_0/\partial x - z\partial^2 w/\partial x^2 \\ e_{yy} &= \partial v/\partial y = \partial v_0/\partial y - z\partial^2 w/\partial y^2 \\ \varepsilon_{xy} &= \partial u/\partial y + \partial v/\partial x = \partial u_0/\partial y + \partial v_0/\partial x - 2z\partial^2 w/\partial x\partial y \end{aligned} \tag{3.53}$$

Partial differentials have been used because u, v and w are functions of both

x and y. That is $\varepsilon_{xx} = (\varepsilon_{xx})_0 - z\chi_{xx}$

$$\varepsilon_{yy} = (\varepsilon_{yy})_0 - z\chi_{yy}, \qquad \varepsilon_{xy} = (\varepsilon_{xy})_0 - z\chi_{xy} \tag{3.54a}$$

$$\begin{bmatrix} \varepsilon_{xx} \\ \varepsilon_{yy} \\ \varepsilon_{xy} \end{bmatrix} = \begin{bmatrix} (\varepsilon_{xx})_0 \\ (\varepsilon_{yy})_0 \\ (\varepsilon_{xy})_0 \end{bmatrix} - z \begin{bmatrix} \chi_{xx} \\ \chi_{yy} \\ \chi_{xy} \end{bmatrix} \quad \text{or} \quad [\varepsilon] = [\varepsilon_0] - z[\chi] \tag{3.54b}$$

3.8.2.1 Laminated composite isotropic plate. It has been shown [10] that for isotropic plates the resultant in-plane forces, namely two axial (N_{xx}, N_{yy}) and one shear (N_{xy}), and moments, namely two bending moments (M_{xx}, M_{yy}) and one torque (M_{xy}), may be obtained by integrating across the thickness of the plate giving

$$\begin{aligned} N_{xx} &= \int_{-t/2}^{t/2} \sigma_{xx}\, dz = Et/(1-\nu^2)\left[\frac{\partial u_0}{\partial x} + \nu\frac{\partial v_0}{\partial y}\right] \\ N_{yy} &= \int_{-t/2}^{t/2} \sigma_{yy}\, dz = Et/(1-\nu^2)\left[\frac{\partial v_0}{\partial y} + \nu\frac{\partial u_0}{\partial x}\right] \\ N_{xy} &= \int_{-t/2}^{t/2} \sigma_{xy}\, dz = Et/2(1+\nu)\left[\frac{\partial u_0}{\partial y} + \frac{\partial v_0}{\partial x}\right] \end{aligned} \tag{3.55}$$

$$\begin{aligned} M_{xx} &= -\int_{-t/2}^{t/2} \sigma_{xx} z\, dz = Et^3/12(1-\nu^2)\left[\frac{\partial^2 w}{\partial x^2} + \nu\frac{\partial^2 w}{\partial y^2}\right] \\ M_{yy} &= -\int_{-t/2}^{t/2} \sigma_{yy} z\, dz = Et^3/12(1-\nu^2)\left[\frac{\partial^2 w}{\partial y^2} + \nu\frac{\partial^2 w}{\partial x^2}\right] \\ M_{xy} &= -\int_{-t/2}^{t/2} \sigma_{xy} z\, dz = Et^3/12(1+\nu)\left[\frac{\partial w^2}{\partial x \partial y}\right] \end{aligned} \tag{3.56}$$

The distribution of the stress σ_{xx}, σ_{yy} and σ_{xy} is shown in Figure 3.13(b) and the forces and moments are shown in Figure 3.14.

3.8.2.2 Laminated composite orthotropic plate. Firstly, consider a composite manufactured from a series of laminae having similar properties and the composite having a symmetric cross-section about the centreline of the secton. For this case, the relationship between in-plane stresses and strains along the principal axes 1 and 2 for orthotropic properties in the plane of the composite plate but isotropic properties across its thickness is defined by

$$\begin{bmatrix} \sigma_{11} \\ \sigma_{22} \\ \sigma_{12} \end{bmatrix} = \begin{bmatrix} Q_{11} & Q_{12} & Q_{13} \\ Q_{21} & Q_{22} & Q_{23} \\ Q_{31} & Q_{32} & Q_{33} \end{bmatrix} \begin{bmatrix} \varepsilon_{11} \\ \varepsilon_{22} \\ \varepsilon_{12} \end{bmatrix} \tag{3.57}$$

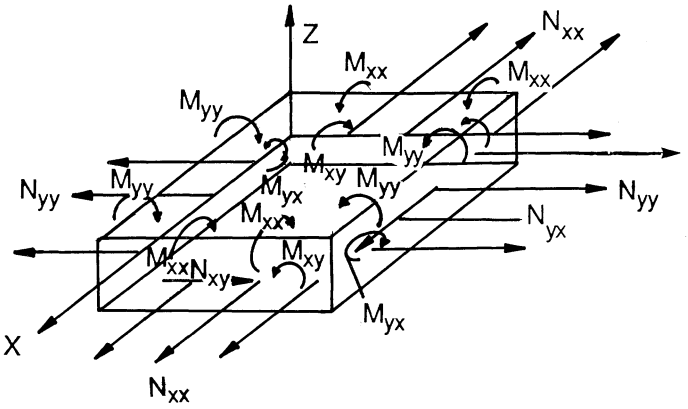

Figure 3.14 Forces and moments acting on rectangular axes.

where

$$Q_{11} = E_{11}/(1 - \nu_{21}\nu_{12})$$
$$Q_{22} = E_{22}/(1 - \nu_{12}\nu_{21})$$
$$Q_{12} = \nu_{12}E_{22}(1 - \nu_{12}\nu_{21}) = Q_{21} = \nu_{21}E_{11}/(1 - \nu_{21}\nu_{12})$$
$$Q_{33} = G_{12}$$

If the stress–strain relationship is defined about the arbitrary axes (x, y), a coupling effect will take place between the normal and shear stresses; the relationship is then given as

$$\begin{bmatrix} \sigma_{xx} \\ \sigma_{yy} \\ \sigma_{xy} \end{bmatrix} = \begin{bmatrix} \bar{Q}_{11} & \bar{Q}_{12} & \bar{Q}_{13} \\ \bar{Q}_{21} & \bar{Q}_{22} & \bar{Q}_{23} \\ \bar{Q}_{31} & \bar{Q}_{32} & \bar{Q}_{33} \end{bmatrix} \begin{bmatrix} \varepsilon_{xx} \\ \varepsilon_{yy} \\ \varepsilon_{xy} \end{bmatrix}$$

or

$$[\sigma] = [\bar{Q}][\varepsilon], \qquad [\sigma] = [\bar{Q}]([\varepsilon_0] - z[\chi]) \tag{3.58}$$

where the composites of matrix $[\bar{Q}]$ are functions of the material properties in the principal material directions and are of similar form to eq. (3.8).

If the mid-plane strains $[\varepsilon]_0$ and the curvature $[\chi]$ are known, eq. (3.58) may be used to calculate the stresses at any point in any ply.

The overall components of stress acting on the laminates are

$$[N] = \int_{-t/2}^{t/2} [\bar{Q}][\varepsilon_0]\,dz - \int_{-t/2}^{t/2} [\bar{Q}][\chi]z\,dz \tag{3.59}$$

$$[M] = \int_{-t/2}^{t/2} [\bar{Q}][\varepsilon_0]z\,dz - \int_{-t/2}^{t/2} [\bar{Q}][\chi]z^2\,dz \tag{3.60}$$

since $[\varepsilon_0]$ and $[\chi]$ are assumed to be uniform throughout the thickness, eqs. (3.59) and (3.60) are reduced to

$$N = [A][\varepsilon_0] + B[\chi] \tag{3.61}$$

$$M = [B][\varepsilon_0] + [D][\chi]$$

$$\begin{bmatrix} N \\ M \end{bmatrix} = \begin{bmatrix} A & B \\ B & D \end{bmatrix} \begin{bmatrix} \varepsilon_0 \\ \chi \end{bmatrix} \tag{3.62}$$

Combining eqs. (3.61) and (3.62) yields the laminate constitutive equation

$$\begin{bmatrix} N_{xx} \\ N_{yy} \\ N_{xy} \\ M_{xx} \\ M_{yy} \\ M_{xy} \end{bmatrix} = \left[\begin{array}{ccc:ccc} A_{11} & A_{12} & A_{13} & B_{11} & B_{12} & B_{13} \\ A_{21} & A_{22} & A_{23} & B_{21} & B_{22} & B_{23} \\ A_{31} & A_{32} & A_{33} & B_{31} & B_{32} & B_{33} \\ \hdashline B_{11} & B_{12} & B_{13} & D_{11} & D_{12} & D_{13} \\ B_{21} & B_{22} & B_{23} & D_{12} & D_{22} & D_{23} \\ B_{31} & B_{32} & B_{33} & D_{13} & D_{32} & D_{33} \end{array}\right] \begin{bmatrix} \varepsilon_{xx} \\ \varepsilon_{yy} \\ \varepsilon_{xy} \\ \chi_{xx} \\ \chi_{yy} \\ \chi_{xy} \end{bmatrix} \tag{3.63}$$

where ε_{xx}, ε_{yy}, ε_{xy} are the in-plane strains and χ_{xx}, χ_{yy}, χ_{xy} are the laminate curvatures.

From eq. (3.63), the submatrices A_{ij}, B_{ij} and D_{ij} are the summations of the ply stiffnesses where A_{ij} is used to evaluate in-plane stress, B_{ij} is used to evaluate the combination of the in-plane stresses and bending moments and D_{ij} is used to evaluate the bending moments.

Secondly, if the composite is manufactured from laminae having different properties but with a symmetric cross-section about the centreline of the section as shown in Figure 3.15a, then the in-plane and out-of-plane behaviour will be uncoupled and the equations will be similar to those for the orthotropic plate first considered. The form of the equation, however, will be more complicated.

The in-plane forces and out-of-plane moments per unit width acting on a rectangular plate consisting of say three orthotropic laminae (each manufactured from an individual lamina) can be expressed as

$$[N] = ([\bar{Q}]_A 2t_0 + [\bar{Q}]_B t_I)[\varepsilon_0]$$

$$([M] = [\bar{Q}]_A\{(2t_0 + t_I)^3/12 - t_I^3/12\} + [\bar{Q}]_B t_I^3/12)[\chi] \tag{3.64}$$

Thirdly, if the composite is manufactured from laminae having different properties and an asymmetric cross-section about the centreline of the section as shown in Figure 3.15(b), the in-plane and out-of-plane behaviour will be coupled and the resulting equations will be more complex than those of the two previous cases.

The in-place forces and out-of-plane moments per unit width acting on a rectangular plate consisting of two asymmetric orthotropic laminae will be

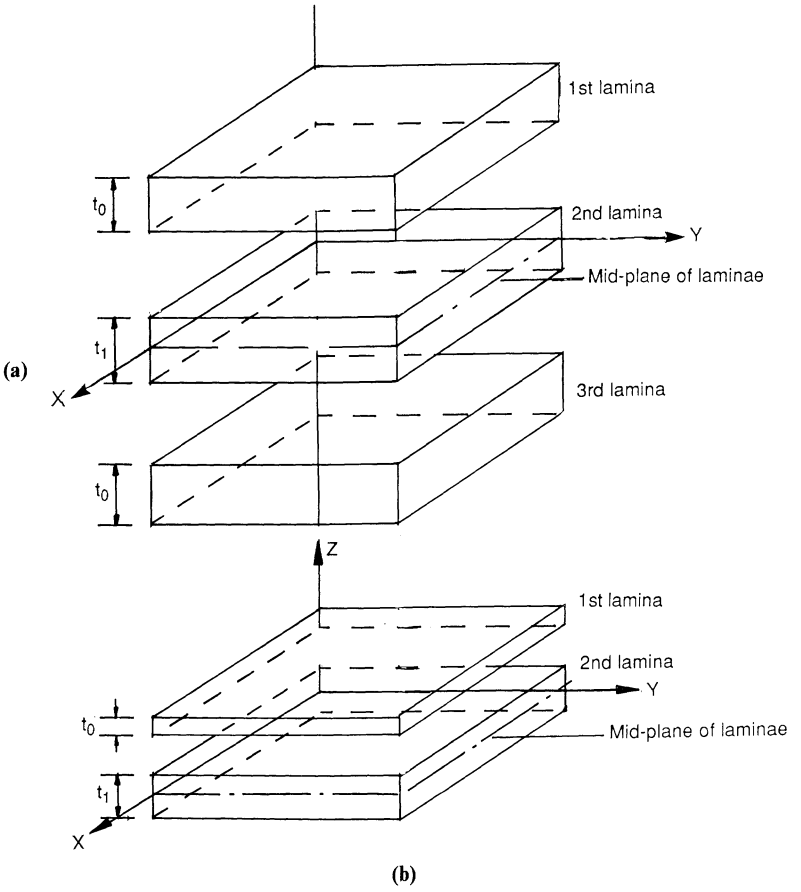

Figure 3.15 Composites manufactured from laminae. (a) Symmetric laminae; (b) asymmetric laminae.

expressed as

$$[N] = ([\bar{Q}]_A t_0 + [\bar{Q}]_B t_I)[\varepsilon_0] + \{([\bar{Q}_A] - [\bar{Q}]_B) t_I t_0/2\}[\chi]$$
$$[M] = ([\bar{Q}]_A - [\bar{Q}]_B) t_I t_0/2[\varepsilon_0] + ([\bar{Q}_A] t_0[t_0^2 + 3t_I^2] + [\bar{Q}]_B t_I[3t_0^2 + t_I^2])[\chi]/12 \quad (3.65)$$

The examples given above have been based on a simple laminate stacking sequence. In practice, a composite consists of a large number of laminae and consequently it is recommmended that further reading should be undertaken [11, 12] to gain a greater understanding of the development of the stiffness properties of multilayered composites. The work has shown that generally for symmetric and asymmetric laminates, the relationship between the

in-plane and the flexural stress resultants and the corresponding strains may be expressed as

$$\begin{bmatrix} N \\ M \end{bmatrix} = \begin{bmatrix} A_{11} & B_{12} \\ B_{21} & D_{22} \end{bmatrix} \begin{bmatrix} \varepsilon_0 \\ \chi \end{bmatrix} \tag{3.66}$$

where B_{12} and B_{21} are equal and are the coupling matrices.

3.9 Design of composites

Chapter 9 describes the design of composites and gives various calculated examples of composites under axial and bending loads. However, in a design office the mathematical description of the complex nature of composites is not easy to formulate by hand and designers are using computer software systems to perform structural analysis of systems manufactured from anisotropic (laminated) composite materials. Although there are some 600 finite element programs available to the structural engineer, when the features are specifically addressed to the applications of structural analysis of composites, the number of suitable software programs decreases to about ten.

Some of the available laminate analyses microcomputer programs are given in [13–16] and these may be used for the failure analysis under any combination of in-plane loads and bending moments applied to the laminate element. All laminate software has similar objectives and methods of operation and are all based on laminate theory, but they may differ in operation. In addition many main frame programs are available to analyse composites; ABAQUS for instance has a procedure specifically for this operation.

References

1. J.E. Ashton, J.C. Halpin and P.H. Petit, *Primer on Composite Materials: Analysis*, Technomic Westport, CT (1969); J.C. Halpin, Revised 2nd edition, *Primer on Composite Materials Analysis*, Technomic, Basel, Switzerland (1992).
2. D. Hull, *An Introduction to Composite Materials*, Cambridge University Press, Cambridge (1981) (reprinted 1990).
3. L.E. Nielsen, *Mechanical Properties of Polymers and Composites*, Marcel Dekker, New York (1974).
4. B.W. Rosen, *Mechanics of Composite Strengthening*, ASM, Metals Park, OH (1965), Ch. 3.
5. P.D. Ewins and A.C. Ham, The nature of compressive failure in unidirectional carbon fibre reinforced plastics, Royal Aircraft Technical Report 730557 (1973).
6. R. Hill, *The Mathematical Theory of Plasticity*, Oxford University Press, London (1950).
7. S.W. Tsai, Structural behaviour of composite materials, NASA Contract Report CR-71 (1974).
8. A.N. Puppo and H.H. Evensen, Strength of anisotropic materials under combined stresses *A.I.A.A. J.* (1972), 468–474.
9. R.M. Jones, Buckling of stiffened multi-layered circular cylindrical shells with different orthotropic moduli in tension and compression, *A.I.A.A. J.* **May** (1971), 917–923.

10. S.P. Timoshenko and S. Woinowsky-Krieger, *Theory of Plates and Shells*, 2nd edition, McGraw-Hill, New York (1959).
11. B.D. Agarwal and L.T. Broutman, *Analysis and Performance of the Fibre Composites*, Wiley, New York (1980).
12. R.M. Jones, *Mechanics of Composite Materials*, McGraw-Hill, New York (1975).
13. ESDU 2022 *Stiffnesses and properties of laminated plates* (ESDU Pac 8335) and ESDU 2033 *Failure of composite laminates* (ESDU Pac 8418), ESDU International, London (1987).
14. MIC-MAC *Think Composites Software*, Dayton (1987).
15. CoALA, WEBBER, ALLAN and LAMHOLE, Cranfield Institute of Technology (1990).
16. LAP, Centre for Composite Materials, Imperial College of Science, Technology and Medicine, London (1991).

Further reading

J.R. Vinson and R.L. Sierakowski, *The Behaviour of Structures Composed of Composite Materials* Martinus Nijhoff, Dordrecht (1987).
K. Ashbee, *Fundamental Principles of Fiber Reinforced Composites*, Technomic, Lancaster, UK (1989).
L. N. Phillips (ed.), *Design with Advanced Composite Materials*, The Design Council, London (1989).
I.M. Marshall and E. Demuts, eds., *Optimum Design of Composite Structures*, Elsevier Applied Science, London (1990).
S.W. Tsai and H.T. Hahn, *Introduction to Composite Materials*, Technomic, Westport (1980).
S.W. Tsai, *Composites Design*, Think Composites Software, Dayton (1987).
A.F. Johnson, *Engineering Design Properties of GRP*, British Plastics Federation (1984).
L. Hollaway, ed., *Engineering Guide to Composite Meterials*, Woodhouse Publishing Ltd., Cambridge (1993).
L. Hollaway, ed., *Polymers and Polymer Composites in Construction*, Thomas Telford, London (1990).
A.F. Johnson and G.D. Sims, *Design Procedures for Plastics Panels*, National Physical Laboratory (1987).
MMGF Design Manual for Extren.

4 Measurements of engineering properties of fibre reinforced polymers

4.1 Introduction

There are two major requirements when designing structural components:

1. the deformation under load must be within the prescribed functional and aesthetic considerations;
2. fracture or rupture should not take place within their scheduled lifetime.

To satisfy these requirements it is necessary to have information on the mechanical characteristics of the material and this chapter discusses the test procedures that enable various properties to be obtained. Test methods are by no means trivial and routine. The accuracy of any numerical solution for the design of composites is highly dependent on the mechanical properties given to the composite during the computation and unless tests are performed accurately to determine these values, the design solution can be greatly in error. Composite materials present a special challenge to materials and design engineers because of their directionally dependent properties. The experimental values obtained from a test procedure are highly dependent on the method used and therefore all tests should be performed according to recognized codes of practice.

4.2 Uniaxial tension

The deformational characteristics of polymer fibre composites under uniaxial tension have been discussed in section 2.13 and it was stated that there are three different ways in which uniaxial tension can be applied to a specimen. These correspond to:

1. a constant rate of strain (constant rate of elongation);
2. a constant rate of stress (constant rate of loading);
3. a constant stress (creep tests).

(a) The British Standards Institute BS 2782 [1] (≡ EN61, equivalent ISO/R527, ISO 3268) describes the constant rate of strain tests and lays down test procedures which lead to secant and tangent moduli values. Clearly, for these values to be intelligible, it is necessary to state the rate of strain.

(b) To apply a constant rate of stress to a specimen is difficult because standard

testing equipment does not generally have this facility. If, however, this test is used, it is necessary to define the rate of stress.

(c) Probably the most relevant tensile test for structural applications of composites is the constant stress one; this relates directly to the long- and short-term loadings of structural systems in practice. Recommendations for the time dependence of polymers are given in BS 4618 [2] (no equivalent ISO) in which standard constant load tests are defined; the concept of these tests has been discussed in sections 2.9.2 and 2.13.

As the ultimate tensile strength of polymer and polymer composite materials under long duration loading varies with time and stress levels, it is necessary to define this strength in terms of a series of curves of maximum nominal tensile stress versus time.

4.2.1 Tension test procedure

The uniaxial tension test is the most fundamental method for the determination of data such as material specification and design of structural components. For unidirectional and woven composites, the following values are measured: $E_{11}, E_{22}, \nu_{21}, \sigma_{11}, \sigma_{22}$. For multidirectional, symmetric composites the following values are measured: $(E_{11})_0, (\nu_{21})_0, (\sigma_{11})_0$. Parallel straight-sided specimens with tabs bonded to the ends are used. Table 4.1 shows the recommended dimensions [3] and Figure 4.1 shows the geometry of the specimen.

1. End tabs
   (a) Composite material of the parent material or aluminium plates is generally used. The 90° specimens are often tested without tabs.
   (b) The length of tab is determined by the adhesive shear strength and the tensile strength of the composite. The length is 50 mm minimum.
   (c) The tab thickness varies with specimen thickness and is 0.5–2.0 mm.
   (d) The bond surface is prepared by sanding and cleaning with an appropriate solvent.

Table 4.1 Recommended specimen dimensions

Orientation (°)	Width (mm)	Length (mm)	Thickness (mm)
0	10–20	100–150	1.0 (nearest mouldable)
90	10–20	100–150	2.0 (nearest mouldable)
Multidirectional[a]	$9t$	Not less than $W(1 + 1/\tan\theta)$ or 100 ± 1 whichever is greater	1.0–4.0 depending on laminate configuration

[a] t is the thickness of the specimen and θ is the angle between the fibres and longitudinal axis.

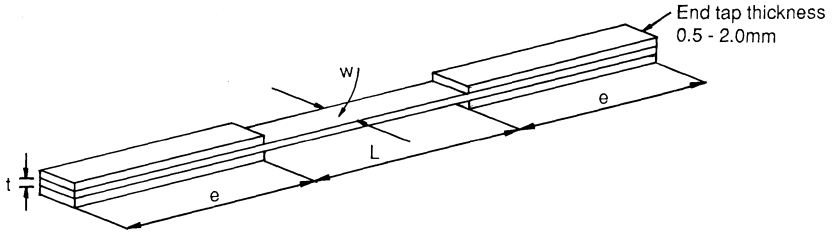

Figure 4.1 Tensile test specimens (after [3]).

For unidirectional fibre reinforced polymers

(a) Longitudinal tensile strength and modulus of elasticity

Dimensions

$t = 1.0$ mm* (nearest mouldable thickness)
$w = 10$–20 mm
$L = 100$–150 mm
$e = 50$ mm minimum.
* tolerances

Width and thickness must be uniform to ± 0.04 mm.
Fibre alignment must be parallel with the specimen longitudinal axes within 0 degrees 30 seconds.

(b) Transverse tensile strength and modulus of elasticity

Dimensions

$t = 2.00$* (nearest mouldable thickness)
$w = 10$–20 mm
$L = 100$–150 mm
$e = 50$ mm minimum.
*tolerances

Width and thickness must be uniform to ± 0.04 mm.
Fibre alignment must be parallel with the specimen longitudinal axis within 0 degrees 30 seconds.

Multidirectional fibre reinforced polymer.

Dimensions

$e = 50$ mm minimum.
$w = 9$ t minimum, typically 10 t (absolute minimum = 20 mm).
$t = 1.0$ to 4.0 mm. depending laminate configuration.
L not less than $w(1 + 1/\tan\phi)$ or 100 ± 1 mm whichever is the greater.

Tolerances

Edge of specimen must be parallel to ± 1.0 mm. Specimen must be flat and end tab faces parallel and aligned to within ± 0.05 mm. For small angles of ϕ ($< 15°$), L may be reduced to $w/\tan\phi$.

2. Specimen cutting
   (a) A diamond impregnated saw is used with water cooling.
   (b) Specimen edges should be parallel to within ± 0.25 mm.
3. Test procedure
   (a) The width and thickness are measured at several places.
   (b) Load is applied through a set of serrated wedge section grips in order to provide sufficient lateral pressure to prevent slippage.
   (c) A constant strain rate to cause failure within 30–60 min is recommended [3]. However, this may not be feasible for many toughened composites which can fail at strains in excess of 8–10%. In this case, the strain rate should be selected so that at least 90% of the anticipated failure load is applied in the range 30–60 s. Either a constant cross-head speed or loading rate corresponding to the strain rate is acceptable.
   (d) The strain is measured during test.

4.3 Compressive tests

The compressive strength is a difficult property to determine. A slight load applied to the specimen during the test will cause premature buckling failure before a compressive failure occurs. In order to prevent buckling, a number of compression test rigs have been developed; probably the best known is the Celanese fixture which is shown in Figure 4.2. The specimen has the dimensions 110 mm long and 10 mm wide. End plates of length 50 mm and width 10 mm are fixed on either side of the specimen at both ends; the thickness of these plates is between 0.5 and 2.0 mm. The gauge length is 10 mm which is a compromise between the requirement to eliminate Euler buckling and the need to avoid end tab effects while providing adequate space for strain gauges.

The test rig is placed between the two platens of a compressive testing machine; one of the platens has a spherical seat to minimize eccentricity of the line of action of the load. The test procedure has limitations; because of the short 'working' length of the specimen, end effects will be encountered and composites consisting of off-axis angle plies cannot be tested.

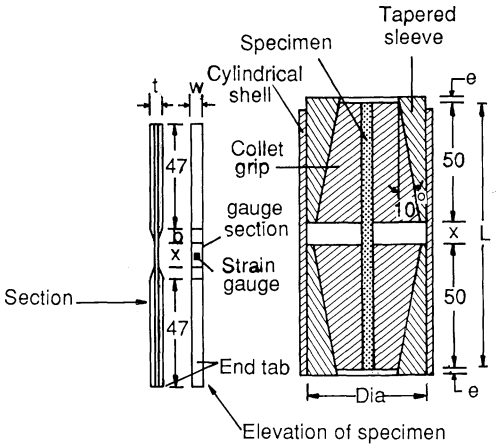

Figure 4.2 Compressive specimen test (Celanese fixture).

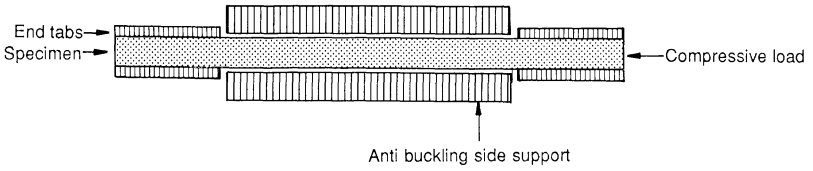

Figure 4.3 Compressive specimen with antibuckling devices.

An alternative test procedure is one in which side supports to the specimen are used; this is shown in Figure 4.3.

4.4 In-plane shear tests

To measure the in-plane shear modulus and shear strength, a number of procedures can be adopted.

4.4.1 The uniaxial tensile test on a symmetric ±45° coupon

Figure 4.4 shows the specimen and the locations of two strain gauges positioned in the x, y axes direction. From the measured longitudinal and transverse strain data, the required properties may be obtained. Noting that the shear stress σ_{12} is half of the applied stress for a tensile test in general and for the $\pm 45°$ laminate in particular and that $\varepsilon_{12} = (1 + \nu_{xy})\varepsilon_{xx}$, then $\sigma_{12} = \sigma_{xx}/2$ and $\nu_{xy} = -\varepsilon_{yy}/\varepsilon_{xx}$. Thus $\varepsilon_{12} = (\varepsilon_{xx} - \varepsilon_{yy})$. It follows that

$$G_{12} = \frac{\sigma_{xx}}{2(\varepsilon_{xx} - \varepsilon_{yy})} \tag{4.1}$$

An incremental procedure should be used to take account of the non-linear stress–strain relationship. The tangent modulus at different strain levels of the $\pm 45°$ tensile response curve is found and used in conjuction with the above.

4.4.2 Off-axis test

The shear modulus of a laminate can be determined by utilizing eq. (3.11). From a tensile test of a unidirectional laminate with the load in the fibre direction, the modulus E_{11} and Poisson's ratio ν_{12} can be determined. From a similar test, but with the load normal to the fibres, the modulus E_{22} can be determined. Using this information, together with the results of a third tension test with the load at an angle θ to the fibre direction (off-axes tensile test), the shear modulus G_{12} can be determined.

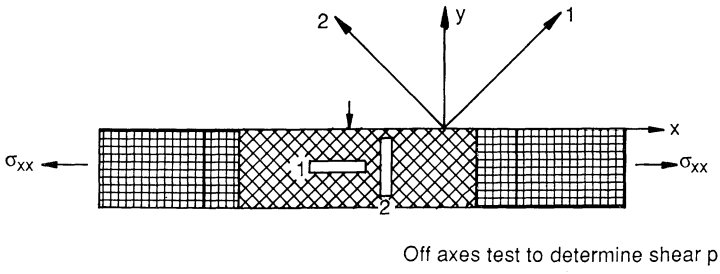

Figure 4.4 Method of test for in-plane shear strength and modulus of composite (±45° laminate).

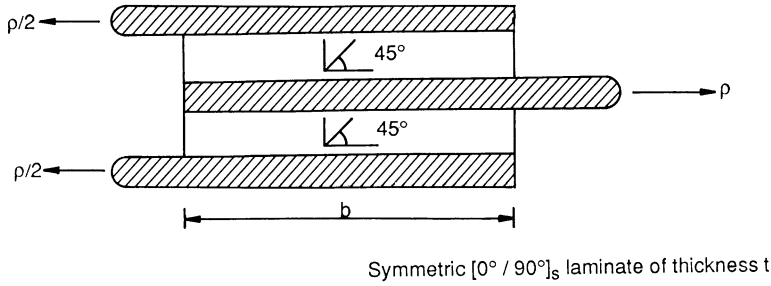

Figure 4.5 Schematic representation of a three-rail shear test.

The above procedure does not provide a means of determining the total stress/strain response as eq. (3.11) is a stiffness equation only.

If the strains were measured in three directions on the above specimen (i.e. 0°, 90° and 45° to direction 1) and were transformed to the fibre direction, then a plot of σ_{12} against ε_{12} gives the required shear behaviour. It has been suggested [4, 5] that a 10° off-axis specimen will give reasonable results with this technique.

4.4.3 Rail shear test

A flat rectangular plate with [0°/90°] symmetric laminate is tested in a two-rail or three-rail fixture; Figure 4.5 shows the test set-up. The strain is measured at 45° to the applied load. If the applied load is P and the cross-sectional area is A (i.e. $b \times t$), then

$$\sigma_{12} = P/2A \quad \text{and} \quad \varepsilon_{12} = 2\varepsilon_{45^\circ}$$

Thus (4.2)

$$G_{12} = \frac{\sigma_{12}}{\varepsilon_{12}}$$

If a [0°/90°] symmetric laminate is considered to be orthotropic, then its constitutive relation can be expressed as

$$\begin{bmatrix} \varepsilon_{xx} \\ \varepsilon_{yy} \\ \varepsilon_{xy} \end{bmatrix} = \begin{bmatrix} S_{11} & S_{12} & 0 \\ S_{21} & S_{22} & 0 \\ 0 & 0 & S_{33} \end{bmatrix} \begin{bmatrix} N_{xx} \\ N_{yy} \\ N_{xy} \end{bmatrix} \tag{4.3}$$

where N_{xx}, N_{yy}, N_{xy} are the applied loads and ε_{xx}, ε_{yy} and ε_{xy} are the laminate strains with respect to the reference axes (see section 3.3.1) and the S_{ij} matrix is the compliance for the laminate.

If a shear load only is applied, then from eq. (4.3)

$$\varepsilon_{xy} = S_{33} N_{xy} = \frac{\sigma_{xy}}{G_{12}} \tag{4.4}$$

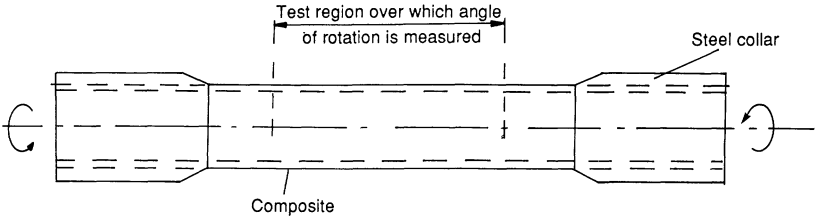

Figure 4.6 Schematic representation of a torsion tube.

As N_{xy} has a dimension of force/unit length, then

$$S_{33} = \frac{1}{G_{12}t}$$

For this laminate, the principle stress and strain axes do coincide so eq. (4.4) can be expressed as

$$G_{12} = \frac{\sigma_{12}}{\varepsilon_{12}} \quad \text{or} \quad G_{12} = \frac{P}{4A\varepsilon_{45^\circ}} \tag{4.5}$$

From eq. (3.34) the failure strength of the composite is

$$\sigma_\theta = \frac{\sigma_{12}^*}{\sin\theta\cos\theta}$$

4.4.4 Torsional shear of a thin-walled tube

A torque is applied to a thin-walled circular cross-section tube about its longitudinal axis; Figure 4.6 shows a schematic representation.

This test is probably one of the most difficult to perform, because in applying a shear force to the specimen other forms of loading are also unavoidably present. However, torsion testing machines were developed by ICI Polymer Division in 1969, and these were subsequently modified to incorporate the use of air bearings to reduce the machine friction to negligible proportions. The machine is limited to small shear strains of approximately 0.2%; consequently, the shear modulus can be calculated from the slope of the straight line plot of the angle of twist of the specimen against the applied torque using the standard linear elastic solution to the torsion of prismatic bars.

Specimens may be strained by using an interrupted step-loading technique analogous to that used in the tensile tests, and by observing the twist at say, 100 s after the application of the load, the 100 s isochronous torque versus angle of twist curves are obtained. If should be noted, however, that because of the limitations of the apparatus, this approach may only be used with small

cross-section polymer specimens and that the apparatus for the investigation of GRP could be similar but would have to be more robust.

The torsional test therefore applies practically a pure shear stress, which is uniform around the circumference and along the length of the specimen. Since the wall thickness is small compared with the tube diameter, the shear strain gradient through the thickness is negligible.

The shear stress σ_{12} may be calculated from

$$\sigma_{12} = T/2\pi r_m^2 t, \qquad \text{where } r_m \text{ is the mean radius of the cylinder}$$

$$\varepsilon_{12} = \varepsilon_{45^\circ} - \varepsilon_{45^\circ} \tag{4.6}$$

(i.e. the strain measured at $\pm 45^\circ$ to the longitudinal axis) and

$$G_{12} = \frac{\sigma_{12}}{\varepsilon_{12}}$$

4.5 Flexural tests

To enable the bending stiffness modulus to be determined, a four-point flexural test can be undertaken; Figure 4.7 gives the notation for this test. The analysis for this test is

$$E_{11} = 11PL^3/64bt^3\delta \tag{4.7}$$

where δ is the displacement of the beam at centre span relative to the support reaction. The specimen should be deflected until tensile or compressive rupture occurs or the maximum fibre strain at the outer fibres is reached. Deflection should not exceed 10% of the span. For deflections larger than this, correction factors should be applied.

4.6 Interlaminar shear tests

4.6.1 The three-point load interlaminar shear test

The test set-up for estimating the interlaminar shear strength is shown in Figure 4.8. The method, based on elementary beam theory, is used to obtain the interlaminar shear strength of unidirectional reinforced polymers. The

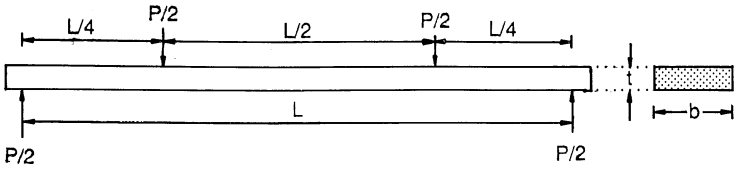

Figure 4.7 Four-point flexural test.

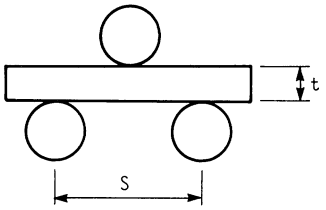

Figure 4.8 Method of test for interlaminar shear strength of fibre-reinforced polymers.

Dimensions from [3]
t = specimen thickness
s = span between supports = $5t \pm 0.5$ mm
b = specimen width = $5t_n \pm 0.25$ mm
ρ = failure load
t_n = nominal specimen thickness = 2.0 mm
support roller diameter = 6 mm

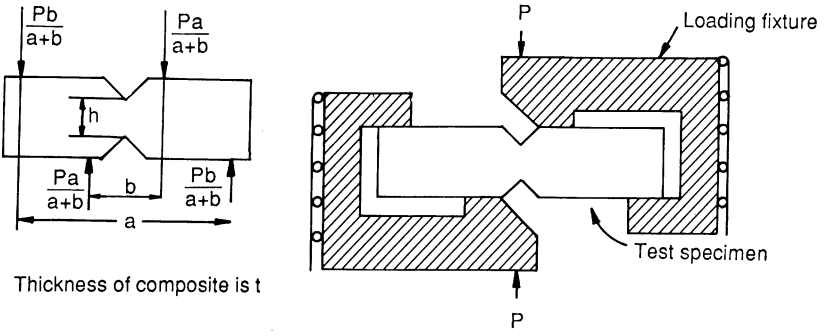

Figure 4.9 Schematic representation of the Iosipescu shear test.

analysis for this test is

$$\sigma_I = 3P/4bt \tag{4.8}$$

The test may not be suitable for design data generation because the failure of the composite under interlaminar shear does not always occur at the neutral plane. It is therefore important to know the actual location of the fracture and the fracture mode. The span to depth ratio should be selected in order to introduce interlaminar shear fracture mode.

4.6.2 Iosipescu shear specimen

This method uses a strip specimen which is loaded by two opposite moments to produce shear forces in the middle section where it is matched to force failure between the notch edges. The technique may be used for both in-plane

and interlaminar shear evaluation. The Iosipescu loading method is shown in Figure 4.9. It should be noted that stress concentrations do exit at the notched root, which is a function of the notched angle, loading level and material anisotropy. As in other shear test methods, the failure of the Iosipescu specimen is not a pure shear failure; a mixture failure mode initiates the specimen fracture which is dependent upon the composite lay-up. The analysis for this test is

$$\sigma_{12} = P(b-a)/(a+b)ht, \qquad G_{12} = \frac{\sigma_{12}}{\varepsilon_{12}}$$

4.7 Impact behaviour

Composite materials suffer some limitations regarding impact conditions; probably the most significant is their response to localized impact loading, such as that imparted by a dropped tool or flying debris. In recent years, many research programmes [6–8] have been undertaken in an attempt to understand the impact response of these materials.

4.7.1 Impact test techniques for composite materials

The impact test fixture should be designed to simulate the loading conditions to which a composite component is subjected in operational service and then to reproduce the failure modes and mechanisms likely to occur. There are two separate conditions which should be considered; these are the low velocity impact by a large mass (dropped tool) and the high velocity impact by a small mass. The former is generally simulated by means of a falling weight

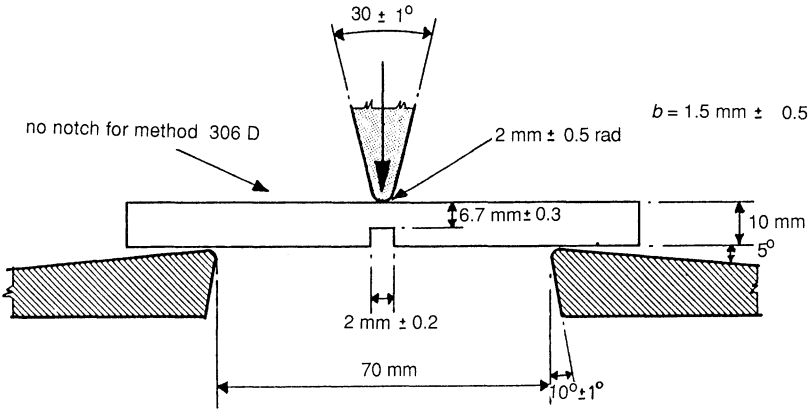

Figure 4.10 Specimen mounting for Charpy test (BS 2782).

or a swinging pendulum and the latter by using a gas gun or some other ballistic launcher. However, because of the lack of experimental standards, a wide variety of testing techniques is presently being employed in order to assess the dynamic response of reinforced polymers; this makes a direct comparison difficult.

4.7.1.1 Low velocity impact. Equipment currently used for simulating the low velocity impact response of composite materials includes the Charpy and Izod pendulums, the drop-weight impact test and hydraulic machines that are designed to perform both in-plane and out-of-plane testing at velocities up to 10 m/s.

Charpy pendulum. Many of the early impact studies on composite materials were undertaken using the Charpy method, originally developed for testing metals. Figure 4.10 shows a diagram of the specimen mountings for this test. The equipment is simple and can be instrumented, and therefore can give information on the process of energy absorption and dissipation in composites. The specimen is supported in a horizontal plane and impacted by the swinging pendulum directly opposite the notch. In addition, by instrumenting the impactor with a strain gauge, the variation of the impact force with time can be determined.

The Charpy test is only suitable for ranking the impact performance of continuous fibre composites and as a first stage in determining the dynamic toughness of these materials.

Izod test. The test set-up and procedure are similar to those outlined for the Charpy test. The specimen is clamped in a vertical plane as a cantilevered beam and impacted by a swinging pendulum at the unsupported end. This test also is best suited as a tool for ranking the impact resistance of composite materials.

Drop weight impact tests. Here a weight is allowed to fall from a predetermined height to strike the test specimen or plate supported in the horizontal plane. In general, the impact event does not cause complete destruction of the test specimen and the weight rebounds, enabling a residual energy component to be determined if necessary. The incident velocity of the impactor can be determined from the equation of motion or by using optical sensors located just above the target. Frequently the impactor is instrumented, enabling the force/time characteristics to be determined; it may also contain a displacement transducer to determine energy dissipation during impact. One advantage of this test compared with the Charpy and Izod tests is that a wider range of geometries can be investigated. The types of impactor heads range from the hemispherical to blunt cylinders and sharp points; the first shape is the most usual.

Hydraulic test machine. In recent years, a number of workers (e.g. [9]) have used hydraulic test machines for assessing the deformation and failure characteristics of materials at high rates of strain; the strain history of the specimen is measured, using bonded strain gauges or optical transducers. One advantage of this technique is that the test specimens permit the evaluation of the basic properties of materials, such as tensile strength, modulus of elasticity and interlaminar fracture toughness, without the contact effects associated with the falling weight hammer. The mass of the load cell and gripping system should be as low as possible so that the inertia effects resulting from these components do not interfere with the true material response.

4.7.1.2 High rate impact test. The Hopkinson bar technique is similar to the previous test procedure in that it permits the determination of the variation of basic material properties as a function of rate of strain. The equipment and experimental technique have been discussed in [10].

The gas gun impact test. Impact testing at ballistic rates of strain can be achieved using a high pressure gun. The velocity of the impactor can be determined just prior to impact using optical sensors. Generally the test is not completely destructive, but frequently results in large-scale damage.

4.7.2 Observations on the impact tests

It may be observed from the above that a wide variety of impact testing procedures, specimen geometries and data reduction techniques are currently being employed; the most relevant of these must be used for a particular structural situation. Pendulum techniques such as the Charpy and Izod tests often require specimen geometries that are not representative of the prototype component and consequently are suitable only for ranking the impact response of composites; the drop weight rigs and gas gun provide more representative tests for assessing the impact response.

4.8 Non-destructive testing techniques

The non-destructive tests applied to composites have mainly been developed from those used in the testing of metals, although it must be said that only ultrasonic and radiography are commonly used with composites. Dye penetrants have been used to find the surface breaking defects but they have the disadvantage that it is difficult to remove the penetrant and this can affect subsequent repairs. In addition, one of the most common defects found in composites is the delamination parallel to the surface of the structures and in this case the dye is less effective than that of a surface breaking transverse crack. When the defect, such as delamination, runs parallel to the

surface of the structure, a low frequency vibration or thermography has been used to detect the problem.

References [11–14] discuss the range of non-destructive testing (NDT) techniques available to investigate defects in composites and bonded joints. These references also discuss techniques that are still in various stages of development, such as fibre optics, shearography, corona discharge, Raman spectroscopy and dielectric measurements. In this section, only the technique commonly used to detect defects is discussed.

The ultrasonic test technique is the most widely used method for NDT of composites and bonded joints. It can be used to detect voids and de-bonds and has the potential for locating very small defects, such as porosity. The ultrasonic tests can be undertaken by using a single transducer in pulse-echo mode or two transducers in through-transmission mode. These methods are very sensitive but have the disadvantage of requiring a couplant between the transducer and the test structure because of the severe impedance mismatch between air and solid material. It is necessary, therefore, that the transducers are coupled to the structure through a liquid or solid medium; this can be achieved by immersing the system in a liquid bath. If the components are large, water jet probes are used; this technique has been discussed in [14].

There are several different ultrasonic methods of measurement; the basic equipment uses either water or gel coupling. These methods are:

1. ultrasonic velocity measurement;
2. ultrasonic backscattering;
3. ultrasonic spectroscopy;
4. echo-amplitude measurements at normal incidence.

A discussion of these methods has been given in [15] and is not repeated here.

There are also different methods of displaying the test results; the most common are the A, B and C scans. The A scan provides information on the time history of the echoes received by the transducers. The B scan gives information of time on the vertical axis and position on the horizontal axis and enables an image of the cross-section of the component to be built up. The C scan provides information on the amplitude of the particular echo on the surface of the composite at each selected point, generally using a grid scanning mechanism. This produces a plan of the defective positions but provides no information regarding their depth.

Thermographic methods for NDT may be divided into two types:

1. the passive technique in which the response of the test structure to an applied heating or cooling transient is monitored;
2. the active technique in which heat is produced by applying cyclic stress to the structure, either by a fatigue load or by a resonant vibration.

In both techniques the surface temperature of the structure is monitored,

generally by the use of an infrared camera, and irregularities in the temperature distribution will reveal the presence of defects. The capital cost of setting up and operating this system is high and the sensitivity of the test may not be adequate in all cases.

A number of low frequency vibration techniques may be used in NDT, but the equipment costs are generally high. However, the coin-tap test, in which the region of the structure to be tested is tapped with a coin and the sound noted is an effective and cheap qualitative method. The defective areas sound duller than the non-defective areas. Defective areas in structures can be detected by impacting them with an instrumented hammer containing a force transducer and monitoring the output. This technique provides a measure of the integrity of a structure; the equipment is portable, relatively cheap and ideal for use in the field. However, the sensitivity may not be sufficient for all cases, particularly where the defects are at significant depths into the composite.

The detection of defects in composites has been developed to a certain degree, but an understanding of its significance is still in its infancy.

References

1. BS 2782 Determination of tensile properties, Method 1003 1977 [≡ EN61, = ISO R527, ISO 3268]*, British Standards Institution, London (1983).
2. BS 4618 Recommendations for the presentation of plastics design data (no equivalence in ISO), British Standards Institution, London (1970).
3. CRAG Technical Report, 88012, *CRAG Test Methods for the Measurement of the Engineering Properties of Fibre Reinforced Plastics*, ed. P.T. Curtis, Ministry of Defence, Farnborough, Hants., UK (1988).
4. J.M. Daniel and T. Liber, Lamination residual stresses in hybrid composites, Parts 1–4 NASA CR-135085, ITTRI-D6073-11 (1976).
5. C.C. Chamis and J.H. Sinclair 10° off-axis test for shear properties of fibre composites, SESA Spring Meeting.
6. P.W. Manders and P.C. Harris A parametric study of composite performance in compression after impact testing *SAMPE J* **22** (6) (1986), 47–51.
7. K.K.U. Stellbrink, Improved impact damage tolerance in *Proc. European Symp. on Damage Development and Fracture Processes in Composite Materials* eds. 1. Verpoest and M. Weveis (1987).
8. S. Rechak and C.T. Sun, Optical use of adhesive layers in reducing impact damage in composite laminates, in *Composite Structures*, Vol. 2, *Damage Assessment and Material Evaluation*, Elsevier Applied Science, London (1987), 18–31.
9. P. Beguelin and M. Barbizat, Caractérisation mécanique des polymères et composites à l'aide d'une machine d'essais rapides, in *Proc. 5th Journée Nationale DYMAT*, Bordeaux, France (1989).
10. J. Harding, Impact damage on composite materials, *Sci. Eng. Composite Mater.* **1** (1989), 41–68.
11. Y. Bar-Cohen, NDE of fibre-reinforced composite materials—a review, *Mater. Eval.* **44** (1986), 446–454.
12. W.N. Reynolds, Non-destructive testing (NDT) of fibre-reinforced composite materials, *Mater. Design* **5** (1985), 256–270.
13. R. Prakash, Non-destructive testing of composites, *Composites* **11** (1980), 217–224.

14. C.C.H. Guyott, P. Cawley and R.D. Adams, The non-destructive testing of adhesively bonded structure: a review, *J. Adhesion* **20** (1986), 129–159.
15. R.D. Adams and P. Cawley, A review of the defect types and non-destructive testing techniques for composites and bonded joints, Paper presented at Seminar on *Bonding and Repair of Composites*, organised by Butterworth Scientific Ltd and RAPRA Technology Ltd. (1989).

*The symbol ≡ indicates in identical standard, i.e. a BSI publication identical in every detail with a corresponding international standard ISO. The symbol = indicates a (technically) equivalent standard, i.e. a BSI publication in all technical respects the same as a corresponding international standard ISO although the wording and presentation may differ quite extensively. The symbol ≠ indicates a related but not equivalent standard, i.e. a BSI publication, the content of which to any extent at all short of complete identity or technical equivalence, covers subject matter similar to that covered by a corresponding international standard ISO.

5 Processing techniques: thermoplastic polymers, thermosetting and thermoplastic composites

5.1 Introduction

Polymer materials must be reinforced with fibres if they are to be used structurally and in so doing a wide range of composites with varying mechanical properties may be obtained by altering:

(a) the relative proportions of thermosetting polymers and fibres;
(b) the type of each component employed;
(c) the fibre orientation within the resin matrix;
(d) the method of manufacture of the composite.

The fibre orientation within the matrix will be dependent on the type of reinforcement used; consequently, it will be clear that the three main types of composites which can be manufactured will depend on whether unidirectional strand, bidirectional strand or cloth, or chopped strand mat reinforcement is used.

This chapter is divided into two parts: the first part concentrates on the manufacturing techniques for fibre reinforced thermosetting polymer composites and the second part discusses production techniques for unreinforced thermoplastic polymers and for fibre reinforced thermoplastic polymer composites.

PART 1

5.2 Processing methods for the manufacture of reinforced thermosetting polymers

There are various techniques for the manufacture of fibre reinforced thermosets; these methods may be considered under three headings:

(a) the manual process;
(b) the semi-automatic process;
(c) the automatic process.

The manual process covers methods such as hand lay-up, spray-up (both of which are known as contact moulding), pressure bag and autoclave moulding. The semi-automatic process includes cold pressing, compression moulding

and resin injection; the automatic processes are those such as pultrusion, filament winding and injection moulding.

The processes may be considered under two main headings. The first is the open mould system in which, during the moulding operation, the material is in contact with the mould on one surface only; the surface of the product in contact with the mould is able to reproduce the surface of the mould completely. This system is generally adopted for civil/structural engineering applications. The second process is the closed mould technique in which the composite is shaped between two matched dies. This method is generally employed for the manufacture of relatively small components, not necessarily associated with the building trades.

The pressure bag techniques are further developments of the contact moulding methods and may be considered to lie somewhere between the open and closed mould processes. In the pressure bag technique, a pressure is exerted on the open face of the laminate so that:

(a) the finished product will be more densely compacted;
(b) a high, fibre volume fraction is achieved in the finished product;
(c) the exposed face of the laminate will be of a higher quality than that attained by ordinary contact moulding.

It is important to mention here that the polymerization process of the thermosetting polymer is an exothermic reaction and heat will be given off through this reaction. In addition, some closed mould techniques require heat during fabrication of the composite. Consequently, during cooling of the composite from the curing temperature, residual stresses will develop because of the differential coefficients of thermal expansion (CTE) parallel and perpendicular to the fibre in particular, and the different CTE of the composite constituents in general.

Two types of residual stresses can be distinguished:

1. The micro-residual stresses associated with the local geometry within the plies; micro-cracking of a matrix leads to a decrease in residual bending strains (unsymmetrical laminates, see section 3.8.2.2), reduced deformation and a reduction in the value of the CTE. It is possible that moisture will then enter the micro-cracks.
2. The macro-residual stresses associated with a gross average stress through the cross-ply; the parameters that affect the more general distortion of the laminates are:
   (a) variation in thickness;
   (b) stacking sequence;
   (c) fibre angle orientation.

If these parameters are not properly designed, curvature and warping of the structural system will take place after the composite has cooled down to room temperature.

5.2.1 *Open mould techniques*

Although the open mould techniques are not exclusive to polyester resins, this polymer is probably the one most used and the production methods take full advantage of two important characteristics of it; it does not require heat or pressure for complete polymerization to occur although some form of pressure is an advantage for greater compaction. There are many variations of the open mould technique, but in the following sections only the principal ones are given.

5.2.1.1 The hand lay-up technique. In this technique, only one mould is used and this may be either male or female. Most materials are suitable for mould making, but probably the most common is GRP. A suitable master pattern is prepared and from this, GRP moulds may readily be made. Figure 5.1(a) shows the hand lay-up operation. To prevent bonding of the composite materials to the mould during manufacture, a release agent is applied to the mould and then allowed to dry before any lay-up is undertaken.

The durability of a GRP composite unit is dependent on the quality of the material at the surface of the unit which is exposed to the atmosphere. Consequently, it is necessary to protect the polymer and fibres by a resin rich area known as a gel coat. This latter is a specially prepared resin, often containing additions and pigments to give weathering resistance and colour to the surface of the composites. The gel coat can be reinforced with a surface tissue mat (section 2.8.1); this also has the function of balancing the composite throughout its cross-section:

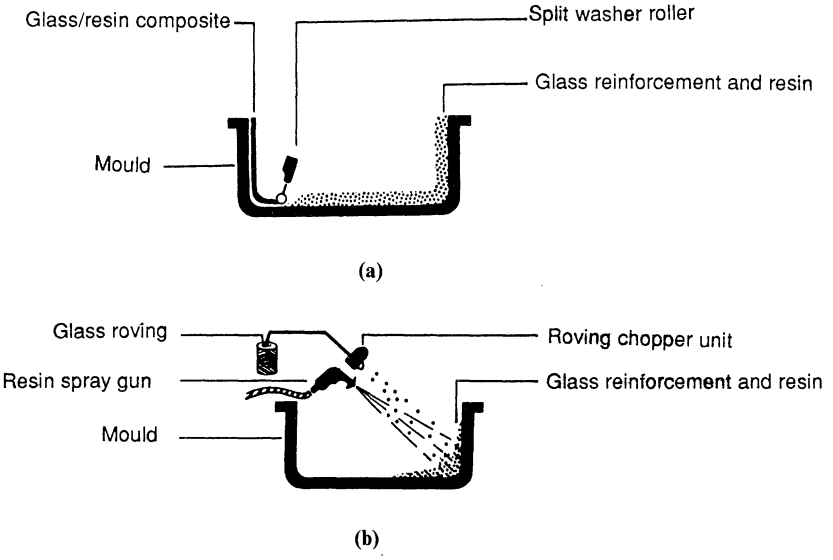

Figure 5.1 (a) Hand lay-up moulding method. (b) Spray-up technique.

(i) to protect the glass fibre from external influences, the main one being moisture penetration to the interface of the fibre and matrix, with consequent breakdown of the interface bond;
(ii) to provide a smooth finish and reproduce precisely the surface texture of the mould.

The thickness of the gel coat should be controlled to about 0.35 mm and should be uniform throughout. If uneven thicknesses do occur, different cure rates over its surfaces will result, with induced stresses in the resin coat causing crazing.

After the gel coat has become tacky but firm a liberal coat of resin is brushed over it and the first layer of glass reinforcement is placed in position and consolidated with brush and roller. The glass fibre may be in the form of chopped strand mat or woven fabric, which is precut to the correct size. Subsequent layers of resin and reinforcement are then applied until the required thickness of the composite is reached.

It is very important that the composite unit should be correctly cured for optimum life span. Ideally units should be placed in an oven for varying lengths of time depending on the temperature of the oven. If the unit is to be cured in the fabrication shop at room temperature it would normally take about 28 days. If, however, the unit is placed in an oven at say 60°C, an exposure time of 8 h would be required. An oven could take the form of heaters placed in a foil enclosure. Polyester resin systems are used with this

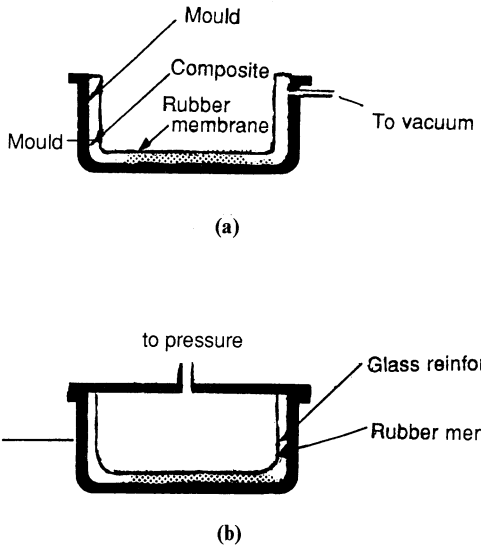

Figure 5.2 Spray-up moulding technique. (a) Vacuum bag moulding method; (b) pressure bag moulding method.

process. Epoxy resin systems can be used but the gel coats available for use with these resins cure relatively slowly.

5.2.1.2 Spray-up technique. The spray-up technique as shown in Figure 5.1(b) is less labour intensive than the hand lay-up method. During the spray-up operation, glass fibre roving is fed continuously through a chopping unit, and the resulting chopped strands are projected onto the mould in conjunction with a resin jet. The glass fibre/resin matrix is then consolidated with rollers. The technique requires considerable skill on the part of the operator to control the thickness of the composite and to maintain a consistent glass/resin ratio.

Although the labour content in this method is less than in the hand lay-up technique, it is considerable in both techniques, and the quality of the finished composite is highly dependent on the skill of the operators. The two processes are relatively simple and the low tooling cost can result in considerable versatility from the designer's point of view. Very large mouldings have been produced by these methods.

After the initial polymerization of the composite, and when it has been demoulded, the unit must be cured; the curing procedure is usually an exposure to a temperature of 60°C for 8 h.

Polyester systems are used with this process. A similar spray technique can be employed with epoxy resins but because of the difficult mixing ratios of resin to curing agent, the polyester spray equipment is generally unsuitable. The resin and curing agent would be either pre-mixed and sprayed through a single-component spray gun or a two-component gun filled with an appropriate metering pump.

5.2.1.3 Pressure bag technique. Pressure bag techniques are practical and low cost methods for the fabrication of closed vessels. Three different procedures are discussed in which the normal contact moulding has been undertaken and before curing has proceeded, a rubber membrane is placed over the component and sealed at the boundary of the mould; one of the following techniques is then used for greater compaction of the laminate. Polyester and epoxy resin systems are equally suitable for processing by pressure bag techniques as are glass, carbon and synthetic fibre reinforcements.

Vacuum bag. A vacuum is created under the membrane. The pressure is equivalent to about 1 atm being applied to the surface of the moulding which forces out air and excess polymer. A protective sheet of cellophane is place on the surface of the composite to prevent any deleterious effect of the resin on the vacuum bag. A 55% glass resin ratio by weight is possible using this technique. Figure 5.2(a) illustrates the moulding.

Pressure bag. In this process, a pressure of about 3 atm is applied directly

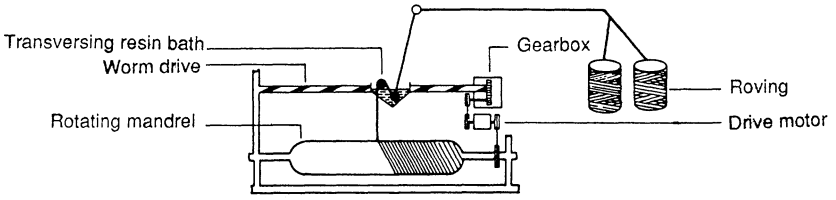

Figure 5.3 Filament winding technique.

to the rubber membrane. As the pressures applied in this method are much greater than in the vacuum bag method glass resin ratios by weight can be increased to about 65% with a corresponding increase in mechanical properties. Figure 5.2(b) shows the pressure bag moulding.

Autoclave. The autoclave process is a modification of the pressure bag method; a pressure up to 6 atm is developed within the autoclave, thus producing a high quality composite with a glass resin ratio by weight of up to 70%. However, the cost of production also increases.

5.2.1.4 Filament winding technique. In filament winding, continuous strands or rovings of reinforcement are passed through a bath of activated resin and then wound onto a rotating mandrel. The angle of helix is determined by the relative speeds of the traversing bath and the mandrel. If resin pre-impregnated reinforcement is used, it is passed over a hot roller until tacky and is then wound onto the rotating mandrel. Figure 5.3 illustrates the process. After completion of the initial polymerization, the composite is removed from the mandrel and cured; the composite unit is then placed into an enclosure at 60°C for 8 h.

5.2.2 Closed mould techniques

The production of fibre matrix composites by moulding techniques using matched dies has been undertaken for many years. The hot press moulding technique is usually selected as being the most economical, while the cold press technique is an intermediate one between the slower open mould systems which are essentially for large products, and the faster but more expensive hot press moulding system in which long runs of small to medium composites are produced. Resin injection and pultrusion techniques are other systems in the closed mould group.

The matched die processes utilize pressure and sometimes heat to produce mouldings with a good finish on both surfaces of the composite. Compared with the open mould technique, this system enables a higher glass content to be used in the composite with improved mechanical properties. It also achieves uniform dimensional properties with lower labour costs.

There are basically three manufacturing processes under this heading:

(a) matched die process;
(b) pultrusion process and the pull-winding process;
(c) resin injection process.

5.2.2.1 Matched die process. The four processes and the materials used in association with them are described in the following sections; each of the methods comes under the heading of a matched die process. Components which are produced from matched dies are complex in shape, consequently randomly orientated fibres are generally used in one of three ways depending on the press system and the moulding technique employed.

The first material system is known as preform moulding where chopped fibres are bonded together in the form of a mat conforming to the shape of the article being made; the mat is known as a preform. This mat is manufactured by projecting chopped rovings onto a rotating fine metal mesh screen which is shaped to the required dimensions; the fibres are held on the screen by applying a suction behind it. The strands are held together by spraying the preform with a resinous binder in the form of a powder or an emulsion, and the whole is transferred to an oven at 150°C for 2–3 min, after which time the preform is ready for the press.

The second material system is the sheet moulding compound (SMC) or prepreg. This material is a polyester resin based material which consists of a mixture of chopped strand mat or chopped fibre, resin, fillers, catalyst and pigment. The fibres vary in length and content, between 12 and 55 mm and 20 and 35% by weight, respectively. They are produced and supplied in the form of a continuous sheet wound into a roll and protected on both sides by sheets of polythene film; the latter are removed before loading into the press. Figure 5.4 show the SMC manufacturing procedure. The desired composite shape and rapid cure are obtained by the application of heat and pressure in the mould and as the material flows uniformly to produce a homogeneous composite, complex and deep draw mouldings can be produced. It is necessary to comply with the correct conditions for moulding; these include using a suitable press and a mould designed specifically for the material, charging

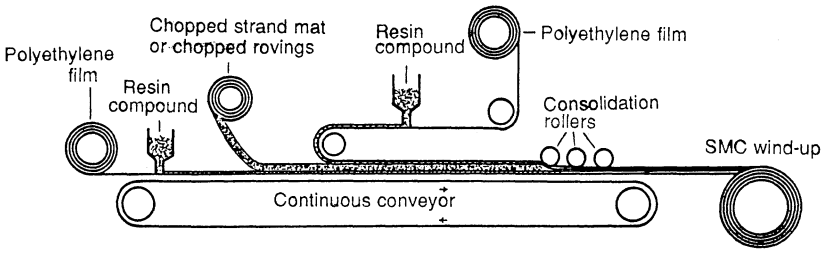

Figure 5.4 The SMC manufacturing procedure.

the mould in the correct manner and using the optimum temperature, pressure and curing time. Moulding pressures of between 3.5 and 14.0 MN/m^2 and moulding temperatures of between 125 and 155°C are generally required; the lower pressures and temperatures are used for moulding simple flat shapes and the higher values for the more complex mouldings. An advantage of this material system is that no liquid resin is involved and the prepreg sheets can be prepared to the design size by cutting.

The third material system is the dough moulding compounds (DMC) or bulk moulding compound and is an unsaturated polyester resin, an unsaturated cross-linking monomer such as styrene, suitable mineral fillers and fibrous reinforcement which is usually chopped strands. The fibres vary in length and content between 3 and 12 mm and 15 and 20%, respectively. Because DMC flows readily, it may be moulded by compression transfer or injection and the pressure required to produce a component is relatively low so that large mouldings can be produced without much difficulty. Curing takes about 2 min for moulding temperatures in the region of 120–160°C although this will depend on the section thickness. These compounds do not give such high composite mechanical properties as the SMC because of the geometry of the component parts, but they can be used for intricate mouldings. Both SMC and DMC have particular uses in the wide field of appliances and fittings for the building industry, but have not been extensively used in the structural applications of polymers.

Hot press moulding system. In the hot press moulding technique, glass fibre reinforcement and a controlled quantity of hot curing catalysed resin are confined between heated matched polished metal dies brought together under pressure Figure 5.5 shows the technique. The fibre/matrix material may be in the form of preform or sheet moulding compound. The dies may be manufactured from steel, cast iron or aluminium but the highest quality surfaces are obtained from dies of chrome-plated steel. The pressures that are involved in the manufacture will vary depending upon the process being undertaken but will normally be in the range from 400 to 4000 kN/m^2 and the mould temperature will be between 120 and 150°C. The application of heat will ensure that rapid curing takes place and consequently no subsequent curing is required.

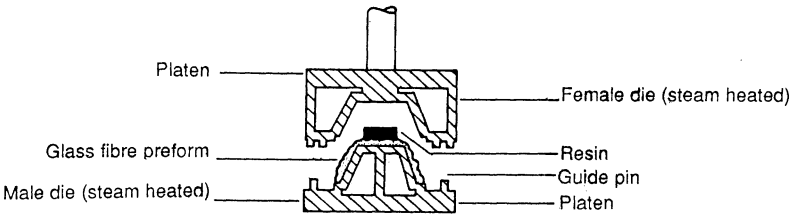

Figure 5.5 Hot press moulding technique.

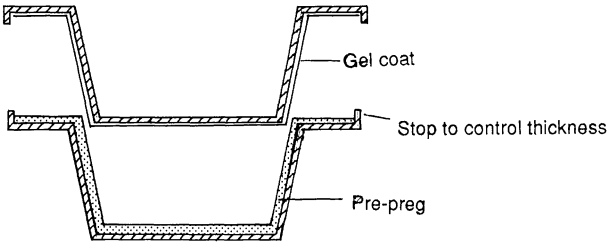

Figure 5.6 Cold press moulding technique.

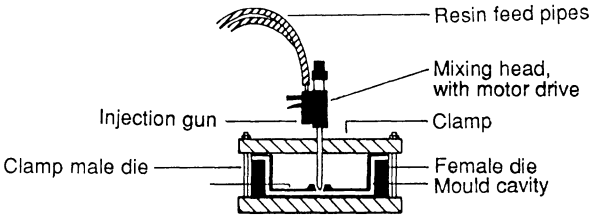

Figure 5.7 Resin injection process.

Cold press moulding system. In the cold press moulding technique, matched tools can be used at much lower pressures and temperatures than those for hot press mouldings; consequently, the cold press moulding system can employ polymer material in the manufacture of the moulds although this does limit the pressures that can be applied. Activated polymer is poured onto the top of the reinforcement and the mould is then closed; the polymer spreads throughout the fabric under the mould pressure, which may be as low as 100 kN/m^2. Curing of the composite is necessary after demoulding to ensure full polymerization. Figure 5.6 shows the cold press moulding system.

5.2.2.2 Resin injection. In this process, glass fibre reinforcement is placed in position in the bottom mould and allowed to extend beyond the sides of the moulds. Figure 5.7 illustrates the resin injection process. The top mould is then placed in position over the bottom one and secured; thus the reinforcement is held firmly in position while the resin is injected. A pressure of about 400 kN/m^2 is sufficient for most mouldings, and when resin seeps through holes specially placed at the highest point of the mould, the resin inlet socket is then sealed.

5.2.2.3 Pultrusion process. The pultrusion technique is one of the few fully automated continuous processes used in the reinforced plastics industry. Constant section shapes are produced by pulling strands, together with any additional required layers of fabric, through a heated die; the strands have

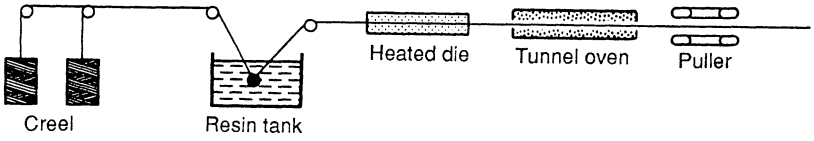

Figure 5.8 Pultrusion technique.

been previously impregnated with resin. Figure 5.8 shows a diagrammatic representation of the process. The products are generally straight and can take most geometrical cross-section shapes, although recently some products which are curved in the longitudinal direction have been manufactured.

The production procedure can essentially be divided into three steps which are assigned to corresponding parts of the production line:

(a) feed-in and impregnation;
(b) shaping and curing in a heated die;
(c) pulling and cut-off.

The greatest technical problems appear in (a) and (b).

The fabric and strand reinforcement are drawn from creels and are passed through a resin bath. After picking up an excess of matrix, the saturated fibre is passed through a number of wiper rings into the shaper and heated die. This processing section is an important part because the final product depends on the cure with which the reinforcement material is fed in and impregnated.

The shaped composite is gripped firmly between rubber blocks and is pulled through the die at a predetermined speed to enable curing of the composite to take place. For economic reasons, the highest possible operating speed is desired but this is influenced by two factors. The first is the curing rate and the second is the time required for excess solvents to be drawn off from the composite. Some solvents have to be retained in the material to enable it to be sufficiently flexible during the production process, but the excess solvent must be renewed to prevent environmental exposure to it.

The processing techniques for producing pultrusion sections can be divided into three categories:

(a) the horizontal pultrusion process;
(b) the vertical pultrusion process;
(c) the lamination process with film tape.

The details of these three processes have been discussed in [1] and are not repeated here.

5.2.2.4 Pullwinding. The pullwinding process is an extension of the pultrusion technique for the manufacture of mainly closed sections. Figure 5.9 shows a diagrammatic representation of a five layer tube system. The process combines

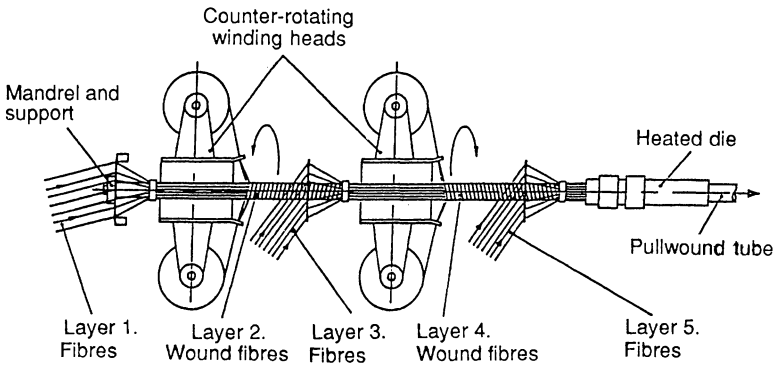

Figure 5.9 Five-layer tube on a double head pullwinder (by kind permission of Pultrex Ltd.).

the continuous fibres used in the pultrusion technique with continuous wound hoop direction fibres; these latter provide crushing and hoop resistance. There are many different types of fibre and resin combinations as well as various fibre orientations to enable the composite to be engineered into an efficient system. The general principle is to combine the undirectional fibres with those wound around them to give combinations of 0° (unidirectional) and 90° (hoop) fibre layers; fibres in the 0° direction could also be combined, during the manufacturing process, with randomly orientated fibres or those orientated at some angle θ to the 0° direction.

PART 2

5.3 Processing methods for the manufacture of unreinforced thermoplastic polymer items

The processing methods for thermoplastic polymer items generally require that they are produced in one operation; this may require the production of sheets, rods or complex shapes. The processing stages such as heating, shaping and cooling would normally be undertaken as a simple event or a repeated cycle.

The principal processing methods for thermoplastic polymers are:

(a) extrusion;
(b) injection moulding;
(c) thermoforming;
(d) calendering.

One of the most important methods for processing polymers is extrusion. The thermoplastic polymer material usually in the form of granules or powder is placed in a hopper and from there it is fed into a rotating screw which is

inside a heated barrel. The screw channel depth is reduced along the barrel so that the material is compacted and at the extremity of the extruder, the melt passes through a die to produce the finished article.

By using the appropriate die in the extrusion technique, a wide range of products can be produced. Some of the more common of these are:

(a) profile products;
(b) film-blowing polymer sheet;
(c) blow-moulding hollow plastics articles;
(d) co-extrusion;
(e) highly orientated grid sheet.

5.3.1 Profile products

A range of profiles such as edging strips, pipes, window frames, etc. can be manufactured by the extrusion process. However, it is not an easy technique to apply and success depends on the correct design of the extrusion die; the extruded profile is manufactured to the approximate size and then sizing units are used to obtain the correct dimensions.

5.3.2 Film-blowing polymer sheet

Currently the commonest method of producing polymer sheets and film is by the film blowing process. Thermoplastic polymer from the extruder passes through an annular die to form a thin tube; a supply of air to the inside of the tube prevents it from collapsing and may also be used to inflate it to a larger diameter. When the polymer is cooled, it passes through collapsing guides and nip rolls and is stored on drums. By varying the air pressure in the polymer tube, biaxial orientation of the molecules of the polymer can be achieved and this in turn controls the circumferential orientation.

5.3.3 Blow moulding

This method was originally developed from the glass blowing technology to produce hollow plastic articles. However, currently a wide range of technical mouldings can also be made by this method. A number of variations on the original process are in existence but only extrusion blow-moulding is discussed.

In the extrusion blow-moulding technique, a molten polymer tube, known as the parison, is extruded through an annular die and a mould then encloses it. An internal pressure forces the polymer against the sides of the mould. This method can be used to manufacture cold water storage tanks, general containers, etc; the materials that are generally used are polypropylene, polyethylene and PET.

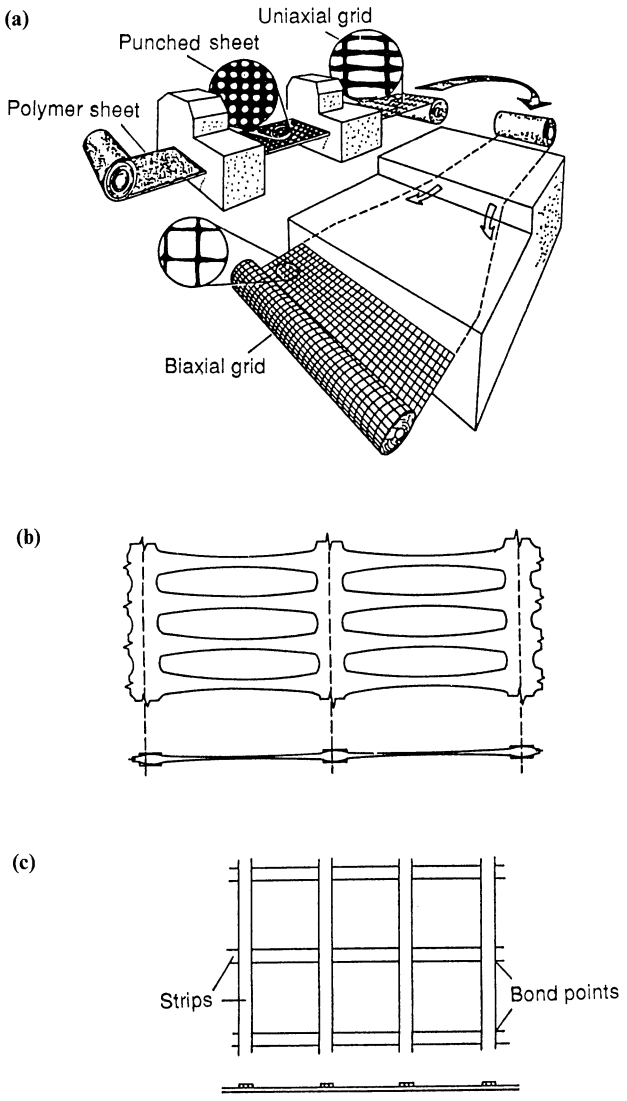

Figure 5.10 (a) The manufacturing process for sheet-formed grids (after [2]). (b) Punched sheet geogrids stretched in the longitudinal direction only. (c) Cross-laid strip geogrids.

5.3.4 Co-extrusion

If it is necessary to use a multilayer plastic composite to satisfy a correct combination of in-service properties, the co-extrusion process, when two or more polymers are combined into a single process, is employed to produce

a multilayer film. Generally, the adhesion between the different polymer layers is not good and an adhesive film is used.

5.3.5 Highly orientated grid sheets

Continuous sheets of thermoplastic polymers, generally polypropylene or polyethylene are extruded to very fine tolerances and with a controlled structure. A series of holes are stamped out in the sheet to a particular pattern and are returned for re-use. The perforated sheet is stretched in the transverse direction to give a highly orientated tolerance in that direction with a tensile strength of that of mild steel. If necessary, the sheet can also be stretched in the longitudinal direction to give a mesh of biaxial strength. The stiffness of the material can be increased ten-fold. It should be remembered, however, that the stiffness is low initially. The stiffness of the non-orientated HDPE, for instance, is only $1\,GN/m^2$; however, when it has been formed into an orientated molecular structure, its stiffness value increases to $10\,GN/m^2$. Practical uses of this material are given in section 6.11. Figure 5.10(a) shows the manufacturing process for sheet-formed grids and Figure 5.10(b) illustrates the punched sheet geogrids stretched in the longitudinal direction only. Figure 5.10(c) shows the cross-laid strip geogrids.

5.4 Processing methods for the manufacture of reinforced thermoplastic composites

The mechanical properties of thermoplastic polymers are considerably improved by the addition of fibres. The manufacturing techniques used to produce the reinforced thermoplastic composites are similar to those used to produce the thermoplastic polymer; for example the extrusion, the blow moulding and the thermoforming of short fibre reinforced thermoplastic processes. Probably the most important technique is injection moulding where the added fibres are short and randomly orientated. The melt viscosity is higher in the reinforced polymer process and consequently the injection pressures are higher. In addition, the stiffness of the reinforced composite is greater than that of the unreinforced polymer, the cycle time is less but the increase in stiffness can affect the ejection from the mould; consequently, the design of the mould has to be modified from that of the unreinforced polymer mould. To overcome this difficulty, glass fibre reinforcement impregnated with a thermoplastic polymer to form a prepreg can be manufactured and then thermoformed into the required shape. The reinforcement may consist of unidirectional continuous fibre strands, woven rovings and a continuous random mat; a combination of these reinforcements may also be used. The polymers which are currently being exploited include polypropylene, poly-

amides, polysulphone, polyparaphenylene terephthalamide and polyether-etherketone; the last three require high temperature applications and are members of the family of aromatic polymers.

These materials are intended to compete with the wet lay-up systems, with the sheet moulding compounds (section 5.2.2.1) and the prepregs based on thermosetting polymers. The principle of fabrication is to preheat the sheet and then to shape it by pressing, or stamping, between heated discs. Because there is no chemical curing operation as there is with the thermosetting resins, the process offers a faster production rate; the process may be compared with metal pressing.

The mechanical property and surface finish of the composite will determine the constitution of the material. Continuous aligned strands and woven cloth will give the highest mechanical properties, but will limit the flow possibilities of the polymer, so that the materials containing this form of reinforcement would be suitable only for panels of shallow curvature. For the more complex shapes, randomly orientated fibres or continuous random mat fibres are used; these latter fibre arrays allow maximum flow but there is a danger that the polymer may flow into the extremities of the mould and so cause a danger of non-uniform fibre distribution.

5.4.1 Film stacking process

The film stacking technique is a thermoforming process. The product is manufactured from two components; a prepreg of cloth reinforcement and a matrix in the form of films. The manufacturing process consists of alternating layers of the prepreg with polymer film of complementary mass. It is designed to give the correct fibre volume ratio. The whole is placed into one part of a split mould; the two half moulds are brought together and heat and pressure are applied to them. This manufacturing technique is used mainly for the production of high technology composites in the aerospace and space industries. Reinforcing films such as glass, carbon and Kevlar have all been used successfully, glass being particularly useful in short-wave electrical applications such as radomes.

5.5 Manufacturing faults

The properties of materials can degrade during the life span of a structure if cracks are present in the matrix. As a result of the complexity of composite materials, quantitative information regarding the effects of this is difficult to produce except for specific in-service conditions. However, a general overview of defects that can occur in these materials is described in the following sections.

5.5.1 *Porosity*

The term porosity is also known as resin voids or void content and usually occurs if the cure pressure is applied too late in the cure cycle thus causing air to be trapped throughout the lay-up; this defect is not usually confined to a restricted area within the composite. Voids can also be formed in the manual and semi-automated processes as a result of inadequate roller compaction.

Clearly a high volume of voids within the lay-up causes some reduction in load transfer throughout the composite. Voids also act as an area for moisture retention and can have a marked effect on the overall properties of the composite.

5.5.2 *Prepreg gaps and fibre alignment*

A unidirectional prepreg is produced by rolling and flattening several bundles of fibres which are then impregnated. Inadequate monitoring at the production stage can result in gaps in a fibre sheet or disturbance of the fibre direction, consequently there should be strict quality control of the prepreg during manufacture. In addition, during the manufacture and handling of the prepreg it is possible for fibres to become detached and to form whorls during manufacture or misalignment during lay-up.

5.5.3 *Prepreg joints*

There are three types of prepreg joints, those that are perpendicular and those that are parallel to the fibre direction in directional reinforcement, and the side by side joints relevant to the randomly orientated fibre. The first two types are found specifically in the film stacking procedure but all three types can be found in hot press moulding techniques.

The first type is not recommended except where the prepreg joint is in a low stress area. The second type is much less critical to the integrity of the fabrication. As the composite is laminated to the required thickness, the joints would be staggered in the thickness direction. It is important to ensure that no entrapped air bubbles are allowed to form during lay-up of the prepregs particularly over complex curved surfaces as this will cause delaminations. These are particularly deleterious to a laminate as the whole basis of strength and stiffness of the composite structure is modified, particularly with respect to compressive loads.

5.5.4 *Resin micro-cracks*

Resin micro-cracks can be caused during the cure cycle if the correct temperature cycle is not adhered to. Resin rich zones are sites for the initiation of cracks within the resin but it is possible for them to be created throughout

the laminate. Fibre rich areas can also give rise to micro-cracking in the direction of the fibres.

5.5.5 Resin shrinkage

Thermosetting polymers shrink during curing; polyester resin has a shrinkage of the order of 5–10% by volume and the corresponding value for epoxy resins is of the order of 2% by volume. It may be argued that, because of the shrinkage, the polymer 'grips' the fibres more firmly than if no shrinkage took place.

References

1. L. Hollaway, Pultrusion, in *Development in Plastics Technology*, 3rd edition, eds., A. Whelan and J.L. Craft, Elsevier Applied Science, London (1986), Ch. 1.
2. R.V. van Zanten, *Geotextiles and Geomembranes in Civil Engineering*, Balkema, Rotterdam (1986).

6 End-use performance properties of structural polymer composites

6.1 Introduction

To a structural engineer the in-service and the miscellaneous properties of materials are just as important as the mechanical properties; indeed the long-term in-service characteristics of a material are interrelated with its mechanical properties.

Durability is an aspect of performance that embraces most physical as well as mechanical and aesthetic properties and is therefore one of the most important qualities to be considered when polymers are used externally on buildings. It is necessary that polymers show a degree of resistance to the degradative action of the weather and although most polymers are, to a certain degree, chemically inert, their surfaces and mechanical properties may change when exposed to the atmosphere, which is not desirable. Architects see the 'mellowing' of traditional materials as a gain in aesthetic appeal but wish polymers to retain their pristine condition to achieve a particular effect and do not regard any physical change as desirable. To the user, change in appearance is often the most significant form of deterioration, but aesthetic properties and limits of acceptability are the most difficult to define. These points are discussed in subsequent sections.

The chapter is divided into three parts. The first part has a section on the specification and quality control for civil engineering polymers. Thermal and chemical properties, sound insulation, light transmission and abrasion resistance are also discussed. The second part discusses the durability of glass fibre reinforced polymers in relation to their mechanical and physical properties, and the various standards relevant to fire. It describes how improved fire performance may be imparted to polymer structures through specific provisions as used in the construction industry. The third part introduces the end-use performance of geosynthetics.

PART 1

6.2 Specification and quality control

The procedure for controlling a product's performance is known as quality assurance; the quality of the finished product will therefore be dependent on

this assurance. To be able to ensure that the components meet all the necessary requirements, it is essential to write a specification covering all aspects of performance and to ensure that the finished product meets this specification. The specification should include:

(a) raw material quality;
(b) an adequate design of all components;
(c) sufficient detail consistent with design requirements for the manufacture of the finished components.

Because there are several different manufacturing processes for glass reinforced polymers ranging from high output, high investment press moulding to low output, low investment hand lay-up, the quality control problems for the various processes are different. Once product, tool design and press operating techniques have been established, the hot press moulding automated stages involve fewer quality control problems compared to, say, the hand lay-up and spray-up techniques which are carried out at ambient conditions and in open moulds with little or no mechanization.

The quality control for reinforced polymer mouldings is covered by the BS 4549 [1] (no ISO equivalent) and is based on performance criteria. This control must be assessed by a routine programme of testing. Probably the most important part of BS 4549 is Part 1 which deals with mouldings such as chopped strand mats or randomly deposited glass fibre. This material is discussed in detail as an example of these types of specifications.

(a) *Materials*: If the materials' specifications are to comply with a BS specification, the suppliers must guarantee the material to this standard.
(b) *Selection of test specimens and frequency of testing*: Test specimens for the assessment of hardness and residue on ignition must be taken from the actual composites. For other tests, specimens with identical fabrication histories are sufficient. An adequate number of samples must be selected to be representative of the product quality and appropriate tests undertaken.
(c) *Preliminary examination.* Each component must be examined visually for defects such as protruding fibres, pits, blisters, eroding and cracks, voids, bubbles, resin rich or resin starved areas, surface tackiness and presence of foreign matter (see section 6.8).
(d) *Dimensions.* Tolerances on dimensions of the components must be agreed between the architect and fabricator. Tolerances for the thickness of a composite are given in Table 6.1 (derived from Table 1 in BS 4549, Part 1).
(e) *Glass content.* If the nominal glass content is specified as $N\%$, the variation must be within $(N-2.5)\%$ to $(N+7.5)\%$. If during the manufacture of a composite, no mineral fillers are used, the residue on ignition can serve as a quick control to the glass content. Alternatively, if mineral fillers are used, BS 2782 *Determination of loss on ignition, Part 10: Method 1002*

Table 6.1 Tolerances for the thickness of composite values (after BS 4549 Part 1 19, Table 1)

Nominal thickness (mm)	Open mould (mm)	Closed mould (mm)
Up to but not including 1.5	$-0.25 + 0.50$	± 0.20
1.5 but not including 3.0	± 0.75	± 0.30
3.0 but not including 6.0	± 1.1	± 0.50
6.0 but not including 12.0	± 1.5	± 0.75
12.0 but not including 25.0	± 2.0	± 1.4
25.0 and over	± 3.0	± 1.9

[2] (equivalent EN60, ≠ISO 1172) may be used as a basis for determining the glass content.

(f) *Degree of cure.* The degree of cure of a composite may be estimated by the Barcol hardness of the material. The minimum value should be at least 90% of the Barcol value specified by the resin manufacturer. The Barcol value is temperature dependent and therefore the test temperature with a tolerance of $\pm 2°C$ on the minimum Barcol values for a range of temperatures must be specified. In certain cases, it may also be necessary to determine the hardness of the gel coat.

It should be noted that the requirements of BS 4549, Part 1 are not always satisfied, particularly in the open mould process. Some fabricators have difficulty in satisfying the tolerances for the thickness of the composite and for the variation of the glass content.

6.3 Thermal properties

The thermal properties of glass reinforced polymers are important when used for structural components. Unreinforced or unfilled polymers have a very high coefficient of expansion which creates design and detailing problems when used in conjunction with traditional materials. Table 6.2 contains typical thermal properties of GRP components and compares them with conventional engineering materials. An effect of incorporating glass fibres and fillers in the polymer materials is to reduce the coefficient of thermal expansion to a composite value of the same order as that for aluminium.

The thermal conductivity of all polymers is low, as shown in Table 6.2; consequently, glass reinforced polymers of sufficient thickness are good insulators and when used with glass fibre wool or foamed polymers, the composite construction has an extremely low *U*-value. When reinforced polymers are used as the faces of an insulating sandwich construction, the resulting composite has a low thermal conductivity.

The temperature limit at which resins begin to lose their rigidity is known

Table 6.2 Thermal properties of some engineering materials

Material	Coefficient of linear expansion ($°C \times 10^{-6}$)	Thermal conductivity (W/m°C)
Steel	11.3	46.0
Aluminium	23.0	140.0–190.0
Timber	5.4–54	0.124–0.24
Concrete	13.0	0.98
Glass fibre	8.6	1.02
Polyester resin	50–100.0	0.11–0.28
Glass fabric with polyester resin	9.0–11.0	0.3–0.35
Woven fabric with polyester resin	11.0–16.0	0.2–0.3
Hand lay-up CSM laminate	22.0–36.0	0.2–0.24
SMC	20.0–28.0	

as the heat deflection temperature (HDT). If the resin is reinforced, this value rises by almost 20°C. The heat deflection temperature represents a limiting factor in design as creep of the material under load becomes appreciable when approaching this temperature. BS 4994 [3] does not permit the use of resins at temperatures greater than (HDT -20)°C.

British Standard Specification 8208 [4] (no ISO equivalent) assesses the suitability of cavity walls. The factors affecting the internal environment of a building together with appropriate design recommendations and the thermal insulation of buildings are controlled by the building regulations.

6.4 Chemical resistance properties

The chemical resistance of GRP laminates is dependent on the composition of the composite, the type of polymer, the surface finish and the degree of cure. In addition, the weather and water resistance of the polymer composite is a function of the quality of the gel coat which is the surface exposed to the atmosphere.

Generally, under normal environmental conditions, acidic and alkaline attack on the composite will not be the concern of the structural engineer; the main requirement is that the polyester and epoxy have been properly cured. If, however, these acidic and alkali conditions are found, they will aggravate the effects of moisture on the polymer.

GRP is used to fabricate process plant items such as storage tanks, reaction vessels, pumps, values, etc. and the associated connecting pipework, and in these cases design procedures must be closely followed. Several methods are currently used to select the design stress, the most common of which is based on the division of the ultimate tensile strength by a design factor, usually in

the range 8–16. Alternatively, the design stress may be obtained from long-term stress–rupture or fatigue data. Design stress obtained in this way may be further reduced by the application of arbitrary factors to take account of manufacturing variables and other considerations such as the chemical environment.

Selection of GRP for a chemical duty has traditionally been based on the results of exposure of unstressed laminates to the environment for periods up to 1 year. These tests satisfy the ASTM requirements or in the case of severe environments such as sulphuric and hydrochloric acid, have been the subject of detailed analyses to determine the effects of temperature, concentration and permeation. The suitability of the material is based on the residual mechanical properties (typically hardness, flexural strength and stiffness) and on visual observation of any blistering and delamination. However, while the strength retention data give information on the mechanisms of chemical attack and hence allow decisions to be taken on the suitability of GRP for a particular environment, the information so obtained is of limited value for design purposes.

The important variables that should be addressed when considering the environmental testing of GRP are:

(a) resin type;
(b) fibre array and type;
(c) gel coat thickness and reinforcement;
(d) catalyst system and cure schedule;
(e) fibre/matrix ratio;
(f) additives (such as fillers, fire retardant waxes, etc.);
(g) effects of air inhibition;
(h) types of exposure;
(i) thickness of composite.

The most widely used resin types to provide various degrees of chemical resistance are:

(a) orthophthalic giving low chemical resistance;
(b) isophthalic, terephthalic giving medium chemical resistance;
(c) biphenol, hot acid, vinyl ester, furance and epoxy giving high chemical resistance

6.4.1 Effects of chemicals on polymers

Water diffuses very slowly into glass reinforced polymers and reaches equilibrium after 1 year. At room temperature, the percentage increase in weight due to absorption of water is about 0.3% whereas at 80°C, the equivalent percentage is 1.0. There is a reduction in strength as water diffuses into the polymers and after 1 year bisphenol polyester laminates will have

a strength retention value of only 60%. Isophthalic polyester laminates have a large decrease in strength as water diffuses into it and after 9 months the strength retention value is only 20%. Orthophthalic polyester laminates have very poor strength retention of only 20% after 1 month.

If there is a strong chemical affinity between the laminating resin and the attacking chemical, then the small molecules (solvent) can diffuse through the polymer and affect the mechanical properties. Generally, physically absorption causes:

(a) losses in strength and stiffness;
(b) increase in toughness and creep rate of the polymer.

Thus the invading molecules destroy some of the chemical bonds in the resin and the mechanical properties are degraded.

If the attacking chemical is from an acidic effluent such as that found in chemical waste pipes, it is possible to incorporate a thermoplastic liner; these have been successfully incorporated into GRP equipment. The liners include

(a) PVC;
(b) polypropylene;
(c) PVDF;
(d) PTFE;
(e) polyethylene.

However, the lined systems may have a limited use in organic environments because of the diffusion of the organics through the liner and subsequent attack on the reinforcing laminate.

6.4.2 Natural weathering of polymers

Polymers that are exposed to natural weathering will deteriorate but the degree of deterioration will be dependent on a number of factors. These may be listed as:

(a) the type of resin used for the gel coat and for the lamination of the composite;
(b) the orientation of the composite relative to the sun's rays;
(c) the ultraviolet component of the sunlight on the composite which is dependent upon item (a);
(d) the action of the weather on the composite in different climates and situations;
(e) the proportion of 'impurities' in the polymer (i.e. fire-retardant additives, etc.);
(f) the provisions of the required level of quality control to ensure a suitable production environment, a correct fabrication procedure and an adequate cure for the resin.

6.4.2.1 *The gel coat.* The durability of polymer composites is mainly dependent on the quality of their exposed surface. Consequently, it is necessary to protect this surface, and particularly any exposed fibre which could be attacked by the atmospheric moisture, by using a gel coat. This coat is the most important part of the laminate and great care must therefore be taken during the formulation of the resin and its application to the composite by brush or spray in a uniform thickness of about 0.4–0.5 mm. If the gel coat is too thin it may not fully cure and the glass fibre in the composite might show through it. Conversely, if it is too thick, it may craze or crack, with a consequent reduction in impact strength. A variation in thickness of the gel coat will cause different rates of curing and it is advisable to reinforce it by a glass fibre surface tissue.

6.4.2.2 Orientation of the composite to the sun's rays. The orientation of the composite to the sun's rays has a significant effect on its rate of deterioration. For instance, a GRP composite panel that is inclined towards the direction of the sun will weather less well (from the sun's ultraviolet rays) than one that is shielded from it. Conversely, the panel that is shielded from the rays of the sun will take longer to dry out and therefore will weather less well, from that effect, than the one that is facing the sun.

6.4.2.3 Ultraviolet component of sunlight. The ultraviolet component of sunlight degrades the composite and the short wavelength band at 330 nm has the most effect on polyesters. It is manifested by a discoloration of the polymer and a breakdown of the surface of the composite. Ultraviolet stabilizers are incorporated into the polyester resin formulations to obviate this problem. The inclusion of these stabilizers in epoxy resin formulations seems to have little effect regarding the discoloration and there is no evidence that continuous exposure to sunlight affects the mechanical properties of these polymers.

6.4.2.4 Action of weather on composites. BS 4618 [5] (no ISO equivalent) recommends natural weathering trials to be made with exposure times of 3 months, 6 months, 1, 2, 4, 6, 8 and 10 years and such longer periods as are necessary. Climates are broadly classified into five different types.

1. hot and wet;
2. hot and dry;
3. mesothermal;
4. temperate;
5. cold.

It is recommended that trial conditions should simulate those of normal service; in addition, certain other tests should also be performed. For instance,

the effects of periodical cleaning should be observed on a second series of specimens.

During weathering tests, the specimens under examination are assessed against control specimens stored under defined conditions, for any or all of the following:

(a) dimensions;
(b) visual appearance;
(c) mechanical properties;
(d) biological attack.

6.4.2.5 Fillers. Fillers and pigments have a major effect on the appearance and durability of polymers. Pigmented polymers absorb incident infrared and visible radiation and this process tends to accelerate the rate of degradation by raising the temperature of the composite; this is particularly noticeable in hot climates; epoxy resins also tend to degrade in a similar way in hot climates.

The majority of long-term estimates on the quality and behaviour of polymer composites have been derived from accelerated tests but inevitably these have limitations which are principally due to:

(a) the difficulty of correlating the results of the accelerated laboratory tests with normal weathering conditions;
(b) the lack of an interrelationship of polymer materials.

6.4.2.6 Quality control. The quality control for the manufacture of the GRP composites has been discussed in section 6.2. Probably the main complaint regarding their appearance and performance can be traced to the inadequate or poor procedure methods for the cure of the material. If the polymer is undercured, some of the resulting defects that will appear during the life of the composite are discussed in section 6.8.

6.5 Sound insulation

In all buildings, sound transmission must be reduced to a minimum. The ideal way of achieving this is to incorporate heavy bulk materials in the construction. As with many other materials, reinforced polymers are not normally used in bulk and consequently sound reduction is difficult to achieve. The required degree of sound insulation may be provided by utilizing a composite design. In a sandwich construction this can be achieved by a filled foam core or by using plaster board as a lining material in which the sound is reflected or absorbed.

Expanded polystyrene is sometimes used as ceiling tiles but these do not absorb sound by porosity as do most acoustic tiles. They can, however, give

a measure of absorption when mounted on battens with an air space between the tiles and the backing surface.

British Standard Specification 8233 [6] and British Standard Code of Practice 153, Part 3 [7] give guidance in the design of building elements and components to ensure adequate sound insulation and noise reduction for various types of buildings and locations.

6.6 Light transmission property

The light transmission of a translucent GRP composite exposed to the atmosphere for a number of years is dependent upon the type of resin used and the resin content. Scott Bader [8], has observed a 14% reduction of light transmission over 5 years in the Crystic 191E resin reinforced with glass mat of fibre/matrix ratio 30:70% by weight and with a gel coat containing surface tissue. The same composite without a gel coat has a reduction of 30% and a resin glass mat with a fibre/matrix ratio of 35:65% by weight has a reduction of about 70%; these examples are all over the same period of time.

The accumulation of dirt on the internal surface of GRP laminates used as roof units is a further cause of reduction of light transmission and it is advisable to make provision for periodic cleaning of such surfaces. Common problems with fire-retardant resin laminates are discoloration, variations in the hue, and the appearance of dirt particles on the surface of translucent laminates.

6.7 Abrasion resistance

Abrasion resistance is dependent on hardness and toughness of the composite material. Polyester and epoxide resins are hard polymers and the addition

Table 6.3 Typical abrasion resistance of GRP laminates

Material	Surface roughness (μm)		Wear (μm)
	As received	After 1200 cycles test with abrasive cleaner	
Good gel coat on laminate	0.25–0.76	1.0	64
Poor gel coat on laminate	0.25–0.76	5.3	192

of glass fibre has little effect upon this physical property of the composite. However, to obtain improved abrasion resistance of composites, it is essential to use a gel coat with surface tissues. Table 6.3 gives typical abrasion resistance values for 'good' and 'poor' gel coats.

PART 2

6.8 Durability

The term *durability* is used to denote the period of time over which a material will perform its allotted task in its given environment. The specification of the durability should state that the components must conform to the performance specification for the expected life of the building; however, for some components, a shorter life may be acceptable. For this to be realistic, the appearance specification will need to incorporate allowances for any anticipated changes.

Durability is often difficult to assess and requires a keen judgement of what constitutes sufficient duration and adequate performance. One year's duration may be adequate when considering a chemical environment and Yovino and Dunwoody [9] have rated the resistance of GRP and other material to aggressive fluids over this period according to performance. On the other hand, the useful life of a composite exposed to the weather as part of a building may be as long as 50 years. This poses a problem when attempting to improve formulations since the results of field performance over limited periods have to be extrapolated to the specific length of time.

Adequate performance is also difficult to assess from a durability point of view because the aesthetic properties that are difficult to quantify may be important. An unacceptable condition for roof lights may be precisely defined in terms of light transmission. In the case of cladding, uneven discoloration and grime accumulation may manifest the changes that are unacceptable but are difficult to define.

Appearance of the exposed surfaces of a polymer composite component may change significantly in weathering and this in some cases may be sufficient to render that article aesthetically unacceptable. Mechanical properties of polymers may also decline in weathering, especially tensile strength and impact strength which are sensitive to surface deterioration.

Crowder [10] has stated that changes in say optical, mechanical and surface appearance are not interrelated. Consequently, observations of a simple property are not an adequate measure of the weathering performance of a polymer material. The phenomena that lead to a failure of polymers due to weathering are complex and vary with different materials. A discussion of the natural weathering of polymers is given in section 6.4.2.

Many problems concerning the appearance and performance of polymer

composites originate from the basic cause of polymer undercure. However, visible flaws and other defects in the composite are occasionally met and become apparent sometime during the life of the structure; some of these are discussed below and a possible remedy is suggested.

(a) *Poor adhesion of the gel coat to the laminating resin*: This defect may be noticed during the handling of the composite component when pieces of the gel coat flake off from the laminating resin or when blisters or undulations on the surface of the composite exist. The cause of the poor gel coat adhesion is usually inadequate consolidation of the laminate or overcure of the gel coat before lamination commences.

(b) *Wrinkling of the composite material*: If the gel coat is undercured, it can be attacked by the monomer in the laminating resin and wrinkling will result. To avoid this problem, the correct resin formulation must be used, the gel coat must not be too thin and the temperature and humidity must be controlled during the manufacturing process.

(c) *Fibre pattern*: The fibre pattern is sometimes visible through the gel coat or noticeable on the surface of the composite. This fault will occur if the gel coat is too thin or the laminating resin and fibre have been laid-up or rolled before the gel coat had hardened sufficiently.

(d) *Bliters in the composite*: Blisters, which are formed when air or solvents are entrapped within the laminate, can extend over a large area of the composite and are observed when composite delamination commences which may be several months after fabrication. Blisters are normally formed because the laminating resin had been undercured or because the moulding has been exposed to excessive radiant heat during curing. If the blister extends into the thickness of the laminate a possible cause is insufficient wetting of the reinforcement. If the laminate has been in contact with water over a long period of time blisters may be formed by the displacement of air from the voids in the composite; these voids are either in or just under the gel coat. The pressure in the voids increases with prolonged immersion in the water until the gel coat cracks and the pressure is released. This effect is more severe in fresh water or water which is heated. To overcome this problem, a compatible resin system should be used and the correct fabrication technique should be employed to give a well compacted laminate with minimum voids.

(e) *Crazing of the surface of the composite*: Crazing appears as fine hair cracks in the surface of the resin. It can occur immediately after manufacture or during its service life. The problem is associated with resin rich areas and is caused by incorrect resin formulations for the gel coat. If the crazing occurs after prolonged exposure to sunlight or chemical attack, it could be the result of under cure or the use of too much filler in the gel coat.

(f) *Poor wetting of mat*: Poor wetting of the mat will occur if the fibre/matrix

ratio is too high for the fabrication process being used. This defect normally occurs on the side away from the gel coat.

(g) *Leaching of the polymer*: Leaching is characterized by a loss of resin from the laminate thus exposing the glass fibre to attack from atmospheric moisture. This problem indicates that there has been either inadequate curing of the composite or there is incompatibility between the resin and in-service use.

(h) *Yellowing of the polymer*: GRP laminates tend to become yellow in colour after exposure to sunlight. It is generally only slight but can be severe in the case of white pigmented laminates. It is the result of absorption of ultraviolet radiation by the resin, however, by adding ultraviolet stabilizers to the resin formulation, it can be reduced considerably. Epoxy resins absorb strongly throughout the ultraviolet region and exposure to sunlight produces yellowing and surface degradation though there is little evidence of this seriously affecting the tensile or flexural strengths or moduli. Ultraviolet stabilisers and absorbers lead to little improvement in the epoxy resin system.

6.9 The fire behaviour of polymers

One of the chief concerns of the architect and engineer using polymers in the construction industry is the problem associated with fire. Because polymer materials are composed of carbon, hydrogen and nitrogen atoms (i.e. they are organic materials) they are all inflammable to varying degrees. It is possible, however, to incorporate additives into the resin formulations or to alter their structure, thereby modifying the burning behaviour and producing a composite with much enhanced fire properties.

The flammability behaviour of materials progresses through five different stages, namely ignition, development, spread, full burning and decay; the first stage is termed reaction to fire and includes flammability, spread of flame, heat release and production of smoke and toxic gases. The fire resistance of a building element is a measure of its ability to confine the fire within a compartment while the unaffected part of the structure remains stable throughout. The fire resisting requirements of different elements of a building are therefore related to the amount of combustion material present in the compartment, their function and their position relative to building boundary lines.

The Building Regulations [11] require that, depending on their use, building components or structures should conform to given standards of fire safety. The fire tests by which these are measured fall into two categories:

(a) reaction to fire: test on materials;
(b) fire resistance: tests on structures.

The test under the headings (a) and (b) above are laid down in BS 476 Parts 4, 5, 6 and 7 and Parts 3 and 8, respectively (Part 3 covers tests on roofs) [12] (this reference gives relevant British Standard Specifications and indicates the relative equivalents to ISO). It is clear then that the behaviour of composite materials in a fire depends on a number of factors, such as:

(a) ease of ignition;
(b) surface spread of flame;
(c) fire penetration.

Many trials for fire behaviour exist and most countries have their own particular methods, often requiring large specimen samples and special equipment; the following sections are some of the tests used in the United Kingdom.

6.9.1 Reaction to fire: test on materials

6.9.1.1 Non-combustibility test for materials. BS 476 Part 4 1970 (1984) defines non-combustibility and investigates whether the material, with or without a coating, meets the definition. In this test a thermocoupled cuboid sample is placed in a furnace at 750°C and the sample should not flame for more than 10 s or raise the original temperature of the furnace by more than 50°C. Polymers that would normally have more than 4% organic content are unlikely to meet these conditions.

6.9.1.2 Method of test for ignitability. BS 476 Part 5 (1979) discusses the readiness with which a material will ignite (namely the conditions at the start of the fire only). A 10-mm long flame is directed on to the centre of a vertical specimen, but it must be said that this test alone does not assess the ignitability of the polymer.

6.9.1.3 Method of test for fire propagation. BS 476 Part 6 1981 (1989) discusses the test required to measure the ignitability, the thermal characteristics and the rate at which heat is released from the specimen. Sample specimens of dimensions 228 mm^2 and nominal thickness not greater than 50 mm are mounted as one vertical side of a non-combustible cubical furnace. Initially, the specimen is subjected to a heat intensity of 1.8 kW and after 2.75 min, the intensity is altered to 1.5 kW for the 20-min test duration.

The emitted gases are directed through a chimney and cowl arrangement and the time–temperature curve for these gases is plotted at various intervals up to the maximum time of 20 min. The results are compared with those obtained from a known non-combustible material. An 'index of performance' I is calculated using the following expression:

$$I = \sum_{0}^{t_1} \frac{\theta_m - \theta_c}{10t} + \sum_{t_1}^{t_2} \frac{\theta_m - \theta_c}{10t}$$

Table 6.4 Classification for the spread of flame test

Spread of flame at 1.5 min	Spread of flame at 10 min	Classification
Not more than 165 mm; tolerance on one specimen 25 mm	Not more than 165 min; tolerance on one specimen 25 min	Class 1
Not more than 215 mm; tolerance on one specimen 25 mm	Not more than 455 mm; tolerance on one specimen 25 mm	Class 2
Not more than 265 mm; tolerance on one specimen 25 mm	Not more than 710 mm; tolerance one one specimen 25 mm	Class 3
Exceeding Class 3 limits		Class 4

where θ_m is the temperature rise in degrees centigrade recorded for the material at time t, θ_c is the temperature rise in degrees centigrade recorded for the non-combustible material at time t and t is the time in minutes from the beginning of the test. Generally two indices are calculated: one between 0 and 3 min and the second between 0 and 20 min; these should not be greater than 6 and 12, respectively.

6.9.1.4 Method of test for the surface spread of flame. BS 476 Part 7 determines the tendency of the material to allow a flame to spread along the surface of a specimen coupon of surface area $225 \times 900\,mm^2$, the length and thickness equal to that of the composite under consideration where this does not exceed 50 mm; six specimens are used in this test. A $1\,m^2$ radiant panel mounted vertically and producing approximately 300 kW is situated at approximately 225 mm from the short edge of the samples which are also mounted vertically with their longitudinal axes horizontal. The hotter ends of the specimens are then ignited for 1 min by a small flame of approximately 90 mm in length. The spread of flame for all specimens is measured and falls into one of the categories laid down in Table 6.4.

6.9.2 Fire resistance: tests on structures

In BS 476 Parts 3 and 8, fire resistance applies only to structures and not to the individual materials of which the elements are made. It is generally measured in length of time (e.g. $\frac{1}{2}$ h, 1 h etc.). The fire resistance tests enable the assessment of the ability of building components to retain their structural stability and to resist the passage of flame or hot gases.

6.9.2.1 Test methods and criteria for the fire resistance of elements of building construction. The test components should be representative of the element of construction in terms of fixings, finishes and manufacture, and the component should include at least one of each type of joint. Before the heating test, a load bearing component is subjected to the equivalent working stresses for the complete structure and this load is maintained during the

test period: the standard time for the test is 6 h at a temperature of 1200°C. During the test, observations are made on:

1. *Stability*: The deformation of the specimen and any collapse or other factors that could affect its stability are noted. In non-load bearing construction, failure is assumed to occur when collapse of the specimen takes place. Load bearing structures should support the test load during the prescribed heating period and for a further 24 h.
2. *Integrity*: The presence of cracks or other openings are noted. Failure is assumed to occur if flaming or hot gases pass through these openings and is determined by holding a cotton wool pad close to the aperture in the component at frequent intervals and for not less than 10 s, in order to observe whether the hot gases cause it to ignite.
3. *Insulation*: The temperature conditions of the unexposed face of the specimen are noted by continuous recordings.

External fire exposure roof test. BS 476 Part 3 (1975) specifies that two successive tests should be performed: the preliminary ignition test and the fire penetration and surface ignition test. In the former, the specimen is exposed to a flame for 1 min, and on its removal, observations are made for any continued flaming on the upper surface or fire penetration to the underside. If penetration does occur, no further test is undertaken.

In the fire penetration and surface ignition test, three specimens are tested and radiant heat of $14.6 \pm 0.5\,kN/m^2$ is applied to the upper surface of each for 60 min and may be extended to a maximum of 90 min unless penetration has occurred before this time. After the specimen has been exposed to the radiant heat for 5 min, the test flame is moved slowly over the surface at varying intervals and for 1 min duration. The time and occurrence of any flaming on the upper and lower surfaces and the development of holes and fissures are noted. Visual observations of changes in appearance, flaming and dripping are made and the minimum distance of the lateral flame spread on the upper surface is measured. The results are expressed in letter notation as follows:

The letter X indicates that:

(a) the duration of flaming exceeds 5 min after the withdrawal of the test flame,
(b) the maximum distance of flaming in any direction is greater than 370 mm.

The letter P indicates that:

(a) the duration of flaming is less than 5 min,
(b) the maximum distance of flaming in any direction is less than 370 mm.

The extent of surface ignition shall be given at 60 min or at the time of penetration to the nearest 25 mm. The classification P60, therefore, indicates

Table 6.5 Notation for results of penetration test

Penetration time	Letter code
More than 1 h	A
More than $\frac{1}{2}$ h	B
Less than $\frac{1}{2}$ h	C
Fails preliminary test	D

Table 6.6 Notation for results of spread of flame test

Spread of flame	Letter code
None	A
Less than 534 mm	B
More than 534 mm	C
More than 381 mm in preliminary test	D

that the specimen passed the preliminary test and that the fire penetration did not occur within 1 h.

Although the above classification has been introduced as a British Standard, the notations for classification of earlier standards are still used and are given here.

A prefix Ext F or Ext S is used to denote the flat or inclined test, respectively, followed by two letters denoting the results of the penetration test (given in Table 6.5) and the spread of flame test (given in Table 6.6). The final letter indicates the extent of dripping on the underside of the specimen. The performance of GRP in structural roofing applications should, in general, be at least Ext SAA or Ext FAA.

Methods of tests and criteria for the fire resistance of elements of building construction. BS 476 Part 8 (1972) gives tests to be undertaken on structural elements. The specimen part defines the sample size as $3\,m^2$ and forms one wall of the furnace and the temperature increase inside the furnace follows the curve shown in Figure 6.1; the thermocouples measure the temperature rise on the surface of the panel away from the fire. The failure of the sample is defined as an average rise in temperature of 140°C with one individual thermocouple giving a temperature rise greater than 180°C. In addition, failure would be defined when hot gases or flame penetrate through the sample or collapse of the sample panel takes place.

These two conditions define the point at which the through-the-thickness thermal conductivity and the collapse of the panel or roof occur (see Table 6.6 for the classification for the spread of flame test).

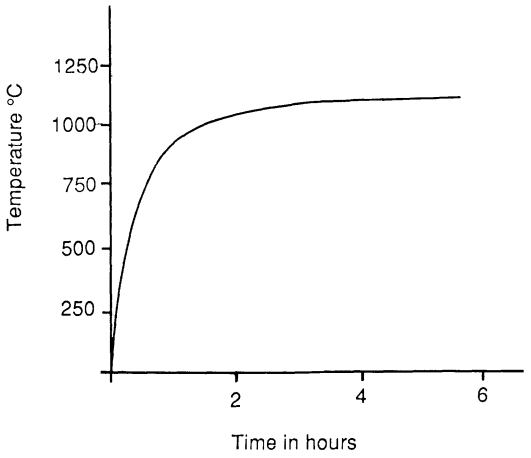

Figure 6.1 Temperature–time curve inside a furnace (fire resistance curve).

6.9.3 Smoke generation characteristics

In addition to assessing the combustion and flame spread properties of polymers, it is also necessary to investigate their smoke generation characteristics; smoke and evolved gases can create physiological hazards due to reduced visibility through smoke and state of panic.

Experimental procedures for the assessment of toxicity and irritancy of smoke are not well developed and are covered mainly by authorities such as the Ministry of Defence and the aircraft industries, who produce their own specification for use under a particular code of reference.

The aircraft industries have produced their own technical specifications which are intended to establish a combined fire hazard standard test produce. The Fire–Smoke–Toxicity (FST) Test Specification [13] considers the aspects of flammability, density of the smoke emitted and the toxicity of the smoke gases applicable to aircraft parts and is intended to be used inside the pressurized portion of the fuselage of large commercial transport category aircraft.

The Naval Engineering Standard (NES) [14] details one of a series of test methods for determining the combination characteristics of materials. The test explores the smoke production potential of a small sample of material. The method is based on the ASTM Special Technical Publication No. 422 (1967) 166–204, which is now superseded by ASTM E662: 1979 Specific Optical Density of Smoke Generated by Solid Materials. The NES 713 Issue 3 [15] is the standard for the determination of the toxicity index of the products of combustion in terms of small molecular species arising when a small sample of a material is completely burnt in excess air under specified

conditions. The test does not necessarily determine the total toxicity of all constituents of the products of combustion.

6.9.3.1 Optical density of smoke. The British Standard method for the measurement of the specific optical density of smoke generated by materials is given in BS 6401 (1983) [16]. In this method, a specimen of specified form and thickness up to 25 mm is exposed vertically to a radiant heat source of 2.5 W/cm^2 in a closed cabinet, with or without the application of a pilot flame. The smoke production from a material varies according to the irradiance level to which the specimen is exposed and it should be noted that the results are based on exposure to one irradiance level only (i.e. 2.5 W/cm^2).

In this test, six specimens are used to determine the percentage light transmission; three of the specimens are tested with the application of the pilot flame and three without. For each specimen, the maximum percentage value of light transmission is determined and from this the appropriate specific optical density is calculated, in terms of the measured percentage light transmittance T using the following expression:

$$D_s = 132 \log_{10} \frac{100}{T}$$

The greater the amount of smoke produced from a specimen, the higher will be the optical density or the lower will be the visibility. The limited data on the performance requirements in terms of the above tests suggest that under non-flaming conditions of combustion, mineral-based products with relatively insignificant quantities of combustible materials have a low optical density, whereas GRP composite and hardboard have a comparatively high optical density.

6.9.4 Methods of imparting flame retardancy to GRP

A coating of intumescent resin retards combustion of the organic materials present in the main structure of the GRP composite and also significantly reduces the area affected by the flame, drastically reducing the volume of smoke and practically eliminating burning. This resin is specifically formulated and ready to apply by brush as a flow coating, after the addition of a catalyst to a GRP laminate. (It can also be used for coating some conventional materials such as wool and building boards.) A thickness of 0.4–0.5 mm (or 450–600 g/m^2) as recommended, will give a dust free surface in 1 h at 18°C or longer at lower temperatures. It gives fire protection by foaming in situations where GRP laminates are exposed to direct flaming. It would normally be applied to the reverse side of a GRP building panel so that the extension face of the GRP system would possess good weathering properties and the interior surface would provide the fire-retardant properties. The carbonaceous foam and the inert gases that are produced when a flame

is applied to the cured surface insulate the main structure of the GRP laminate against flame for a period of time, dependent on the severity of the heating conditions.

Minerals fillers such as calcium carbonate, china clay and alumina trihydrate impart varying degrees of flame retardancy to GRP. These fillers generally reduce the amount of combustible material by replacing some of the resin in the body of a laminate. In the case of alumina trihydrate, the filler has additional effects of flame retardancy and smoke reduction due to the significant quantity of heat absorbed by the endothermic reaction during the decomposition of this material into alumina and water.

To achieve any significant level of flame retardancy, filler contents higher than 100 parts of filler to 100 parts of resin by weight are required. In the hand lay-up method of GRP production, the filler content is restricted to an upper limit of 75 parts by weight of resin, and is generally about 45. It is, therefore, necessary to add antimony trioxide and chlorinated paraffin in the ratio of between 2 and 15 and between 1 and 10 parts per weight of resin, respectively, depending upon whether class 2 or class 1 is desired.

A paste dispersion of antimony trioxide and a chlorinated organic compound, which is fully compatible with all normal Crystic resins and is readily dispersed by simple mechanical means has been developed by Scott Bader [8]. By replacing 20% of the basic resin with Crystic Prefil F, composites are produced with low surface spread of flame. Cold cure formulations require at least 2% Accelerator E to ensure that the cure is satisfactory.

It will be clear during the reading of this chapter that the degree of degradation of polymers, from whatever source, is highly dependent upon the type of polymer used and, of course, on the quality of the cure process. It is necessary for engineers and architects to seek the advice of the resin manufacturer on the type of polymer that should be used for the specific job and, if required, to have a special resin formulated for the particular application.

6.10 Repair of composite materials

Two types of repair of composite materials may be required as a result of the faults that occur during the moulding operation or during the service life of the composite.

6.10.1 Types of repair

The first type of repair, undertaken at the trimming and finishing stages of the laminate in the factory, will not normally present any difficulties because of the availability of the material and the factory expertise. Any loose resin and reinforcement are removed from the affected area, which is then

roughened, cleaned and dried. New resin and reinforcement are laid-up and the latter is cut to overlap the existing reinforcement to enable a good bond and adhesion to be obtained.

If the laminate is fractured, the whole area is cut out and the existing edges are chamfered so that the area of the hole is larger on the outside (gel coat) surface; this chamfered area is then roughened. If the affected area is large, a temporary mould may have to be made before the release agent, gel coat and laminating resin and reinforcement can be applied.

The second type of repair refers to polymer composites which have been damaged in service; two aspects must be considered. These are:

(a) the damage tolerance of the material and its application;
(b) the NDT techniques that can be used to identify the type and extent of damage in a component.

The first item depends upon the application of the composite. In situations where the design takes into account holes for fixings and fasteners, for example, the design stresses are generally low and consequently the degree of damage that can be tolerated can be determined by a visual inspection. An NDT technique such as ultrasonics (see section 4.8) can then be used to define the repair area. A more sophisticated NDT technique must be used to assess more highly stressed components as critical damage may be below the threshold that is visible on the impact surface.

In order to define the level of damage on a surface of a thin laminate, a tap hammer can be used to estimate the area of delamination. Ultrasonics, however, must be used with a thick laminate. Although interpretation of the results from both methods requires considerable technical experience, these methods are probably the most popular NDT techniques currently used.

Other methods for damage detection include infrared thermography, X-ray tomography and computerized vibro thermography, but all these techniques are difficult and expensive to use in the field. Optical fibres embedded in the structure and acoustic emission have also been successfully used to detect damage in composite structures. In addition 'bruisable' paints have been developed, based on micro-spheres containing a dye and dispersed in a conventional paint system. When impact takes place, the spheres burst, releasing the dye and indicating the area of impact.

If polymer composites have been damaged in service, they are likely to be contaminated by environmental fall-out, or if they are used in machinery, some parts of cars or airframes, they are likely to be contaminated by a film of hydraulic fluid or grease which would be difficult, if not impossible, to remove completely by cleaning. In addition, the material will have been degraded by exposure to the in-service environment; this is particularly so if the composite is used in construction and exposed to natural weathering. For these reasons, repairs are never as reliable as replacements, and, furthermore, generally they have to be undertaken *in situ*.

6.10.2 Bonded repairs

The most common type of repair to composite materials is undertaken by the adhesive bond technique, but the exact system used will depend upon the material and method of manufacture of the original composite. For instance, the repairs to hand-lay-up laminates are much easier to perform than those for the high pressure, hot-cured laminates.

Laminate 'patches' are likely to be dimensionally unstable with respect to the original polymer composite. Firstly, the resin in the latter composite will have post-cured and shrunk in service. Secondly, water uptake is likely to be at or near saturation, and consequently the resin will have swelled compared with its original volume. To enable a repair of a damaged polymer composite to be undertaken, it is necessary to provide as near equalization stresses as possible in the repaired and the undamaged materials.

Minor damage can usually be repaired by using a paste adhesive in the affected area. If the delamination has occurred and it is localized, it may be repaired by injecting resin, via a syringe, into the failed area. Large-scale damage necessitates replacements of the affected zone by a precured patch

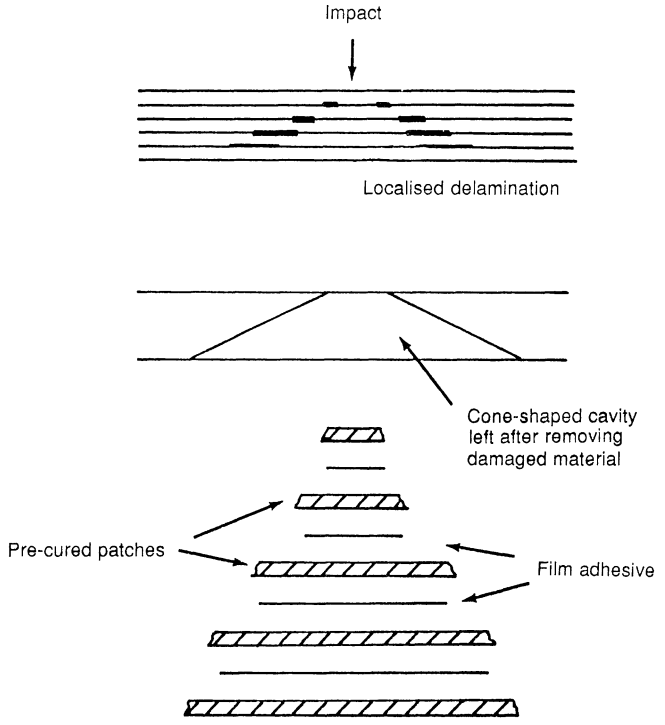

Figure 6.2 Typical lay-up for minor damage to composite materials (application of adhesively bonded precured composite patches).

either bonded or bolted (see section 6.10.3) into position. In both cases, the repair is effected by using an isotropic or quasi-isotropic patch, and for a bonded patch, a typical lay-up would be of the form shown in Figure 6.2.

6.10.3 Bolted repairs

The main problem with bonded repairs to composite structures is the difficulty of inspection and assessment of the patch, in particular, the quality of the bond line; consequently, the quality control of the process has to be very strict. In many instances, where the skills and conditions are not available to enable a reliable bonded repair to be undertaken, bolted connection of patches is preferred. A bolted repair should be able to realize 80% of the original material strength, and this is adequate for most applications encountered in the civil engineering field.

6.10.4 Techniques for modelling and analysis of composite repairs

The modelling and analysis required to support the design of bonded repairs has proved to be difficult. Invariably, simplified assumptions are made to facilitate an analysis: e.g. avoiding considerations of peel stress (see section 8.3) and the use of a one-dimensional analysis for a bonded strip representing the central region of the patch and the parent laminate. As a consequence, the design of a repair is usually supported by extensive and costly test programmes. Kedward [17] has suggested an approach based on the one-directional strip technique and a finite element technique, amenable to multi-directional characterization. The difficulties and high cost of a three-dimensional finite element representation through the adhesive layer are avoided by the use of spring elements to transmit shear and normal stresses between the patch and parent materials. The accuracy of the proposed approach is assessed by comparing the solutions to classical bonded joint problems with closed form or other acceptable solutions for the one-dimensional condition. The generality of the proposed technique also permits the analysis of bolted repairs in a similar manner.

PART 3

6.11 End-use performance properties of geosynthetics

6.11.1 Introduction

This part discusses the use of polymers in the geotechnical engineering industry and the specific mechanical and in-service properties associated with reinforced soil applications. The geotextiles to be considered consist of high

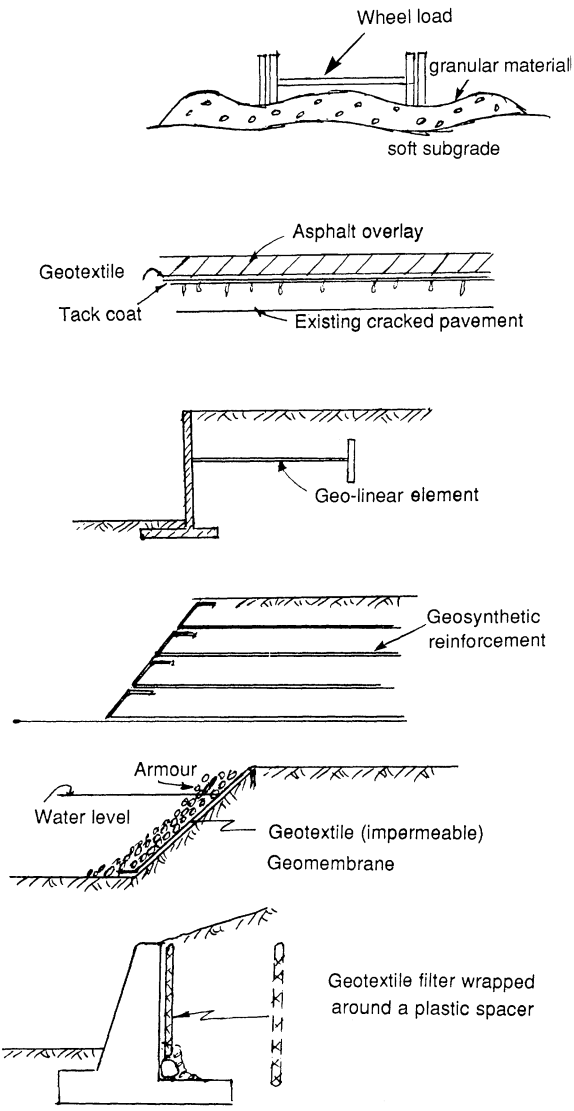

Figure 6.3 Examples of the use of various types of geosynthetics. (1) Geotextile to prevent intermixing of the soft subgrade with granular material. (a) Asphalt overlay to prevent existing cracks in pavement migrating into new overlay surface. (3) Geolinear elements used as anchors. (4) Geogrids to reinforce slopes and retaining walls. (4) Geomembranes to prevent loss of liquid from containment structure. (6) Geocomposites: wide applications from prefabricated drains, flexible skins, etc.

modulus polyester and polypropylene fibres (see sections 2.7.5 and 2.8.4). The design of these systems is generally based on a limit state principle.

6.11.2 The utilization of geotextile reinforcement

The concept of reinforcing soils with 'fibres' is not new. Reeds and vines were used extensively to reinforce clay bricks and granular soil as early as 1000 BC, but it was not until early 1960 that steel strips and later polymer composites were employed in the construction of reinforced soil walls and steep slopes.

The term geosynthetic is used to encompass all polymeric-based finished materials used in geotechnical engineering; this may be defined as a synthetic (polymeric) material used in a soil environment (i.e. conventional and special geotextiles). The general characteristics of the various geotextile types are given in section 2.8.4 and Lawson [18] has discussed fully the uses of these materials. Figure 6.3 gives some examples of the use in construction of various types of geosynthetics.

6.11.3 Geotextile characteristics

There are four main properties that must be considered when determining the suitability of a geotextile for reinforced soils:

1. strength;
2. stiffness and creep;
3. durability;
4. bond.

6.11.4 Strength characteristics

The initial tensile strength and extension characteristics of geotextiles are a function of the tensile properties of the constituent load carrying elements and the geometrical arrangements of these elements within the geotextiles. The tensile characteristics of various geotextile load carrying elements have been related to those of prestressing steel in Figure 6.4 and it can be seen that the tensile strength of some polyaramid fibres can be stronger than that of prestressing steel tendons. The polyaramid fibres, however, are not often used for geotextiles for economic reasons. Polyester fibres, polypropylene tapes and high density polyethylene (HDPE) grids are economic and exhibit good tensile characteristics, although lower than those of the polyaramid fibres; the properties and the respective reinforcing elements are well suited to reinforced soil applications. The constituent fibres are placed in the geotextile in a highly aligned configuration to utilize their load/extension characteristics as efficiently as possible. Properties of the geosynthetics (geotextiles) used for reinforcing soil applications are given in Table 2.6.

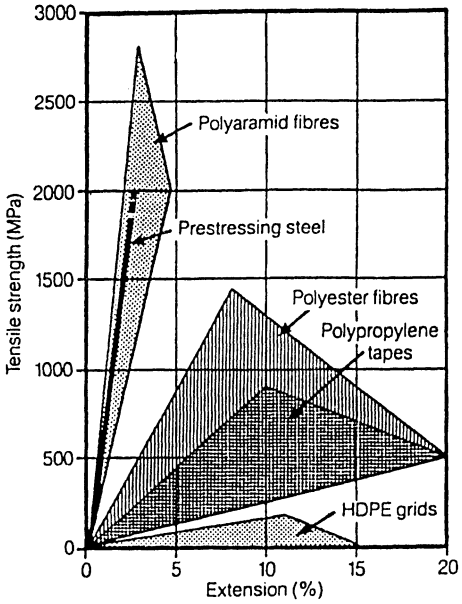

Figure 6.4 Tensile characteristics of some thermoplastic fibres in relation to prestressing steel (after [18]).

Installing the geotextiles in the ground includes handling, placing and compacting the soil around the reinforcement which inevitably results in a reduction of strength but the modulus is unaffected. Jewell and Greenwood [19] have observed the effect of compaction in strength/extension properties of a woven polyester geotextile exposed to the compaction of 37.5 mm diameter crushed limestone. They have shown the strength of the geotextile is reduced to $\frac{2}{3}$ and $\frac{1}{3}$ of its manufactured value for standard compaction and compaction to refusal, respectively. An effective representation of installation damage on the tensile strength of geotextile reinforcement is to use a partial factor applied to the tensile strength of the manufactured geotextile $P_{R(lab)}$ and the installed tensile strength $P_{R(ins)}$:

$$P_{R(ins)} = P_{R(lab)}/f_d$$

where f_d is a partial factor related to the installation damage. The partial factor f_d can only be estimated from tests undertaken on recovered geotextiles from sites and then comparing with the manufactured material strengths.

To quantify the long-term strength capability of geotextile reinforcement, the long-term extension and stiffness must be determined; either the isochronous creep curves or creep coefficients (see section 2.9.2) can be used for this purpose.

Isochronous creep curves depict the change in shape of the load/extension

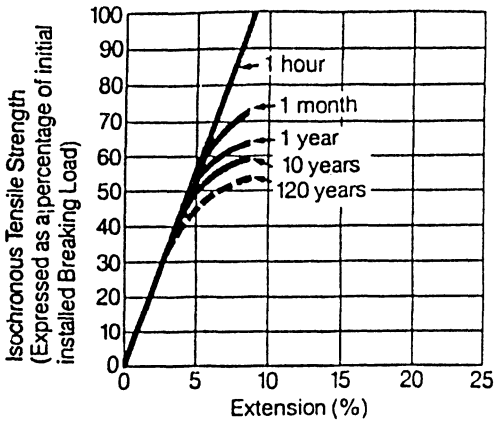

Figure 6.5 Isochronous creep curves for high modulus polyester fibre (after [20]).

curve of the reinforcements at different points in time. Figure 6.5 shows the isochronous creep curves for a commercially available high modulus polyester fibre based geostrip. It can be seen that there is little change in the load/extension curve over time for load levels at or below 40% of the initial ultimate tensile strength (less than 1% creep extension); this is typical for all high modulus polyester fibres. Figure 6.6 shows a set of isochronous creep curves for a commercially available woven polypropylene geotextile. The curve shows a significant change in stiffness with time (under a sustained load) for all load levels. It is seen that at a working stress level of 20% of the initial ultimate tensile strength of the material, the long-term creep extensions can be expected to approach 5–6%. Creep coefficients proved a

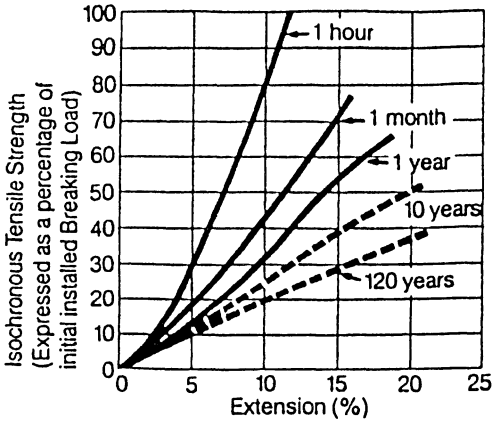

Figure 6.6 Isochronous creep curves for high modulus polypropylene tape woven geotextiles at 23°C (after [20]).

convenient means of comparing the rate of creep of different polymeric materials. Note that the creep coefficient increases for increasing applied load for all polymer types, with polypropylene and HDPE materials more highly affected. There is also a significant increase in the rate of creep from a low value for polyaramid fibres through polyester fibres and HDPE grids to a high value for polypropylene fibres and grids.

6.11.5 Durability

Polymers used in geotextiles are highly durable but nevertheless a considerable amount of research and testing has been carried out to assess precisely their long-term durability. However, the testing period is still short-term compared with the design life of a typical reinforcing geogrid element and the use of stress–rupture curves to determine the long-term load carrying capacity of the geotextile reinforcements are utilized. If the available creep data do not cover the full design life of the reinforcement, then extrapolation of the data is required, subjected to the inclusion of a material partial factor of safety which takes account of uncertainties associated with extrapolation of time dependent results such as the environment.

6.11.6 Effects of oxidation

Degradation due to oxidation occurs as a result of heat (thermo-oxidation) and exposure to ultraviolet light (photo-oxidation); the latter is not a problem as the material is installed underground. Minimal oxidation occurs with polyester, but polyethylene and polypropylene can be attacked and particularly the latter polymer.

During the processing and use of polyolefins, anti-oxidants are added but as they are consumed the resistance of the polymer to oxidation decreases. The quantity of anti-oxidant present, the consumption rate and its leaching out from the polymer all play a part in the final rate of oxidation of the polymer. The rate of oxidation is also influenced by the presence in the surrounding environment of certain heavy metal ions (e.g. iron, manganese and copper) and the evaluation of the effects of these factors is still continuing.

6.11.7 Effects of hydrolysis

Hydrolysis occurs when water molecules react with polymer molecules with a consequent loss of strength. The polyolefins are not susceptible to hydrolysis but the polyester is. Hydrolysis is a very slow reaction and is affected by:

1. *Humidity*: tests are usually conducted at 100% relative humidity which conforms to a soil suction $pF \leqslant 3$ which covers granular soils;
2. *Polyester structure*: specifically the molecular weight; the higher the molecular weight the lower will be the rate of hydrolysis;

3. *Temperature*: a rise of temperature from 20°C to 30°C increases the rate of hydrolysis four-fold;
4. *External catalyst*: polymers can be protected from alkaline environments by coatings of polyethylene or PVC, although in time water can migrate very slowly through the coatings, the latter acts as a barrier to the migration of inorganic ions and consequently the environment inside the casings remains essentially neutral.

6.11.8 The effects of external chemicals

The durability of the polyolefins is high and these polymers would not normally be affected by ground conditions. However, if oil or chemical spillage took place in large doses, and depending on the chemical involved, it is estimated that polyolefins would have a reduction of about 10% in the tensile properties; stress–rupture limits need to be defined and this can only be estimated by an investigation.

As already stated, polyesters are susceptible to hydrolysis and therefore care should be taken if they come into contact with cement/water materials.

References

1. BS 4549, Guide to quality control requirements for reinforced plastics mouldings, (Part 1: Polyester resin mouldings reinforced with chopped strand mat or randomly deposited glass fibres) (no ISO equivalence), British Standards Institution, London (1970).
2. BS 2782, Determination of loss on ignition, Part 10: Method 1002 1979 ($\equiv$EN60, $\neq$ISO 1172)*, British Standards Institution, London (1989).
3. BS 4994, Specification for design and construction of vessels and tanks in reinforced plastics, (no ISO equivalence), British Standard Institution, London (1987).
4. BS 8208, Guide to assessment of suitability of external cavity walls for filling with thermal insulants, Part 1: Existing traditional cavity construction (no ISO equivalence), British Standards Institution, London (1985).
5. BS 4618, Resistance to natural weathering, Section 4.2 (no ISO equivalence), British Standards Institution, London (1972).
6. BS 8233, Code of practice for sound insulation and noise reduction (no ISO equivalence), British Standards Institution, London (1987).
7. British Standards Code of Practice 153, Sound insulation, Part 3 (no ISO equivalence), British Standards Institution, London (1972).
8. Scott Bader, *Crystic Polyester Handbook* (1990).
9. J. Yovino and G.T. Dunwoody, *Symp. on Reinforced Plastics and Composites*, Sydney (1970) paper 18.
10. J. Crowder, Building Research Station, Garston, Herts, private communication.
11. HMSO, *The Building Regulations*, HMSO, London (1989). (Explanatory book: *The Building Regulations Explained and Illustrated* 8th edition, eds V. Powell-Smith and M.J. Billington) (1989).
12. BS 476: (a) External fire exposure roof test, Part 3: 1958, British Standards Institution, London (1950) (this standard has been withdrawn but is still cited in the UK Building Regulations; the test method is very similar to the 1975 version but the classification method is different); (b) External fire exposure roof test, Part 3: 1975, British Standard Institution, London (1975) (designed to measure the ability of a representative section of a roof, roof light, dome light or similar components to resist penetration by fire, when its external surface

is exposed to heat radiation and flame; also measures the extent of surface ignition). (c) Non-combustibility test for materials, Part 4: 1970 (1984) British Standard Institution, London (1984) (includes definition of non-combustibility; determines whether materials, with or without coatings, used in construction or finishing of buildings meet the definition) [≡ ISO/R1182]* (this standard is used for the building regulations only); (d) Method of test for ignitability, Part 5: 1979, British Standards Institution, London (1979) (measurement of ignitability characteristics of essentially flat and rigid building materials and composites when subjected to a small flame) [≡ ISO/R1183]*; (e) Method of test for fire propagation for products, Part 6: 1981, British Standards Institution, London (1981) (a method to determine the fire performance of products used as internal linings in buildings, takes account of the combined effects of factors such as the ignition characteristics, the amount and rate of heat release and thermal properties of products in relation to their ability to accelerate the rate of fire growth) [≡ ISO/R1183]*; (f) Method for classification of the surface spread of flame of products, Part 7: 1987, British Standards Institution, London (1987) (method for measuring the lateral spread of flame along the surface of a specimen in the vertical position, together with a classification system on the rate and extent of flame) [≡ ISO/R1183]*; (g) Test methods and criteria for the fire resistance of elements of building construction, Part 8: British Standards Institution London (1972) (method of test and criteria for determining fire resistance of walls and partitions, floors, flat roofs, columns, beams, suspended ceilings protecting steel beams, doors and shutter assemblies, glazing and ceiling membranes; replaced by Parts 20–23 of BS 476 but remains current as it is cited in legislation. [= ISO/TR 6167 and ≠ ISO 834]*; (h) Method for assessing the heat emission from building materials, Part 11 1982 (1988) British Standards Institution, London (1988) (no ISO equivalence); (i) Method for determination of the fire resistance of elements of construction (general principles), Part 20 (1987) (≠ IOS 834)*, (this BS replaces BS 476 Part 8 (1972) which remains current as it is cited in legislation).

13. Airbus Industrie Technical Specification, Fire–Smoke–Toxicity (FST) test Specifications (1989).
14. Naval Engineering Standard, Determination of the smoke index of the products of combustion from small specimens of materials, Ministry Standard of Defence Controllerate of the Navy, NES 711, Issue 2 (1985).
15. Naval Engineering Standard, Determination of the toxicity index of the products of combustion from small specimens of materials, NES 713, Issue 3 (1985).
16. BS 6401, Method for measurement in the laboratory of the special optical density of smoke generation by materials (no ISO equivalence), British Standards Institution, London (1983).
17. K.T. Kedward, *Jointing and Repair*. Short course on composite materials technology—mechanics, design and manufacture, held at University of Surrey, 13–17 July (1992).
18. C.R. Lawson, Geosynthetics in *Polymers and Polymer Composites in Construction*, ed. L. Hollaway. Thomas Telford, London (1990) Ch. 10.
19. R.A. Jewell and J.H. Greenwood, Long term strength and safety in steep soil slopes reinforced by polymer material. *Geotextiles and Geomembranes*, **7** (1988), pp. 81–118.
20. *Geotextiles—Designing for Soil Reinforcement Handbook*, Exxon Chemical Geopolymers Ltd. (1989).

*The symbol ≡ indicates an identical standard, i.e. a BSI publication identical in every detail with a corresponding international standard ISO. The symbol = indicates a (technically) equivalent standard, i.e. a BSI publication in all technical respects the same as a corresponding international standard ISO although the wording and presentation may differ quite extensively. The symbol ≠ indicates a related but not equivalent standard, i.e. a BSI publication, the content of which to any extent at all short of complete identity or technical equivalence, covers subject matter similar to that covered by a corresponding international standard ISO.

7 Low density rigid foam materials, sandwich construction and design methods

7.1 Introduction

In previous chapters, the properties and fabrication techniques of a single skin composite of GRP, capable of being used for small components as well as large folded plate structures, have been discussed. If it is necessary to increase the stiffness of the overall cross-section of the composite or the individual laminates, a sandwich construction consisting of the reinforced polyester composites bonded to a low density core may be used. The face then generally supports the bending moments and axial forces within the composite cross-section and the core takes the majority of the shear. The core may be of low density polymer and four types of foam which are not exhaustive but which are used in the construction industry and which will be considered in this chapter are:

(a) rigid polyurethane;
(b) phenolic;
(c) polyvinylchloride;
(d) polystyrene.

The first two polymers are thermosetting resins and the last two are made from thermoplastic resins.

After the above four forms have been discussed, some design methods for sandwich construction are given. Within one chapter, it is impossible to deal fully with the design methods of sandwich construction. The chopped strand mat polymer is the laminate used mainly in the construction industry as the face material of sandwich construction; consequently the design methods given here are generally applicable only to isotropic faces and isotropic core materials.

7.2 Rigid polymer foams

A description of the rigid polymer foams has been given in section 2.7.3. The gas in the foam is distributed in voids referred to as 'cells', while the solid polymer encloses these voids to form the cell walls. A foam in which the cells are discrete or disconnected units and whose gas phase is not continuous is

said to have a 'closed cell' structure and is essentially air and vapour tight, while a foam in which the cells are interconnected and whose gas is continuous is said to have an 'open cell' structure. With this latter foam, free movement of air and vapour through the volume of material is permitted. Most rigid polymer foams, however, are neither completely open nor completely closed celled but are characterized by a 'fraction' of open or closed cells.

The arrangement of the gas and solid in a polymer foam depends largely on the forces that exist during the expansion of the polymer:

(a) the gas pressure which causes the material of the cell wall to flow as the volume of the cell increases;
(b) the viscoelastic reaction forces of the polymer which resist its flow;
(c) the surface tension forces which cause the flow of material from the cell walls to the point at which they intersect.

The most favoured cell structure is one resulting in a minimum surface tension for the expanding polymer.

Density, when applied to a rigid polymer foam refers to its bulk density, which is defined by the ratio of total weight/total volume of the polymer and gaseous components. Obviously, the gaseous component contributes considerably to the volume of the foam, while the solid polymer component contributes almost the entire weight.

The division of polymers, as given in section 2.7 is, of course, relevant to foams. As shown in Table 2.3 phenolic and polyurethene foams are thermosetting polymers which, apart from the polyester and epoxy resins already discussed, are the most commonly used in the construction industry. Expanded unplasticized PVC which is a thermoplastic material is also used in the industry.

7.3 Phenolic foam (PF)

Foamed phenol-formaldehyde resin (phenolic foam) is available in boards and slabs to BS 3927 [1]. It is a rigid thermosetting resin with good chemical and temperature resistance, as well as a high resistance to water vapour transmission and water uptake; these properties are carried over into the foam.

The range of densities available at present vary from $30\,kg/m^3$ up to $150\,kg/m^3$. For particular applications, large cell structures can be provided or high density foams (up to $500\,kg/m^3$) can be produced. Generally, phenolic foams are available in rectangular block form up to $2000 \times 1000 \times 50\,mm^3$ and in square blocks up to $1000 \times 1000 \times 500\,mm^3$.

The foam achieves the highest classifications of the BS 476 fire tests Parts 5 and 7 and produces an optical smoke obscuration to Part 9 of less than

5%, compared with between 50 and 90% for most commercial grades of polystyrene and polyurethane foam. Phenolic foam burns in a similar way to natural timber, giving off only carbon dioxide, carbon monoxide and water, without the intermediate evolution of carbon laden smoke. As the combustion temperature progressively increases to above 200°C, the foams undergo gradual oxidation to become a carbonaceous structure, without any intermediate softening or dripping or any significant smoke, fume or flame production. The resulting rigid foam-char protects the remaining structure from the primary heat source.

Because of the inert nature of phenolic foam, only concentrated acids and alkalis can attack it chemically; it is resistant to hydrocarbons, dilute alkalis and acids, methylalcohol, seawater, petrol and diesel oil. It also resists the solvents used in the adhesives and varnishes which are currently employed in building construction and it is claimed by one manufacturer that despite its acid catalyst, it presents no particular corrosive problems with respect to metals. It is able to resist attack by fungi, bacteria, insect and rodent sources, even after prolonged exposure.

Permali Gloucester, UK produces a phenolic based, rigid, closed cell foam (Plasticell) to meet the fire resistant properties; Table 7.1 gives typical properties. The foam material does not support combustion, is self-extinguishing and produces very little smoke and toxicity and is often used as the core material in structural sandwiches; it can readily be combined with polyester, epoxide or phenolic resin based laminates to produce the sandwich panels. The Plasticell foams are produced without the use of chlorofluorocarbons (CFC).

Table 7.1 Typical properties of phenolic foamed polymer (source: Permali (technical literature), Gloucester, UK)

Typical properties	Values	Methods
Density (kg/m^3)	100.00	BS 4370
Compressive strength (MPa)	0.90	BS 4370
Compressive modulus (MPa)	40.0	BS 4370
Thermal strength (MPa)	1.1	BS 4370
Flexural modulus (MPa)	55	BS 2782
Shear strength (MPa)	0.3	BS 1137
Limiting oxygen index	41	ASTM 02863-77
Smoke index	6	NES 711
Toxicity	2	NES 713
Thermal conductivity (W/m K)	0.036	BS 874
Water absorption (%)	2	ASTM C 272-53
Surface spread of flame	Class I	BS 476 Pt. 7; 1971

7.4 Rigid polyurethane foam

Chemically, rigid polyurethane foam is the most complex of all the polymer foams. The basic raw materials to manufacture urethane foam are polyol, MDI (*meta*-phenylene di-isocyanate), water and a blowing agent. The auxiliary materials are the catalysts (amine and tin) and finally the stabilizer (silicone surfactant); these materials are metered and mixed in the mixing chamber. During this time tiny air bubbles are formed or introduced by injection. The MDI/water reaction develops carbon dioxide gas at which time the liquid becomes creamy. This reaction is catalysed by the amine catalyst. The gas from this reaction enters the bubbles, which have already been formed by the air, and expands them causing the reaction mixture to foam. Simultaneously the MDI/polyol reaction is proceeding; this is catalysed by the tin catalyst. The two reactions proceed concurrently; the polyurethane provides the solid matrix and the blowing reaction expands the reacting mass. Should a blowing

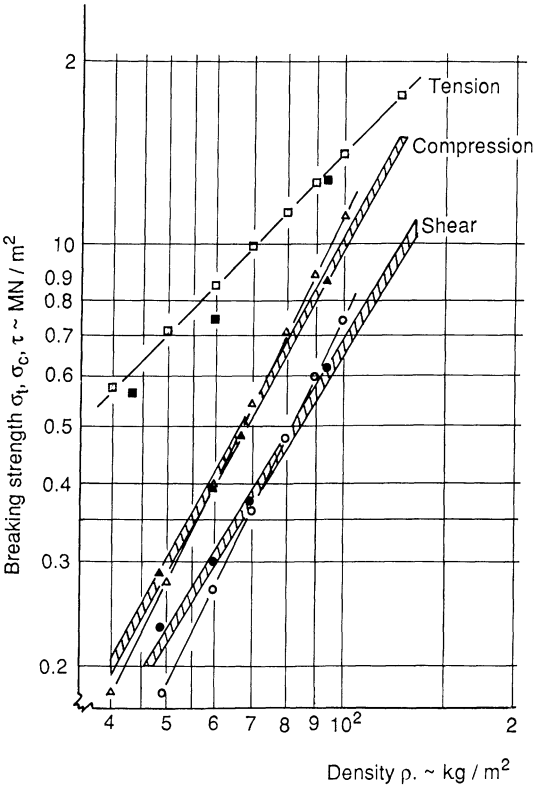

Figure 7.1 Density versus buckling strength of polyurethane foam (after [2]). Measured values indicated by filled symbols, calculated values by open symbols. Cross-hatched region results from [3].

agent be present, the heat from the reactions will cause evaporation of the low boiling point material thus providing a further expansion of the bubbles. The silicone surfactant stabilizes the bubbles so that uniform expansion can proceed without collapse of the walls of the bubbles.

The important foam properties are its density and hardness. In standard, polyether polyol based polyurethane foam, the density and hardness of the material are related as shown in Figure 7.1. In practice, higher hardness/density ratios may be required and this property may be achieved by using different raw materials and often without the need for modification of the foam production process. Hardness changes can also be effected by increasing the amount of MDI over that necessary for a complete 1:1 reaction. If an excess of 10% of MDI is used, it is expressed as an index of 110. Slabstock foam is normally run with an index between 105 and 110. At an index of 115, an asymptotic values of hardness is reached.

The property generally used to describe foam is its density and this changes with the amount of water and/or blowing agent; to increase the density, the blowing action is reduced. Other properties such as resilience and durability are also improved. The walls of the foam are filled with a gas mixture which has a low value of conductivity and which is less than that of still air. The cell walls do not readily allow the gas to diffuse through them. In service, there may be times when the foam has free access to air and it may diffuse inwards until an equilibrium condition is reached, at which point the conductivity of the foam will be that of still air.

The main advantages of polyurethane over other foams lie in its excellent low thermal conductivity (0.02 W/m^2 per °C) (the foam gains its good insulation value from the chlorofluorocarbon blowing agent trapped inside the cell walls), good high temperature resistance (up to 120°C), low vapour permeability and the property of *in situ* foaming. The behaviour of the foam in fire is not good although flame-retardant grades are available by adding halogen-containing compounds at the time of mixing. Fire tests on small coupons are laid down in BS 4735 [4].

7.5 Expanded PVC foam

Expanded PVC is a thermoplastics foam based on polyvinyl chloride resins or co-polymers of polyvinyl chloride. It can be produced either by a mechanical blowing process or by one of several chemical blowing processes. It has an almost completely closed-cell structure and therefore a low water vapour transmission and low water absorption; it has a tridimensional grid structure which gives a high thermal stability. This foam polymer tends to be expensive and therefore its use in the construction industry is limited to specific applications. It tends to be stronger and more rigid than the above mentioned cellular polymers and its low vapour transmission is an advantage when

Table 7.2 Typical mechanical properties of six standard expanded PVC foams (source: Permali, Gloucester, UK)

Properties	Standard grades					
Density ($kg\,m^3$)	40	55	75	100	300	400
Compressive strength at 23°C (MPa) (ISO R844)	0.40	0.80	1.5	2.0	8.9	14.0
Compressive modulus (MPa) (NFT 56–101)	21.5	38.1	61.3	90.4	357	470
Shear strength (MPa) (ISO 1922)	0.40	0.60	1.2	1.481	Bond failure	Bond failure
Shear modulus (MPa) (ISO 1992)	9.20	13.60	15.10	27.58	Bond failure	Bond failure
Flexural strength (MPa) (ISO 1209)	0.70	1.4	2.20	2.60	12.8	20.5
Tensile strength (MPa) (ISO 1926)	0.70	1.3	—	2.8	14.1	—

condensation might be a problem. Because of its rigidity, it is often used in sandwich constructions to increase the stiffness of the composite; however, care must be exercised if it is used as a building material because it tends to collapse in fire; although it does not support combustion and is self-extinguishing.

Permali, Gloucester, UK are the largest producers of rigid expanded PVC (known as plasticell) in the UK. Their products are available in six special grades, each with different qualities but with high impact resistance combined with good compression values consistent with their densities.

Typical mechanical properties for the six standard grades are given in Table 7.2.

7.6 Urea formaldehyde (UF)

Although urea formaldehyde is not a structural material, it is relevant to introduce the foam here because of its applications in the construction industry. It is produced from a liquid system by mixing resin, water and foaming hardener in a special machine. The foam leaves the mixing machine head or gun in a relatively soft fluid state, but quickly hardens into a rigid cellular mass. The foam has a density of $8\,km/m^3$, and is one of the lightest polymer cellular materials.

7.7 Uses and manufacturing processes of polymer foams

The rigid foam polymers can be sold or used in several ways. The chemicals can be mixed and reacted in a machine that makes a continuous block of

foam; these blocks are known as buns or bunstock. Buns can then be cut into half rounds or other special shapes which are used to insulate pipes and tanks.

Slices of rigid foam can be sandwiched between flexible materials (e.g. foils) or rigid materials (e.g. GRP composites or metals). These sandwich systems are called structural laminates (see section 7.9).

The rigid foam polymers may also be poured in place. The formulation consisting of polyol, isocynate, catalysts and blowing agents will be different for each practical requirement to enable the chemicals to flow or rise as quickly or slowly as necessary. The chemicals can be mixed and injected into a mould or cavity such as a hollow door, the walls of a truck or a rail freight container or into the cavity of a building. This method is known as pour-in-place. The foam exerts pressure as it rises and consequently clamps or jigs are needed to support the mould.

The chemical can be mixed and poured onto a moving conveyor between two continuous surfaces such as foil or thin sheets of steel, aluminium, paper or polymer composites. This forms a laminate which is often used as a panel to insulate buildings.

Polymers are organic materials and will therefore burn. However, special formulations have been developed to make the various foams more resistant to ignition (see section 6.9). Fire retardant additives can be included in the formulations to offer extra protection in fire hazard situations. In one special formulation, the isocyanate is encouraged to react with other isocyanates to form polyisocyanurate; this process is called trimerization. However, when the foam is used as insulation on interior walls or ceilings of buildings it must be cured with an approved thermal barrier as a safety precaution against fire.

A flexible foam polymer can be produced by changing the formulation and using a long-chain polyol and a special blowing agent. In flexible foams, the great majority of cells are open in contrast to the rigid foam where normally more than 95% of the cells are closed. The main use of this type of foam polymer is in automative seating and packaging.

Rigid integral skin foams are those that during the manufacturing process are formed with a thick skin on either side of a rigid (or flexible) foam by forcing the surface cells to collapse. This is achieved with pressure (packing the mould) using cold moulds and particular types of polyols and isocyanates.

By omitting the blowing agent and reacting only the polyol, isocyanate and catalysts, the resulting polymer will not foam. This form of polymer is known as an elastomer. It can be made very soft and flexible, similar to a rubber, or it may be made hard and rigid with a high modulus.

The most common method of manufacture for moulding polyurethane elastomers, for instance, is by casting. The polyol, isocyanate and catalysts are mixed and poured, either by hand or by machine, directly into an open mould with no additional pressure. This method can be used for the manu-

facture of small parts and to provide insulation for electrical components such as transformers. In the reaction injection moulding (RIM) process, chemicals are mixed by injecting thin streams of reactants at each other at high pressure; this causes instantaneous mixing of the streams. The mixed chemicals are then forced into a closed, vented mould. This method is used where large complex parts must be made quickly (e.g. in a high volume industry such as in automative plants to make bumpers, etc.)

7.8 Mechanical testing of rigid polymer foams

As low density foam polymers are usually anistropic, the strength will vary with the direction of measurement. It also varies with the rate of stressing although the effect of the strain rate decreases as the rigidity of the polymer increases. Highly cross-linked polymers show little change in compressive stress with change in strain rate. As a group, these polymers are unlikely to find application in high efficiency sandwich structures, although the stiffness of the continuum forming a folded plate is considerably increased with the utilization of a sandwich construction of chopped strand mat faces and foamed polymer core.

Tables 7.3(a) and (b) give typical values of the mechanical properties of

Table 7.3(a) Typical properties of standard and Nilfam polyisocyanurate polyurethane foams manufactured by Coolag Ltd

Property	Standard foam	Nilfam polyisocyanurate
Density (kg/m^3)	32	40
Compressive strength (kPa)		
In direction of rise	172	206
In direction across rise	124	—
Thermal conductivity of polyurethane foam (W/mK)	0.022	0.022

Table 7.3(b) Typical mechanical properties of foam polymers with density of 32 kg/m^3

Property	Maximum	Typical value at 10% strain
Compressive strength (ISO 844–1985)		
In direction of rise (kPa)	200	140–180
In direction across rise (kPa)	120	130–180
Tensile strength (ISO 1926–1979)		
In direction of rise (kPa)	350	
In direction across rise (kPa)	250	
Shear strength (ISO 1922–1982) (kPa)	160	
Flexural modulus (BS 4370–1968) (kPa)	3000	

some foamed polymers but it is usually necessary to undertake laboratory tests to determine the strength and stiffness of the particular form or core material to be used. The mechanical properties which are generally required are:

(a) compressive strength;
(b) flat-wise tensile strength;
(c) shear test.

These latter tests may be divided into three basic types [5]:

(a) in plane shear, in which the shear distortion takes place entirely in the plane of the composite material;
(b) twisting-shear, in which the cross-section of the composite (in bar or thin-sheet form) undergoes a twisting-type shear deformation;
(c) thickness shear, sometimes called transverse shear or interlaminar shear (in the case of laminates), in which the composite material sheet undergoes shearing deformation in a plane normal to the plane of the sheet.

It is the first shear type that is described in section 7.8.3 and which is of importance when considering sandwich beams and slab construction.

7.8.1 Compressive strengths

To determine the compressive characteristics of rigid polymer foams used as core materials in structural sandwich constructions, it is necessary to undertake a compressive strength test. The characteristics are determined in directions perpendicular and parallel to the plane of the facings corresponding to directions *T* and *L* of Figure 7.2; this is how the foam core is placed in an actual sandwich. The test procedure is laid down in ASTM designation C365 [6].

The significance of the test is that it produces information on the behaviour of rigid plastics-foams under uniaxial compressive loads: the compressive

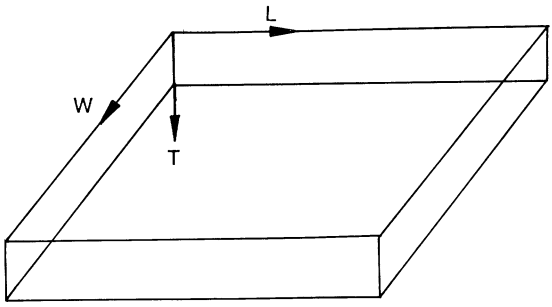

Figure 7.2 Diagram illustrating planes within a core material of sandwich constructions.

stress, σ_c, is defined as

$$\sigma_c = \frac{\text{compressive load}}{\text{initial cross-sectional area of the specimen}}$$

If the maximum load is reached at less than 10% deformation, the compressive strength is

$$\sigma_c = \frac{\text{maximum compressive load}}{\text{initial cross-sectional area of the specimen}}$$

If the maximum load is not reached before 10% deformation, the compressive strength is given at 10% relative deformation, i.e.

$$\sigma_c = \frac{\text{compressive load at 10\% deformation}}{\text{initial cross-sectional area of the specimen}}$$

7.8.2 Flatwise tension test

This method covers the procedure for determining the tensile properties of rigid polymer foams for use as the core material in sandwich construction. Properties are determined in a direction normal to the plane of the facings as the foam core is placed in the sandwich construction in direction T and corresponding to the rise direction of the foam. Basically, the test requires the specimen to be bonded between two steel loading blocks and plates must be sufficiently stiff to keep the bonded surface as flat as possible.

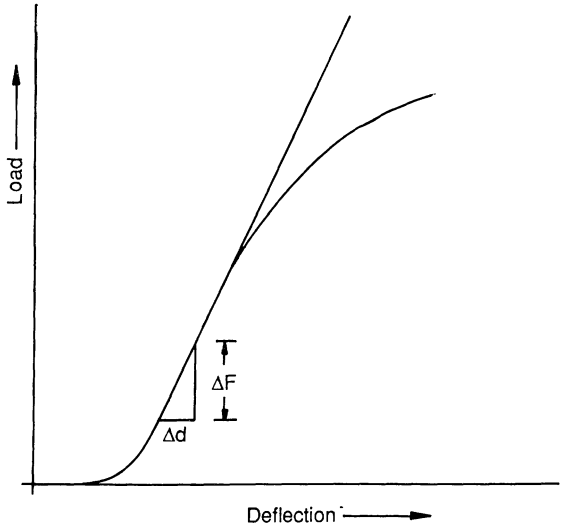

Figure 7.3 Typical flatwise tension test result.

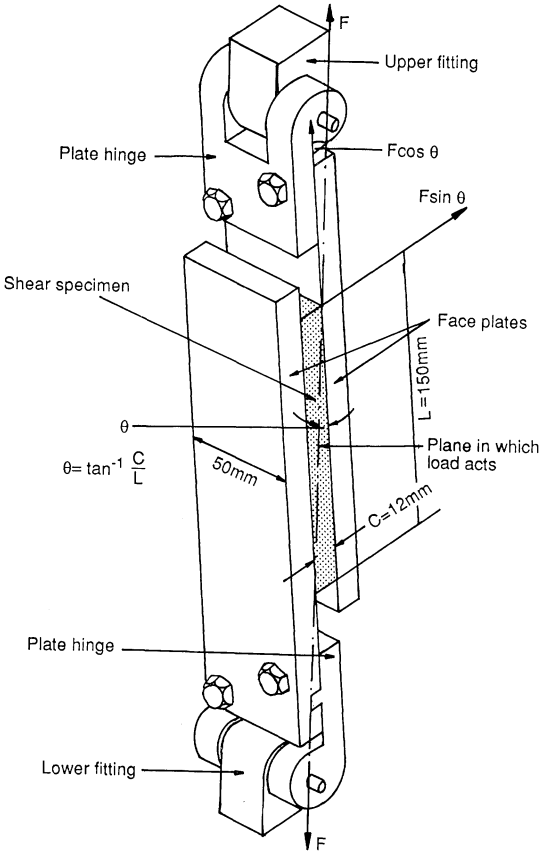

Figure 7.4 Shear test for determining the shear strength of a foam core.

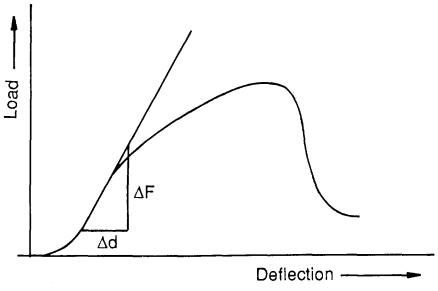

Figure 7.5 Typical recording of load versus deflection for shear test.

American Standard Test Methods for determining the tensile properties of rigid plastics foams are given in [7, 8]; these standards require specimens to be lathe turned to specific dimensions. The significance of the test lies in the information it provides on the behaviour of rigid polymer foams when loaded in tension. In the design of sandwich construction, a knowledge of the ultimate tensile strength of the core material is usually sufficient; it will help to decide whether the face wrinkling will resist either the facing tearing from the core or buckling into the core.

A typical recording of load versus deflection is shown in Figure 7.3,

$$\text{Tensile stress } \sigma = \frac{\text{tensile load}}{\text{cross-sectional area}}$$

7.8.3 Shear test

This method covers the procedure for determining the shear properties of rigid polymer foams for use as core materials in structural sandwich constructions. Figure 7.4 gives details of single shear tests for determining the shear strength and stiffness in the *LT* and *TW* planes. Samples of the core material are bonded to two thick plates and loaded in the direction as shown in Figure 7.4.

The standard shear test method is laid down in ASTM designation C273-61 [9]. A typical recording of load against deflection for a shear test is given in Figure 7.5. If the shear stress across the width of the specimen is assumed constant, then the shear stress, τ, and the shear strain, γ, are defined as

$$\tau = \frac{\text{shear load}}{\text{area of shear}} = \frac{F \cos \sigma}{Lb}$$

$$\gamma = \frac{r}{c}$$

where r is the movement of one face relative to the other and c is the thickness of specimen. The shear modulus, G, is

$$G = \frac{cF \cos \sigma}{Lbr}$$

7.9 Sandwich laminates: beams

The sandwich beam is defined in the glossary and is manufactured by sandwiching a core of low density material of thickness c between two faces of thickness t. It is likely that the beam will be structurally efficient only if the faces are much stronger and stiffer than the core material and if the

density of the core material is much lower than the faces; these conditions are usually met in practice.

The flexural rigidity El of a sandwich beam, which is usually given the symbol D, is the sum of the flexural rigidities of the two separate parts of the composite, namely the core and the faces, measured about the centroidal axis of the whole section. From Figure 7.6, it will be clear that

$$D = E_f \frac{bt^3}{6} + E_f \frac{btd^2}{2} + E_c \frac{bc^3}{12} \tag{7.1}$$

where E_f and E_c are the modulus of elasticity of the faces and core, respectively.

The first term on the right-hand side of the equation represents the local stiffness of the faces bending stiffness about their own centroidal axes (D_f). The third term represents the bending stiffness of the core. In practice, the

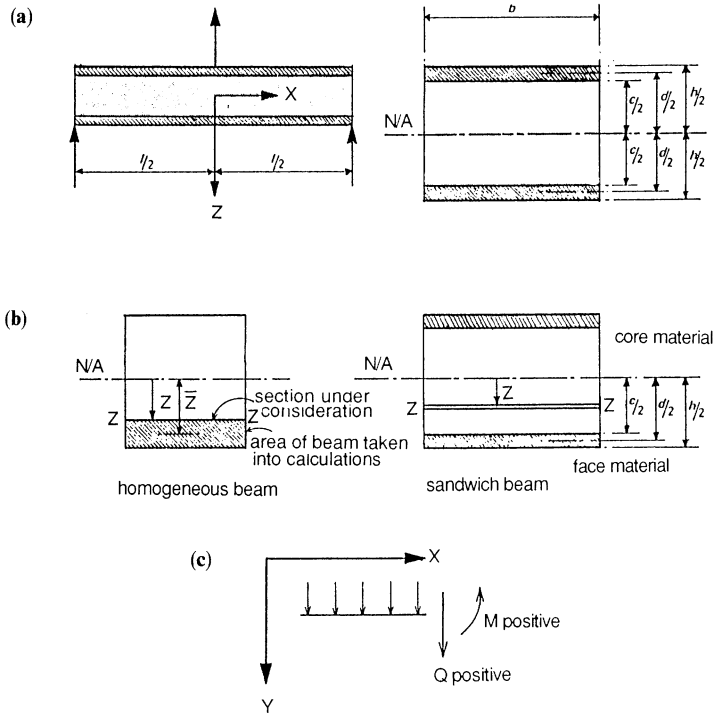

Figure 7.6 Sandwich beam dimensions and sign convention: (a) dimensions of sandwich beam for flexural rigidity equations; (b) dimensions for shear stress equations; (c) the sign convention adopted for the stress resultants is shown. The positive direction of the external forces required to balance the coordinates x, y and z. Consequently, the relationship between the curvature and bending moment is $M = -EI(d^2z/dx^2)$, deflection $= w$, moment $M = -D(d^2w/dx^2)$, $Q = dM/dx$, slope $= dw/dx$, shear force $Q = -D(d^3w/dx^3)$, $q = -dQ/dx$, curvature $= d^2w/dx^2$, distributed load $q = D(d^4w/dx^4)$.

second term is the dominant one and provided the first and third terms are less than 1% of the second, then they may be discounted.

Therefore, provided

$$\frac{E_f bt^3/6}{E_f(btd^2)/2} < \frac{1}{100}, \qquad \frac{E_c bc^3/12}{E_f(btd^2)/2} < \frac{1}{100}$$

that is

$$\frac{d}{t} > 5.77 \quad \text{and} \quad \frac{E_f}{E_c}\frac{t}{c}\left[\frac{d}{c}\right]^2 > \frac{100}{6} \tag{7.2}$$

$$D = E_f \frac{btd^2}{2} \tag{7.3}$$

Under this condition, the stresses in the faces may be determined by the use of ordinary bending theory. As the sections remain plane and perpendicular to the longitudinal axis, the strains at any point distance z below the centroidal axis are Mz/D. The sign convention for bending of beams is given in Figure 7.6. The stresses in the faces are

$$(\sigma_f)_{max} = \frac{Mz}{D}E_f = \pm\frac{MhE_f}{2D} \tag{7.4}$$

Similarly the stresses in the core are

$$(\sigma_c)_{max} = \frac{Mz}{D}E_c = \pm\frac{McE_c}{2D} \tag{7.5}$$

7.9.1 *Shear stress in the core*

The assumptions in the ordinary bending theory lead to the shear stress distribution in a homogeneous beam at a depth $\bar{z}$ below the neutral axis as

$$\tau = \frac{Qaz}{bI} \tag{7.6}$$

where Q is the shear force, a is the area of the section of the beam at section under consideration (see Figure 7.5), z is the distance of the centroid of area a to the centroidal axis of the beam, b is the width of the beam at the section under consideration and I is the second moment of the area of the whole section of the beam. For a composite sandwich beam the shear stress in the core is

$$\tau = \frac{Q}{Db}\sum a\bar{z}E \tag{7.7}$$

where D is the flexural rigidity of the entire section and E is the modulus

of elasticity of the various component sections above the section under consideration.

Considering Figure 7.6

$$\sum a\bar{z}E = \left[E_f bt\frac{d}{2}\right] + \left[\frac{c}{2} - z\right]\left[\frac{c}{2} + z\right]\frac{b}{2}E_c$$

$$= E_f\frac{btd}{2} + \left[\frac{c^2}{4} - z^2\right]\frac{bE_c}{2}$$

Therefore

$$\tau = \frac{Q}{D}\left[E_f\frac{td}{2} + \frac{E_c}{2}\left\{\frac{c^2}{4} - z^2\right\}\right] \tag{7.8}$$

The maximum core shear stress will occur at $z = 0$ and the minimum core shear stress will occur at $z = \pm c/2$.

If the ratio of the maximum core shear stress to the minimum core shear stress is within 1% of unity, that is

$$\left(1 + \frac{E_c}{E_f}\frac{c}{t}\frac{c}{d}\frac{1}{4}\right), \quad \text{where } 4\left(\frac{E_f}{E_c}\frac{t}{c}\frac{d}{c}\right) > 100$$

it may be assumed that the core is too weak to contribute to the shear stress and this stress may be considered constant across the core; the last term on the right-hand side of eq. (7.8) is then ignored and the constant shear stress in the core is

$$= \frac{Q}{D}\frac{E_f td}{2}$$

If in addition to the above, the condition associated with eq. (7.2) is also satisfied, then the shear stress in the core is

$$\tau = \frac{Q}{bd} \tag{7.9}$$

Figure 7.7 shows the shear stress distribution in the sandwich beam.

In using eqs (7.4), (7.5) and (7.9) for the stresses in bending and shear, the beam is defined as a thin face one (see definition in the glossary) and the following assumptions have been made:

1. A core with a low modulus resulting from a cell structure is considered to be a continuous elastic material.
2. In sandwich constructions of GRP faces and foam cores, the faces are much stronger, stiffer and denser than the core. Therefore, the contribution of the core to the overall stiffness of the sandwich construction is small and may be neglected. Consequently, the direct stresses that arise in the

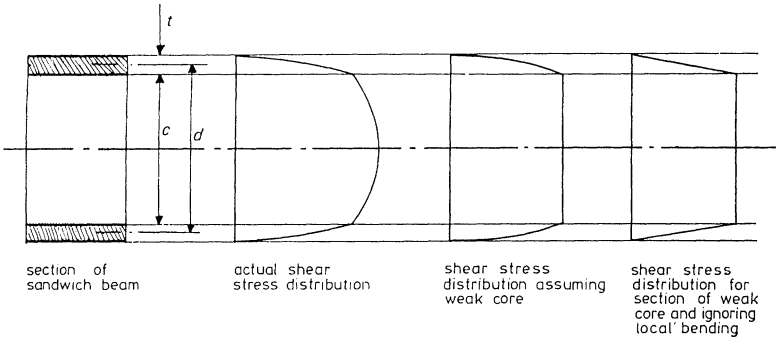

Figure 7.7 Shear stress distribution for sandwich beam.

core under bending are small and may also be neglected; the shear stresses in planes perpendicular to the faces are uniform across the thickness of the core.

3. The core is assumed to be sufficiently stiff in the direction normal to the faces to maintain them the correct distance apart; this assumes stiffening members are placed under concentrated loads.

7.9.2 Thin face sandwich beams

The total deflection w of the beam can be regarded as the sum of the primary deflections (bending deflection), w_1, and the secondary deflections (shear deflection), w_2. The primary deflection may be calculated by the ordinary theory of bending and the secondary deflection also by this theory based on

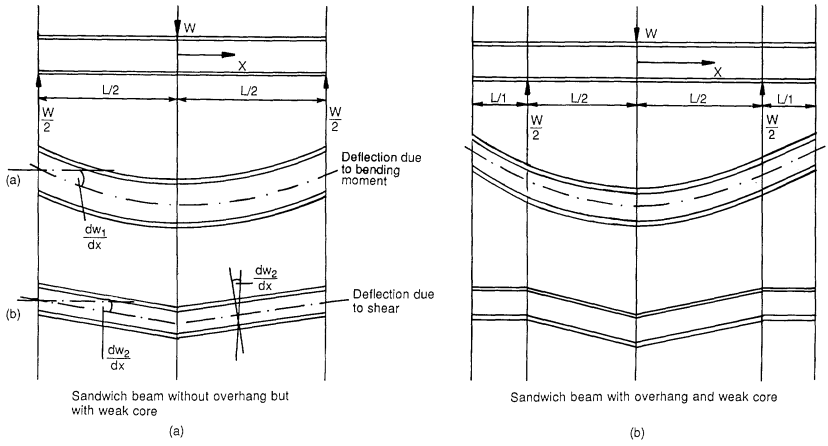

Figure 7.8 Deflection of a sandwich beam under a centrally applied load.

the combined flexural rigidity of the faces as they bend locally about their own separate centroidal axis.

The central deflection of a sandwich beam under a central point load can be represented as shown in Figure 7.8(a). The primary displacement occurs when plane cross-sections remain plane and perpendicular to the longitudinal axis of the beam. This is illustrated in Figure 7.9 by a short length of beam where abcdefg, which was straight in the undeformed sandwich, remains straight and perpendicular to the axis of the beam after bending.

The rotation of this line dw_1/dx gives the slope of the beam and the stresses are related to the displacements by the simple theory of bending. Similarly, Figure 7.9 also shows a short length of beam which has undergone a secondary displacement which occurred when the faces bent about their own individual centroidal axes but underwent no axial extension or contraction. The lines, abc and efg, are perpendicular to the longitudinal axis of the beam. The rotation of these lines is equal to the slope of the beam dw_2/dx. Therefore,

$$\frac{dw_2}{dx} = \gamma \frac{c}{d} = \frac{Q}{bdG_c}\frac{c}{d}$$

$$= \frac{Q}{AG_c}, \quad \text{where } A = \frac{bd^2}{c} \quad \text{and} \quad G_c = \text{modulus of rigidity.} \tag{7.10}$$

The deflection due to shear at the centre of the beam carrying a single point load at this position is obtained by integrating eq. (7.10) and is given as

$$w_2 = \frac{W}{4AG_c} \tag{7.11}$$

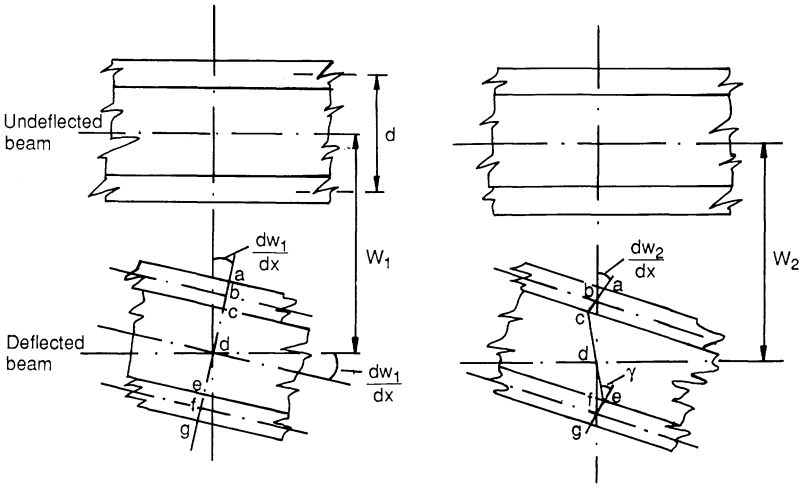

Figure 7.9 Primary and secondary deflections of a short length of beam.

so the total deflection due to bending and shear for this beam is

$$w = \frac{WL^3}{48D} + \frac{WL}{4AG_c} \tag{7.12}$$

This equation is a simplified form of eq. (7.15) in which $D/D_Q L^2$ and D_f/D are both relatively small; it therefore applies essentially to thin face sandwich beams (see also example 9.10).

Generally, for a thin face beam under a statically determined and symmetrically loaded condition, the total deflection may be determined by the addition of the primary and secondary deflections calculated separately, utilizing in each case the total load on the beam. To calculate the deflections for very thin faces or thick faces, it is necessary to use modifications of the above formula.

7.9.3 Thick face sandwich beams

For thick face sandwich beams, the first term on the right-hand side of eq. (7.1) cannot be ignored. The flexural rigidity of the beam is then

$$D = E_f \frac{btd^2}{2} + E_f \frac{bt^3}{6} \tag{7.13}$$

The shear stiffness D_Q has been defined [10] as the shear force that must be applied to the beam to produce a unit slope in the secondary mode of deformation. If dw_2/dx is equal to unity, then $\gamma = d/c$ and the shear stress in the core is $G_c d/c$ and the shear force carried by the whole cross-section of the beam is

$$D_Q = \left[G_c \frac{d}{c}\right] b \left[\frac{t}{2} + c + \frac{t}{2}\right] = G_c \frac{bd^2}{2} \tag{7.14}$$

7.9.4 Characteristic behaviour of a sandwich beam

A sandwich beam under load exhibits characteristic behaviour which depends on the three non-dimensional parameters: D_f/D (the ratio of the face stiffness to the total stiffness of the sandwich), $D/L^2 D_Q$ (the ratio of the total flexural stiffness to the product of the shear stiffness and the square of the span) and L_1/L (the ratio of the length of overhang and length of beam).

The total deflection due to bending and shear at the centre of the beam carrying a single point load at this position and having an overhang L_1 (see Figure 7.8(b)) is

$$w = \frac{WL^3}{48D} + \frac{WL}{4D_Q}\left[1 - \frac{D_f}{D}\right]^2 S_1 \tag{7.15}$$

If w is normalized with respect to w_1, where w and w_1 are defined above

(section 7.9.2), the dimensionless quantity r, is obtained as

$$r_1 = [1 + 12D/L^2 D_Q](1 - D_f/D)^2 S_1$$

Allen [10] has drawn a complete family of curves of r_1 versus $D/D_Q L^2$, each curve representing a particular value of D_f/D; these curves define only the deflection of a sandwich beam with a central point load and no overhang. These curves are shown in Figure 7.10. Allen shows that:

(a) At one limit of the relationship, where $D/D_Q L^2 < 0.01$, r_1 approaches unity, the span L is large and $w = WL^3/48D$ and the deformation is almost wholly due to the primary mode.

(b) At the other limit of the relationship where $D/D_Q L^2 > 1000$, r_1 approaches the value D/D_f, the span L is short and

$$w = \frac{WL^3}{48 D_f} \tag{7.16}$$

(c) Between these two limits ($0.01 < D/D_Q L^2 < 1000$) the deformation is a combination of the primary and secondary deflections and the stresses in the beam are complicated. In Figure 7.10, the curve ABCG has been

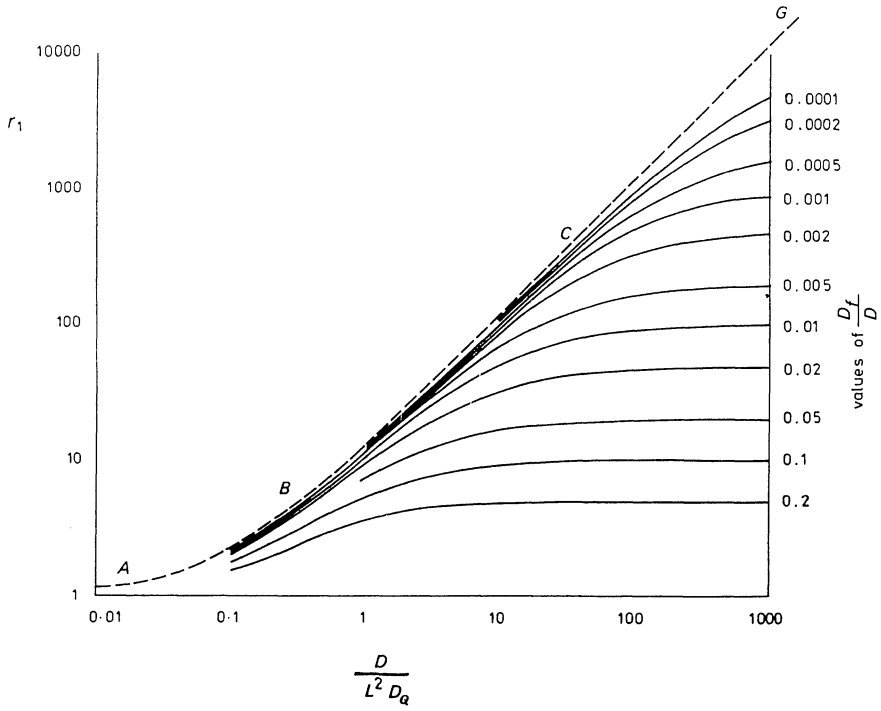

Figure 7.10 Family of curves for r_1 plotted against parameter $D/L^2 D_Q$ (based on [10, Figure 6.5]).

plotted for the result of a thin face sandwich and it is evident that for $D/D_Q L^2 < 10$, the curve essentially defines the sum of the deformation due to ordinary bending and the deformation due to shear strain in the core.

Similar graphs to that shown in Figure 7.10 can be constructed to illustrate the way in which deflections, bending moments, shear forces and critical loads depend on D_f/D and on $D/D_Q L^2$ for a wide range of sandwich beams. Allen [11] has given an outline of the method of solution with formulae, to calculate the coefficient for beams with central point load and uniformly distributed load. The formulae and coefficient for a simply supported beam with a central point load and with a uniformly distributed load have been reproduced at the end of this chapter (appendix).

In the analysis of sandwich constructions involving narrow beams (a narrow beam is defined as one in which b is less than the core depth c; conversely, a wide beam is one in which b is much greater than c), the lateral expansions and contractions of faces take place without causing unduly large shear strains in the core. The stress condition is therefore in a state of unidirectional stress and the ratio of stress to strain is equal to E. When local bending stresses are set up in the face of the sandwich, they act as thin plates in cylindrical bending and the ratio of stress to strain in this case is $E/(1-\nu^2)$. However, as these strains are usually of secondary importance, the ratio may be taken as E without undue inaccuracy. For wide beams, the strains in the lateral directions are restrained by the core and therefore are assumed to be zero. In this case, the ratio of the longitudinal stress to strain is $E/(1-\nu^2)$.

7.10 Buckling of sandwich struts with thin faces

The maximum axial compressive force that a pin-ended elastic strut can support before it becomes unstable is equal to the Euler load P_E given by

$$P_E = \frac{\pi^2 D}{L^2} \tag{7.17}$$

where D is the flexural rigidity. In a sandwich strut in which the core material is of low modulus, it is likely that shear deformations within the core will occur; these reduce the stiffness of the strut member.

For a thin face and an antiplane core (see definition in the glossary), the flexural rigidity is given by

$$D_1 = E_f b t d^2/2$$

When the strut deflects, the shear stress distribution is similar to that given in Figure 7.6 and the total displacement is the addition of the displacement

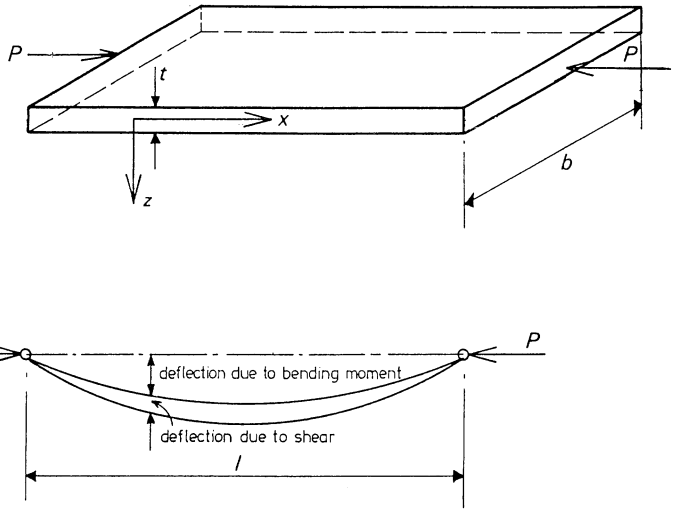

Figure 7.11 Deformations of a buckled strut.

due to ordinary bending (w_1) and that due to shear deformation of the core (w_2).

The buckled strut is shown in Figure 7.11 and at any cross-section, the moment $= P(w_1 + w_2) = -D_1 w_1''$. Allen [11] has shown that this equation yields a differential equation in w_1.

$$w_1''' + \alpha^2 w_1' = 0$$

The solution of this equation with correct boundary conditions (i.e. $(w_1 + w_2) = 0$ at $x = 0$ and at $x = L$) leads to the critical load of the sandwich strut:

$$P = \frac{P_E}{1 + P_E/AG}; \quad P_E = \pi^2 D_1 / L^2 \tag{7.18}$$

In the above formulae for thin faces, it has been assumed that the strut is narrow and that it bends anticlastically. If the strut is wide and bends cylindrically the value for E_f should be replaced by $E_f/(1 - v_f^2)$ (see definition in the glossary).

7.11 Buckling of sandwich struts with thick faces

In the case of a pin-ended sandwich strut with thick faces, Allen [11] has shown that the critical load is

$$P_{cr} = P_E \left[\frac{1 + (P_{Ef}/P_c) - (P_{Ef}/P_c)(P_{Ef}/P_E)}{1 + (P_E/P_c) - (P_{Ef}/P_c)} \right] \tag{7.19}$$

where $P_E = \pi^2 D/L^2$ is the Euler load of strut when there are no shear strains in the core, $P_{Ef} = \pi^2 D_f/L^2$ is the sum of the Euler loads of the faces, considered as two independent struts and P_c is the critical load for shearing instability. Equation (7.19) may be rewritten as

$$\frac{P_E}{P_{cr}} = \frac{1 + \pi^2 \dfrac{D}{D_Q L^2}\left[1 - \dfrac{D_f}{D}\right]}{1 + \pi^2 \dfrac{D}{D_Q L^2}\left[1 - \dfrac{D_f}{D}\right]\dfrac{D_f}{D}} \tag{7.20}$$

P_E/P_{cr} is the ratio of the Euler load of a strut (of the same dimensions as the sandwich strut) to the critical load of the sandwich strut, and if this ratio is plotted against $D/D_Q L^2$, for various values of D_f/D, it may be shown that the results resemble those given in Figure 7.10 where P_E/P_{cr} is substituted for r_1. This means that the true ratios $D/D_Q L^2$ and D_f/D can be calculated for any situation, and by referring to Figure 7.10 it will be evident what type of sandwich behaviour can be expected. The same reasoning may be applied when considering the buckling of sandwich beams as was applied to the bending of sandwich beams in section 7.9.4.

(a) If $D/D_Q L^2 < 0.01$, ordinary bending theory may be used and shear deflection ignored.
(b) If the calculated values of $D/D_Q L^2$ and D_f/D are such that the plotted points lie on or near the line ABCG, local bending of the faces is not likely to be important. The beam or column will then have ordinary bending deflections in addition to deflection due to shear in the core.
(c) If the plotted points lie well below the line ABCG, then local bending of the faces is expected and the thick face theory must be used.

7.12 Wrinkling instability of faces of sandwich struts with cores of finite thickness

In addition to the critical load on a sandwich strut there is an additional component that could cause failure of the strut by introducing a local instability, known as wrinkling, and that is associated with the short wavelength ripples in the faces. Wrinkling may also be present in the compression faces of sandwich beams. The short wavelength wrinkling instability of the faces could occur at a lower axial load than the critical buckling load. Analyses of this problem have been made by Gough *et al.* [12] and by Hoff and Mautner [13].

The wrinkling theory refers only to local bending of the faces and ignores completely their membrane strains. On the other hand, it will be realized that ordinary buckling theory is concerned only with the overall stability of the sandwich component. Wrinkling and other forms of local instability of sandwich beams and struts have been well documented by Allen [11]. The

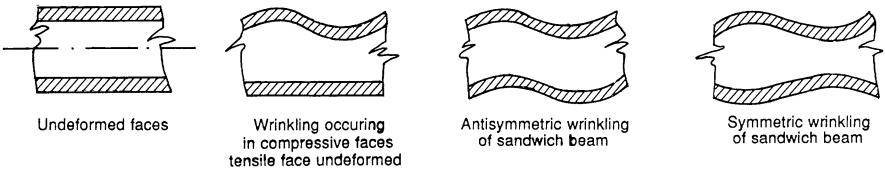

Figure 7.12 Wrinkling instability.

theory is too extensive to quote here and therefore only the results for use by designers are presented.

There are three types of wrinkling instability:

(a) the sandwich beam develops wrinkling in the compressive face; the tensile face remains perfectly flat;
(b) the antisymmetrical wrinkling in sandwich struts;
(c) the symmetrical wrinkling in sandwich struts.

There are three types of wrinkling instability:

The stress at which wrinkling commences in the faces of axially loaded struts and panels with isotropic cores such as phenolic or polyurethane foamed plastics (which for design purposes are assumed isotropic), is given by

$$\sigma = BE_f^{1/3}E_c^{2/3} \tag{7.21}$$

where E_f is the modulus of elasticity of the strut face material $= E_f/(1-\nu_f^2)$ for wide panels, E_c is the modulus of elasticity of the core material and B is the buckling coefficient. Hoff and Mautner [13] have quoted an empirical value for B of 0.4. This must only be considered an approximate quantity.

7.13 Buckling of sandwich panels

This section gives the essential equations for determining the critical edge force per unit length of sandwich panels. The panel considered will be of the form shown in Figure 7.13; the notation is as for sandwich beams. It is supported on four sides and bends in two directions.

The assumptions made in the following discussions are:

(a) deflections are small, therefore the ordinary theory of bending is valid;
(b) there is no extension of the middle section of the panel, therefore the membrane forces are unaffacted by displacements in the z-direction;
(c) as the faces are thin, local bending stiffness within them is neglected.

7.13.1 Buckling of thin face sandwich panels

The critical buckling edge load per unit length in the x-direction for a thin face sandwich is

$$P_{cr} = \frac{\pi^2 D_2}{b^2} K \tag{7.22}$$

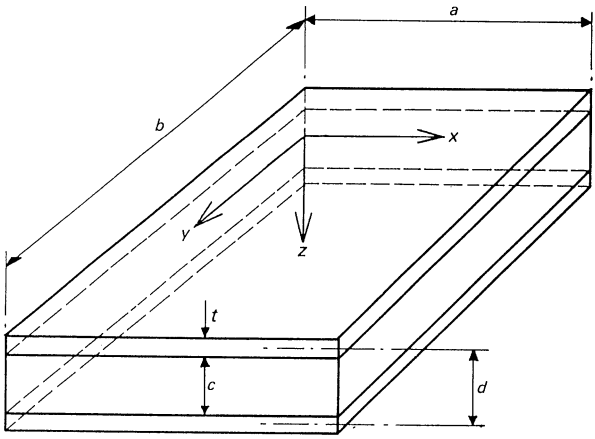

Figure 7.13 Sandwich panel with equal faces a = length of panel, b = width of panel.

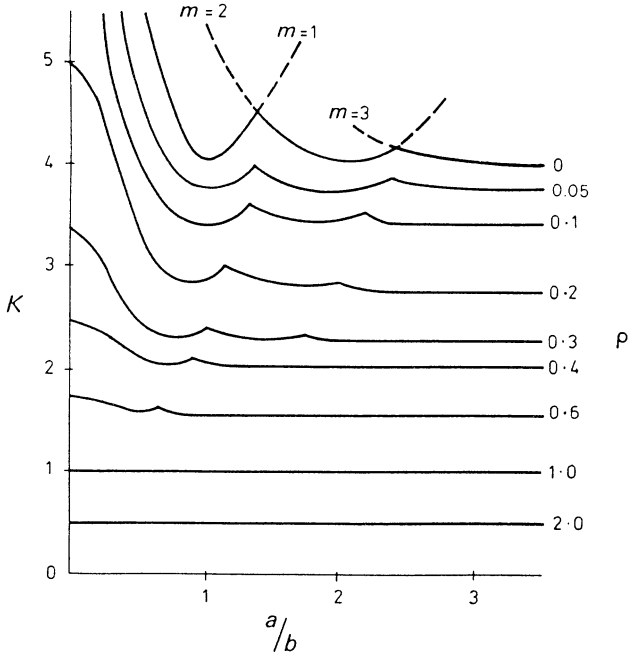

Figure 7.14 Relationship between K and a/b for known values of ρ (eq. (7.23)) (based on [11, Figure 5.4]).

(this load causes buckling in the m, n mode) where $D_2 = E_f t d^2/2(1-v_f^2)$ is the flexural rigidity of the panel per unit length, b is the width of the panel, K is the dimensionless coefficient $= \{mb/a + (n^2 a/mb)\}^2/\{(1+\rho[(m^2b^2/a^2)+n^2]\}$ and a is the length of the panel.

$$\rho = \frac{\pi^2}{b^2}\left(\frac{E_f d^2 t}{2(1-v_f^2)}\right)\left(\frac{c}{G_c d^2}\right)$$

$$= \frac{\pi^2}{2(1-v_f^2)}\frac{E_f}{G_c}\frac{tc}{b^2}$$

$G_c d^2/c$ is the shear rigidity of the panel per unit length or $\rho = \pi^2/b^2$ times the ratio of the flexural rigidity to the shear rigidity. The dimensionless coefficient K may be obtained from Figure 7.14 knowing the ratio a/b and ρ. Equation (7.22) may be used for an isotropic face (viz. a CSM laminate) and an assumed isotropic foamed polymer core.

To determine the buckling load of a panel with thin or very thin faces, it is necessary to find the mode that gives the smallest critical load. For any value of m this critical load value will exist when $n = 1$. Therefore, the dimensionless coefficient K may be obtained from Figure 7.14 when values of a/b and ρ are known. It should be noted that the curves in this figure ignore the effect of D_f on the secondary deformation and they can only be relied upon if D_f/D and $D/D_Q L^2$, for the plate, combine to give a point in Figure 7.10 that is close to the line ABCG.

7.13.2 *Buckling of thick face sandwich panels*

The critical buckling edge load per unit length in the x-direction for a thick face sandwich is

$$P_{cr} = \frac{\pi^2 D_2}{b^2} K_t \tag{7.23}$$

where P, a, D_2 are as defined in eq. (7.22),

$$K_t = K + \left[\frac{mb}{a} + \frac{n^2 a}{mb}\right]^2 \left[\frac{t^2}{3d^2}\right] \tag{7.24}$$

where K is the dimensionless coefficient in eq. (7.22). The dimensionless coefficient K_t may be obtained from Figure 7.15 when the values of a/b and ρ are known and when $t/d = 0$ and 0.3. These values of t/d represent the extreme values of any practical sandwich.

Equation (7.23) may be utilized for an isotropic face and isotropic core (i.e. faces of a chopped strand laminate and an assumed isotropic foamed polymer core).

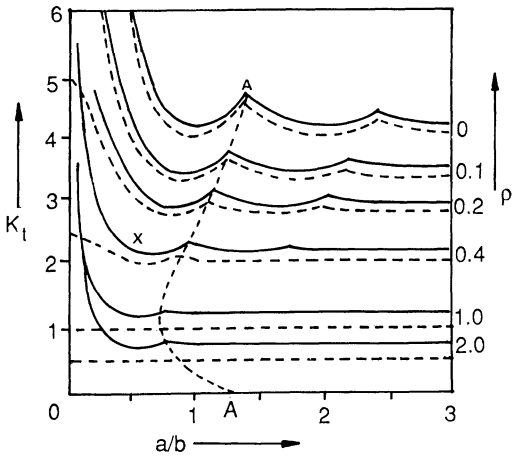

Figure 7.15 Buckling coefficient K_t in eq. (7.24). Simply supported isotropic sandwich panel with thick faces and uniform edge load in the x-direction. Broken and full lines represent the extreme case, $t/d = 0.03$, respectively (based on [11, Figure 6.3]).

7.14 Bending of simply supported panels with uniform transverse load

The maximum transverse deflection of a sandwich panel, consisting of an isotropic thin face and isotropic core, due to a uniform transverse load q per unit area is given by Allen [11] as

$$w_{max} = \frac{qb^4}{D_2}[\beta_1 + \rho\beta_2] \tag{7.25}$$

where b is the width of the panel in the y-direction.

$$D_2 = E_f t d^2/2(1 - v_f^2)$$

where ρ is the flexural and shear rigidity ratio and is given in eq. (7.22). β_1 and β_2 are coefficients which are given in Figure 7.16.

Timoshenko and Woinowsky-Krieger [14] have given an equivalent formula, eq. (7.26) for a homogeneous plate. It is necessary to obtain the numerical factor α which depends upon the ratio a/b of the sides of the plate; the value of the maximum deflection computed from eq. (7.26) yields a similar result to that obtained from eq. (7.25):

$$w_{max} = \frac{qb^4}{D}\alpha \tag{7.26}$$

where α may be obtained from [14, Ch. 5, Table 8].

The formulae quoted above should be used only when small transverse

deflections of the panel take place. If large deflections are experienced then Alwan [15] should be referred to.

Corresponding membrane stresses in the faces and shear stresses in the core may be obtained from the following equation [11]. The direct stresses in the faces are:

$$\sigma_{xx} = \frac{qb^2}{dt}[\beta_3 + \nu\beta_4] \tag{7.27}$$

$$\sigma_{yy} = \frac{Qb^2}{dt}[\beta_4 + \nu\beta_5] \tag{7.28}$$

The maximum stresses are located at the centre of the plate ($x = a/2$, $y = b/2$, Figure 7.13). The shear stresses in the faces are:

$$\sigma_{xy} = \frac{qb^2}{dt}[1 - \nu]\beta_5 \tag{7.29}$$

The maximum value is located at the corners of the slab ($x = 0$, $y = 0$). The shear stresses in the core are

$$\sigma_{zx} = \frac{qb}{d}\beta_6 \tag{7.30}$$

and are located in the middle of the side of length b ($x = 0$, $y = b/2$),

$$\sigma_{yz} = \frac{qb}{d}\beta_7 \tag{7.31}$$

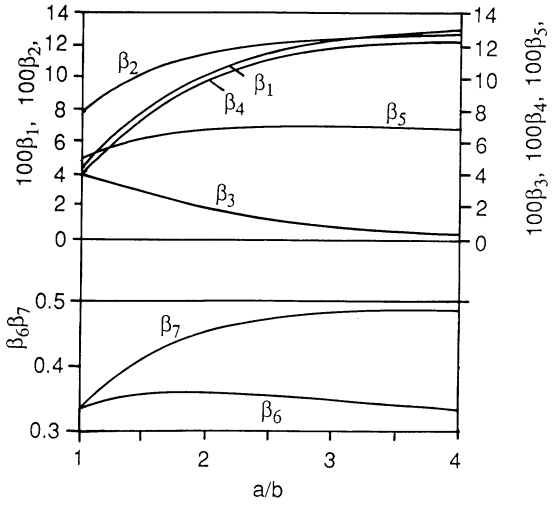

Figure 7.16 Values of $\beta_1 - \beta_7$ in eqs. (7.25)–(7.31). Isotropic panel with very thin faces (based on [11, Figure 5.5]).

and are located in the middle of the side of length a ($x = a/2$, $y = 0$), where d and t have been defined in Figure 7.13 and β_3–β_7 may be obtained from Figure 7.16.

In the above equations, the stresses are independent of the shear stiffness of the core and are identical with those obtained when the shear deformations in the core are neglected. Consequently, the results given by Timoshenko and Woinowsky-Krieger [14] could also be used to determine the stresses in a sandwich plate.

7.15 Simply supported sandwich panels with edge load and uniform transverse load

Allen [11] has discussed this topic fully for general sandwich constructions and Benjamin [15] has also quoted formulae which may be used to investigate the problem. However, the formulae derived by Allen incorporate a number of coefficients, all of which are dependent on dimensionless parameters. It is recommended that reference be made to the above for information concerning edge load and uniform transverse load on simply supported sandwich panels.

7.16 Summary: a guide for design of sandwich beams and struts and panels with edge loads

Figure 7.10 gives an important graphical result as it shows immediately which type of sandwich behaviour can be expected. It may be used as an approximate design guide when the parameter values D/L^2D_Q and D_f/D are known and where the quantity r_1 may be taken as an approximate estimate for:

(a) the ratio of (deflection of a sandwich beam of span L)/(deflection of simple beam of the same dimensions and load);
(b) the ratio of (Euler load of a simple strut of length L)/(the critical load of a sandwich strut of the same dimensions);
(c) the ratio of (deflection of a sandwich panel)/(deflection of an equivalent simple panel); the panel is supported on four sides, with the shorter span of length L and with a transverse load applied to it;
(d) the ratio of (critical edge load on a simple panel)/(critical edge load of an equivalent sandwich panel); the panel is supported on four sides with shorter span of length L.

The graph may be interpreted as follows:

(a) When the ratio D/L^2D_Q is less than 0.01 (i.e. for very large spans or cores with high shear moduli), r_1 approaches unity. This implies that the shearing deformations of the core are not important and the panel may be analysed by the application of the ordinary bending theory.

(b) If the calculated values of D/L^2D_Q and D_f/D give plotted points close to the curve ABCG, the behaviour of the member is as for an ordinary beam, column or panel with the addition of shear deflection in the core. Most practical sandwiches with flat faces have values of $D_f/D \geqslant 0.01$ and $c/t \leqslant 5$ which will give points close to the curve ABCG provided $D/L^2D_Q < 1$.

(c) If the plotted points lie close to the horizontal region of the D_f/D curve, then the composite action of the sandwich has been largely lost and the faces act as independent beams or columns.

Having established the dimensions of the sandwich component, it is advisable to undertake a laboratory test to verify the deflections.

Appendix

The total deflection due to bending and shear at the centre of a beam carrying a single point load at this position is

$$w = \frac{WL^3}{48D} + \frac{WL}{4D_Q}\left[1 - \frac{D_f}{D}\right]^2 S_1$$

The total deflection due to bending and shear at the centre of a beam carrying a uniformly distributed load q per unit length is

$$w = \frac{5qL^4}{384D} + \frac{qL^2}{8D_Q}\left[1 - \frac{D_f}{D}\right]^2 S_2$$

The coefficients S_1 and S_2 are defined as

$$S_1 = 1 - \frac{\sinh\theta + \beta_1(1 - \cosh\theta)}{\theta}$$

$$S_2 = 1 + \frac{2\beta_2}{\theta}(1 - \cosh\theta)$$

$$\beta_1 = \frac{\sinh\theta - (1 - \cosh\theta)\tanh\phi}{\sinh\theta\tanh\phi + \cosh\theta}$$

$$\beta_2 = \frac{1}{\theta}\left[\frac{1 + \theta\tanh\phi}{\sinh\theta\tanh\phi + \cosh\theta}\right]$$

$$\theta = \frac{1}{2}\left[\left(\frac{D}{L^2D_Q}\right)\frac{D_f}{D}\left(1 - \frac{D_f}{D}\right)\right]^{-1/2}$$

$$\phi = 2\theta\frac{L_1}{L}$$

The above equations are given for simply supported beams with overhangs of value L_1. The various symbols have been defined in the chapter.

References

1. BS 3927, Specification for rigid phenolic foam (PF) for thermal insulation in the form of slabs and profiled sections. British Standards Institution, London (1986).
2. G. Menges and F. Knipschild, Stiffness and strength—rigid plastics foams, in *Mechanics of Cellular Plastics*, ed. N.C. Hilyard, Applied Science Publishers Ltd, London (1982) Ch. 2A, pp. 27–72.
3. P. Grosskopf and Th. Winkler, *Auslegung von GFH-Hartschaum-Verbundwerkstoffen*, Kunststoffe (1973) pp. 881–888.
4. BS 4735, Laboratory methods for assessment of the horizontal burning characteristics of specimens no larger than 150 mm × 50 mm × 13 mm (nominal) of cellular plastics and cellular rubber materials when subjected to small flame. British Standards Institution, London (1974).
5. L.J. Broutman and R.H. Krock, in *Composite materials, Vol. 18, Structural Design and Analysis*, Part II, ed. C.C. Chamis, Academic Press, London (1985).
6. Flatwise compressive strength of sandwich cores, American Society for Testing Materials Standard, designation C365.
7. Tension test of flat sandwich constructions in flatwise planes, American Society for Testing Materials Standard, designation C297–61.
8. Tests for tensile properties of rigid cellular plastics, American Society for Testing Materials Standard, designation D1623–64.
9. Shear test in flatwise plane of flat sandwich construction or sandwich core, American Society for Testing Materials Standard, designation C273.
10. H.G. Allen, Analysis and design methods used in plastics sandwich panel construction, in, *Use of Load Bearing and Infill Panels*, ed. L. Hollaway, Manning Papley (1977) Ch. 6.
11. H.G. Allen, *Analysis and Design of Structural Sandwich Panels*, Pergamon Press, Oxford (1969).
12. G.S. Gough, C.F. Elam and N.D. De Bruyne, The stabilisation of a thin sheet by a continuous supporting medium, *J. R. Aero. Soc.* **44** (349) (1970) 12–43.
13. N.J. Hoff and S.E. Mautner, Buckling of sandwich-type panels, *J. Aero-Sci.* **12** (3) (1945) 285–297.
14. S. Timoshenko and S. Woinowsky-Krieger, *Theory of Plates and Shells*, McGraw-Hill, New York (1959).
15. A.M. Alwan, Large deflection of sandwich plates with orthotropic cores, *J. AIAA* **2** (10) (1964) 1820–1822.
16. B.S. Benjamin, *Structural Design with Plastics*, 2nd edn, Van Nostrand Reinhold Co., New York (1982).

8 Bonding and bolting composites

8.1 Introduction

This chapter introduces the principles behind the behaviour of the adhesively bonded and the mechanically bolted joints in composite structures. There are a number of reviews representing the state-of-the-art for the theoretical analyses of both types of joints [1–8]; in addition, Matthews [9] discusses the design techniques for bonded and bolted joints and gives a number of design curves.

The physical nature of fibre/matrix composites does introduce problems that are not encountered with metals. The fibre type and arrangement (i.e. whether the composite has been manufactured from random reinforcement, woven fabric, unidirectional filaments, etc.) as well as resin type and fibre volume fraction influence the behaviour of the joint. The strength of the adhesively bonded joint is dependent on the joint type and geometry (see section 8.2) and the bolted joint is dependent on the geometry, bolt size, washer size, damping force hole size tolerance and clamping force. The latter parameter is the force in the through-thickness direction caused by tightening the bolt and is of critical importance in the design of bolted joints.

In composite structures, jointing has a special significance and poses a major challenge to the engineer, a joint in a composite structure has to be addressed at the following levels:

(a) the micromechanics level, at the fibre-matrix interface;
(b) the macromechanics level, at the interfaces between layers as characterized by the free edge problem;
(c) the structural level, at the interfaces between two or more separate components as in the conventional joint.

8.2 Adhesive bonded joints

In the past, the bonding of polyester composite components had apparently presented some difficulties as it was felt that the parts to be joined should be bonded in the 'green' state; this belief was based on the performance of polyester resin when used as the bonding agent. Epoxy based composites have not presented such a problem although there has been and still is the problem of interlaminar stability. Thermoplastic polymers have always

presented difficulties because of their poor 'wetting' characteristics. However, surface modification techniques have overcome this particular difficulty to a certain degree. It should be mentioned here that under certain circumstances a more satisfactory procedure for the jointing of thermoplastic polymers and composites might be either the heat or solvent welding techniques.

Currently the epoxy and the acrylic based toughened adhesives are used for general application and have proved over the years to be very versatile and easy to use, durable, robust and relatively free from toxic hazards; the toughened adhesives exhibit high pull strengths.

Composites are not generally homogeneous throughout their thickness as many thermosetting polymer composites have a gel coat; resin rich surface layers are brittle and when overloaded are liable to display a brittle failure. An appropriate resin should be chosen, such as a compliant one, which will distribute the applied load over a large area, thus reducing the stress taken by the friable surface of the composite.

When designing joints special case must be taken to ensure efficient load transfer through the joint. Bonded joints are most efficient when subjected to shear loads and least efficient when subjected to peel load (see section 8.3), thus joints should be designed so that they are only subjected to shear

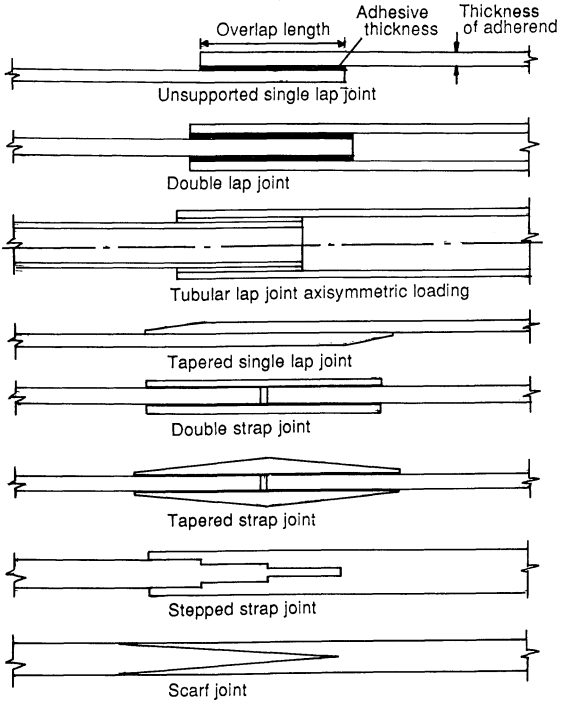

Figure 8.1 Lap joint system for tubes.

loads whenever possible. In practice, pure shear loads can only rarely be achieved and therefore peel forces have to be considered. The highest peel stress loading is generally found at the edge of the joint and is affected by the relative rigidities of the adherends and the properties of the adhesive [10].

Adhesive bonding has other functions apart from transferring load form adherend to adherend. Bonding can be used to increase the structural efficiency of a laminate structure. Stiffeners are also generally bonded to thin plates to prevent local buckling, in which case very little load is transmitted through the glue lines, provided that the structure remains intact. However, the bonding here is important from the point of view of containing local damage.

Flat structural components which are fabricated separately and are then assembled, may be joined in many different configurations of which the most common are shown in Figure 8.1; their uses, from a strength point of view, are given in Figure 8.2. If tubular members are to be joined, a lap system (see Figure 8.3) capable of bonding overlapping co-axial tubes would be used (see section 8.4); this is shown also in Figure 8.1.

By investigating Figures 8.1 and 8.2, it will be clear that the simpler and cheaper configurations cannot sustain the high load levels of the more elaborate systems, no matter how much quality workmanship is employed in their manufacture.

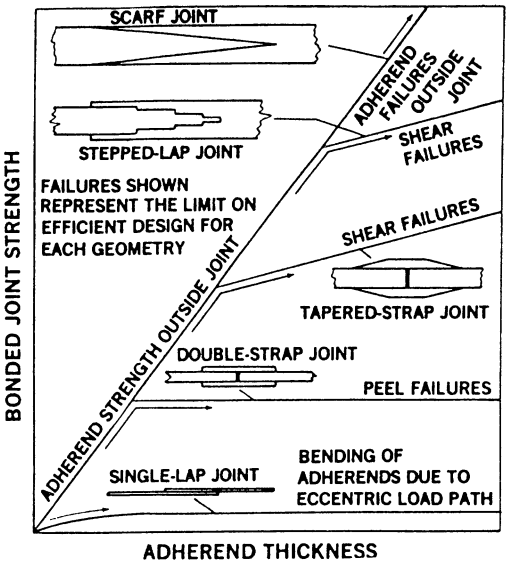

Figure 8.2 Relative strength of joints (after [5]). Note: (i) to provide an increase in joint strength requires an increase in joint sophistication; (ii) the less sophisticated joint strengths are not increased by increasing the adherend thickness, failures are initiated generally by high peel stresses; (iii) The more sophisticated joints fail by the development of high shear stresses but these failure stresses will increase in value if the thickness of the adherend is increased.

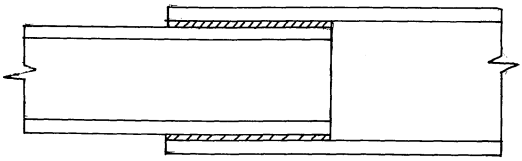

Figure 8.3 Tabular lap joint axi-symmetric loading.

The single lap joint is unlikely to be as strong as the adherends, but with an adequate overlap-to-thickness ratio in excess of 50:1, the eccentricity in load path is relieved by the transverse deflections under tensile load and a relatively high structural efficiency can be developed. This type of joint is efficient for an in-plane shear transfer but should not be used in a compressive load situation. Greater joint efficiency is achieved by tapering the ends of the adherends of a single lap joint, the taper prevents excessive peel stresses from developing at the ends of the joint and increases the shear strength of the joint by causing a reduction of the peak value of the shear stress.

8.3 Modes of failure

There are four distinct modes by which adhesively bonded joints can fail. These are

(a) a failure of the adherend;
(b) a shear strength failure of the adhesive;
(c) a mode associated with the failure of the adhesive under a peel load;
(d) a failure by delamination of the fibrous composite adherends.

These modes are illustrated in Figure 8.4. Item (a) occurs in the strongest joint, in that the load level is 100% of the strength of the adherend in which failure takes place. In this case the strength of the joint is linearly proportional to the thickness of the laminate.

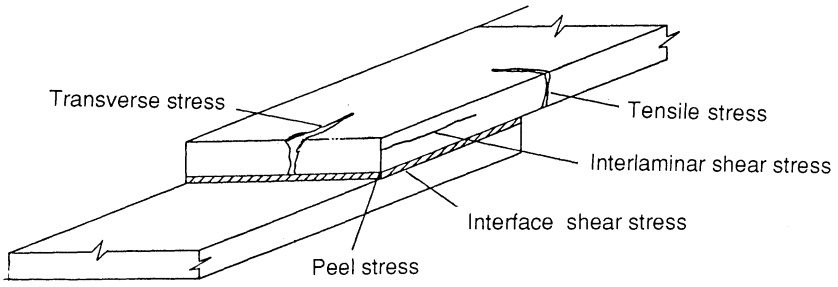

Figure 8.4 Failure modes of an adhesively bonded joint.

Item (b) is an adhesive failure of the bond between the adherend and the adhesive. The shear strength of the bonded joint is proportional to the square root of the laminate thickness. This form of failure must not be confused with a cohesive one which implies a failure wholly within the adhesive materials whereas an adhesive failure is the failure of the bond between the adhesive and adherend.

The peel stress in item (c) is a tensile stress which develops its maximum value near the free end of a double or a single lap joint. The stress is developed in association with the shear stresses and can be particularly severe in thick double lap joints (high peel stresses are developed in single lap joints). The low interlaminar tension strength of composite laminates limits the thickness of the adherends which can be bonded together efficiently by lap joints. The inner laminate of the adherend splits locally due to peel stresses, thus destroying the shear transfer capacity between the inner and outer piles. This overloads the outer filaments which break in tension and the failure progresses through the adherend thickness; this process is illustrated in Figure 8.5. The peel stress induced failure occurs within the laminate as soon as the peel stress exceeds the interlaminar tension; this latter strength is far less than the peel strength of typical structural adhesives.

The peel stress can be reduced to a minimum by having an adequate overlap length in the range $50t$–$100t$ with an upper limit on thickness of the order of 1.5 mm. If the thickness of the adherends is greater than 1.5 mm, the efficiency of the joint can be retained provided the ends of the adherends are tapered [11]. Smith and Pattison [12] have shown that the joint efficiency is only 30% when a simple lap joint is used but this value can be increased to 60% with a butt strap joint, 70% with a scarf joint and 90% with a stepped joint. Consequently, for high technology joint situations, a scarf or stepped joint should be used rather than a simple lap joint.

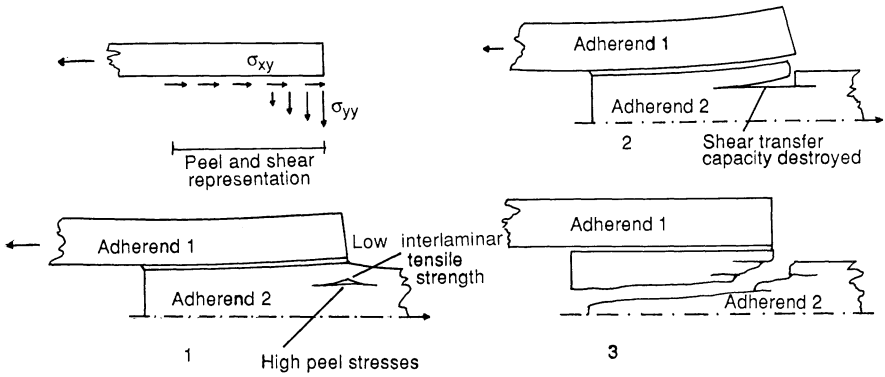

Figure 8.5 Delamination of thick adherends in a lap joint.

Real joints will form a fillet of adhesion spew due to the squeezing of the adherends during bonding (see Figure 8.6); other joints may be specifically manufactured to have spew fillets at the free end of the joint. These fillets reduce the high stress concentrations in the joint. It has been shown [3] that when a spew fillet does exist, the maximum shear stress is reduced to 70–80% of its value without the fillet; actual magnitude depends upon the geometry of the joint.

The important characteristics of the state of stress and strain in the adhesive are the maximum and minimum shear strain and the maximum induced adhesive peel stress. Figure 8.7 shows the relationship between the adhesive shear stress and strain versus length along the joint overlap when it is assumed that the material has an elastic perfectly plastic relationship. As discussed earlier, when the composite is under a high load, the composite adherend could delaminate before the ultimate peel stress is reached; this is illustrated in Figure 8.7.

Practical details to reduce the above maximum stresses and strains without any loss in shear strength of the joint, are illustrated in Figure 8.8 where:

(a) the adherend of the cover plate is tapered;
(b) the adhesive layer is thickened locally (to make the bond material more flexible);
(c) a spew fillet is incorporated at the end of the adherend or strap plate.

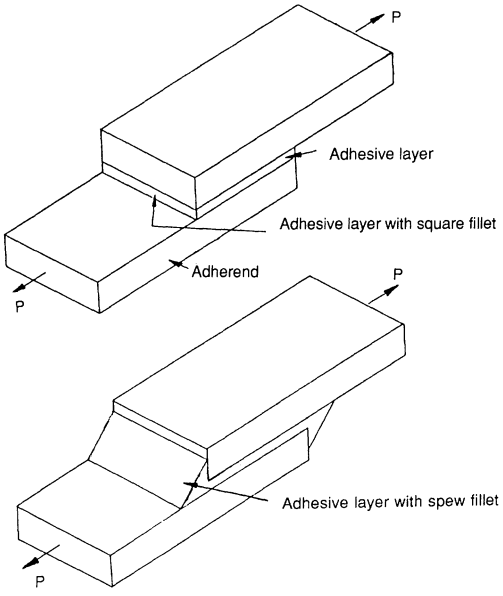

Figure 8.6 Square fillet and spew fillet lap joint.

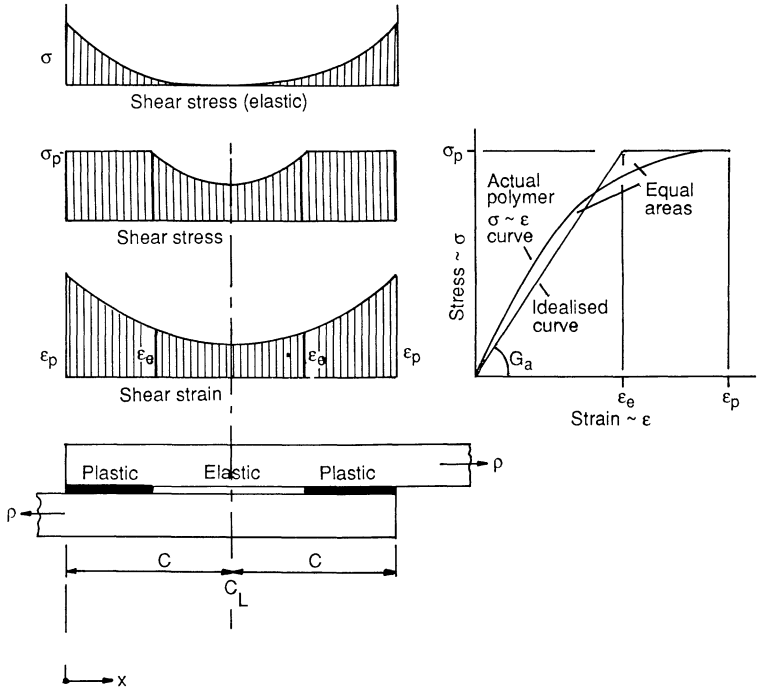

Figure 8.7 Relationship between adhesive shear stress and strain versus length along joint overlap. ε_e = elastic limit strain, ε_p = ultimate shear strain, and σ_p = ultimate shear stress.

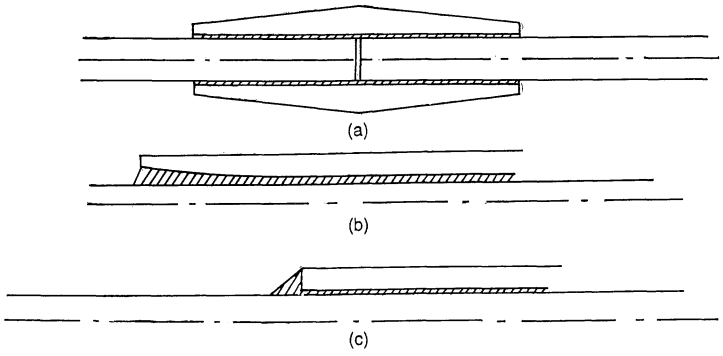

Figure 8.8 Practical details to reduce maximum stresses and strains in the adhesive.

The degree of taper and thickening of the adhesive layer in items (a) and (b), respectively, is not critical.

The adhesive shear stresses are shown in Figure 8.9 as a function of bond overlap when the possibility of premature failure (mentioned in items (a), (b) and (c) above) has been eliminated.

There is significant shear lag effect in the double strap joint, this affects the splice plate through-thickness stresses at the point where the adherends butt together. It is recommended that the splice plates have a thickness of one-half of the adherend thickness.

If the joint failed in the adherend [mode (a)] under a direct tensile or compressive load, the strength of the joint is proportional to the thickness of the adherend. If the joint failed in mode (b), the shear strength of the joint is proportional to the square root of the thickness of the adherend and failure of the joint in mode (c) indicates that the peel strength of the joint is

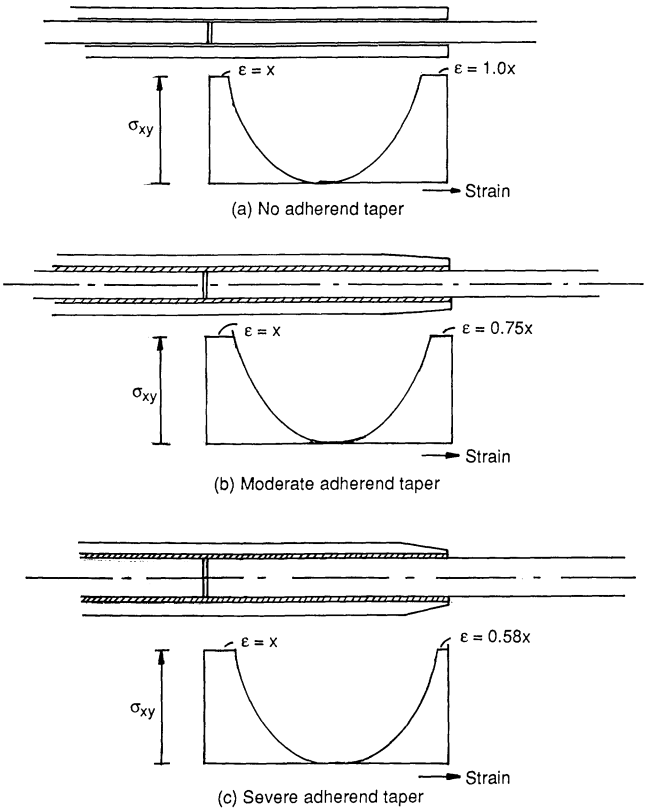

Figure 8.9 Adhesive shear stresses as a function of taper of the cover plate. (a) No adherend taper; (b) moderate adherend taper; (c) severe adherend taper.

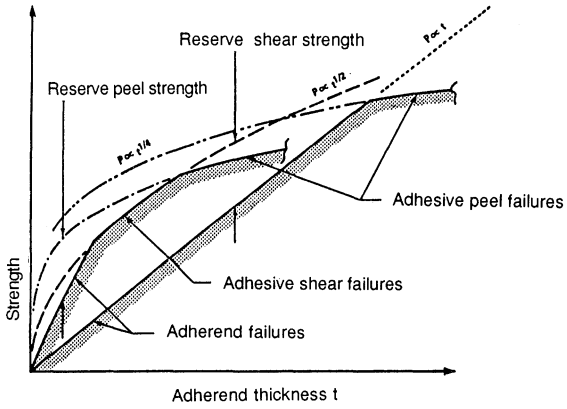

Figure 8.10 Strength of joint versus adherend thickness. Relative values of adherend and peel stresses (after [5]).

proportional to the composite thickness to the quarter power. Figure 8.10 shows the strength of the joint plotted against adherend thickness. It will be seen that the efficiency of adhesively bonded joints and their failure mechanisms are a function of the adhesive thickness. The main reason for this is that the adhesive layers are most efficient when their thickness lies between 0.125 and 0.5 mm. Although thicker joints could develop higher failure loads, it is likely that flaws (see section 8.8) within their thickness will form during the manufacture of the joint with a consequent reduction in joint ultimate strength.

8.4 Tubular lap joints

The mechanism of load transfer in a tubular joint is via differential straining of the adherends and the generation of an adhesive shear stress. A peel stress is produced by the combined actions of adherend bending and differential radial displacements of the tubes due to the Poisson ratio effect of the axial loading.

8.4.1 Jointing closed section members

Closed section members and in particular tubular members are generally manufactured by the pultrusion (see section 5.2.2.3) or filament winding techniques (see section 5.2.1.4) and the composites made by these methods, especially the first mentioned, generally have a high percentage of unidirectionally aligned fibres; this will cause difficulties when these members require to be joined to another member.

The method of bolting these members to form joints at their ends is not advisable. Members under tensile forces would fail by shear (see section 8.9.2); a bonded joint is therefore desirable but the fabrication of this type of connection presents some difficulty. These systems are discussed below.

Various jointing configurations for the axial loading of composite tubes have been proposed and are shown in Figure 8.11. The diagrams (a)–(d) are self-explanatory; the vent in examples (c) and (d) is to allow the air to be expelled in the wet joint or to allow an access for the resin to be pumped into the adhesive region in the dry joint. Diagram (e) shows the crimp bonded aluminium end cap which has been threaded and diagram (f) shows the composite end cap positioned on a composite tube; an optimum method of analysis for the cap bonded ends is given by Hollaway *et al.* [14]. Green and Phillips [15] describe the crimp bonded jointing technique where aluminium end fittings are crimped and bonded onto the ends of composite tubes. These are efficient in terms of the ultimate magnitude of tensile and compressive loads that the joint can take; the crimped aluminium sleeve could be threaded and screwed into the appropriate joint.

There are drawbacks, however, to the use of the crimped bonded aluminium end fitting:

1. the structural system, because it contains aluminium, cannot be used in a corrosive environment;
2. a complete aluminium structural system might be more appropriate if aluminium is to be used as a component part of the structure.

Hollaway and Baker [16] have developed a composite end cap specifically for forming nodal joints in skeletal systems although it can be used for

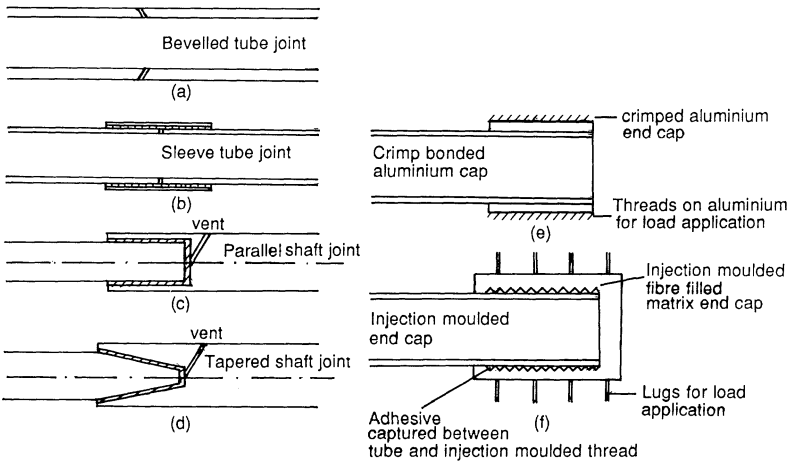

Figure 8.11 Diagrammatic representation of tabular joints for axial or torsional loading.

jointing the ends of the composite tubes to a support. The end cap is manufactured by the injection moulded technique using glass-filled nylon or glass-filled polyester (see section 5.2.2.2) and consists of an inner core and outer sleeve which are jointed at the base of the cap. The outer surface of the inner core and the inner surface of the outer sleeve have a thread moulded into them. A full description of the end cap is given in [16] and Figure 8.12 show the elevation and cross-section.

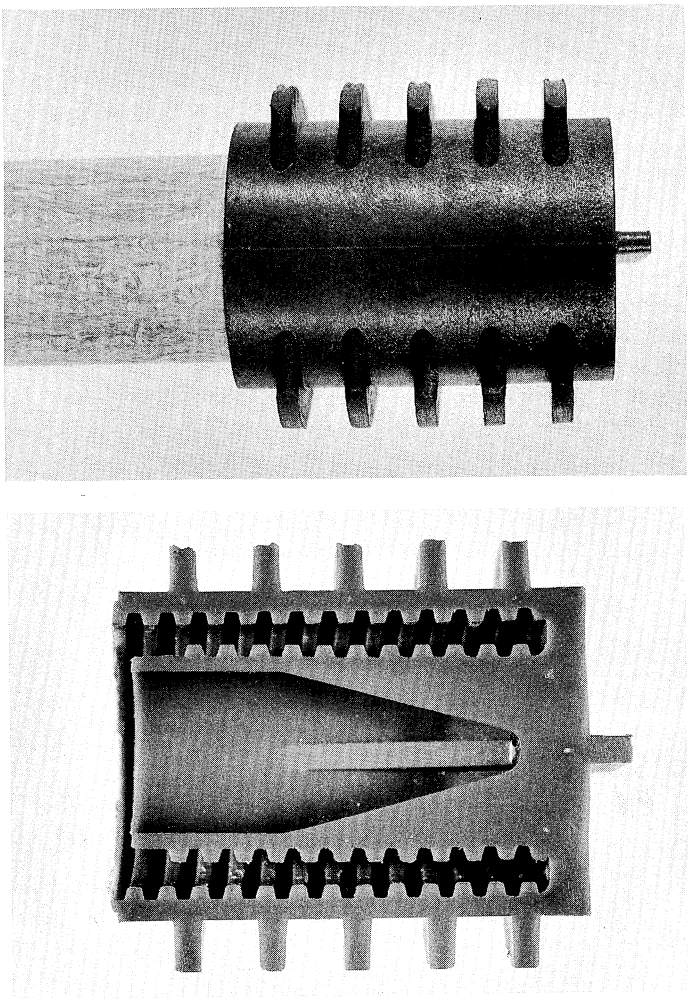

Figure 8.12 (a) Composite end cap for forming nodal joints. (b) Section through composite end cap for forming nodal joints.

8.5 Theoretical solutions to bonded joints

To undertake the theoretical solution to bonded joints, two methods are predominant. The first is a numerical procedure which uses a mathematical treatment employing the classical theory of elasticity and introduces assumptions to enable the solution to be formulated; authors differ in the assumption made depending upon the aims of the analyses. The second procedure uses the finite element theory and this technique is capable of a general analyses that is free of assumptions.

When the numerical procedure is employed the following assumptions are made:

1. The condition of plane strain loading is invariably imposed for the single and double lap joint. This implies that the state of stress at every cross-section in the *xz* plane is identical and renders the joint a two-dimensional analysis problem. This allows the mathematical solution to be treatable, or in finite element theory, it dramatically reduces the computer storage requirements; the tubular joint is analysed as an axi-symmetric body.
2. The adhesive layer is always isotropic and has a thickness smaller than that of the adherends. It may be assumed, therefore, that the adhesive stresses are constant in the through-the-thickness or transverse direction. The only components of stress that are usually considered significant and therefore included in the analyses are the adhesive peel and shear stress components.
3. The classical theory of elasticity is utilized by most workers to treat the adherends as either a thin beam which may undergo in-plane stretching and bending actions or as a thin plate that may also account for transverse normal and shear deformations.
4. The load on the joint is generally tensile and in-plane for continuum systems or axial in the case of tubular joints.

8.5.1 Single lap joint: elastic analyses

The elastic analyses for single lap joints have been outlined by Hollaway [10] and only the basic principles are discussed here.

The first analysis of the stress distribution for an adhesive layer is usually attributed to Volkersen [17] in 1938. As the analysis considered only shear deformation in the adhesive caused by differential in-plane straining of the adherends, it is often referred to as the shear lag method; the mechanism of the stress transfer for the shear lag method is shown in Figure 8.13. The complex shear and peel stress distribution in the adhesive is shown in Figure 8.14.

Goland and Reissner [18] were the first authors to account for the out-of-plane bending associated with the eccentricity in the load path of a single

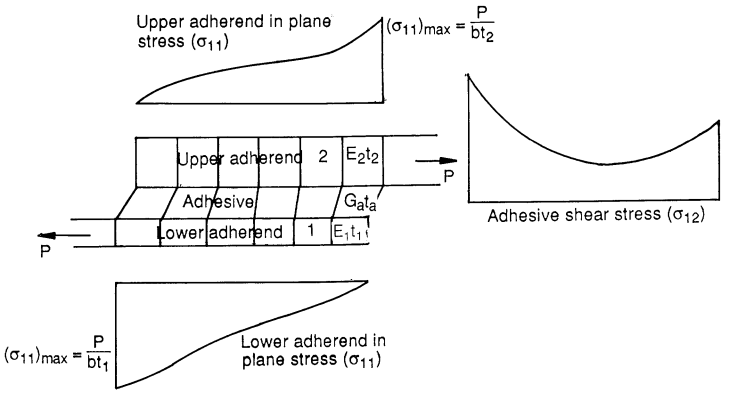

Figure 8.13 Stress distribution for a simple shear lag model. E = modulus of elasticity; G = modulus of rigidity; t = thickness of component.

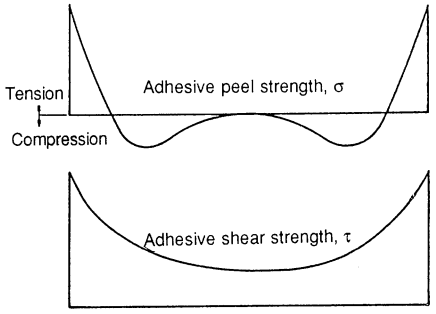

Figure 8.14 Adhesive shear and peel stress distributions for a single lap joint.

lap joint; this is now considered to be the classic bonded joint analysis. Figure 8.15 illustrates the behaviour of the single lap joint and it will be clear that the presence of the bending stresses requires long overlaps to allow the adherends to bend gently rather than abruptly when the adhesive shear is of secondary importance to the moment stress.

Several investigators, notably Renton and Vinsen [19] and Allman [20] have produced analyses which model the adherends to include bending, shear and normal stresses and have set the adhesive shear stress to zero at the overlap ends. These improvements on the original analysis of Goland and Reissner have culminated in the general treatment by Yuccoglu and Updike [21]. These authors analysed embalanced orthotropic adherend plates where the principal material directions coincided with the joint axis system. The adherends were allowed to undergo in-plane, shear and bending deformations.

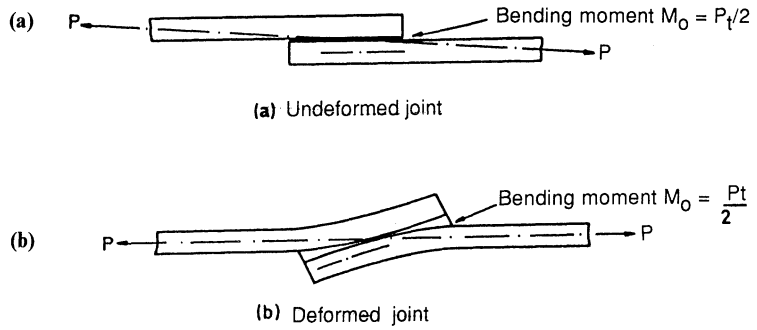

Figure 8.15 Single lap joint. (a) Unloaded single lap joint; (b) loaded single lap joint showing an aligned neutral axis.

A numerical solution technique for the fundamental equations and the boundary conditions are necessary and Yuccoglu and Updike have suggested the multisegment method of integration. Joint rotation is ignored, although boundary conditions can be applied to simulate this rotation. The authors concluded that for practical purposes, the transverse shear deformations in the adherends can be neglected unless the adherends are extremely thick and deformable in shear.

8.5.2 Double lap joint: linear classical theory

The double lap joint is a more efficient joint configuration compared with the single lap one as it overcomes, to a certain extent, the undesirable rotation by applying the load symmetrically. However, the joint still suffers from an eccentric loading path and as a consequence, the adhesive stress shown in Figure 8.16 is developed; the peel stress, which is also shown in this figure, is different from that of the single lap joint (cf. Figure 8.14).

8.5.3 Single and double lap joint: non-linear analysis

The non-linear classical theories of Grimes *et al.* [22] and Hart-Smith [23] have considered the shear stress only to be non-linear. Hart-Smith used the shear-lag model which is adopted to provide the elastic plastic differential equation for adhesive shear stress; only the shear stress is considered to be non-linear. The adhesive shear stress–strain curve is expressed as a continuous mathematical function and the Volkersen equations [24] are written in a finite difference form. A numerical solution is obtained for the adhesive elastic-plastic stress using these equations in an iterative computer routine. The ultimate load is predicted once the limiting value of the shear strain is reached.

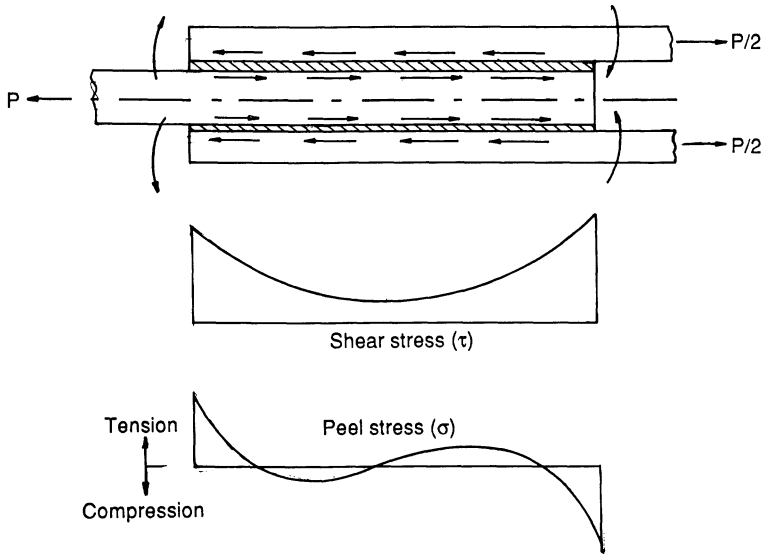

Figure 8.16 Adhesive stress distributions for the double lap joint.

The Volkersen theory, which neglects adhesion bonding, does offer the advantage of reducing the differential equations from a seventh to a second order system. This enables a closed form expression to be obtained which gives the ultimate load of joints having a long overlap length, based upon a plastic adhesive failure.

It has already been stated that a mathematical solution is difficult to perform and the analysis is more readily executed by the finite element technique which is free from assumptions except those implicit in the numerical nature of the analysis.

There are a number of numerical solutions which have examined various aspects of bonded joints from the point of view of linear and non-linear problems; these have included an examination of balanced double lap joint and the influence of an adhesive spew fillet on the glue line stress distribution [25, 26]. The elastic stress distribution for an unbalanced double strap joint using orthotropic carbon fibre reinforced polymer adherends is given by Wright [27, 28].

8.6 Adhesive stress–strain characteristics

The analysis of bonded joints is dependent upon the non-linear stress-strain curve of the adhesive layer in shear. Figure 8.17 shows a typical shear stress/shear strain characteristic for both ductile and brittle adhesive as measured

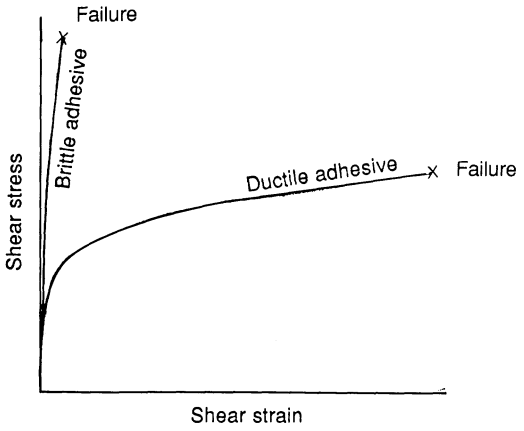

Figure 8.17 Typical shear stress–shear strain characteristic for a brittle and a ductile adhesive (after [5]).

by the napkin-ring or thick-adherend test specimen [11]. The shear strength can be expressed by the strain energy to failure per unit bond area of the adhesive layer rather than by individual strength properties such as peak shear stress. Consequently, the load transfer from adherend to adherend is by non-linear behaviour of the adhesive whether it behaves in a brittle or ductile manner; in the case of a ductile adhesive, the contribution of the linear elastic behaviour is only about 10%. Therefore, the elastic analyses of adhesive joints are not applicable.

As with polymers generally, the adhesive stress–strain characteristic is sensitive to the environment; there could be as much as a 50% drop in the adhesion shear strength, as measured by a coupon test specimen when the temperature rises from 23°C to 80°C. The energy to failure, however, of structurally proportioned joints over these temperatures is very similar. Hart-Smith [11] has discussed the errors that may be incurred in trying to relate the performance of structurally bonded joints to results from test coupons. He has suggested that a radically different approach should be adopted to characterize adhesives by a rational selection for a particular application. It is recognized, however, that certain test data are required as the bases for design.

Hart-Smith [29] has suggested various linear and non-linear adhesive models and these are shown in Figure 8.18. The elastic/perfectly plastic model has the same strain energy to failure as the actual stress–strain curve and predicts the ultimate strength of bonded joints. To estimate the internal stresses associated with low loads, the perfectly elastic model can be used, but the above comments should be observed; for intermediate loads, the elastic-plastic strain hardening model is preferred.

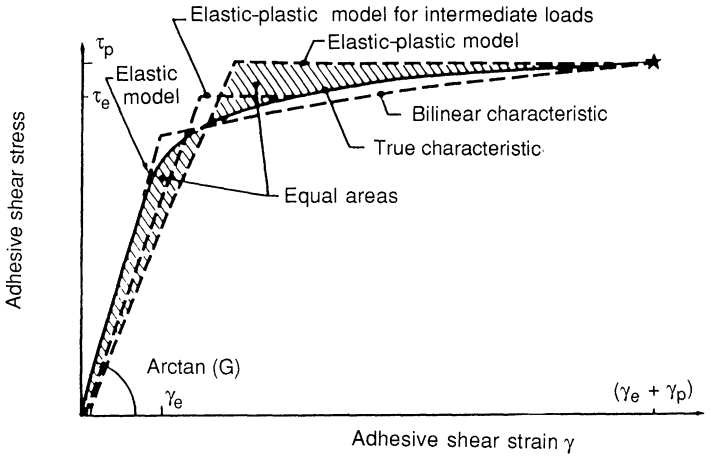

Figure 8.18 Adhesive shear stress–strain curves and mathematical models (after [5]).

Hart-Smith [5] assumed that failure of the joint occurs when the adhesive reaches its limiting shear strain. Figure 8.19(a) shows the adhesive shear stress and shear strain for a double lap joint as the applied load is increased. Figure 8.19(b) shows the effect of lengthening the overall length of a double lap joint loaded to such a value as to cause plastic deformation in the adhesive regions. A solution is then sought for these equations which satisfies

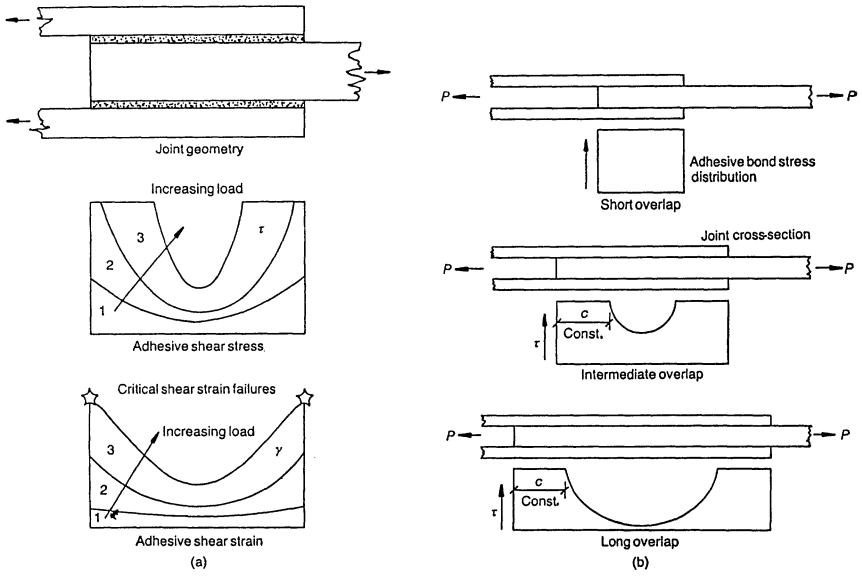

Figure 8.19 The effect of lap length on the adhesive shear stress distribution in a double lap joint.

the usual boundary conditions and also ensures continuity of adhesive strains at the elastic-plastic boundary.

The following points have been suggested by Hart-Smith for the design of joints:

1. the non-linear characteristic of an adhesive layer through idealized elastic-plastic representation should be used;
2. a simplified (Volkersen-type) analysis method should be adopted which includes non-linear and thermal mismatch effects;
3. the regions of high peel stress should be designed-out rather than developing detailed and complex analyses (this also reduces the possibility of transverse failure in composite adherends);
4. the lowest stresses in the elastic trough should be restricted by limiting the length of the trough to avert the tendency for creep accumulation under long-term loading.

8.7 Physical considerations during the bonding operations

In addition to the structural design of the joint, other considerations must be reviewed; these include:

(a) the selection of an adhesive compatible with the adherends;
(b) the in-service properties of the adhesive to give adequate life span;
(c) the surface preparation of the adherend.

Item (a) has been discussed briefly in section 8.2.

8.7.1 In-service properties of adhesives

The in-service properties of the adhesive used in the joint must be known fully; however, this is a particularly difficult task to undertake as the pitfalls of trying to relate the performance of bonded structural joints to results from test coupons are great and there is really no correlation between the small test results and the prototype values. This problems is not unique as generally it is difficult to relate composite small scale test results to prototype structures.

8.7.2 Surface preparation

The surface preparation of the adherends is of vital importance. If GRP adherends are to be joined, it was previously thought advisable to undertake the bonding operation while the laminating resin was still in the 'green' state; at this time the surface may require wiping with an acetone soaked cloth only, although some abrasion of the surface may be desirable. When the bonding operation has been accomplished, the curing cycle of the GRP

adherends must be completed by exposing them to elevated temperatures. With the improved adhesive bonding technology, components that are fully cured at the time of bonding can have a joint efficiency of up to 90%.

The surface preparation procedure for fully cured adherends is as follows:

(a) all traces of release agent must be removed by washing with water or white spirit/MEK or a proprietary cleaner;
(b) the surface of the adherend must be abraded preferably down to the reinforcement;
(c) If the GRP is to be bonded in a particular area, a strip of woven glass cloth may be applied to the laminate during lay-up (if this is an open mould process) and then peeled off while the resin is still in the 'green' state. This leaves the underlying reinforcement partially exposed and provides an ideal surface for bonding.

8.8 Flaws in adhesive bonds

Hart-Smith [30, 31] has shown that adhesive bonds are much more tolerant of flaws than is generally recognized. This most critical location in a bonded joint regarding the high stress situation is generally at the free end of the overlap and flaws tend not to occur in this position; air bubbles tend to be trapped in the interior of the joint where the stresses are usually low in magnitude. He found that local flaws have no effect on the strength of the bonded joint unless they were so large that they shifted the high stress concentrations away from the free boundaries to an area adjacent to the flaws.

Occasionally adhesive bonding and mechanical fastening are used together to provide a fail-safe characteristic. Adhesive bonding in the vicinity of the fastener holes provides a fail safe load path to protect thin and moderately loaded structures. In the case of thick and highly loaded structures, mechanical fasteners would be provided to prevent a catastrophic failure in the high stress region of the adhesive joint which may contain some initial damage. Figure 8.10 shows the relative strength of the composite and the bonded joints for thick and thin structures and the relative sensitivity of adhesive shear and peel stresses; the positions of the failure paths where the adherends become stronger than the adhesives are also shown.

8.8.1 Adherend thermal mismatch

High strength adhesives are usually cured at temperatures well above the normal operating temperatures of the joint. Consequently, when a mismatch in the coefficient of thermal expansion exists between the adherend and the adhesive, significant thermal stresses may be developed. This effect is particularly acute when carbon fibre/epoxy polymer is joined to aluminium; the most severe condition for the joint is at the lowest operating temperature.

8.9 Mechanical joints

8.9.1 Introduction

Mechanical joints find application where bonding is impractical, uneconomic, or where parts may have to be removed or replaced at some time; in addition the mechanical joint is generally preferred for on-site assembly.

The design methods that have been established for structural joints in metals are mainly applicable to those for composites. However, because of the physical nature of composites, problems are introduced that are not encountered with metals; each composite jointing system has to be designed independently because of the anisotropic properties of the material.

The behaviour of the joint is dependent on the composite's stiffness, strength, low interlaminar shear and through-the-thickness tensile strength and these in turn are influenced by the fibre type and array, resin and the fibre volume fraction. It is also dependent on the type of joint, geometry, bolt size, washer size clamping force, hole size and tolerance.

The advantages of mechanical joints over the adhesively bonded ones include the capability for repeated assembly, absence of environmental effects particular to polymers (such as inhomogeneous swelling in aqueous environments), ease of inspection and no specific surface preparation of the components to be jointed. There are disadvantages; probably the greatest is that in forming the joint, some of the material of the component part has to be removed; this causes higher stress levels and areas of stress concentration within the vicinity of the bolts. A mechanical connection does tend to be bulky and may incur a weight penalty but this is unlikely to cause problems in the construction industry.

Hart-Smith [32] has shown that adding mechanical fasteners to a well designed bonded joint does not achieve any significant advantage. This is due to the high rigidity of bonded joints which prevent the load transfer through the mechanical fasteners until the adhesive has failed. However, if the bonded joint is subjected to eccentricity, the addition of end fasteners prevents the peeling action and therefore improves the strength. The second option seems more promising but it suffers from the relatively small bonding area and the moments that have to be transmitted through the adhesive.

Although it is well established that bonded joints can show higher efficiencies than mechanical joints [33], the latter are preferred for on-site assembly for the following reasons:

(a) the quality control procedures for such joints are less complicated than those for bonded joints;
(b) there is no need for the sophisticated surface preparation operations that are required for bonded joints;
(c) damaged and incorrectly assembled members are readily dismantled;

(d) the removal of members to enable inspection of other parts of the structure is possible;
(e) the joint is able to take the design load immediately after it is assembled;
(f) the bolted joints present higher confidence under poor on-site working conditions.
(g) the load is distributed uniformly over the thickness of the member.

These points outweigh the following disadvantages:

(a) lower efficiency compared to bonded joints due to the weakening of the members by holes;
(b) higher weight penalty due to the use of metal fasteners, although composite fasteners can be used;
(c) if there is no skilled labour, the drilling operation may damage the material;
(d) the cost of the joint increases rapidly with size of the joint.

The three main mechanical fastenings systems are:

(a) the screw;
(b) the rivet;
(c) the bolt.

8.9.2 The failure modes

Although bolted joints made of composite materials show failure modes similar to the failure modes of steel joints, the following effects of the material properties have to be noted:

1. *the tensile failure mode* can occur at much lower loads due to the high stress concentrations resulting form the anisotropy of the material;
2. *the bearing failure mode* of composite materials depends heavily on the stacking sequence of the layers and on the presence of a washer (the interlaminar shear strength is low);
3. *the shear failure mode* can occur at relatively low loads particularly in pultruded materials due to the high percentage of longitudinal fibres;
4. *the cleavage failure mode* is a mode of failure which is initiated by transverse tensile failure ahead of the bolt, followed by tensile failure on the minimum area cross-section;
5. *the bending failure mode* is a combination of the cleavage failure and induced bending in front of the hole fastener;
6. *the pull-through of the fasteners* is a further cause of failure of the joints;
7. *the shearing of bolts*: if steel bolts are used shearing failure is very unlikely, but small diameter bolts are liable to bend because of the lower stiffness of the composite compared to that of the bolt.

Basic experimental data are usually obtained from a single bolt configuration;

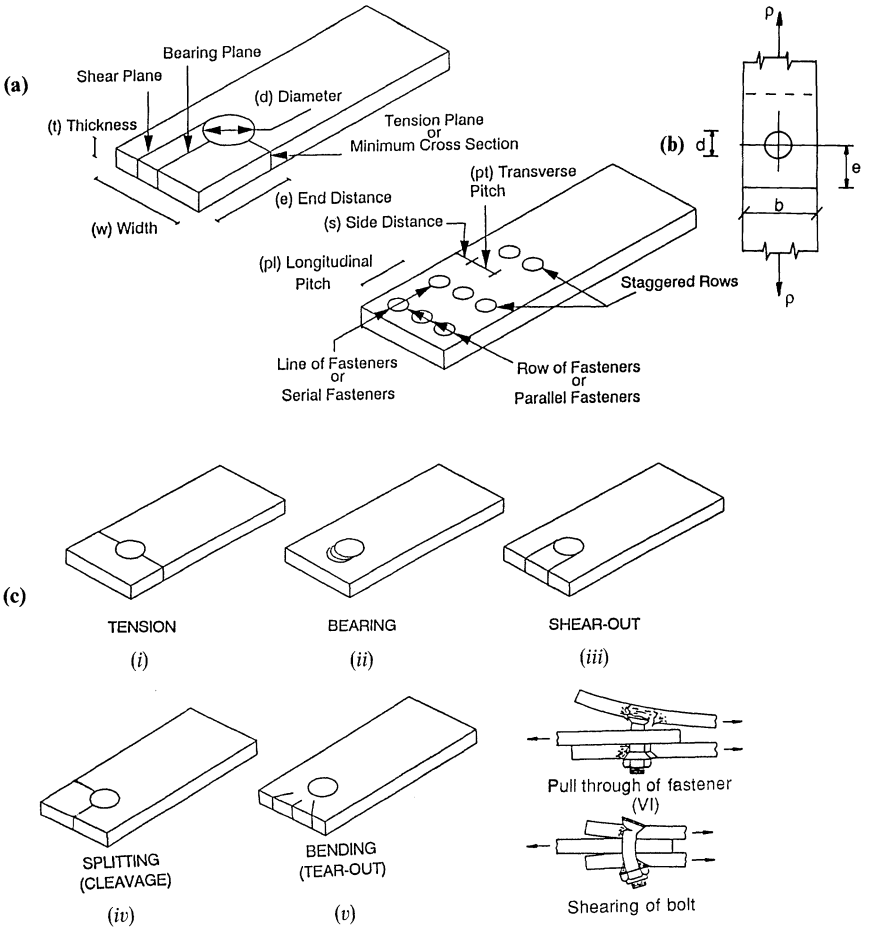

Figure 8.20 Failure modes of bolted connections. (a) Joint nomenclature; (b) notation; (c) joint failure modes.

the seven failure modes are shown in Figure 8.20. As a combination of modes can occur during the failure of a joint, very often no single failure mode is clearly defined. However, bearing mode damage can generally be identified because the pin damages the composite area adjacent to the loaded part of the hole; this type of failure is not catastrophic unlike the other three composite modes.

Tension failure. A tensile failure stress is given by

$$\sigma_a = P_{ult}/bt \text{ on the gross area}$$

$$\sigma_n = P_{ult}/(b - nd)t \text{ on the net area}$$

As fibre/matrix composites are essentially elastic to failure, stress concentrations will develop and these will tend to give rise to low net failure stresses; the greater the degree of anisotropy in the region of the hole, the lower will be this stress value.

Bearing failure. The bearing failure stress is given by

$$\sigma_\Delta = P_{ult}/n\,dt$$

Compressive stresses are developed around the loaded half of the circumference of the bolt or rivet hole. The distinction between bearing and tension failure is largely determined by the joint geometry; the most important parameters are the width to diameter ratio and the fibre array. The clamping effect from the lateral constraint provided by a tightened bolt is another parameter that will enhance the strength of the joint.

Shear failure. The shear failure stress is given by

$$\sigma = P_{ult}/2et$$

When the line of action of the load is in the direction of the fibres, the joint shear strength of unidirectional fibre/matrix composites is low compared with the in-plane shear strength.

The difference between the two strengths will give rise to stress concentrations. If fibres are placed at $\pm 45°$ to the line of action, the shear strengths are high and the stress concentrations will therefore be low. Consequently, fibre orientation has considerable influence over the shear failure strength of joints. There appears to be little information on the case histories for GRP but Collings [36] has shown that for a CFRP composite, the shear strength of a $\pm 45°$ fibre orientation is about 100 MN/m^2 but that of a 0° CFRP composite is only 23 MN/m^2. Combining 0° plies with $\pm 45°$ plies increases the shear performance to give strengths greater than either 0° or the $\pm 45°$ composites alone. He has also shown that a reaction in the degree of anisotropy of a composite, together with a strengthening of potentially weak planes of failure, lead to a decrease in the magnitude of the stress concentration and an increase in shear strength.

Cleavage-tension failure. Cleavage-tension failures are the result of the material being orthotropic and the line of action of the load being parallel to one of the orthotropic axes. To correct this potential failure mode, fibres are required to be placed in the non-axial direction.

Bending failure. The bending failure tends to occur in laminates with mainly directionally aligned fibres together with randomly oriented fibres where the dimensions b and e are large compared to d.

Pull-through failure. Pull-through failure is usually associated with single shear joints in which rivets and countersunk rivets are employed, although double shear joints are also exposed to this load. As in single and double lap bonded joints, peel forces are set up as the composite components tend to straighten under load, thus imposing an out-of-plane bonding situation in the joint. This situation introduces out-of-plane transverse loads and imposes tensile forces in the rivets and through-the-thickness shearing of the rivet head through the laminate thickness.

The strength of countersunk fastener joints in composites is reduced by the non-uniform bearing stress associated with the usually concurrent rotation of the fastener under single shear and by the reduction in strength after the initial failure due to the greatly reduced clamp-up. The countersunk head should not penetrate more than $\frac{1}{3}$ to $\frac{1}{2}$ of the laminate thickness depending upon the operating bearing stress in the shank.

8.10 The influence of various parameters on the failure mechanisms of bolted composites

8.10.1 The geometric factors

The geometric factors include the width (b), the laminate thickness (t), the end distance (e) and the bolt diameter (d). Composite materials are unable to take advantage of plasticity and yield at the bolt hole (unlike isotropic materials) and therefore the effect of stress concentration on the net tensile strength of the plate is dependent on its width. In addition, the ultimate net and gross tensile strengths of a laminate are dependent on the ply orientation. These two parameters, therefore, are interrelated and cannot be discussed separately. Generally the joint width (or fastener pitch) is chosen so that the mean tension failure stress and the ultimate bearing strength of the material are reached simultaneously.

The effect of end distance on the shear strength of the material is also highly dependent on the fibre lay-up of the composite. For most orthotropic composites, the ultimate shear stress decreases with increase in end distance. The absence of 90° (or $\pm 45°$) plies in combination with an excess of 0° plies (where the application of the load is parallel to the 0°) results in failures by shear, in which parallel plugs of material are sheared from the parent material. It is necessary, therefore, that a combination of 0° plies with $\pm 45°$ plies increases the shear performance to give strengths greater than either the 0° or the $\pm 45°$ laminates alone. It will be clear that a reduction in the degree of anisotropy of a laminate in addition to the strengthening of weak planes of failure will lead to a decrease in the magnitude of stress concentrations and an increase in the shear strength of the composite.

Hart-Smith [6] has characterized the strength of single-hole bolted joints

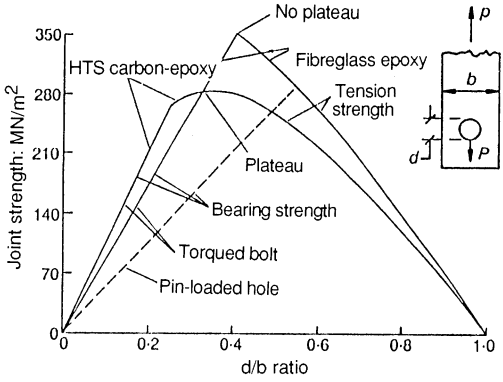

Figure 8.21 Relationship between bearing and tension failures for carbon/epoxy and fibre glass/epoxy laminates as functions of joint geometry (after [29]).

as a function of the joint geometry and has produced a relationship between the joint strength and the ratio of bolt diameter to strip width (d/b); this relationship is shown in Figure 8.21. The values given in this figures are for 6.35 mm diameter bolts in double shear in a quasi-isotropic composite manufactured from high tensile strength carbon fibres and epoxy matrix, but the general form would be relevant for almost any fibrous composite. When the strip width is large, bearing failures are the criterion for failure but as the bolt becomes large, compared with the width of the strip, there is a change in failure mode to that of tension 'through-the-hole' section. Figure 8.21 shows that the peak strength of the joint occurs either at the tension-failure mode or at an abrupt transition between that and the bearing-failure mode. Hart-Smith has shown that for both cases, the failure has a definite value for the ratio of d/b and this is nearer to 1:3 than to the value of 1:4 which is usually associated with bolted joints. He has also stated that bearing failures are more desirable than tensile ones because they are less catastrophic. However, if a bearing failure does occur, it will be associated with a reduced joint strength compared with that for a tensile failure.

In addition, Hart-Smith has shown that glass-fibre epoxy composites have a higher ratio of tensile-to-bearing strength than do the carbon epoxy laminates. Figure 8.21 shows an abrupt change between the two modes where the maximum strength value lies between ratio d/b values of 1:3 and 1:4.

8.10.2 Fibre orientation, resin type and method of manufacture

The type of resin, fibre and its orientation (as discussed above) and stacking sequence have a major influence in determining the strength of bolted joints. The highest bearing strengths are attained for lay-up containing around 50%

of 0° plies and in the presence of ±45° plies, the compressive strength of the constrained 0° plies is improved [34].

8.10.3 Bolt fit

The bearing strength of the composite is highly dependent on the bolt hole dimensions. For maximum strength, the bolt hole in the composite and in the washer should be reamed to size. Normally, however, the holes are fractionally larger than those of the bolt and in this case the bearing strengths are reduced in value, some by as much as 25% of the 'reamed' condition.

8.10.4 Clamping force

Probably the most significant factor that influences the strength of bolted joints compared with pinned joints is the presence of washers. These prevent the composite splitting in its through-the-thickness direction whereas the pinned connections provide no such resistance.

By increasing the bolt tightening torque and hence clamping force, the bearing strength is increased, however, it is possible that an overtightened bolt could damage the composite but with reasonable care the bearing strength of a tightened bolt can increase to four times that which can be taken by a pin. A finger tightened bolt can increase the bearing strength by a factor of two [35, 36].

One of the advantages for composite systems is that orthotropic properties can be tailored for any specific application. This implies a need for bolted joint strength data for a large variety of laminate patterns and the design of composite structures can then be quite a complex and expensive task. The main reason for using orthotropic composites derives mainly from stiffness considerations, and the necessity to develop adequate strength at bolt holes and cut-outs tends to restrict the choice of fibre patterns to those that do not deviate far from a quasi-isotropic pattern. Hart-Smith [29] has suggested that there should not be more than three-eighths or less than one-eighth of the volume of the fibres in any one of the laminate directions (i.e. 0°, +45°, −45° and 90°).

If orthotropic laminates are required to be bolted, it is suggested that modification to the material properties in the location of the fastener should be made; these modifications can be achieved by incorporating extra arrays of fibres to provide near isotropic material properties around the hole. Stress concentrations in carbon fibre/polymer matrix composites can be reduced considerably by incorporating glass 'softening' strips in the vicinity of the hole. In the case of glass fibre/polymer matrix composites, 'softening' can only be achieved by increasing the randomly orientated content of the fibre in order to approach the quasi-isotropic material condition that is required.

References

1. L.J. Hart-Smith, *Developments in Adhesives–2*, ed. A.J. Kinloch, Elsevier Applied Science, London (1981).
2. F.L. Matthews, P.F. Kilty and E.W. Godwin, A review of the strength of joints in fibre-reinforced plastics, Part 2. Adhesively bonded joints, *Composites* **13** (1982) 29.
3. R.D. Adams and W.C. Wake, *Structural Adhesive Joints in Engineering*, Elsevier Applied Science, London (1984) Chs. 1,2.
4. E.W. Godwin, F.L. Matthews and P.F. Kilty, Strength of multi bolt joints in GRP, *Composites* **13** (1982) 268–273.
5. L.J. Hart-Smith, Adhesively bonded joints for fibrous composite structures, McDonnell-Douglas Co., Douglas Paper 7740, Long Beach, CA (1986).
6. L.J. Hart-Smith, Design and analysis of bolted and riveted joints in fibrous composite structures, McDonnell-Douglas Co., Douglas Paper 7739, Long Beach, CA (1986).
7. W.A. Lees, A review—the design and assembly of bonded composites, *Composite Structures*, ed. I.M. Marshall, Elsevier Applied Science, London (1991) Ch. 36.
8. C.J. Poon, Literature review on the design of mechanically fastened composite joints, Structures and Materials Laboratory, Material Aeronautical Establishment, National Research Council, Canada NRCC/NAE Aeronautical NAE-AN-37, NRC No. 254442 (1986).
9. F.L. Matthews, Bonded and bolted joints, *BPF Design Guide*, ed. L. Hollaway, Woodhead Publishing (1993) Ch. 3.
10. L. Hollaway, Adhesive and bolted joints, *Polymers and Polymer Composites in Construction*, ed. L. Hollaway, Thomas Telford, London (1990) Ch. 6.
11. L.J. Hart-Smith, Differences between adhesive behaviour in test coupons and structural joints, Douglas Aircraft Co., McDonnell Douglas Corporation, Paper 7066, presented to ASTM Adhesives Committee D-14 meeting, Phoenix, AZ (1981).
12. C.S. Smith and D. Pattison, Design with fibre reinforced materials, *I. Mech. E. Conf.*, London (1977) paper C230/77.
13. J.L. Lubkin and E. Reissner, Stress distribution and design data for adhesive lap joints between circular tubes, *Trans. ASME* **78** (1956) 1213.
14. L. Hollaway, A. Romhi and M.J. Gunn, Optimisation of adhesive bonded composite tubular section, *Composite Structures* **16** (1990) 125–179.
15. A.K. Green and L.N. Phillips, Crimp-bonded end fittings for use on pultruded composite sections. *Composites* **13** (3) (1982) 219–224.
16. L. Hollaway and S. Baker, The development of nodal joints suitable for double-layer skeletal systems made from fibre matrix composite. In: *Proc. Int. Conf. on Space Structures*, ed. H. Nooshin, Elsevier Applied Science, London (1984) pp. 908–913.
17. O. Volkersen, Die nietkraftoerteilung in ubeansprunchten nietverbindungen mit konstanten loshonquersch nitten. *Luftfahrtforschung* **15** (1938) 41.
18. M. Goland and E. Reissner, Stresses in cemented joints, *J. Applied Mech.* **11** (1944) 17.
19. W.J. Renton and J.R. Vinson, *J. Adhesion* **7** (3) (1975) 175.
20. D.J. Allman, *Quarterly J. Mechanics Appl. Maths* **30** (1977) 415.
21. V. Yuccoglu and D.P. Updike, Bending and shear deformation effects in lap joints, *J. Eng. Mech. Div.* **17** (1981) 55.
22. G.C. Grimes, L.F. Greimann, T. Wah, G.E. Commerford and W.R. Blackstone, The development of non-linear analysis methods for bonded joints in advanced filamentary composites structures, Southwest Research Institute, San Antonio, USA, Contract report No. AFFDL-TR-72-97 (1972).
23. L.J. Hart-Smith, Adhesive-bonded double-lap joints, Douglas Aircraft Company, NASA CR-112235 (1973).
24. O. Volkersen, Recherches sur la théorie des assemblages collés, *Construction Metallique* **4** (1965).
25. R.D. Adams and N.A. Peppiat, Stress analysis of adhesive bonded lap joints, *J. Strain Anal.* **9** (1974) 185.
26. R.D. Adams and N.A. Peppiat, Stress analysis of lap joints in fibre reinforced composite material, *Fibre Reinforced Plastics*, ICI, London (1977) p. 45.
27. M.D. Wright, Stress distribution in carbon fibre reinforced plastics joints, *J. Composites* **II** (1980) 46.

28. M.D. Wright, The stress analysis of a butt strap joint in CFRP, *J. Composites* **9** (1978) 259.
29. L.J. Hart-Smith, Design and empirical analysis of bolted or riveted joints, *Jointing Fibre-Reinforced Plastics*, ed F.L. Matthews, Elsevier Applied Science, London (1987) Ch. 6.
30. L.J. Hart-Smith, Further developments in the design and analysis of adhesive-bonded structural joints, Douglas Aircraft Co., McDonnell Douglas Corporation, Paper 6922, presented to ASTM Conference on Jointing of Composite Materials (STP 749), Minnesota (1980).
31. L.J. Hart-Smith, Effects of flaws and porosity on strength of adhesive-bonded joints. Douglas Aircraft Co., McDonnell Douglas Corporation Report MDC-J4699 (1981); USAF Contract Report AFWAL-TR-82-4172 (1982).
32. L.J. Hart-Smith, Bonded-bolted composite joints, *J. Aircraft* **22** (1985) 993–1000.
33. J.H. Stockdate and F.L. Matthews, The effect of clamping pressure on bolt bearing loads in glass fibre-reinforced plastic, *Composites* **34** (1976).
34. F.L. Matthews, E.W. Godwin and P.F. Kilty, The design of bolted joints in GRP, Technical Note TN82-105, Department of Aeronautics, Imperial College, London, UK (1982).
35. T.A. Collings, On the bearing strength of CFRP laminates, *Composites*, **13** (1982) 241.
36. T.A. Collings, Experimentally determined strength of mechanically fastened joints, *Jointing Fibre-Reinforced Plastics*, ed F.L. Matthews, Elsevier Applied Science, London (1987) Ch. 2.

9 Numerical examples of fibre-matrix composites

9.1 Introduction

This chapter is devoted to the practical solution of problems associated with polymer composite structures and components. The most efficient configuration for a fibre/matrix composite is one that contains a unidirectional fibre array; problems associated with this configuration are solved as well as those containing off-axis unidirectional arrays. If loads are such that unidirectional composites are inadequate then the bidirectional fibre arrangements can be used in practice and solutions for these systems are given.

The solutions to problems in this chapter have been obtained by hand calculator to acquaint the reader with the method applicable to composite materials. However, in a design office, computer programs are available because generally it is not easy to describe mathematically the complex nature of composites and to perform structural analysis of systems manufactured from these anisotrophic (laminated) materials; both the design of the material and the analysis of the structural system must be undertaken simultaneously.

The various computer software packages that are available for laminate analysis tend to be designed to operate on specific computers and to vary in the quality of their computing capability. It is possible to have a mesh generation option as well as a range of coloured, shaped and illustrated options to display the model and applied loads. It is also possible to obtain software that has static, dynamic and thermal capabilities and to be able to analyse hundreds of laminae with many different ply materials in the composite. Some software can evaluate the laminate stiffness and compliance matrices and can calculate the laminate equivalent elastic and physical engineering constants.

To give the reader further experience in design techniques and in long-term performance characteristic evaluations of composite structural systems, it is suggested that further reading [1, 2] may be of benefit. Reference [1] contains case histories of composite structural systems which have been erected over the last two decades.

9.2 Axial tensile forces in composite systems

The following six examples illustrate the methods of analyses for polymer composite systems under an axial tensile load.

Example 9.1

This example utilizes the law of mixtures as given in section 2.4. It is required to obtain the stress at a point of matrix rupture and the elastic modulus of a composite consisting of unidirectional glass fibres in a polyester matrix under a tensile force. The composite has the following geometric and mechanical properties (see Figure 9.1).

Resin ratio by volume	$= 65\%$
Area of composite $= 25 \times 2$	$= 50\,\text{mm}^2$
The ultimate stress in the matrix	$= 62.0\,\text{MN/m}^2$
The modulus of elasticity of the glass fibres	$= 70\,\text{GN/m}^2$
The modular ratio of the composite	$= 20$
Area of glass in composite $= 50 \times 0.35$	$= 17.5\,\text{mm}^2$
Area of matrix $= 50 \times 0.65$	$= 32.5\,\text{mm}^2$

Equation (2.6) states

$$\sigma_c A_c = \sigma_m A_m + \sigma_f A_f$$

$$\sigma_c A_c l_c = \sigma_m A_m l_m + \sigma_f A_f l_f$$

$$50 \times \sigma_c = \sigma_m 32.5 + \sigma_f 17.5$$

where

$$l_c = l_m = l_f \tag{9.1}$$

Equation (2.8) states

$$\varepsilon_c = \varepsilon_f = \varepsilon_m$$

$$\frac{\sigma_c}{E_c} = \frac{\sigma_f}{E_f} = \frac{\sigma_m}{E_m}$$

Therefore

$$\sigma_f = \sigma_m \frac{E_f}{E_m} = \sigma_m 20 \tag{9.2}$$

Substituting eq. (9.2) into eq. (9.1),

$$\sigma_c = \frac{62.0}{50}[32.5 + 17.5 \times 20] = 474.3\,\text{MN/m}^2$$

Figure 9.1

The composite elastic modulus

$$E_c = E_{11} = E_m V_m + E_f V_f$$
$$= \frac{70}{20} \times 0.65 + 70 \times 0.35$$
$$= 26.78\,\text{GPa}$$

From section 2.6 for short fibre composite materials, when the fibres are randomly oriented, the elastic modulus is given by eq. (2.27) where the value of the coefficient β is 0.375.

Therefore assuming the same geometrical and mechanical properties as given at the beginning of the question,

$$E_c = E_{11} = \beta E_f V_f + E_m V_m$$
$$= 0.375 \times 70 \times 0.35 + (70/20)\,0.65$$
$$= 9.19 + 2.28$$
$$= 11.47\,\text{GPa}$$

Example 9.2

Strain gauge readings were taken on a loaded composite system and at a particular location on the composite, the strain measurements were $\varepsilon_{xx} = 3.5 \times 10^{-3}$, $\varepsilon_{yy} = 5.2 \times 10^{-4}$ and $\varepsilon_{xy} = 5.2 \times 10^{-3}$. The manufacturer of the prepreg, which was used in the construction, gave the values of Q_{11}, Q_{22} and Q_{33} as 138 GPa, 13.8 GPa and 6.9 GPa, respectively, and $\nu_{12} = 0.2$. What is the state of stress in the ply axis direction and in the coordinate axis (reference axes) which is 30° to the ply axis?

From eq. (3.7a),

$$\begin{bmatrix} \varepsilon_{11} \\ \varepsilon_{22} \\ \varepsilon_{12}/2 \end{bmatrix} = \begin{bmatrix} m^2 & n^2 & 2mn \\ n^2 & m^2 & -2mn \\ -mn & mn & m^2 - n^2 \end{bmatrix} \begin{bmatrix} \varepsilon_{xx} \\ \varepsilon_{yy} \\ \varepsilon_{xy}/2 \end{bmatrix}$$

where $m = \cos\theta$ and $n = \sin\theta$.

$$\begin{bmatrix} \varepsilon_{11} \\ \varepsilon_{22} \\ \varepsilon_{12}/2 \end{bmatrix} = \begin{bmatrix} 0.75 & 0.25 & 0.866 \\ 0.25 & 0.75 & -0.866 \\ -0.433 & 0.433 & 0.5 \end{bmatrix} \begin{bmatrix} 3.5 \times 10^{-3} \\ 5.2 \times 10^{-4} \\ (5.2/2) \times 10^{-3} \end{bmatrix} = \begin{bmatrix} 0.005 \\ -0.001 \\ 0 \end{bmatrix}$$

Equation (3.3) gives the stress–strain relationship for an orthotropic composite as

$$\begin{bmatrix} \sigma_{11} \\ \sigma_{22} \\ \sigma_{12} \end{bmatrix} = \begin{bmatrix} Q_{11} & Q_{12} & 0 \\ Q_{21} & Q_{22} & 0 \\ 0 & 0 & Q_{33} \end{bmatrix} \begin{bmatrix} \varepsilon_{11} \\ \varepsilon_{22} \\ \varepsilon_{12} \end{bmatrix}$$

where

$$Q_{11} = \frac{E_{11}}{1 - \nu_{12}\nu_{21}} = 138\,\text{GPa}$$

$$Q_{22} = \frac{E_{22}}{1 - \nu_{21}\nu_{12}} = 13.8\,\text{GPa}$$

$$Q_{12} = Q_{21} = \frac{\nu_{21}E_{11}}{1 - \nu_{12}\nu_{21}} = \frac{\nu_{12}E_{22}}{1 - \nu_{12}\nu_{21}}$$

$$\nu_{21} = (E_{22}/E_{11})\nu_{12} = 0.02$$

$$Q_{33} = 6.9\,\text{GPa}$$

$$\begin{bmatrix}\sigma_{11}\\ \sigma_{22}\\ \sigma_{12}\end{bmatrix} = \begin{bmatrix}138 & 2.76 & 0\\ 2.76 & 13.8 & 0\\ 0 & 0 & 6.9\end{bmatrix}\begin{bmatrix}0.005\\ -0.001\\ 0\end{bmatrix} = \begin{bmatrix}687\\ 0\\ 0\end{bmatrix}\text{MPa}$$

Therefore the state of stress in the major fibre direction is 687 MPa. The stresses in the direction 30° to the principal material axis are given by eq. 3.5(b).

$$\begin{bmatrix}\sigma_{xx}\\ \sigma_{yy}\\ \sigma_{xy}\end{bmatrix} = \begin{bmatrix}m^2 & n^2 & -2mn\\ n^2 & m^2 & 2mn\\ mn & -mn & (m^2 - n^2)\end{bmatrix}\begin{bmatrix}\sigma_{11}\\ \sigma_{22}\\ \sigma_{12}\end{bmatrix} = \begin{bmatrix}515\\ 173\\ 297\end{bmatrix}\text{MPa}$$

Therefore the stresses in the off-axes direction are

$$\sigma_{xx} = 515\,\text{MPa}, \qquad \sigma_{yy} = 173\,\text{MPa}, \qquad \sigma_{xy} = 297\,\text{MPa}$$

Example 9.3

Consider a tensile force which is applied at an angle θ to the principal axis of a composite material made of glass fibre/polyester resin (see Figure 9.2).

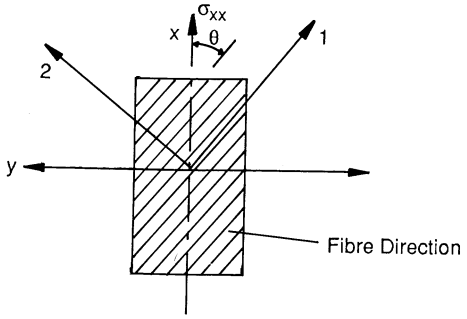

Figure 9.2

The stress σ_{xx} is equal to 3.5 MPa and makes an angle θ of 60° with respect to the principal fibre direction. Investigate the state of stress of the laminate by examining the failure laws, given in section 3.7, when the laminate has the following properties.

$$E_{11} = 30\,\text{GPa}, \qquad E_{22} = 4\,\text{GPa}, \qquad G_{12} = 1.2\,\text{GPa}$$

$$\nu_{12} = 0.28, \qquad \nu_{21} = 0.067$$

$$(\sigma^*_{11})_t = 1200\,\text{MPa}, \qquad (\sigma^*_{22})_t = 45\,\text{MPa}, \qquad (\sigma^*_{12})_t = 35\,\text{MPa}$$

$$(\varepsilon^*_{11})_t = 0.033 = (\varepsilon^*_{11})_c, \qquad (\varepsilon^*_{22})_t = 0.002 = (\varepsilon^*_{22})_c, \qquad (\varepsilon^*_{12})_t = 0.0078 = (\varepsilon^*_{12})_c$$

Maximum stress failure criterion. This theory states that failure will occur if any stress along the principal direction of the laminate exceeds the specified allowable (see section 3.7.1).

It is first necessary to transform the given stress σ_{xx} along the direction of the principal material axis. From eq. (3.33),

$$\begin{aligned} \sigma_{11} &= \sigma_{xx}\cos^2\theta = \sigma_\theta \cos^2\theta = 0.875\,\text{MPa} \\ \sigma_{22} &= \sigma_{xx}\sin^2\theta = \sigma_\theta \sin^2\theta = 2.625\,\text{MPa} \\ \sigma_{12} &= -\sigma_{xx}\sin\theta\cos\theta = 1.515\,\text{MPa} \end{aligned} \tag{9.3}$$

Therefore

$$\begin{aligned} \sigma_{11} &= 0.875 < \sigma^*_{11} \quad (\sigma^*_{11} = 1200\,\text{MPa}) \\ \sigma_{22} &= 2.625 < \sigma^*_{22} \quad (\sigma^*_{22} = 45\,\text{MPa}) \\ \sigma_{12} &= 1.515 < \sigma^*_{12} \quad (\sigma^*_{12} = 35\,\text{MPa}) \end{aligned}$$

Maximum strain failure criterion. This theory states that failure occurs when the strain along the principal material axis exceeds the allowable strain in that direction (see section 3.7.2).

From Hooke's Law for orthotropic materials (from eq. (3.4)),

$$\begin{aligned} \varepsilon_{11} &= \frac{\sigma_{11}}{E_{11}} - \nu_{21}\frac{\sigma_{22}}{E_{22}} \\ &= \frac{\sigma_{11}}{E_{11}} - \nu_{12}\frac{\sigma_{22}}{E_{11}} \left(\frac{\nu_{21}}{E_{22}} = \frac{\nu_{12}}{E_{11}}\right) \\ \varepsilon_{11} &= \frac{1}{E_{11}}[\cos^2\theta - \nu_{12}\sin^2\theta]\sigma_{xx} \end{aligned} \tag{9.4}$$

Similarly,

$$\varepsilon_{22} = \frac{1}{E_{22}}[\sin^2\theta - \nu_{21}\cos^2\theta]\sigma_{xx} \tag{9.5}$$

$$\varepsilon_{12} = \frac{1}{G_{12}}[\sin\theta\cos\theta]\sigma_{xx} \tag{9.6}$$

Therefore from eq. (9.4)

$$\varepsilon_{11} = 0.0000047 < (\varepsilon^*_{11})_t \quad (\varepsilon^*_{11} = 0.033)$$

from eq. (9.5)

$$\varepsilon_{22} = 0.0006 < (\varepsilon^*_{22})_t \quad (\varepsilon^*_{22} = 0.002)$$

from eq. (9.6)

$$\varepsilon_{12} = 0.0013 < (\varepsilon^*_{12})_t \quad (\varepsilon^*_{12} = 0.0078)$$

where $\theta = 60°$ and the material properties have been given at the beginning of the example.

The interaction failure criterion. The third theory is the interaction one (see section 3.7.3) and states that the failure occurs under a combined set of stresses. From the current example the interactive criteria given by eq. (3.46) is used.

Referring to eq. (3.46), the applied stress may be computed.

$$\sigma_{11} = \sigma_{xx}\cos^2\theta, \qquad \sigma_{22} = \sigma_{xx}\sin^2\theta, \qquad \sigma_{12} = \sigma_{xy}\sin\theta\cos\theta$$

Therefore eq. (3.46) may be written as

$$\left(\frac{\cos^2\theta}{\sigma^*_{11}}\right)^2 - \left(\frac{\cos\theta\sin\theta}{\sigma^*_{11}}\right)^2 + \left(\frac{\sin^2\theta}{\sigma^*_{22}}\right)^2 + \left(\frac{\sin\theta\cos\theta}{\sigma^*_{12}}\right)^2 < \frac{1}{\sigma^2_{xx}} \tag{9.7}$$

Therefore using the values given in the example where $\theta = 60°$, the left-hand side of the equation becomes

$$\left(\frac{0.25}{1200}\right)^2 - \left(\frac{0.433}{1200}\right)^2 + \left(\frac{0.75}{45}\right)^2 + \left(\frac{0.433}{35}\right)^2 = 0.0016$$

the right-hand side of eq. (9.7) = 0.0816. Therefore the composite does not fail.

Example 9.4

A compressive force is applied to the composite shown in Figure 9.3 where the line of action of the load is at an angle θ equal to 60° to the direction of the principal axis. The stresses σ_{xx}, σ_{yy} and σ_{xy} are equal to 3.5, 7.0 and 1.5 MPa, respectively.

$$(\sigma^*_{11})_t = 1200\,\text{MPa}, \qquad (\sigma^*_{11})_c = 2450\,\text{MPa}, \qquad \nu_{12} = 0.28$$

$$(\sigma^*_{22})_t = 45\,\text{MPa}, \qquad (\sigma^*_{22})_c = 225\,\text{MPa}, \qquad \nu_{21} = 0.067$$

$$(\sigma^*_{12}) = 35\,\text{MPa}$$

The stresses must be translated from the x,y axes to the principal material

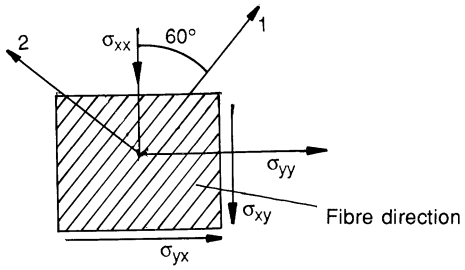

Figure 9.3

directions. Thus using eq. (3.5a),

$$\begin{bmatrix} \sigma_{11} \\ \sigma_{22} \\ \sigma_{12} \end{bmatrix} = [T] \begin{bmatrix} \sigma_{xx} \\ \sigma_{yy} \\ \sigma_{xy} \end{bmatrix}$$

Therefore

$$\begin{bmatrix} \sigma_{11} \\ \sigma_{22} \\ \sigma_{12} \end{bmatrix} = \begin{bmatrix} \frac{1}{4} & \frac{3}{4} & \frac{\sqrt{3}}{2} \\ \frac{3}{4} & \frac{1}{4} & -\frac{\sqrt{3}}{2} \\ -\frac{\sqrt{3}}{4} & \frac{\sqrt{3}}{4} & -\frac{1}{2} \end{bmatrix} \begin{bmatrix} -3.5 \\ +7.0 \\ -1.5 \end{bmatrix} = \begin{bmatrix} 3.08 \\ 0.424 \\ 5.297 \end{bmatrix}$$

Comparing the stresses calculated in the right-hand column with the allowable values, indicates that the lamina is within the safe stress limits, i.e.

$$\sigma_{11} < (\sigma^*_{11})_t, \qquad \sigma_{22} < (\sigma^*_{22})_t, \qquad \sigma_{12} < (\sigma^*_{12})_t$$

Investigating shear stresses. For homogeneous isotropic materials, the direction of the shear stress can be either positive or negative and it is of little consequence in determining the strength of such materials. However, with orthotropic composite materials the signs are of great importance. Consider the following two cases in which the laminates consist of $-45°$ orientated fibres and are loaded with positive and negative shears as shown in Figure 9.4(a) and (b), respectively. It will be seen that the two laminae are loaded differently along the principal material axes direction (the fibre direction). In the case of positive shear, a tensile stress is developed in the transverse direction and compression stresses in the fibre direction; the reverse is true for the negative shear.

The shear strengths of laminae are dependent on the transverse strengths of the composite, and clearly, with the positive shear and negative fibre orientation, there is a lower apparent strength than with the negative shear

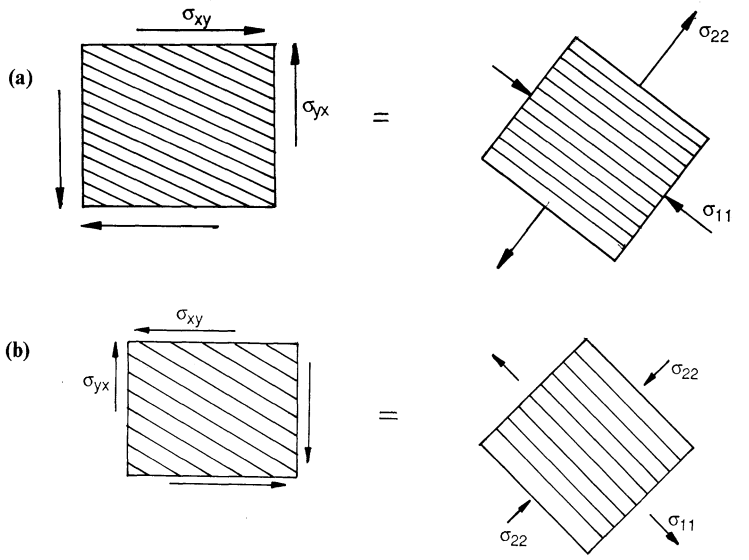

Figure 9.4

and negative fibre orientation. Consequently the off-axes shear of laminae must be carefully studied and the applied direction of the shear stress must be understood.

The maximum strain failure criterion. This cirterion is analogous to the maximum stress failure criterion in that stresses are simply replaced by allowable strain values; the assumption is that the material remains elastic up to failure. Thus

$$\varepsilon_{11} = \frac{\sigma_{11}}{E_{11}} - \nu_{12}\frac{\sigma_{22}}{E_{22}} = \left[\frac{3.08}{30} - 0.067 \times \frac{0.424}{4}\right] \times 10^{-3} = 0.0000956$$

$$\varepsilon_{22} = \frac{\sigma_{22}}{E_{22}} - \nu_{12}\frac{\sigma_{11}}{E_{11}} = \left[\frac{0.424}{4} - 0.293 \times \frac{3.08}{30}\right] \times 10^{-3} = 0.0000759$$

$$\varepsilon_{12} = \frac{\sigma_{12}}{G_{12}} = 0.00441$$

Comparing these values with the ultimate:

$$(\varepsilon^*_{11})_c = 0.033, \qquad (\varepsilon^*_{22})_c = 0.002, \qquad (\varepsilon^*_{12})_c = 0.0078$$

shows that the calculated values are satisfactory.

The interactive failure criterion. The interactive theory is used to investigate whether failure occurs under a combined set of stresses. The interaction

theory (see section 3.7.3) states that

$$\left(\frac{\sigma_{11}}{\sigma_{11}^*}\right)^2 - \left(\frac{\sigma_{11}}{\sigma_{11}^*}\right)\left(\frac{\sigma_{22}}{\sigma_{11}^*}\right) + \left(\frac{\sigma_{22}}{\sigma_{22}^*}\right)^2 + \left(\frac{\sigma_{12}}{\sigma_{12}^*}\right)^2 < 1$$

The left-hand side of the above equation is

$$\left(\frac{3.08}{1200}\right)^2 - \left(\frac{3.08}{1200}\right)\left(\frac{0.424}{1200}\right) + \left(\frac{0.422}{45}\right) + \left(\frac{5.297}{35}\right)^2$$

which is less than unity and therefore will lie inside the failure envelope and the lamina will not fail.

Example 9.5

A polymer composite consists of glass fibre woven rovings in a polyester resin. The ultimate tensile strength in the principal axes 1 and 2 of the composite material (the fibre direction) and the ultimate tensile strength at 45° to these axes are

$$\sigma_{11}^* = 288\,\text{MPa}, \qquad \sigma_{22}^* = 260\,\text{MPa}, \qquad \sigma_{45}^* = 81.4\,\text{MPa}$$

It is required to determine the ultimate tensile strength of the composite at 30° to direction 1 (see Figure 9.5).

From the interactive theory, the failure of the composite occurs under a combined set of stresses and eq. (3.48) may be written as

$$\frac{1}{(\sigma_{xx}^*)^2} = \frac{\cos^4\theta}{(\sigma_{11}^*)^2} + \frac{\sin^4\theta}{(\sigma_{22}^*)^2} + \frac{\sin^2\theta\cos^2\theta}{(\sigma_{12}^*)^2}$$

where θ is the off-axis angle

The relationship for the ultimate tensile stresses in the above composite principal axis (1, 2) and the reference axes (x, y) at an angle θ to the principal

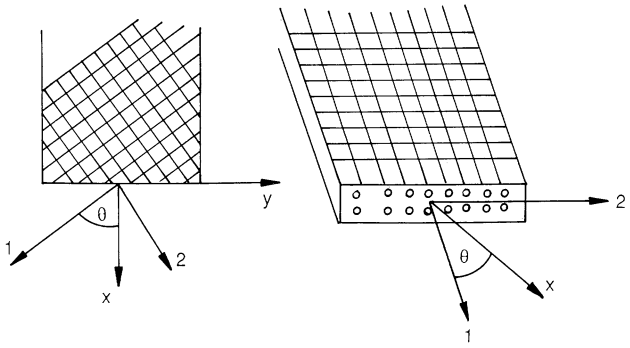

Figure 9.5

axis are given by

$$\frac{1}{(\sigma^*_{xx})^2} = \frac{\cos^4\theta}{(\sigma^*_{11})^2} + \frac{\sin^4\theta}{(\sigma^*_{22})^2} + \frac{\sin^2\theta\cos^2\theta}{(\sigma^*_{12})^2} \tag{9.8}$$

where σ^*_{xx}, σ^*_{11} and σ^*_{22} are the ultimate strength values 81.4 MPa, 288 MPa and 260 MPa, respectively. $\theta = 45°$, therefore $\sigma^*_{12} = 41.64$ MPa.

Using eq. (9.8) again with $\theta = 30°$, $\sigma^*_{xx} = 92.91$ MPa (the ultimate tensile strength of the composite with an off-axis angle of 30°).

Example 9.6

A composite system is manufactured from a composite material of chopped strand mat glass fibre reinforcement and polyester resin of 10 mm thickness and this is sandwiched between laminates consisting of woven rovings of glass fibre in a polyester resin matrix; these latter composites have thicknesses of 1.5 mm. It is required to find the ultimate tensile load/metre width that the composite system can carry when the line of action of the applied tensile load is 15° off-axes (see Figure 9.6 and Table 9.1).

The chopped strand mat glass fibre composite is assumed to be isotropic in behaviour, but the woven roving composite has orthotropic material properties and therefore the values of the ultimate stress (σ^*_{xx}) and modulus of elasticity at an off-axes angle of 15° must be computed.

From the rearrangement of eq. (3.48) and where $\theta = 45°$,

$$\left(\frac{1}{\sigma^*_{12}}\right)^2 = \frac{1}{\sin^2\theta\cos^2\theta}\left[\frac{1}{(\sigma^*_{xx})^2} - \frac{\cos^4\theta}{(\sigma^*_{11})^2} - \frac{\sin^4\theta}{(\sigma^*_{22})^2}\right]$$

$$\sigma^*_{12} = 31.4 \text{ MPa}$$

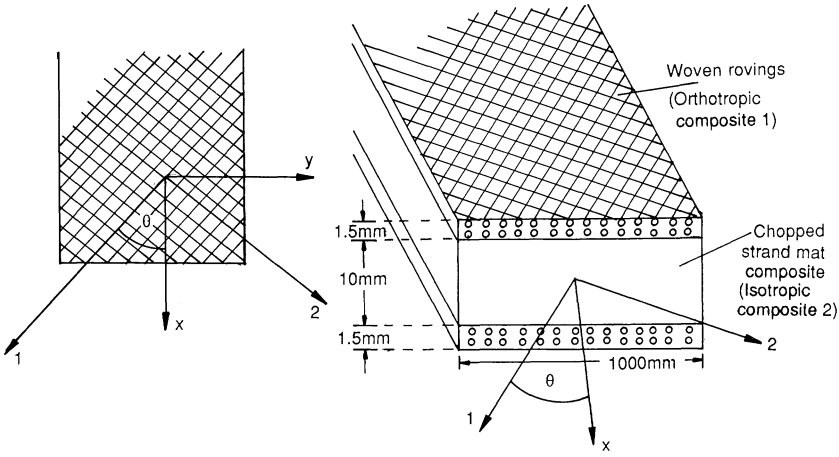

Figure 9.6

Table 9.1

	Chopped strand mat	Woven rovings
Ultimate tensile strength values (MPa)		
σ_{11}^*	65.0	123.0
σ_{22}^*	65.0	95.0
$\sigma_{xx} = \sigma_{45}^*$	65.0	58.0
Modulus of elasticity (GPa)		
E_{11}	7.0	13.45
E_{22}	7.0	12.41
G_{12}	–	3.59
ν_{12}	–	0.20

Again from eq. (3.48) and where $\theta = 15°$,

$$\left(\frac{1}{\sigma_{15}^*}\right)^2 = \frac{\cos^4\theta}{(\sigma_{11}^*)^2} + \frac{\sin^4\theta}{(\sigma_{22}^*)^2} + \frac{\sin^2\theta\cos^2\theta}{(\sigma_{12}^*)^2}$$

$$\sigma_{15}^* = 90.77\,\text{MPa}$$

From eq. (3.11), to enable the engineering constants to be determined,

$$\frac{1}{E_{xx}} = \frac{\cos^4\theta}{E_{11}} + \frac{\sin^4\theta}{E_{22}} + \left[\frac{1}{G_{12}} - \frac{2\nu_{12}}{E_{11}}\right]\cos^2\theta\sin^2\theta$$

$E_{15} = 12.40$ GPa, where $\theta = 15°$.

At any section within the composite system, the strains in the woven roving composite must be equal to the strains in the chopped strand mat composite. If this condition does not hold there can be slippage between the individual composites or slippage between fibre and matrix in either of the composites.

In the off-axes direction of 15° to the principal material direction, the strain relationship is

$$(\varepsilon_{15})_1 = (\varepsilon_{15})_2$$

where the subscripts 1 and 2 refer to composites 1 and 2,

$$\frac{(\sigma_{15}^*)_1}{(E_{15})_1} = \frac{(\sigma_{15}^*)_2}{(E_{15})_2}$$

Therefore

$$(\sigma_{15}^*)_1 = (\sigma_{15}^*)_2 \times \frac{(E_{15})_1}{(E_{15})_2}$$

or

$$(\sigma_{15}^*)_2 = (\sigma_{15}^*)_1 \times \frac{(E_{15})_2}{(E_{15})_1}$$

By computing the above two stress values, it will be noted that the ultimate stress in the woven roving composite (composite 2) is the critical one. Consequently, at failure of this composite ($\sigma^*_{15} = 90.77$ MPa), the stress in the chopped strand mat glass fibre composite is 51.24 MPa.

Thus the total load applied to the composite is

$$A_1(\sigma)_1 + A_2(\sigma^*_{15})_2 = (10 \times 51.24 + 3 \times 90.77)10^{-3}\ \text{MN/m width}$$
$$= 784.71\ \text{MN/m width}$$

Composites are laminated to a required thickness firstly to sustain high planar loads in various directions and secondly to enable lateral loading to be taken by the composite in bending.

In the case of single lamina, only planar effects are considered as the thickness is too small for the plate to take bending. As the thickness is increased by applying more laminae whose properties in any given direction are different, the material across the thickness may be non-uniform. This non-uniformity of the cross-sectional characteristics may introduce interaction between the planar and flexural action from which bending can occur. The following examples develop the procedures for the design of polymer composite plates.

Example 9.7

Unidirectional fibre array Consider a polymer composite consisting of a number of laminae in which all the plies have parallel fibres and the material principal directions (i.e. the fibre axes 1,2) are the same as the plate axes (i.e. the coordinate axes x, y and $\theta = 0$). The design procedure is as follows (see Figure 9.7).

From eq. (3.63),

$$A_{11} = E_{11}\text{h}/(1 - \nu_{12}\nu_{21}), \qquad A_{22} = E_{22}\text{h}/(1 - \nu_{12}\nu_{21})$$
$$A_{12} = \nu_{12}E_{22}\text{h}/(1 - \nu_{12}\nu_{21}), \qquad A_{33} = G_{12}\text{h}$$

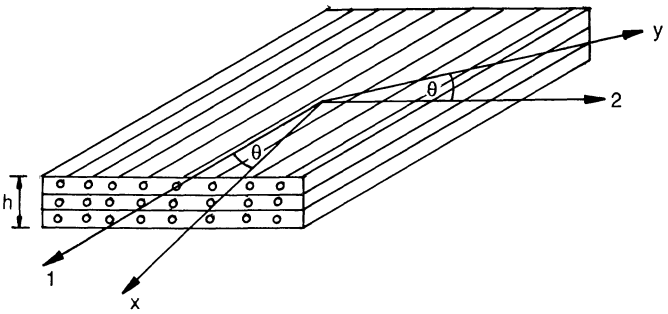

Figure 9.7

$$D_{11} = E_{11}h^3/12(1 - v_{12}v_{21}), \qquad D_{22} = E_{22}h^3/12(1 - v_{12}v_{21})$$
$$D_{12} = v_{12}E_{22}h^3/12(1 - v_{12}v_{21}), \qquad D_{33} = G_{12}h^3/12$$

The laminate failure loads are

$$N^*_{xx} = h\sigma^*_{11}, \qquad N^*_{yy} = h\sigma^*_{22}, \qquad N^*_{xy} = h\sigma^*_{12}$$

The bending moments at failure are

$$M^*_{xx} = h^2\sigma^*_{11}/6, \qquad M^*_{yy} = h^2\sigma^*_{22}/6, \qquad M^*_{xy} = h^2\sigma^*_{12}/6$$

(a) If the orthotropic material properties are required in the plate coordinate axes (x, y) at an angle θ to the material principal axes $(1, 2)$ then eq. (3.5b) can be used to transform stresses from axes $(1, 2)$ to the axes (x, y) coordinate system resulting in eqs. (3.58) and (3.59).

(b) If the polymer composite is fabricated from a number of laminae in which the reinforcement is of various types (i.e. a mixture of randomly orientated, bidirectional and unidirectional fibres), the composite stiffness properties $[A]$ and $[D]$ and the failure loads in terms of laminate structure, ply orientation and ply material properties are required.

Cross-ply laminate

Consider a cross-ply composite in which alternate unidirectional plies are orientated at 0° and 90° to the plate element. If the cross-ply is symmetric about the mid-plane, then it will possess orthotropic properties and the in-plane stiffness properties are as follows (see Figure 9.8).

From eq. (3.63),

$$A_{11} = h/(1 - v_{12}v_{21})[V_fE_{11} + (1 - V_f)E_{22}]$$
$$A_{22} = h/(1 - v_{12}v_{21})[(1 - V_f)E_{11} + E_{22}V_f]$$

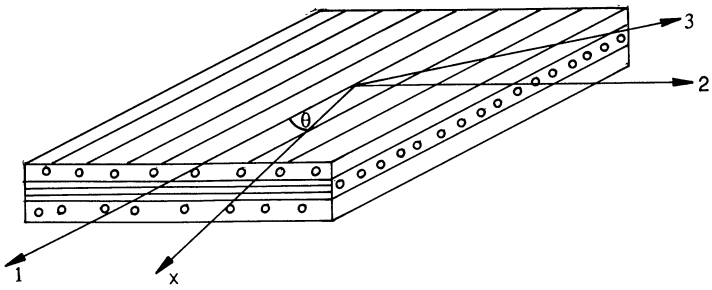

Figure 9.8

Angle-ply laminates

Angle-ply laminates which are symmetric about their mid-plane and also balanced by having an equal number of $+\theta$ and $-\theta$ plies are orthotropic materials (Figure 9.9). In the case where they consist of a large number of thin plies, the material is specially orthotropic and their stiffness properties are homogeneous; the value of the components in the matrices $[A]$ and $[D]$ in eq. (3.63) are

$$(A_{11}, A_{12}, A_{22}, A_{33}) = h(\bar{Q}_{11}, \bar{Q}_{12}, \bar{Q}_{22}, \bar{Q}_{33})$$
$$(D_{11}, D_{12}, D_{22}, D_{33}) = (h^3/12)(\bar{Q}_{11}, \bar{Q}_{12}, \bar{Q}_{22}, \bar{Q}_{33})$$

where $\bar{Q}_{11}, \bar{Q}_{12}, \bar{Q}_{22}, \bar{Q}_{33}$ are given in eq. (3.8).

It should be noted that if the angle-ply laminates have a small number of plies, they are not specially orthotropic since they may have bending/twisting coupling terms present and anti-symmetric angle-ply laminates may have bending/extension coupling terms.

The failure mode of an angle-ply composite is complex and failure does depend on ply angle. For a laminate which is loaded uniaxially in the x direction, the initial damage is frequently found to be a shear failure in the plies particularly when θ is less than 45°. The shear stress mode failure is given by eq. (3.34) (i.e. $\sigma_\theta^* = \sigma_{11} \sin\theta\cos\theta$) where σ_{12}^* is the unidirectional ply ultimate shear strength and therefore the in-plane load N_{xx}^* and the bending moment M_{xx}^* are

$$N_{xx}^* = h\sigma_{12}^*/\sin\theta\cos\theta$$
$$M_{xx}^* = (h^2/6)\sigma_{12}^*/\sin\theta\cos\theta$$

To undertake composite analyses and design by hand computation is complicated and time consuming. Consequently, in order to simplify laminate design several micro-computer programs based on laminated plate theory are now

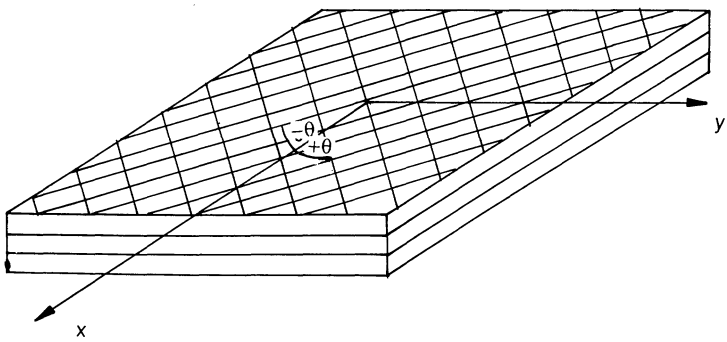

Figure 9.9

commercially available and are widely used. These software packages differ in operational details with MIC-MAC [3] using a spreadsheet and CoALA [4] and ESDU [5] programs using the conventional input/output format. These programs are available on floppy disks suitable for running on micro-computers such as the Macintosh, IBM PC and compatibles.

9.3 Buckling of members under axial compression forces

There are various types of buckling. The Euler buckling of a column is historically the earliest and can occur when a slender column is loaded in compression. The column is unable to carry any load greater than the buckling one. Plates and shells also buckle under in-plane loading and also develop 'local' buckling in the form of waves or ripples along the plate. This form of buckling, however, does not necessarily mean collapse of the structure as it can usually withstand loads beyond that required to initiate buckling. The post-buckling behaviour of a plate must be ascertained if loads beyond the critical are anticipated.

If a load P is applied along the axis of a column, which is initially perfectly straight, it will remain straight until a critical value P_E of the load is reached; this is the Euler critical load. At this point the column becomes unstable and buckles.

If the compressive stress in every lamina of a viscoelastic composite is less than the proportional limit of the material, the critical load formula is

$$P_E = \frac{\pi^2 D}{(kL)^2} \tag{9.9}$$

where D is the flexural rigidity of the composite, L is the length of the member and k is the column's equivalent length factor.

If the column is under the action of a critical load and either

(a) the proportional limit of the material is exceeded and therefore the stress–strain relationship is non-linear; or
(b) the material, although elastic, does not follow Hooke's law but has a compressive stress–strain relationship as shown in Figure 9.10. Then as the column buckles, bending will occur about the centroidal axis of the cross-section and there are corresponding increases and decreases in compressive strains towards the concave and convex sides, respectively, of the buckled column. Consequently, the instantaneous value of the modulus corresponding to the increase in the applied strain on the compressive side of the strut (the concave side) is the tangent value E_t; this quantity is a function of the applied stress. The modulus of elasticity on the opposite side of the composite (the convex side), representing a decrease in strain, is defined by the initial modulus of elasticity value E_I.

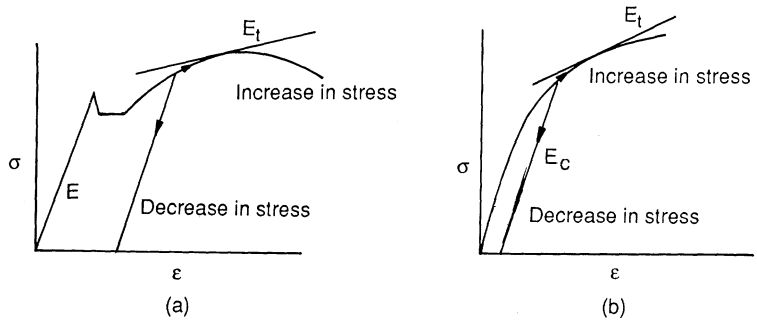

Figure 9.10 Stress–strain relationships for ductile and viscoelastic materials: (a) ductile material; (b) viscoelastic material. E is the modulus of elasticity ($=\sigma/\varepsilon$), E_t is the tangent modulus (non-linear) ($=d\sigma/d\varepsilon$) and E_I is the initial tangent modulus.

The conditions are analogous to a material having two different moduli, one for tension and the other for compression. Therefore, at the point of buckling, the equivalent modulus will be a function of both E_I and E_t and is usually referred to as the reduced modulus E_r; it will also be dependent on the position of the lamina in the composite. The value of the reduced modulus must be formulated for each geometrical section. Timoshenko [6] has shown that for a rectangular section,

$$E_r = \frac{4E_I E_t}{(\sqrt{E_I} + \sqrt{E_t})^2} \tag{9.10}$$

Thus a theory is available that meets the equilibrium condition but it is deficient because a perfectly straight column can not be expected to remain straight above the tangent modulus load (P_t). Bifurcation can occur at a load lower than that given by substituting ($D_r = IE_r$) into eq. (9.9) [i.e. $P_r = \pi^2 D_r/(kL)^2$]; buckling is governed by the incremental flexural rigidity of the member. Therefore the load at which buckling becomes possible is the tangent modulus load P_t and is given by

$$P_t = \frac{\pi^2 D_t}{(kL)^2} \tag{9.11}$$

where $D_t = E_t I$. The true failure load is difficult to obtain theoretically, but it is known to be between the tangent modulus load P_t and the reduced modulus load P_r.

Glass reinforced polymer composites are assumed to be viscoelastic non-linear materials and therefore will approximately follow the above argument.

The controlling parameter in the above equations is the flexural stiffness; the effect of shearing forces on the value of the critical load has been ignored. With materials in which the resistance to shear effects is low, modification to the Euler equation must be made.

From Timoshenko and Gere [7], the buckling load for a pin ended column

$$P_s = \frac{P_E}{1 + (nP_E/AG)} \tag{9.12}$$

where P_E is the Euler critical load given by eq. (9.9), n is a numerical factor depending on the shape of the cross-section ($= 1.11$ for a circular section) and G is the shear modulus. From eq. (9.12), it may be seen that by reducing the value of shear modulus, the Euler critical load is reduced.

Example 9.8

A composite material strut of width 150 mm and of length 600 mm is shown in Figure 9.11 and is composed of:

(a) a composite of thickness 3 mm consisting of an orthotropic fibre-matrix material, with the major fibre axes parallel to the line of action of the load;
(b) a composite of thickness 9 mm consisting of randomly orientated fibre reinforcement in a polymer matrix;

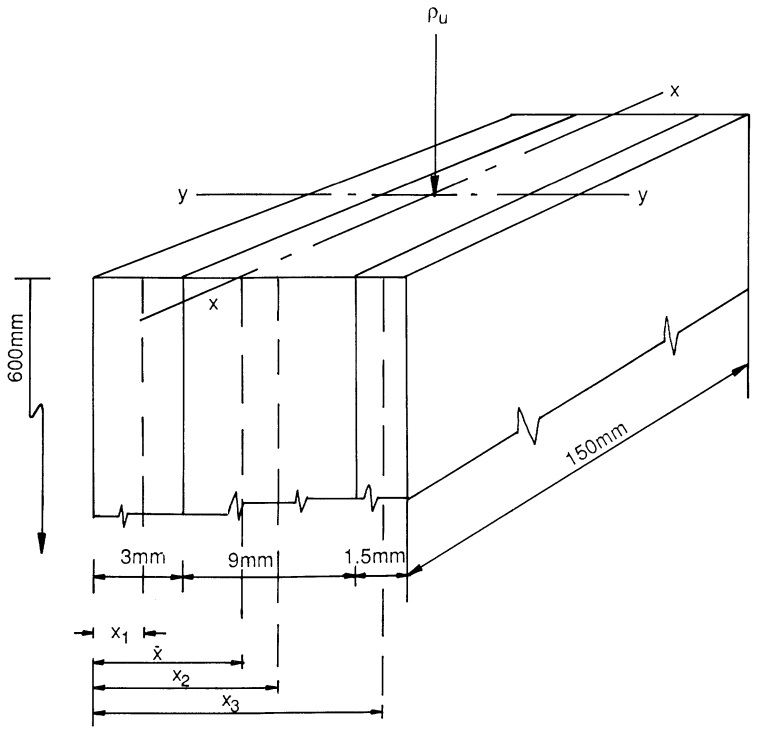

Figure 9.11 Composite material strut. $x_1 = 1.5$ mm, $x_2 = 7.5$ mm and $x_3 = 12.75$ mm.

(c) a composite of thickness 1.5 mm consisting of an orthotropic fibre-matrix material, with the fibre axis parallel to the line of action of the load.

It is required to determine the critical compressive load parallel to their warp directions for pin ended conditions. The value of E_r for the orthotropic composite (material one) in the major fibre direction (direction 1) is equal to 16.8 GPa. The value of E_r for the orthotropic composite (material three) in the major fibre direction (direction 1) is equal to 17.0 GPa.

In solving this problem:

(a) it is assumed that the reduced modulus load is the criterion for failure.
(b) it is necessary to determine the least radius of gyration and hence slenderness ratio and then to compute the critical reduced modulus load. Because there are no general design tables for composite materials, this example will be solved numerically.

The area of composite material 1 is 450 mm^2, area of composite material 2 is 1350 mm^2 and area of composite material 3 is 225 mm^2. The distance of the centroid of the whole section from the free edge of the composite material 1 is

$$\bar{x} = \frac{\Sigma A_i E_i x_i}{\Sigma A_i E_i} \quad \text{(i.e. considering the area stiffness moments)}$$

$$= 6.279 \text{ mm}$$

The composite modulus of elasticity E_c (i.e. this is an average composite material stiffness) is given by

$$E_c = \frac{1}{\Sigma A_i}[\Sigma E_i A_i] = 10.22 \text{ GPa}$$

The stiffness of the overall composite material is

$$E_c I_{xx} = \Sigma E_i \{I_i + A_i x_i^2\}$$

where $A_i x_i^2$ is the parallel axes theorem, x_i is the distance from the centroidal axes of composite i to the x–x axis of the composite structure.

$$I_{xx} = 4159979.7/10.22 = 40702.5 \text{ mm}^4$$

$$\text{Least radius of gyration } r_{yy} = \left(\frac{40702.5}{2025.0}\right)^{1/2} = 4.483 \text{ mm}$$

$$\text{Slenderness ratio} = \frac{l}{r_{yy}} = \frac{600}{4.483} = 133.8$$

$$\text{The critical reduced modulus load} = \{\pi^2 E_r A\}/(I/r_{yy})^2$$

$$= \{\pi^2 \times 10.22 \times 2025.0\}/133.8^2$$

$$= 11.40 \times 10^3 \text{ N}$$

9.4 Bending moments on a composite beam example

To obtain an approximate solution to a polymer composite beam under the action of a bending moment, smeared values of the composite material properties are sometimes taken and then the material is assumed to be isotropic; the following problem is given as an illustration.

Example 9.9

Determine the ultimate load carrying capacity per 10 mm width of a simply supported beam when under a uniformly distributed load. The beam is manufactured using a cloth, woven rovings and randomly orientated mat reinforcement. Figure 9.12 shows the arrangement of the beam. The span of the beam is 300 mm. The composite stiffness and strength values are given in Table 9.2.

As the mechanical properties of the three composite materials are different the centroid of the system must be determined and hence the position of the neutral axes. The bending stresses in any selected composite is given by the equation

$$\sigma = \frac{ME_i x_i}{D}$$

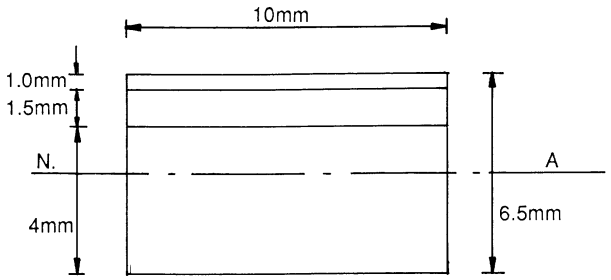

Figure 9.12

Table 9.2 Strength and stiffness values of composites

Reinforcement	Cloth (Cl) fibres (thickness 1.0 mm)	Woven rovings (WR) fibres (thickness 4 mm)	Randomly orientated (RO) fibres (thickness 1.5 mm)
Modulus of elasticity in bending (GPa)	11.0	10.6	7.0
Ultimate strength in bending (MPa)	216.0	195.0	140.0
Ultimate interlaminar shear stress (MPa)	19.0	20.0	22.0

where E_i is the modulus of elasticity of the composite in which the stress is required, x_i is the distance from the NA to the section under consideration and D is the stiffness of the beam. In addition to determining the load carrying capacity of the beam in bending, the interface shear stress between the different composite materials must be determined.

The shear stress at the section under consideration is given by

$$\sigma_{12} = \frac{Q\Sigma E_i A_i x_i}{Db}$$

where $\Sigma E_i A_i x_i$ is the area stiffness moment of all laminae above the section being considered. The distance of the NA from the bottom free edge of the beam is obtained by calculating the area stiffness moments of the three separate composites from this edge and dividing these by the area stiffnesses of the three composites.

$$\bar{x} = (\Sigma A_i E_i x_i)/(\Sigma A_i E_i) = 3.141\,\text{mm}$$

The stiffness of the composite beam is determined by the summation of the product of the modulus of elasticity and the second moment of area of the separate composites. The latter quantity for each composite is obtained by calculating the second moment of area about its own centroidal axis, and using the parallel axis theorem, determining the second moment of area about the composite beam's neutral axis.

$$D_c = [E_c(I_{xx})_c] = \Sigma E_i(I_i + A_i x_i^2) = 2317.05\,\text{GPa mm}^4$$

where the suffices refer to the individual laminae.

The bending stress in any laminate is given by:

$$\sigma = \frac{ME_i x_i}{D_c}$$

where x_i is the distance of the section being analysed from the NA; this must lie in the composite of modulus of elasticity E_i.

The section modulus for the fibre composites are

$$Z_{WR} = \frac{D_c}{E_i x_i} = \frac{2317.05}{10.6 \times 3.14} = 69.61\,\text{mm}^3$$

$$Z_{RO} = \frac{D_c}{E_i x_i} = \frac{2317.05}{7.0 \times 2.36} = 140.26\,\text{mm}^3$$

$$Z_{Cl} = \frac{D_c}{E_i x_i} = \frac{2317.05}{11.0 \times 3.36} = 62.69\,\text{mm}^3$$

The ultimate moments at which the stresses in each of the three composites will reach their ultimate value are

$$M_{CI} = \sigma^*_{CI} Z_{CI} = 13541.04 \text{ N mm}$$

$$M_{WR} = \sigma^*_{WR} Z_{WR} = 13573.95 \text{ N mm}$$

$$M_{RO} = \sigma^*_{RO} Z_{RO} = 19636.40 \text{ N mm}$$

The ultimate moment of resistance for the simply supported composite material beam is 13541.04 N mm and therefore the maximum uniformly distributed load for 10 mm width

$$w = \frac{M \times 8}{L^2} = \frac{13541.04 \times 8}{300^2} = 1.204 \text{ N/mm}$$

The vertical shear force that the composite is able to support is given by

$$Q = \frac{\sigma_{12} D_c b}{\Sigma E_i A_i x_i}$$

It is necessary to consider the shear force at the neutral axis and at the interface planes between the woven roving and the randomly oriented laminate and then to calculate the uniformly distributed load on the minimum value.

(a) The vertical shear strength at the neutral axis within the woven roving composite is

$$Q = \frac{20.0 \times 2317.05 \times 10}{10 \times 3.141 \times 1.571 \times 10.6} = 883.71 \text{ N}$$

(b) Consider the shear plane between the woven roving and randomly oriented composites surface. At the randomly orientated composite surface the shear force is

$$Q = \frac{22.0 \times 2317.05 \times 10}{319.34} = 1054.32 \text{ N}$$

(c) Consider the shear plane between the randomly orientated and cloth composites. At the randomly orientated composites surface the shear force is

$$Q = 1620.63 \text{ N}$$

At the cloth composite surface the shear force is

$$Q = 1399.63 \text{ N}$$

Therefore the minimum ultimate shear strength (condition 'a') = 883.71 N and the ultimate distributed load/10 mm width on beam

$$w = \frac{2 \times Q}{L} = \frac{2 \times 883.71}{300} = 5.89 \text{ N/mm}$$

The ultimate strength in bending controls the ultimate load bearing capacity of the composite material, therefore, $w = 1.204\,\text{N/mm}$.

9.5 Sandwich beam construction

The following three examples deal with the design approach for sandwich beam construction. They illustrate:

(a) a thin face sandwich construction;
(b) a thick face sandwich construction;
(c) a sandwich construction in which the bending stiffness of the face is high.

The behaviour of a loaded sandwich beam depends on two non-dimensional parameters D_f/D and D/L^2D_Q and if these are significant, eq. (7.15) must be used in preference to eq. (7.12).

The following three examples illustrate the method of solution for problems related to beams which are simply supported and carry point loads at the centre. The first problem (Example 9.10) concerns a thin face sandwich beam and it will be noted that the total deflection is given by the sum of the primary and secondary deformations without applying coefficients to the secondary deformations (i.e. eq. (7.12) is used); this is due mainly to the span being relatively large for the size of beam (the value of $D/L^2D_Q = 0.0077$ and is small). The majority of the sandwich beams with GRP faces and foamed polymer core come under this category.

The second problem (Example 9.11) relates to a thick face sandwich beam made from GRP faces and a foam core, and although there is significant stiffness in bending about the faces (the value of $D_f/D = 0.0357$), the value D/L^2D_Q is still small because the overall stiffness of the beam is low in value and the span is relatively large for the beam; the total deflection is given by eq. (7.12).

The third example (Example 9.12) has stiffer faces than the two previous ones; it has a smaller span and therefore the value of $D/L^2\,D_Q$ is comparatively large; consequently the total deflection of the beam is given by eq. (7.15).

Example 9.10

Figure 9.13 shows the cross-section of a sandwich beam. Both faces are a composite of chopped strand glass fibre mat reinforcement and polyester resin (42% glass content by weight) and the core material is a polyurethane foam. The beam is simply supported with a span of 3600 mm and an overhang of 200 mm. The central point load has a value of 2.25 kN. The maximum central deflection must not exceed 25 mm. The material properties are as follows:

$$E_f = 10.00\,\text{GN/m}^2, \qquad \nu_f = 0.2, \qquad G_c = 20\,\text{MN/m}^2$$

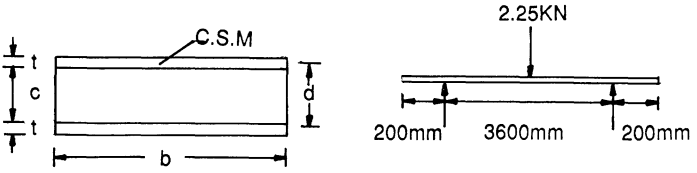

Figure 9.13

The width of the beam and the thickness of the faces are assumed to be 640 mm and 6 mm, respectively. It is required to design the beam.

It will be assumed that the construction is a thin face sandwich beam, and at the end of the example this assumption will be justified.

In a sandwich beam the deflection is usually the criteria for design and as a first approximation, the deflection due to bending moment is

$$w_1 = \frac{WL^3}{48EI}$$

$$EI = \frac{WL^3}{48w_1} = \frac{2.25 \times 3600^3}{48 \times 25 \times 10^6} = 87.48\,\text{kN m}^2$$

For a thin face sandwich beam

$$D = E_f \frac{bd^2t}{2}$$

Therefore

$$d = \sqrt{\frac{87.48 \times 2 \times 10^6}{10.42 \times 640 \times 6}} = 66.126\,\text{mm}$$

As deflection due to shear has also to be considered, assume $d = 70\,\text{mm}$. It is now necessary to determine the properties of the section:

$$I_f = \frac{bt^3}{6} = \frac{640 \times 6^3}{6} = 23040.0\,\text{mm}^4$$

$$\frac{bd^2}{c} = \frac{640 \times 70^2}{64} = 49000\,\text{mm}^2$$

$$I_{\text{total}} = \frac{btd^2}{2} = \frac{640 \times 6 \times 70^2}{2} = 9\,408\,000\,\text{mm}^4$$

$$\frac{E_f}{1-v^2} = \frac{10.00}{(1-(0.2)^2)} = 10.42\,\text{GN/m}^2$$

$$D = I_{\text{total}} \times \frac{E_f}{1-v^2} = \frac{9\,408\,000 \times 10.42 \times 10^3}{10^6} = 98\,031.35\,\text{MN mm}^2$$

$$D_Q = G \times \frac{bd^2}{c} = \frac{20 \times 49000}{10^6} = 0.98\ \text{MN}$$

$$D_f = E_f I_f = \frac{10.42 \times 10^3}{10^6} \times 23040.0 = 240.0768\ \text{MN mm}^2$$

$$\frac{D_f}{D} = \frac{240.08}{98\,031.35} = 0.00245$$

$$\left(1 - \frac{D_f}{D}\right) = 0.99755$$

$$\left(1 - \frac{D_f}{D}\right)^2 = 0.9951$$

As D_f/D is small compared with unity and D/L^2D_Q is very small,

$$\frac{D}{L^2 D_Q} = \frac{98031.35}{3600^2 \times 0.98} = 0.0077$$

S_1 in eq. (7.15) is close to unity and the standard formula for deflection (eq. (7.12)) is used for a thin face sandwich beam.

The total deflection = the primary deformation + the secondary deformation, i.e.

$$w = \frac{WL^3}{48EI} + \frac{WL}{4AG}$$

$$= \left(\frac{2.25 \times 3600^3}{48 \times 98031.35 \times 10^3}\right) + \left(\frac{2.25 \times 3600 \times 10^6}{4 \times 640 \times 64 \times 20 \times 10^3}\right)$$

$$= 22.309 + 2.472 = 24.781\ \text{mm}$$

The bending stress for a thin face sandwich beam is

$$\sigma = \frac{M}{btd} = \frac{2.25 \times 3600}{4 \times 640 \times 6 \times 70 \times 10^{-6}} = 7533.48\ \text{kN/m}^2$$

The shear stress in the core material is

$$\tau = \frac{Q}{bd} = \frac{2.25 \times 16^6}{2 \times 640 \times 70.0} = 27.47\ \text{kN/m}^2$$

It is necessary to justify the use of the simplified moment stiffness and shear stress formula. The moment stiffness $D = E_f\ bd^2t/2$ if the conditions:

(a) $100 > d/t > 5.77$

(b) $\frac{E_f}{E_c}\frac{t}{c}\left(\frac{d}{c}\right)^2 > \frac{100}{6}$

both hold. The shear stress in the core material $= Q/bd$ for the conditions

(a) $\dfrac{E_f}{E_c}\dfrac{t}{c}\dfrac{d}{c} > \dfrac{100}{4}$

(b) the moment stiffness above may be used

In this example all conditions are satisfied.

Example 9.11

A sandwich beam of similar manufacture to that in Example 9.10 and with dimensions shown in Figure 9.14 (where $d/t < 5.77$) is simply supported over a span of 3600 mm. It is to support a central point load of 0.7 kN. The overhang is 200 mm. The maximum central deflection must not exceed 25 mm. The material properties are as follows:

$$E_f = 10.00\,\text{GN/m}^2, \qquad \nu_f = 0.2, \qquad G_c = 20\,\text{MN/m}^2$$

It is required to design the beam.

The solution of this problem is similar to that of Example 9.10 and only the main results are given.

The construction is a thick face sandwich beam. The first approximation, to enable the sizes of the beam to be estimated, is to ignore deflection due to shear

$$w_1 = \frac{WL^3}{48EI}$$

Therefore

$$D = \frac{0.7 \times 3600^3}{48 \times 25 \times 10^6} = 27.216\,\text{kNm}^2$$

$$D = E_f I_{\text{total}}$$

$$I_{\text{total}} = \frac{D}{E_f}$$

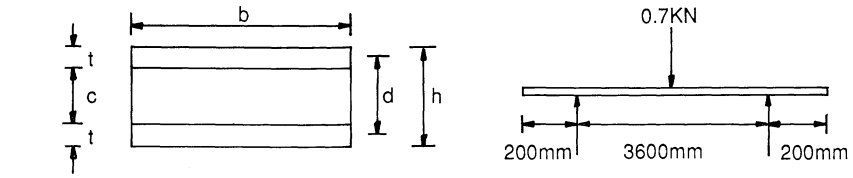

Assume t = 10mm
b = 640mm

Figure 9.14

$$\frac{bt^3}{6}+\frac{btd^2}{2}=\frac{D}{E_f}$$

$$d=\sqrt{\left[\frac{27.216\times10^6}{10.42}-\frac{640\times10^3}{6}\right]\frac{2}{640\times10}}=27.980\,\text{mm}$$

Assume $d=30\,\text{mm}$ (to allow for deflection due to shear).

$$I_f=\frac{bt^3}{6}=\frac{640\times10^3}{6}=106666.7\,\text{mm}^4$$

$$\frac{bd^2}{c}=\frac{640\times30^2}{20}=28\,800\,\text{mm}^2$$

$$I_{\text{total}}=\frac{bt^3}{6}+\frac{btd^2}{2}$$

$$=2\,986\,666.7\,\text{mm}^4$$

$$\frac{E_f}{1-\nu^2}=\frac{10.00}{1-(0.2)^2}=10.42\,\text{GN/m}^2$$

$$D=I_{\text{total}}\times\frac{E_f}{1-\nu^2}=31\,121.065\,\text{MN mm}^2$$

$$D_Q=G\frac{bd^2}{c}=0.576\,\text{MN}$$

$$D_f=E_fI_f=1111.460\,\text{MN mm}^2$$

$$\frac{D_f}{D}=\frac{1111.460}{31\,121.065}=0.0357$$

$$\frac{D}{L^2D_Q}=\frac{31\,121.065}{3600^2\times0.576}=0.00417$$

D_f/D is small compared with unity and D/L^2D_Q is very small.

Therefore S_1 in eq. (7.15) is close to unity and the standard formula for deflection (eq. 7.12) is used for the thick face sandwich beam.

The total deflection = the primary deflection + the secondary deflection, i.e.

$$w=\frac{WL^3}{48EI}+\frac{WL}{4AG}$$

$$=\left(\frac{0.7\times3600^3}{48\times31121.065\times10^3}\right)+\left(\frac{0.7\times3600\times10^6}{4\times28800\times20\times10^3}\right)$$

$$=21.817+1.094=22.911\,\text{mm}$$

Example 9.12

Figure 9.15 shows the cross-section of a sandwich beam. Both faces are made of sheet steel; the top being a trough section of 1.22 mm thickness and the bottom a sheet section of 1.5 mm thickness. The core material is 28 mm thickness and is a low density foamed polyurethane. The width of the beam is 1000 mm and the beam is simply supported with a span of 1200 mm and an overhang of 200 mm. The central point load has a value of 40 kN. The material properties are as follows.

$$E_f = 205\,\text{GN/m}^2, \qquad \nu_f = 0.3, \qquad G_c = 20\,\text{MN/m}^2$$

It is required to design the beam.

The properties of the section are

$$\bar{x} = \frac{\Sigma Ax}{\Sigma A}$$

$$\text{Length of trough section} = (30 \times 2 + 2 \times 20 \times \sqrt{2}) = 116.569\,\text{mm}$$

$$\text{Weight of core material} = 75.0\,\text{kg/m}^3$$

$$\text{Weight of steel} = 7700\,\text{kg/m}^3$$

Therefore

$$\bar{x} = \frac{116.569 \times 1.22 \times 7700 \times 39.36 + 75 \times 28 \times 100 \times 15.5}{116.569 \times 1.22 \times 7700 + 75 \times 28 \times 100 + 100 \times 1.5 \times 7700}$$

$$= 18.7796\,\text{mm}$$

$$h_1 = 20.58\,\text{mm}, \qquad h_2 = 18.78\,\text{mm (both by calculation)}$$

$$c = 28\,\text{mm}, \qquad d = 39.36\,\text{mm}$$

$$\frac{bd^2}{c} = \frac{1000 \times 39.36^2}{28} = 55328.914\,\text{mm}^2$$

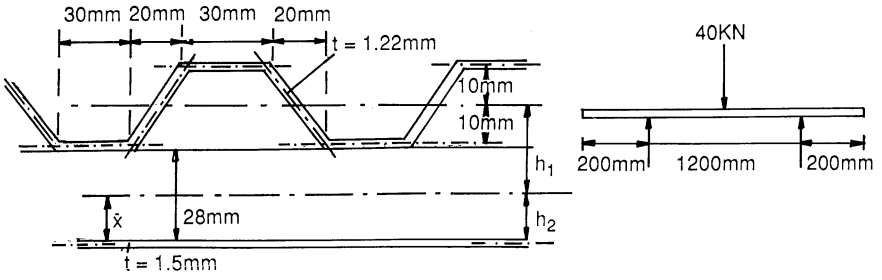

Figure 9.15

$$I_{f1} = \left[(30 \times 1.22 \times 10^2 \times 2) + \left(\frac{1.22 \times 1.414 \times 20^3 \times 2}{12} \right) \right] \times 10$$

$$= 96201.07\,\text{mm}^4 \quad \text{(for whole width of beam)}$$

$$I_{f2} = \frac{1000 \times 1.5^3}{12} = 281.25\,\text{mm}^4$$

$$I_f = 96201.07 + 281.25$$

$$= 96482.32\,\text{mm}^4 \quad \text{(for whole width of beam)}$$

$$I_{total} = (96\,482.32) + (116.569 \times 1.22 \times [20.58042]^2 \times 10)$$

$$+ (100 \times 1.5 \times [18.7792]^2 \times 10)$$

$$= 1\,227\,844.6\,\text{mm}^4 \quad \text{(for whole width of beam)}$$

$$E_f/(1 - v_f^2) = 225\,274.73\,\text{MN/m}^2$$

$$D_Q = 20 \times 55\,328.914 \times 10^{-6} = 1.107\,\text{MN}$$

$$D_f = 225\,274.73 \times 96\,482.32 \times 10^{-6} = 21\,735.029\,\text{MN mm}^2$$

$$D = 225\,274.73 \times 1\,227\,844.6 \times 10^{-6} = 276\,602.36\,\text{MN mm}^2$$

$$D_f/D = \frac{21\,735.029}{276\,602.36} = 0.07858$$

$$(1 - D_f/D) = 0.921$$

$$(1 - D_f/D)^2 = 0.8482$$

$$D/L^2 D_Q = \frac{276602.36}{1200^2 \times 1.107} = 0.17352$$

Overhang $L_1 = 200\,\text{mm}$

$$\theta = \tfrac{1}{2}[(D/L^2 D_Q)(D_f/D)(1 - D_f/D)]^{-1/2} \quad \text{(from appendix, chapter 7)}$$

$$= \tfrac{1}{2}[0.17352 \times 0.07858 \times 0.921]^{-1/2} = 4.461793$$

$$\phi = \frac{4.461793 \times 2 \times 200}{1200} = 1.487$$

$$\beta_1 = \frac{\sinh\theta - (1 - \cosh\theta)\tanh\phi}{\sinh\theta \tanh\phi + \cosh\theta} \quad \text{(from appendix, chapter 7)}$$

$$= \frac{43.374123 - (1 - 43.385679) \times 0.9027685}{43.374123 \times 0.9027685 + 43.385679} = 0.9890$$

$$S_1 = 1 - \left[\frac{\sinh\theta + \beta_1(1 - \cosh\theta)}{\theta} \right]$$

$$= 1 - \left[\frac{43.374123 + 0.9890 \times (1 - 43.385679)}{4.461793}\right] = 0.674$$

From eq. (7.15) the total central deflection

$$= \frac{WL^3}{48D} + \frac{WL}{4D_Q}\left(1 - \frac{D_f}{D}\right)^2 S_1$$

$$= \left(\frac{40 \times 1200^3}{48 \times 276602.36 \times 10^3}\right) + \left(\frac{40 \times 1200 \times 0.8482 \times 0.674}{4 \times 1.107 \times 10^3}\right)$$

$$= 5.2060 + 6.1972 = 11.4032\,\text{mm}$$

The equivalent equation for the total central deflection of a beam carrying a uniformly distributed load is given in the appendix to chapter 7; also given are the relevant coefficients.

Example 9.13

Determine the critical buckling load for a sandwich panel manufactured from faces consisting of composites of chopped strand mat reinforcement and polyester resin (30% glass content by weight) and core material of polyurethane foam. The panel is simply supported at its ends. The modulus of elasticity in compression of the material of the faces is 7.0 GN/m^2, Poisson's ratio is 0.2 and the modulus of rigidity of the core material is 20 MN/m^2 (see Figure 9.16).

The critical buckling load for a thin face sandwich panel $= P_{cr} = (\pi^2 D_2/b^2)K$ (eq. 7.23) where the buckling coefficient K is determined from Figure 7.14 in terms of the length/width ratio of the panel and the quantity ρ where

$$\rho = \frac{\pi^2}{b^2}\left(\frac{E_f d^2 t}{2(1 - v_f^2)}\right)\left(\frac{c}{G_c d^2}\right)$$

Therefore

$$\rho = \frac{\pi^2}{2000^2}\left(\frac{7.0 \times 70^2 \times 6 \times 10^3}{2(1 - 0.2^2) \times 10^6}\right)\left(\frac{64 \times 10^6}{20 \times 70^2}\right)$$

$$= 0.1727$$

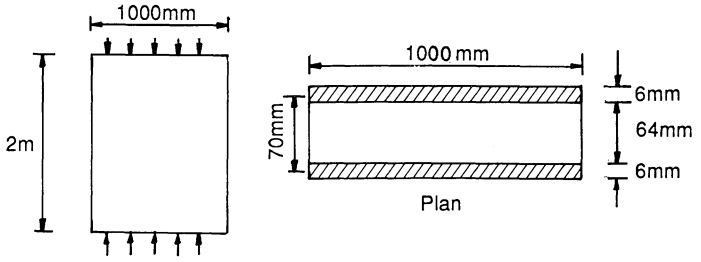

Figure 9.16

$$D_2 = \frac{E_f t d^2}{2(1-\nu_f^2)} = \frac{7.0 \times 6 \times 70^2 \times 10^3}{2(1-0.2^2) \times 10^6}\ \text{MN/mm}^2$$

$$= 107.1875\ \text{MN/mm}^2$$

Buckling coefficient K $= 1.3$

Therefore

$$P_{cr} = \frac{\pi^2 D_2}{b^2} K$$

$$= \frac{\pi^2 \times 107.1875}{10^6} \times 1.3 \times 10^6 = 793.48\ \text{N}$$

Figure 7.13 may only be used if D_f/D and $D/D_Q L^2$ give a point in Figure 7.9 which is close to the line ABCG. It is, therefore, necessary to check.

$$D_f = E_f I_f$$

where $I_f = 6^3/6 = 36.0\,\text{mm}^4$. Thus

$$D_f = \frac{7.0 \times 36.0 \times 10^3}{(1-0.2^2) \times 10^6} = 0.2625\ \text{MN mm}^2$$

$$D = I_{total} \times \frac{E_f}{(1-\nu_f^2)}$$

$$I_{total} = \frac{td^2}{2} = \frac{6 \times 70^2}{2} = 14700.0\,\text{mm}^4$$

$$D = \frac{14700.0 \times 7.0 \times 10^3}{(1-0.2^2) \times 10^6} = 107.1875\ \text{MN mm}^2$$

Therefore

$$D_f/D = 0.00245$$

$$D_Q = \frac{Gd^2}{c} = \frac{20 \times 70^2}{64 \times 10^6}\ \text{MN} = 0.0015312\ \text{MN}$$

$$D/D_Q L^2 = \frac{107.1875}{0.0015312 \times 2000^2} = 0.0175$$

The above values of D_f/D and $D/D_Q L^2$ give a point on the line ABCG of Figure 7.9.

References

1. L. Hollaway, ed., *BPF Composites Design Guide*, Woodhead, Cambridge (1993).
2. L. Hollaway, ed., *Polymer and Polymer Composites in Construction*, Thomas Telford, London (1990).

3. *MIC-MAC*, Think Composites Software, Dayton, OH (1987).
4. *CoALA*, Cranfield Institute of Technology (1987).
5. Engineering Science Data Unit, Failure of Composite Laminates, ESDU 2033, ESDU International, London (1987).
6. S. Timoshenko, *Strength of Materials. Part II Advanced Theory and Problems*, Van Nostrand, New York (1968).
7. S. Timoshenko and J.M. Gere, *Theory of Elastic Stability*, McGraw-Hill, New York (1961).

Glossary

The use and range of applications of fibre reinforced matrix materials have increased considerably over recent years. Consequently, a new technology has been established, involving a number of specialized processes and techniques. Since those working in the area may have widely differing backgrounds, it is useful to define the more important terms used in this book.

Addition polymers Polymers formed into long chain molecules by the chemical reaction of one or more types of monomer units, each of which has a double bond prior to polymerization.

Anisotropic material There are no planes of material property symmetry which pass through a point. Therefore, the material constants at a point change as the co-ordinate system is rotated at the point. An anisotropic material in a plane stress state has six independent elastic constants. Isotropic and orthotropic materials are specialized cases which have a higher degree of symmetry than anisotropic materials.

Antiplane core (associated with sandwich beams) One in which $\sigma_{xx} = \sigma_{yy} = \sigma_{xy} = 0$. Consequently, the shear stresses σ_{zx} and σ_{yz} are independent of z.

Bifurcation A term related to the load deflection relationship of a straight axially loaded strut at critical load. It is a point at which divergent equilibrium states become possible and results at a branch point in the plot of axial load against lateral deflection from which two alternative load deflection plots are theoretically valid.

Buckle The process of wrinkling or bulging of a member as a result of elastic or inelastic strain.

Buckling load The load at which a compression member will collapse in service or fail in a loading test.

CFRP Carbon fibre reinforced polymer.

Chopped strand mats These are chopped strands which are held together by means of a size. The strands are completely randomly orientated and the mats are of uniform thickness. They are produced in various sizes, the most usual being 1 oz/ft^2 and $1\frac{1}{2}$ oz/ft^2 (300 g/m^2 to 400 g/m^2).

Chopped strands These are made from continuous strands which are chopped into short lengths, usually 50 mm.

Condensation polymers Polymers formed by the chemical reaction of at least two monomer units, with, in most cases, production of a by-product of low molecular weight.

Continuous fibre reinforcement Continuous fibres may be defined as fibres which are continuous throughout the whole length of the laminate, resulting in the load being applied directly to them; the stress throughout the length of the fibre is constant.

Co-polymer An addition polymer of at least two monomers.

Critical length The critical length of a fibre is the length which is required for the fibre stress to develop its maximum value when under a particular load condition.

Critical load The load at which bifurcation occurs. It is determined by theoretical stability analysis.

Crystallite The most rudimentary form of an embryonic crystal that can be identified as a certain species under the microscope.

Degree of polymerization An impression of the length of the average molecular chain in a polymer, assessed by an estimate of the average molecular weight and usually stated in terms of the number of repeating units in the chain.

Discontinuous fibre reinforced plastics Discontinuous fibre reinforced plastics refer to plastics whose reinforcing fibres have length-to-diameter (l/d) ratios (know as aspect ratios) varying between 100 and 5000. Whisker reinforcements have l/d ratios between approximately 150 and 2500. Discontinuous glass fibre reinforced polymers which consist of premix thermosetting resins, chopped strand mat-reinforced resins and fibre-reinforced thermoplastics resins have fibres with l/d ratios between 150 and 5000. The ultimate strength and modulus of short-fibre-reinforced composites can approach the values for continuous fibre composites, providing that the short filaments can be aligned unidirectionally and that their length is much greater than the critical length (l) required for shear stress transfer.

Effective width This term refers to the reduced width of plate or angle which, assuming uniform stress distribution, will give the same structural behaviour as the actual section of the plate or angle and the actual non-uniform stress distribution.

Elastomer An elastomer is any member of a class of synthetic polymeric substances possessing rubber-like qualities (especially the ability to regain shape after deformation) and toughness, and which has a glass transition temperature well below ambient temperature.

Fibre Any material in an elongated form such that the ratio of its minimum length to its maximum average transverse dimension is 10:1, its maximum cross-sectional area is 1.975×10 mm (corresponding to a circular cross-section of 0.25 mm diameter) and its transverse dimension is not greater than 0.25 mm.

Fibre composite material A material consisting of two or more distinct physical phases, one of which is a fibrous phase dispersed in a continuous matrix phase.

Filament A continuous fibre.

Flexural rigidity (associated with sandwich beams or struts) Neglecting the local bending stiffness of the faces:

$$D_1 = E_f btd^2/2.$$

Flexural rigidity (associated with sandwich panels) With cylindrical bending and neglecting the local bending stiffnesses of the face:

$$D_2 = E_f t d^2/2(1 - v_f^2)$$

Gelcoat Quick-setting resin used in the moulding process to provide an improved surface for the composite; it is the first resin applied to the mould after the mould release agent and provides enviromental protection to the composite.

GFRP, GRP Glass fibre reinforced polymer.

Glass transition temperature The temperature at which a sudden change in slope of various physical properties versus temperature curves occurs (commonly measured in terms of the standard heat distortion temperature). It almost approximates the temperature below which a polymer fails in a brittle manner and above which it behaves as a leathery or rubbery solid.

Homogeneous materials The material properties do not change from point to point in the body, although they may change with a co-ordinate rotation at the points; thus, as long as the material properties are the same for the same co-ordinate position the material is homogeneous. If this is not true, the material is said to be *heterogeneous.*

Hybrid Composite with two or more constituents: for instance a carbon/glass fibre hybrid. An intralaminar hybrid has plies made from carbon and glass filaments. An interlaminar hybrid has laminates made from two or more different ply materials.

Hydrophilic The property of possessing strong affinity for water.

Hygrothermal effect Changes in properties due to moisture absorption and temperature change.

Isotropic material This term indicates that the material properties at a point in the body are not a function of orientation. The material properties remain constant regardless of the reference co-ordinate system at a point. As a result, the material properties are constant in any plane which passes through a point in the material. All planes which pass through a point in the isotropic material are planes of material property symmetry. Two independent elastic constants are necessary to write the Hooke's Law relationship for two- or three-dimensional stress states.

Kevlar fibre DuPont company trade name for an aramid fibre.

KFRP Kevlar fibre reinforced polymer.

Macromechanics Structural behaviour of composite laminates using the laminated plate theory. The fibre and matrix within each ply are smeared and no longer identifiable.

Matrix A bonding material which adheres to and contains the fibres. Many materials, such as the thermoplastic and thermosetting resins, metals, glass or ceramic materials, can form a matrix. Resins are the most widely used.

Micromechanics Calculation of the effective ply properties as a function of the fibre and matrix properties. Some numerical approaches also provide the stress and strain within each constituent and those at the interface.

Monomer A monomer is the low molecular weight starting material from which a polymer is formed.

Off-axes Not coincident with the symmetry axis.

On-axes Coincident with the symmetry axis.

Orthotropic material Only three mutually perpendicular planes of material property symmetry may pass through a point. Four independent elastic constants must be determined.

PAN A precursor used in the manufacture of carbon fibres. PAN is the abbreviation for polyacrylonitrile.

Peel ply Fabric material applied to a laminate to protect the clean, ready-to-use bonding surface and peeled off prior to curing.

Plane strain Two-dimensional simplification for stress analysis, applicable to the cross-section of long cylinders.

Plane stress Two-dimensional simplification for stress analysis applicable to thin homogeneous and laminated plates.

Plasticizers Materials deliberately added to polymers to reduce their stiffness.

Polymerization The chemical reaction involved when, for example, a liquid polyester resin sets to a solid. A comparatively simple chain molecule becomes a highly complex three-dimensional one.

Pre-preg (a pre-impregnated fibre) An intermediate product consisting of fibres or tows which have been coated with a matrix material such as resin. In the majority of cases the fibres are aligned to give a flat sheet or tape. Usually the resin is not fully cured, so that the aggregate remains flexible and the sheet can be built up in plies to form a composite.

Sandwich beam A sandwich beam has two faces, each of thickness t, separated by a layer or core of low density material of thickness c.

Strand This is associated with filaments of glass fibre. The diameter of a filament is up to 1/400 mm.

Tangent modulus The slope of the stress-strain curve of a material in the inelastic region, at any given stress level as determined by the compression test of a small specimen.

Thermoplastic plastics A material is thermoplastic when it can be softened by heating and hardened by cooling without undergoing a chemical change.

Thermosetting plastics A material is thermosetting when it can be changed or has been changed into a hard infusible product by a non-reversible chemical reaction initiated by the use of heat or curing agents.

Thick face (associated with sandwich beams) One in which the stiffness in bending about its own axis is significant and the thickness of the faces is assumed to have a finite value so that d is not equal to c.

Thin face (associated with sandwich beams) One in which the stiffness in bending about its own axis is assumed to be zero, but the thickness of the faces is assumed to have a finite value so that d is not equal to c.

Very thin face (associated with sandwich beams) One in which the stiffness in bending about its own axis is taken as zero and is sufficiently thin to assume d equal to c.

Whisker Any material that fits the definition of a fibre and is a single crystal.

Wire A metallic filament.

Woven cloth This is a more refined product than woven rovings. It is usually a bi-directional reinforcement.

Woven rovings These are continuous strands which may be unidirectionally or bidirectionally orientated.

Yarn or tow A number of filaments in a bundle which can be handled as a single unit. A tow is usually bigger than a yarn, having thousands of filaments whereas a yarn usually has a few hundred filaments. A yarn may be spun and twined from staple fibre but a tow is formed from constant filaments.

Yield point The maximum stress recorded in a tensile or compressive test of a ductile specimen prior to entering the inelastic region of the material.

Yield stress A term denoting the yield strength or yield point of a material as defined above.

Appendix: ASTM specifications

There is generally no equivalence between the test specification of the American Society for Testing and Materials (ASTM) and the British Standards Institution (BSI) specification. Throughout the book reference has been made to BSI specifications and the equivalent International Standards Organisation (ISO) specifications; this appendix will give some of the more commonly encountered specifications from ASTM for fibre reinforced polymers.

Chemical resistance

Various different test methods are in use.

Resistance of plastics (including cast/hot-moulded/cold-moulded resinous/sheet products) to 50 chemical reagents	ASTM D 543-87(08.01)
Practice for determining chemical resistance of thermosetting resins used in glass fibre reinforced structures (liquid service)	ASTM C 581-87(08.04)
Reinforced plastics contact-moulded laminates for corrosion resistance equipment	ASTM C 582-87(08.04)

Fire and smoke tests

Test method for rate of burning and/or extent and time of burning of self-supporting plastics in horizontal position	ASTM D 635-91(08.01)
Test methods for rigid sheet and plate materials (used for electrical insulation): flammability and flame resistance	ASTM D 229-91(08.01, 10.01)
Test methods for measuring minimum oxygen concentration to support candle-like combination of plastics	ASTM D 2863-87(08.02)
Test method for surface burning characteristics of building materials	ASTM E 84-90a(04.07)
Test method for surface flammability of materials using a radiant heat energy source	ASTM E 162-90(04.07)

Smoke evolution tests

Test method for density of smoke from the burning or decomposition of plastics	ASTM D 2843-77(1988)(08.02)

Mechanical properties

Test methods for compressive properties of liquid plastics	ASTM D 695-91(08.01) [D 695M-91]metric
Test methods for flexural properties of unreinforced and reinforced plastics and electrical insulating materials	ASTM D 790-91(08.01)

Tensile strength and modulus

Various different test methods are in use, utilising different sizes of test specimens and different test speeds.

Apparent tensile strength of ring or tubular plastics and reinforced plastics (by the split disc method NOL ring method	ASTM D 2290-92(08.04, 15.03)
Method for preparation and tension testing of filament wound pressure vessels	ASTM D 2585-68(1990)(15.03)
Test methods for tensile properties of fibre resin composites	ASTM D 3039-76(1989) (15.03)
Test method for flexural properties of fibre-reinforced pultruded plastic rods	ASTM D 4476-85(1990)(08.03)
Test method for in-plane shear strength of pultruded glass-reinforced plastic rod	ASTM D 3914–84(08.03)
Test method for apparent horizontal shear strength of pultruded reinforced plastics rods by short beam method	ASTM D 4475-85(1990)(08.03)
Test method for tensile properties of pultruded glass-fibre reinforced plastic rod	ASTM D 3916-84 (1988) (08.03)
Test method for tensile properties of reinforced thermosetting plastics using straight sided specimens	ASTM D 5083-90(08.03)
Test methods for tensile properties of plastics	ASTM D 638-91 (08.01) ASTM D 638M-91a (for matrix [metric])
Test method for longitudinal tensile properties of fibre glass reinforced thermosetting plastic pipe and resin tube	ASTM D 2105-90(08.04)

Definitions of terms relating to reinforced pultruded products	ASTM D 3918-80(08.03)
Specification for contact moulded glass-fibre-reinforced thermoset resin hoods fabricated by custom contact-pressure/ chemical resistant tanks	ASTM D 4097-88(08.04)

Thermal properties

Test method for deflection temperature of plastics under flexural load	ASTM D 648-82(1988)(08.01)

Coefficient of expansion

Linear expansion	ASTM D 696-91(08.01)

Adhesives

Test method for tensile properties of adhesive bonds	ASTM D 897-78(1983)(15.06)

Rigid cellular polymers

Test method for compressive properties of rigid cellular plastics	ASTM D 1621-73(1979)(08.02)
Test method for tensile/tensile adhesive properties of rigid cellular plastics	ASTM D 1623-78(08.02)
Test method for apparent bending modulus (stiffness) of plastics by cantilever beam method	ASTM D 747-90(08.01)

Plastics (thermosetting) reinforced

Test method for in-plane shear strength of reinforced thermosetting plastics	ASTM D 3846-79(1985)(08.03)
Specification for dimensional tolerance of thermosetting glass-reinforced plastic	ASTM D 3917-84(1988)(08.03)
Test method for tensile properties of pultruded glass-fibre-reinforced plastic rod	ASTM D 3916-84(1988)(08.05)

Index